A Robotic System Using Myoelectrical Control at the Elbow Joint for the Rehabilitation of Persons after Stroke

Rong SONG

A thesis submitted in partial fulfillment of the requirements for
the Degree of
Doctor of Philosophy
in Biomedical Engineering

Department of Health Technology and Informatics
The Hong Kong Polytechnic University

December 2005

CERTIFICATE OF ORIGINALITY

I hereby declare that this thesis is my own work and that, to the best of my knowledge and belief, it reproduces no material previously published or written, nor material that has been accepted for the award of any other degree or diploma, except where due acknowledgement has been made in the text.

_____

Rong SONG

December 2005

ABSTRACT

Robotic systems have been used in stroke rehabilitation to restore upper limb functions. In this study, an innovative myoelectrically controlled robotic system with one degree of freedom (DOF) was developed. The axis of the robotic system was aligned with the elbow joint and a torque from a servo motor was applied directly to the elbow based on the electromyographic (EMG) signal of the subject's affected muscle at the elbow joint. This could help subjects after stroke to perform active elbow training in the horizontal plane. Two control strategies were investigated for the robotic system: the recurrent artificial neural network (RANN) model and proportional control. The RANN model was investigated on six subjects without impairment and three subjects after stroke. After training, the average cross-correlation coefficients between the expected and the predicted torque of subjects without impairment were 0.97±0.01 in the training data and 0.92±0.03 in the test data, respectively. It appeared that the output of the RANN was highly correlated to the expected torque. However, the performance of the RANN model on the three subjects after stroke did not show results as good as that on the subjects without impairment. The average cross-correlation coefficients of the subjects after stroke were 0.73±0.10 in the training data and 0.41±0.07 in the test data, respectively. Proportional control with a resistive load was used as an alternative control strategy. With the application of proportional control, the system could provide assistive extension torque which was proportional to the amplitude of the subject's processed and normalized triceps EMG. The EMG-torque gain was set at 0%, 50%, 100% and 150% for the assistive torque. The system could also provide a resistive load, the level of which ranged from 0%-20% of the maximum isometric voluntary extension (MIVE) torque and the maximum isometric voluntary flexion (MIVF) torque of the affected elbow when the elbow angle was at 90 deg. Effects of the resistive loads and EMG-torque gains on the performance of the elbow extension were investigated on the affected arms of nine subjects after stroke in a tracking experiment. Results showed that the design could enable eight subjects with weak triceps to extend their affected elbows to a more extended position with the assistance of the myoelectrically controlled robotic system except for one subject who could already extend her elbow to the full extension position (0 deg) without the assistance of the system. There was a significant decrease in triceps EMG along with the increase in the EMG-torque gain during the elbow

movement from 90 deg to 60 deg, which implied that it took less effort for subjects after stroke to perform the same movement with a larger gain. Since the myoelectrically controlled robotic system could facilitate elbow movement, its long-term training effect on the functional improvement of the affected arm in three subjects after stroke was investigated in a 20-session training program for four weeks. In each session, there were 18 trials with different combinations of the EMG-torque gain and the resistive load. In each trial, the subject was asked to follow a target trajectory which ranged from 0 deg to 90 deg, and complete five-cycle repetitive elbow flexion and extension with the myoelectrically controlled robotic system. Outcome measurements on the muscle strength at the elbow joint showed that there were increases in the MIVE and MIVF torques of the affected arms of all the subjects after the four-week rehabilitation training. The subjects could also reach a more extended position without the assistance of the robotic system after the four-week rehabilitation training. Moreover, there were a decrease in the modified Ashworth scale and an increase in the Fugl-Meyer score for all three subjects after the four-week rehabilitation training.

In addition, another sinusoidal arm tracking experiment was designed to quantitatively evaluate the elbow control function on nine subjects after stroke in dynamic situations. The movement performance was analyzed in terms of three parameters: root mean square error (RMSE) between the actual elbow angle and the target angle, root mean square jerk (RMSJ) and response delay (RD) at six velocities (10, 20, 30, 40, 50 and 60 deg/s). Results showed the RMSE and RMSJ increased in both the affected and the unaffected arms with the increase in the tracking velocity. The RMSE and RMSJ of the unaffected arms were significantly lower than those of the affected arms at all the velocities studied. The RD of the affected arms was larger than that of the unaffected arms at the velocities of 20, 30, 40 and 60 deg/s. There were significant correlations between the RMSJ and the modified Ashworth scale at the velocities of 10, 20, 30, 40 and 60 deg/s. The sinusoidal arm tracking experiment was also conducted on the three subjects after stroke before and after the four-week training. Results showed that there were decreases in the RMSE and RD of the affected arms after the four-week training, which indicated the improvement of the elbow control function in the affected arms for the three subjects.

Publications and patent arising from the thesis

1. **Song R**, Tong KY. Using recurrent artificial neural network model to estimate voluntary elbow torque in dynamic situation. Medical & Biological Engineering & Computing; 43(4) pp. 473-480 (2005).
2. **Song R**, Tong KY, Tsang SF, A method for the evaluation of the elbow functional control in patients after stroke, The 10th Annual Conference of the International Functional Electrical Stimulation Society (IFESS 2005), Montreal, Canada, July 5-9 (2005).
3. **Song R**, Tong KY, Hu XL and Li L. The Development of a Rehabilitation Robot of Elbow Joint Using Artificial Neural Networks, International Conference on. Computing, Communications and Control Technologies (CCCT'04), Austin, USA, August 14-17, (2004).
4. **Song R**, Tong KY, Hu XL and Li L. An EMG-Driven Rehabilitation Robot, The 11th World Congress of the International Society for Prosthetics & Orthotics, Hong Kong (ISPO2004) August 1-6, pp. 65 (2004).
5. **Song R**, Tong KY,Hu XL, Li L. Torque estimation in voluntary reciprocal elbow flexion and extension based on a recurrent artificial neural network WCCBME Beijing (2004).
6. **Song R**, Tong KY. A surface EMG driven musculoskeletal model of the elbow joint during isometric contraction using a nonlinear optimization method on the muscle activation parameters. Conference on Biomedical Engineering: BME2004, Hong Kong September 23-25, pp. 87-91 (2004).
7. **Song R**, Tong KY, Hu XL, Tsang SF, and Li L. The therapeutic effects of myoelectrically controlled robotic system for persons after stroke-a pilot study. Submitted to IEEE EMBC 2006.
8. Chinese Patent pending. Tong KY, **Song R**. Rehabilitation robotic system and training method using EMG signal to provide mechanical help. Chinese patent application being processed (IP-313A). filed in April 2006.

ACKNOWLEDGEMENTS

I would like to express my deepest thanks to my chief supervisor, Dr. Raymond K. Y. Tong, and my co-supervisor, Prof. Arthur F. T. Mak, for their invaluable guidance, encouragement, patience, and support throughout the period of my study.

I would like to thank Dr. XL Hu, Mr. Le Li, Mr. Vincent Tsang, Mr. Shaomin Zhang and other colleagues in HTI for their helps in subject recruitment, experimental setup and suggestions on many aspects of this research. Without their helps, this study could not have been completed.

I would also like to thank Mr. KC Chen and Mr. CF Tin for giving me help in the mechanical workshop and Ms Diana Chau in the Jockey Club Rehabilitation Engineering Clinic for offering her generous helps in various aspects of this study.

Thanks are given to Professor Daniel Chow for allowing me to use their EMG systems and advising me on statistical analysis.

I am grateful to my friend Mr. XP Liu who provided me many useful materials for my research.

I would like to thank Mr. Sheng Bi for advising me on clinical scales.

I am also grateful to Ms. Sally Ding who helped to correct grammar mistakes in my thesis.

I must thank all the subjects who participated in the experiments. Without their participation, this study would not have been completed.

I would like to thank the financial support from the Hong Kong Polytechnic University.

Finally, this thesis is especially dedicated to my parents and my girl friend. Without their endless encouragement and support, I could not have achieved my goals.

LIST OF ABBREVIATIONS

ANN	Artificial neural network
ANOVA	Analysis of variance
ARM Guide	Assisted rehabilitation & measurement guide
CE	Contractile element
CIMT	Constraint-induced movement therapy
CNS	Central nervous system
CPM	Continuous passive motion
DOF	Degree of freedom
EMG	Electromyography
EEG-EMG	Electroencephalogram-electromyogram
FES	Functional electrical stimulation
HAL	Hybrid assistive leg
ISJ	Integration of square jerk
MA	Moment arm
MAS	Motor assessment scale
MIME	Mirror-image movement enabler
MIVE	Maximum isometric voluntary extension
MIVF	Maximum isometric voluntary flexion
ML	Muscle length
MOI	Moment of inertia
MRP	Motor relearning program
MSS	Motor status scale
MUAP	Motor unit action potential
MULOS	Motorized upper-limb orthotic system
NEMG	Normalized EMG
PE	Passive elastic element
PID	Proportional-Integral- Differential
QOL	Quality of life
RANN	Recurrent artificial neural network
RD	Response delay
RMA	Rivermead motor assessment
RMSE	Root mean square error
RMSJ	Root mean square jerk
ROM	Range of motion
SSE	Sum square error
VR	Virtual reality
WHO	World Health Organization

TABLE OF CONTENTS

LIST OF FIGURES

LIST OF TABLES

CHAPTER 1 BACKGROUND

1.1 Introduction

1.1.1 Stroke

Stroke is a primary cause of serious disabilities and the third leading cause of death in Hong Kong. Approximately 25,000 strokes occur each year in Hong Kong, causing 3,000 deaths and significant disability for many survivors (Fig. 1.1) (Hong Kong Hospital Authority Statistical Report, 2004), and the number of disability increases in recent years because of the increasing population of aged people. The World Health Organization (WHO) has defined stroke as a condition with 'Rapidly developing clinical signs of focal loss of cerebral function, with symptoms lasting more than 24 hours or leading to death, with no apparent cause other than that of vascular origin' (Hatano et al., 1976). There are two main kinds of stroke. One is ischemic stroke which results from occlusion of or low flow in one or more vessels by blood clots or other particles; the other is hemorrhagic stroke which is caused by bleeding. The rupture or blood clot reduces the blood supply to an area of brain and the neurons in this area are affected. Disabilities occur when the neurons in these areas are killed and the abilities or functions they control are disrupted. The types and degrees of disability that follow a stroke vary considerably, depending upon the origin part of the brain and the size of affected area. Generally, stroke can cause five types of disabilities (National Institute of Neurology Disorder and Stroke, US, 2005):

1. Paralysis or problems controlling movement
2. Sensory disturbances including pain
3. Problems using or understanding language
4. Problems with thinking and memory
5. Emotional disturbances

Patients after stroke have often been reported to have a lower quality of life (QOL) than normal subjects of similar age due to the disabilities (Jonkman et al., 1998; Wyller et al., 1998). Post-stroke depression was also reported in these patients with impaired QOL (Angeleri et al., 1993). It is important to help such patients with

disabilities to regain optimal physical, psychosocial, and vocational functioning and allow them to take an active independent role in both family and community life.

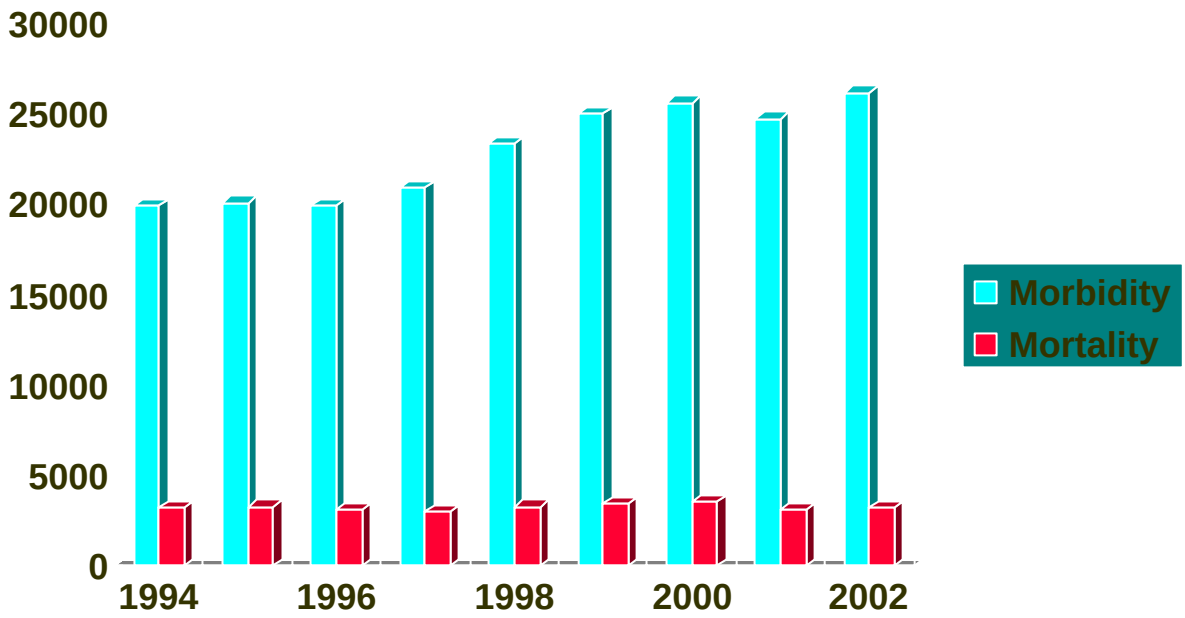

Fig. 1.1 Mortality and morbidity statistics of cerebrovascular disease (Stroke) in Hong Kong from 1994 to 2002 (Hong Kong Hospital Authority Statistical Report, 2004).

Stroke rehabilitation begins during acute hospitalization after the patient's medical condition has been stabilized and continues sequentially in three main settings: hospital, specialized rehabilitation units, and the community (Greshman et al., 1997; Pollack et al., 2002). Since most patients after stroke are affected by hemiplegia or hemiparesis, a neurological impairment that could restrict sensory and motor abilities on one side of the body, the objective of physiotherapy is to focus on helping patients with motor function impairment to restore the lost functions, perform normal activities independently and improve the quality of daily life (Teasell et al., 2003; Sivenius et al., 1985). Different kinds of rehabilitation approaches or rehabilitation with different intensities could result in different outcomes (Dobkin, 2004; Sivenius et al., 1985; Bode et al., 2004). In order to find a better rehabilitation strategy or to design a suitable rehabilitation device for patients after stroke, it is necessary to understand how spontaneous recovery takes place and how it can be facilitated for

maximum recovery. The answers to these questions can reveal what is the mechanism behind the rehabilitation that causes the recovery.

1.1.2 Brain plasticity

Neuroscientific knowledge about basic mechanisms for motor control, cognition, learning, and memory has been developed to explain rehabilitative practices during the last decade. Brain plasticity means ability of the brain to reorganize neural pathways based on new experiences. Brodal (1973) found that stroke might damage the neuromuscular system and this damage was irreversible. Since no neurons could regenerate after stroke, the mechanism behind the rehabilitation could only be explained by intact fibers taking over the function for the damaged ones. It is still not very clear about the recovery process and there are two main explanations. One was that neurons in the unaffected hemisphere region took the place of the functions of the damaged ones (Fisher et al., 1992); the other explanation was that the remaining intact neurons in the same hemisphere took on the functions of the damaged ones. Many techniques and theoretical models have been adopted to investigate the change in the brain caused by different kinds of stimulation. Nelles et al. (2001) used serial positron emission tomography (PET) to study training-induced brain plasticity after stroke. They found that the group who received passive movement improved much more than the control group after treatment. They also found a bilateral improvement of activation in the inferior parietal cortex using statistical parametric mapping after the training. Karni et al. (1995) used functional magnetic resonance imaging (fMRI) of local blood oxygenation to study the neural changes underlying the learning of finger movements. They found that a slowly evolving, long-term, experience-dependent reorganization of the adult primary motor cortex might explain the acquisition and retention of the motor skill. Robertson et al. (1999) studied the brain as a circuit, and rehabilitation of the brain could be viewed as the reconnection of a damaged circuit and the targeted input was useful to reconnect it. Hallet (2001) found that there was a competition between different limbs in the motor cortex. The cortex area of the inactivated muscle diminished in spinal excitability or motor threshold. Increases were also observed in motor output area size and motor evoked potential amplitudes for subjects with stroke after training the muscles, which indicated enhanced neuronal excitability in the damaged hemisphere (Liepert et al., 1998; Johansson, 2000). Brain

plasticity is the basic theory behind physiotherapy. The clinical practice and therapy goals should be integrated with this principle of rehabilitation strategy to improve the outcome of stroke rehabilitation.

Ward et al. (2004) gave hypothesis-driven approaches to neuro-rehabilitation on how to improve the motor performance of a paretic hand based on brain plasticity. The factors that have the possibility of affecting the neuro-reorganization are:

1. Reduction of somatosensory input from the intact hand
2. Increase in somatosensory input from the paretic hand
3. Anesthesia of a body part proximal to the paretic hand
4. Plasticity within the affected motor cortex may be enhanced
5. Activity within the intact motor cortex may be down-regulated
6. Pharmacological interventions may enhance recovery processes acting on adrenergic and dopaminergic neurotransmission

On the basis of this increased understanding of brain plasticity, better interventional strategies and rehabilitation device are being developed, which will optimize the outcome of stroke rehabilitation.

1.1.3 Conventional rehabilitation approaches

Conventionally, therapists design appropriate one-on-one rehabilitation exercises and training protocols based on the patient's ability, which are represented by various approaches.

Bobath is the most commonly used approach for stroke rehabilitation. It is defined as 'a problem-solving approach to assess and treat individuals with disturbances of function, movement and postural control due to a lesion of the central nervous system' (International Bobath Tutors Association, 2000). The therapist tries to optimize and facilitate automatic and volitional movements through specific handling techniques and the techniques are modified or withdrawn depending on the individual's ability to maintain effective task performance (Bobath et al., 1990; Luke et al., 2004). Another commonly used approach is the motor relearning program (MRP). It was first introduced to stroke rehabilitation by Carr and Shepherd in 1982 as a new rehabilitation theory and technique which emphasized specific training of

motor control in everyday activities (Carr and Shepherd, 1987). Motor relearning means goal oriented repetitive movement training. If people lose the special motion function, they can repetitively perform the training of this function which may help him/her to regain the control of the lost function. In order to investigate the effects of these two methods in early post-stroke treatment, Langhammer et al. (2000) carried out a randomized control trial. The results indicated that patients treated by MRP improved more in motor function and stayed fewer days in hospitals than those treated by Bobath. On the other hand, van Vliet et al. (2005) found that there was no significant difference between these two therapy methods in another randomized control trial.

The controversy in the current rehabilitation treatments implies that conventional rehabilitation approaches need to be improved for better outcome and the improvement should depend on increased understanding of brain plasticity and also on the development of rehabilitation devices. The objective of this study is to design a new rehabilitation strategy based on new theory and technology in order to optimize the outcome of stroke rehabilitation.

1.2 Recent rehabilitation approaches and devices

Although conventional therapies have positive effect to restore the motion function, many new rehabilitation approaches and devices are developed for optimal outcome. Conventional approaches are conducted in clinical setting in a one-to-one mode by therapists, which makes the treatment cost expensive, labour intensive and inconvenient for out-patients. For these reasons, patients often received little or no physiotherapy treatment after hospitalization. Although it is important to enhance motor function in the early rehabilitation period, the initial type of physiotherapy does not seem to have any long-term effect on patients' motor function after stroke (Langhammer et al., 2003). On the other hand, long term regular physical training is also needed in order to maintain the function improvement after hospitalization. Therefore, the two important issues that we should focus are how to help the patients after stroke to perform rehabilitation training after discharge from hospital and how to find a better way for them to restore lost functions. With the development of new techniques nowadays, it seems that we can use alternative approaches; patients can perform self-care motor relearning training automatically or the therapist can manage

more patients at a time and even remotely (Lai et al., 2004). It can be a more economical, convenient and efficient way. Several recent rehabilitation approaches or techniques that have been applied in stroke rehabilitation are introduced in the following parts.

1.2.1 Constraint-induced movement therapy (CIMT)

CIMT which is based on limiting the motion of unaffected limbs and trying to push subjects to reuse their affected limbs seems a promising way in the stroke rehabilitation (Sabari et al., 2001; Liepert et al., 1998; Mark et al., 2004). CIMT uses the theory of 'learned non-use'. Subjects after stroke show increased reliance on the unaffected arm since it is difficult for them to use their affected arm. This over-reliance on the unaffected arm interferes with the restoration of their affected arm. A 2-week program of CIMT had shown obvious function improvement in patients with chronic stroke (Stein, 2004). Functional MRI and transcranial magnetic stimulation studies have confirmed the changes in cortical function in association with CIMT training (Liepert et al., 2000, Levy et al., 2001).

1.2.2 Virtual reality (VR)

VR is a kind of visual feedback to guide the patients in the exercise. A virtual-reality system may include three components: (1) a computer or television screen that shows the virtual environment; (2) a device to record kinematics information or other feedback; (3) motivational games that guide the manipulation. The computer technology creates an environment in which the intensity of feedback and training can be well integrated, and the environment will make patients more immersed and active. The VR technique has some applications in stroke rehabilitation (Jack et al., 2001; Deutsch et al., 2004; Broeren et al., 2004). Jack et al. (2001) used a computer-based VR system together with a Cyber glove and a Rutgers force feedback glove to help patients after stroke to restore the functions of hand. The control system can capture the force sensor data from the gloves. After processing and evaluating the data, the system produces the simulation results on the screen. This kind of simulation can guide patients to do different kinds of tasks and the data can be saved into a database for later analysis and application. Fig. 1.2 shows the architecture of their system. Their VR rehabilitation system was evaluated on three patients after stroke in the rehabilitation program and produced positive results in increasing hand-grasp force.

Further investigation is needed to confirm its effect in stroke rehabilitation. VR technique is often not applied alone in stroke rehabilitation; robot training in a VR environment is often combined to motivate patients and facilitate rehabilitation training (Hogan et al., 1992, Krebs et al., 1998).

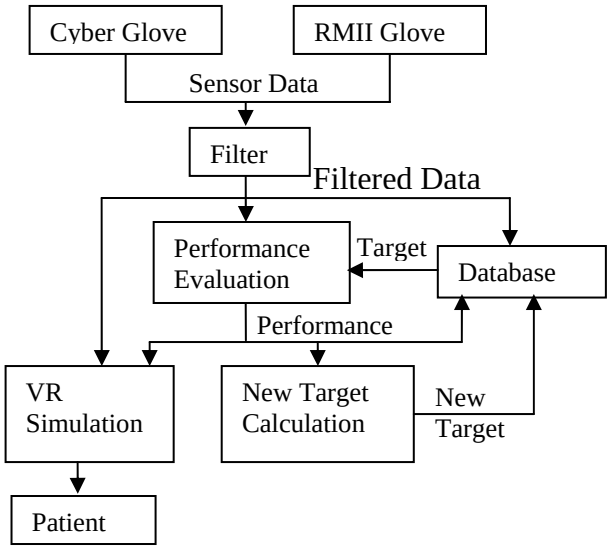

Fig. 1.2 Architecture of the virtual reality (VR) system (Jack et al., 2001).

1.2.3 Electromyographic (EMG) biofeedback

Biofeedback involves translating the physiologic activity of a patient's muscular response into a visual or auditory signal which allows him/her to be aware of the volitional changes in motor unit activity. The subject can facilitate or inhibit the muscular activity depending on the guide. The mechanism by which biofeedback can help to improve the outcome in the rehabilitation may be the reasons that the subjects can gain conscious control over undamaged upper neuron pathways which are in turn able to promote the restoration of missing functions (Morton et al., 1997). In practice, biofeedback is often combined with traditional physiotherapy as a useful complementary unit. EMG biofeedback has been applied on the recovery of upper limb (Basmajian et al., 1982; Inglis et al., 1984) and lower limb (Bradley et al., 1998; Wolf et al., 1983). Stein (2004) expected that robotic and sophisticated biofeedback technologies for motor relearning after stroke might converge into combined training systems.

1.2.4 Functional electrical stimulation (FES)

FES is a type of neural prosthesis used for restoring the neural function that has been damaged (Rushton et al., 1997). FES uses an electrical pulse to activate muscles directly, and it can bypass the brain injury and initiate movement in muscles that are partial or complete paralyzed. In consequence, FES has been used to help subjects with injured nervous system to perform movement and to restore the lost functions through rehabilitation training. Graupe et al. (1989 a, b) used EMG signals to trigger two kinds of FES mode in the rehabilitation of patients with spinal cord injury, and they also used EMG signals to identify muscle fatigue. Cauraugh et al. (2000) conducted a study to determine the effect of EMG-triggered neuromuscular electrical stimulation on the wrist and finger extension muscles in patients after stroke. Chae et al. (1998) designed an EMG-controlled FES system which not only could trigger the wrist training, but also could maintain and terminate the stimulation pulse. Fig. 1.3 showed its control flow. The subject's voluntarily activated EMG signal was captured by the intramuscular EMG electrodes. The amplitude of rectified and integrated EMG signal was used as a command signal. If the command signal exceeded a preset threshold, the stimulator delivered a neuromuscular electrical stimulation to activate the extensor digitorum communis. The stimulation was provided when the EMG signal was above the threshold during the movement of wrist extension. It was a close loop system with human cognitive investment. A sensorimotor integration theory was given to explain the advantage of cognitive investment in rehabilitation (Cauraugh et al., 2000). The EMG signal, which reflected subject's intention, was used to control the electrical stimulation and the movement. When subjects wanted to perform the training, they expressed their intention by increasing their EMG activities of agonists; the electrical stimulation would be triggered if the amplitude of the EMG signals exceeded the preset threshold. Subject not only could control the movements but also could sense the movements by proprioceptive feedback, an afferent signal that returned to the somatosensory cortex. The efferent control signal and the afferent sensory signal formed the sensorimotor cycle. If the control was not only triggered but also held by EMG signals (Chae et al., 1998), then it would give continuous stimulation to brain. This voluntary sensorimotor cycle might enhance the rehabilitation of subjects after stoke, especially help subjects who could not conduct the joint movement by themselves to perform voluntary the rehabilitation training.

Subjects would be more active in the training, if they could control the training by themselves, and they would feel more positively involved when compared to simple passive training.

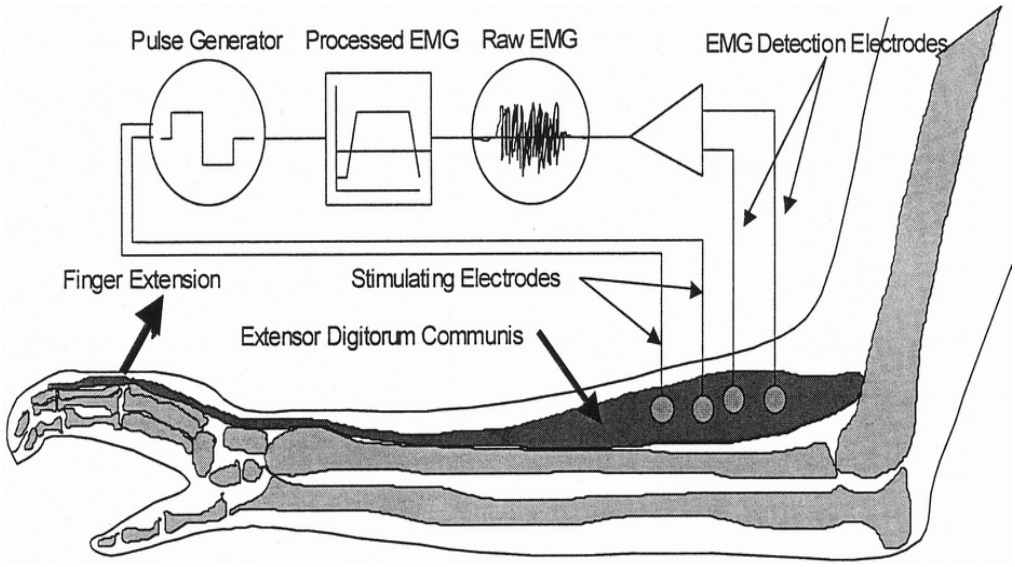

Fig. 1.3 Architecture of the EMG-controlled FES system (Chae et al., 1998).

1.3 Robotic systems in stroke rehabilitation

Motor relearning for upper limb can also be achieved by robotics and automation technology, which has emerged since the 1990s, since exercising the patients' paralyzed limbs may have a positive effect on neurological restoration of the limb function (Hogan et al., 1992). Thus mechanical, repetitive, passive exercises with the assistance of robotic devices are also useful for recovery. Moreover, robotic techniques can quantitatively measure motor recovery during rehabilitation training (Colombo et al. 2005). Van der Helm (1994) reported that a model structure of a robotic system could be divided into four blocks:

1. The linkage system is the mechanical structure of the robot like the human bones, intermediate joints and ligaments.
2. The actuator system by the electrical motor is used to generate forces and power the same as the function of muscles.
3. The sensory system adopts the transducer such as potentiometer and force sensor to measure the position, velocity and force. It is similar to the function of muscle spindles and Golgi tendon organ.

4. The control system is applied to the motor controller such as PID control and Fuzzy logic to control the movement of the robot like the function of central nervous system.

In the studies by Reinkensmeyer et al. (1992), they proposed that the tasks for patients to perform and design choices of a rehabilitation robot were:

1. Manipulations to apply to patient
2. Movement parameters to measure
3. Linkage geometry and strength
4. Number/type/size/location of actuators
5. Number/type/size/location of sensors
6. Means to physically couple to patient
7. Control scheme to implement desired manipulations
8. Sensor processing/fusion to derive key parameters
9. Feedback to give patient

Recently, many robotic devices have been designed for the motor relearning training of stroke rehabilitation. In this section, a review of the recent systems in robot assisted upper limb rehabilitation is given, including the robotic systems which have potential advantage for future applications in stroke rehabilitation.

1.3.1 Mirror-image movement enabler (MIME)

A research group in Stanford developed a robot system named mirror-image movement enabler (MIME) system that could assist or resist elbow and shoulder movements in three-dimensional space (Burgar et al., 2000; Lum et al., 1999) (Fig 1.4). They used a commercial mobile arm to apply forces and torques to the paretic forearm through one of the arm supports. A six-axis force/torque sensor measured the external forces applied to the limb, and the trajectories could be measured by the position encoders mounted at the pivot points of the mobile arm supports. Position and force data were sampled at 105 Hz. It had four kinds of motion mode: passive, active-assisted, active-resisted, and bimanual. The patient could use his/her unaffected arm to control the affected arm by a bimanual position feedback strategy. Motions of

the unaffected forearm commanded the mirror-image movement of the robot, thus moving the affected arm with the intended kinematics. Daily therapy with the MIME in 21 chronic, moderately affected, hemiparetic subjects showed a significant improvement in muscle strength when compared with traditional therapy. The Fugl-Meyer scale of elbow and shoulder of the robot group was higher than that of the control group (Burgar et al., 2000). Lum et al. (2004) also investigated the biomechanical change after rehabilitation training with MIME. Thirteen chronic stroke subjects were trained with MIME for 24 sessions in eight weeks. Improvement of the muscle activation mode was also observed, which was associated with the improvement of the kinematics after training.

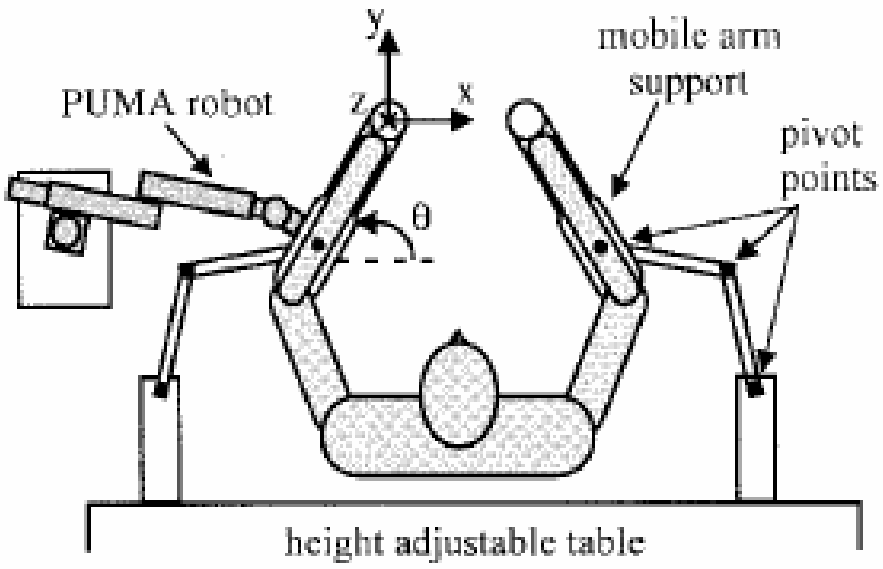

Fig. 1.4 Top view diagram of the MIME system (Burgar et al., 2000).

1.3.2 Assisted rehabilitation and measurement guide (ARM Guide)

The ARM Guide was a rehabilitation system developed at the Rehabilitation Institute of Chicago and the University of California Irvine (Reinkensmeyer et al., 1999; 2000; Kahn et al., 2001). It was designed for reaching training and evaluation of upper limb reaching function (Fig 1.5). The subject's forearm/hand was attached to a specially designed splint which could slide along the linear constraint. A DC servo-motor was connected to the linear constraint and could assist or resist the reaching movement depending on the control strategy. The orientation of the linear bearing could be

changed in two degrees: yaw(Y) and elevation (E). In these two DOFs, resistant torque could be applied by magnetic particle brakes. The position of hand could be measured by an optical encoder and the forces generated by the arm could be measured by a six-axis load cell mounted between the splint and the linear constraint. The subject could receive feedback about movement and force generation of the arm on a video monitor. The ARM Guide could provide a qualitative evaluation of several motor impairments including abnormal tone, incoordination and weakness. In addition, the system had been used as a therapeutic tool for rehabilitation training. Active assist exercises (three times a week for 2 months) on three chronic patients with ARM Guide resulted in a reduction of muscle tone in two patients. Active range of motion, peak velocity and the ability to initiate movement also improved (Reinkensmeyer et al., 2000).

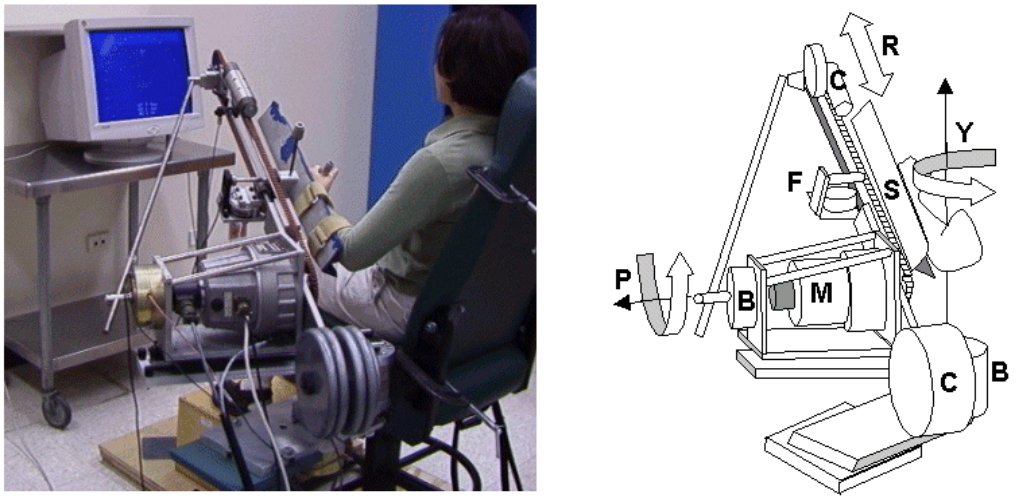

Fig. 1.5 Diagram of the ARM guide (Reinkensmeyer et al., 2000).

1.3.3 MIT-MANUS

MIT-MANUS was developed in the Massachusetts Institute of Technology for the neuro-rehabilitation of upper limb for patients after stroke (Fig. 1.6) (Hogan et al., 1992, Krebs et al., 1998). The key feature of MIT-MANUS was that the control system could react to mechanical perturbation from the manipulator to ensure a gentle compliant trajectory using impedance control shown as follows (Hogan et al., 1985; Krebs et al., 1998):

$$\tau = -J^T(q).[K_p \tilde{x} + K_D \dot{x}] \qquad (1.1)$$

where τ is the output torque, J(q) is the manipulator Jacobian, q is a vector of joint angles, $\tilde{x} = x - x_{desire}$ is a vector of displacement from a nominally desired position, K_p is the stiffness matrix, and K_D is the damping matrix.

Virtual reality techniques were applied to guide the person to perform an arm exercise shown on the screen. Another important characteristic of the MIT-MANUS was its low inertia, which could enable a patient to move it and perform motor relearning training easily. If movement was not finished by the patient, MIT-Manus could move the patient's arm. If the patient could move on his own, the robot provided adjustable levels of impedance (very soft, soft, medium, hard and very hard) depending on the need of the training. The MIT-MANUS could not only guide the arm but also give a resistive force to the movement of a subject's upper limb. The system recorded motions and mechanical quantities such as the position, velocity, and forces applied which were important for the analysis of the motion of the patients. This system had been tested on patients after stroke and the results showed a positive effect on reduction of impairment and improvement of motor performance of the exercised shoulder and elbow (Krebs et al., 1998; 1999; 2000; Volpe et al., 2000; Aisen et al., 1997).

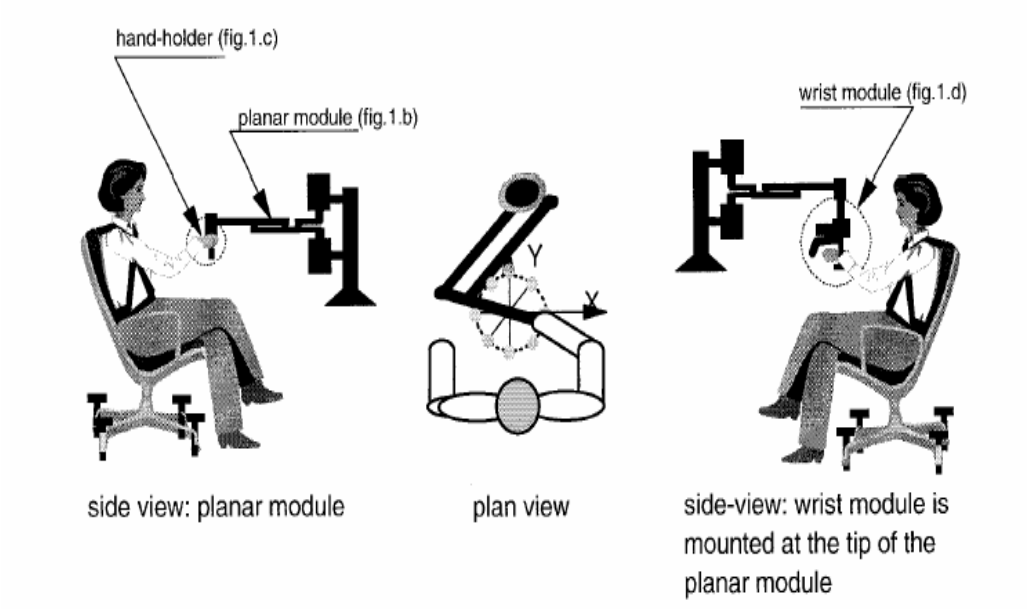

Fig. 1.6 MIT-MANUS: Assembly sketch (Krebs et al., 1998).

1.3.4 Bi-manu-tracking trainer

The bi-manu-tracking trainer was developed by Hesse et al. (2003), which followed the bilateral approach and enabled the bilateral passive and active practice of two movements: forearm pronation/ supination and wrist dorsiflexion and volarextension in a mirror-like or parallel fashion (Fig. 1.7). The amplitude, speed and resistance of both handles could be set at different levels. Daily therapy of 15 minutes with the arm trainer and 45 minutes with comprehensive rehabilitation program that included individual physiotherapy and occupational therapy on 12 chronic patients after stroke for 3 weeks resulted in a reduction on the modified Ashworth scale and there was no improvement in functional tasks.

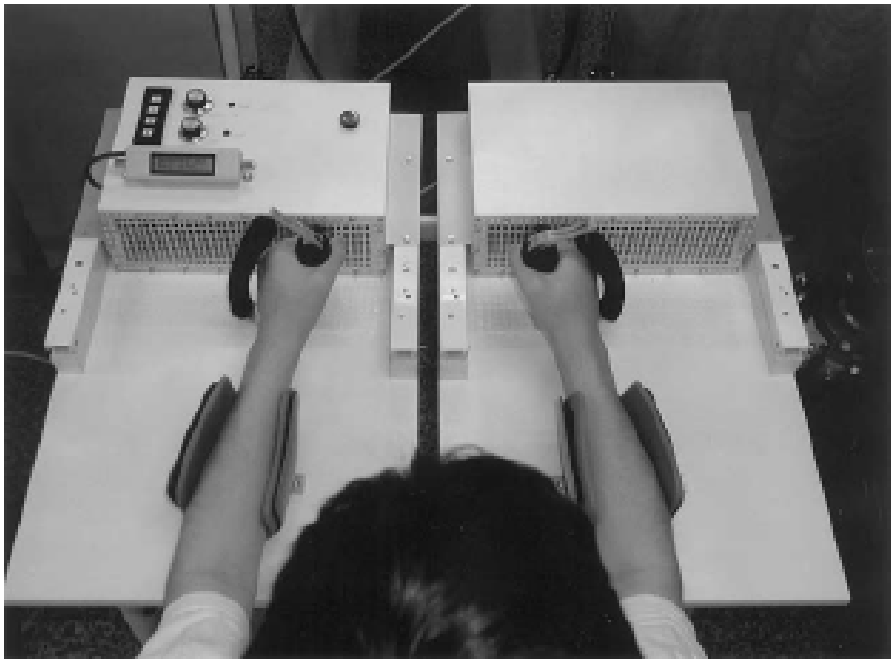

Fig. 1.7 Diagram of the bi-manu-tracking trainer. Patient with left hemiparesis practices a repetitive bilateral pronation and supination movement of the forearm (Hesse et al., 2003).

1.3.5 Colombo's robot

Colombo et al. (2005) also designed a one-DOF wrist manipulator and a two-DOF elbow-shoulder manipulator for rehabilitation of upper limb movements. They used admittance control to reduce the inertia and facilitate the movement. Fig. 1.8 shows

the block diagram of their functional principle. The control system included two control loops. The first is the position, velocity, and acceleration (P, V, A) control of the dc motor and the second is the admittance control. Two groups of chronic patients after stroke were involved in a three-week rehabilitation program including standard physical therapy (45 min daily) as well as treatment by means of robot devices for wrist and elbow-shoulder movements (40 min twice daily). Besides standard clinical assessment scales, they also designed a special task to quantify the patient's ability with the robot-measured parameters but without the robot assistance. After treatment, their motor deficit and disability were improved according to the clinical assessment scales and the robot measured parameters in both groups.

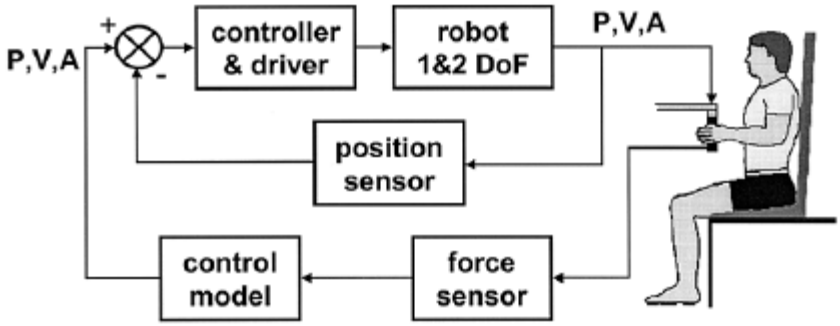

Fig. 1.8 Block diagram of the control system of the Colombo's rehabilitation devices.

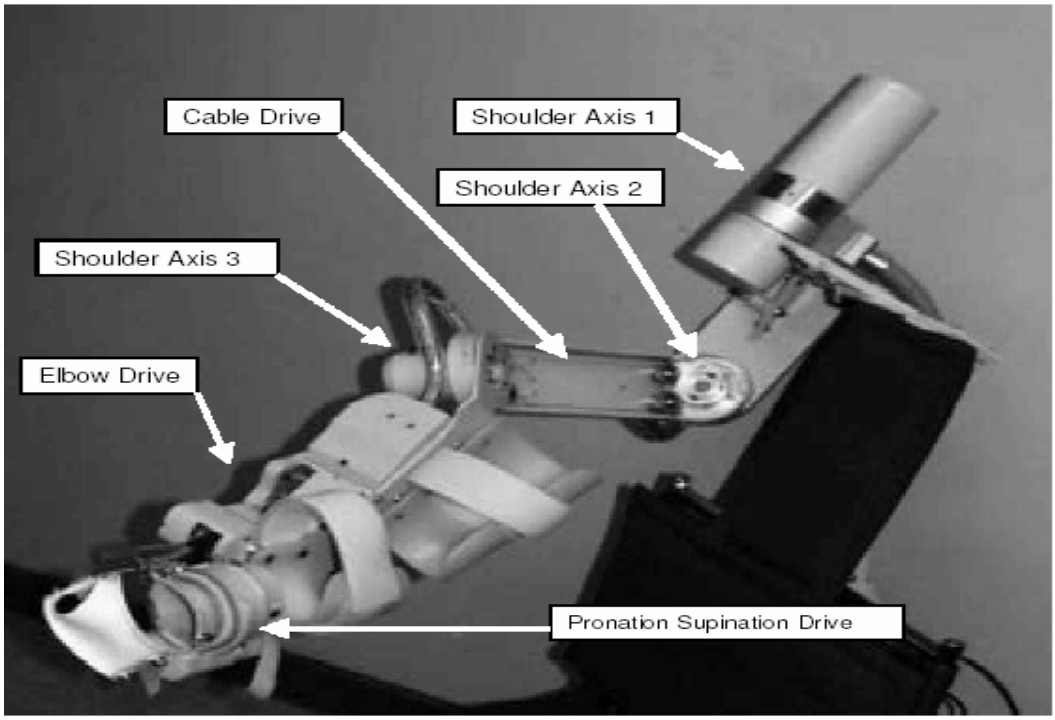

Fig. 1.9 Motorized upper-limb orthotic system. (Johnson et al. 2001)

1.3.6 Other robotic systems

Apart from the above robotic systems, there are also many robotic devices which can be used for rehabilitation treatment for different kinds of motion on the shoulder, elbow and wrist. However, their therapeutic effect has not been evaluated in the rehabilitation training on subjects after stroke.

The University of Newcastle developed a new motorized upper-limb orthotic system (MULOS) (Johnson et al., 2001). The system consisted of a five-DOF electrically powered upper-limb orthosis (three degrees in the shoulder and two degrees in the elbow) and was designed to assist people with disability to perform normal activities of daily life like normal people (Fig. 1.9). It could also work in continuous passive motion (CPM) designed for the therapy of the upper limb to enhance the range of motion. The advantage of this system was that it had multiple-DOF movements that could facilitate rehabilitation of multiple movements, including wrist, elbow and shoulder. The trajectory of the joints could be preprogrammed for a given number of cycles at a chosen speed.

Cozens (1999) developed a robot arm which had an axis aligned with the elbow and could help patients after stroke to perform elbow flexion and elbow extension in the horizontal plane (Fig. 1.10). They proposed an assist feedback control scheme which could detect spasticity from acceleration and provide a ramp torque in the movement if the acceleration was beyond the preset value. The assistive torque would be withdrawn once it reached 2 Nm or elbow movement exceeded a maximum speed (60 deg/s) in order not to transform the exercise into a passive mode. Although the assistive effect had been demonstrated in ten patients with weakness and spasticity, the therapeutic effect had not been reported.

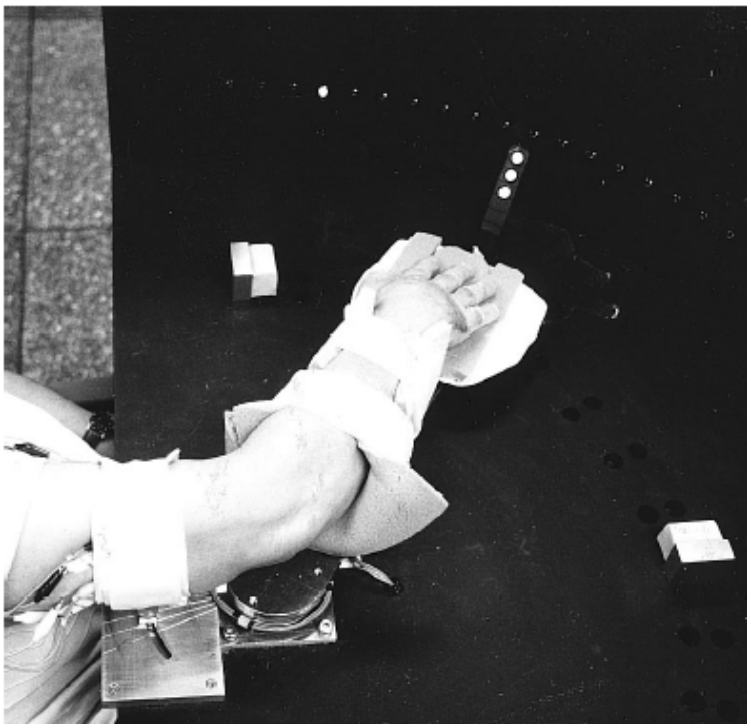

Fig. 1.10 Diagram of Cozens's robotic system (Cozens, 1999)

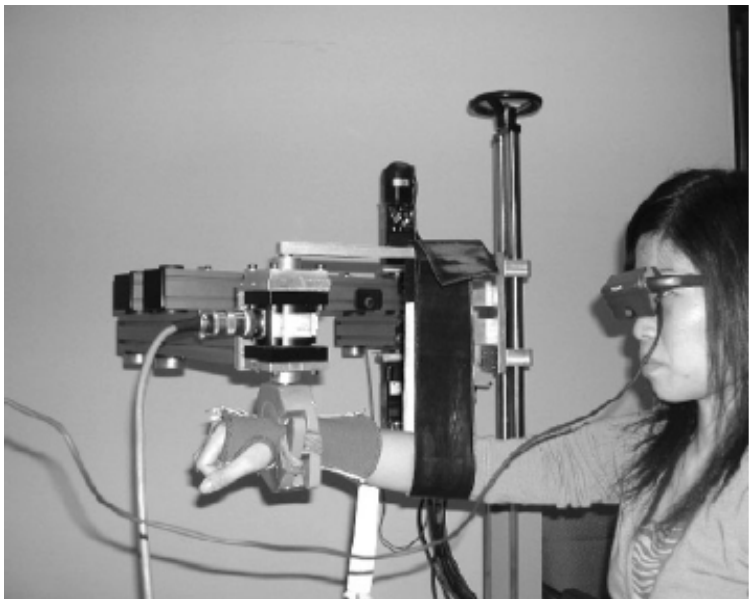

Fig. 1.11 Diagram of Ju's robotic system (Ju et al. 2005).

Ju et al. (2005) developed a rehabilitation robot with a force-position hybrid fuzzy controller, which could guide the patient's wrist to move along planned linear, circular and figure eight trajectories and maintain a constant force along the tangential direction of the movement (Fig. 1.11). The controller was stable in normal subject and further investigation was needed to explore the effect of the robot on the patient with spasticity.

ARMin was another rehabilitation robot developed at the Swiss Federal University of Technology (Riener et al., 2005; Nef et al., 2005). It had a semi-exoskeleton structure with six degrees of freedom which enabled the arm therapy related to activities of daily life. There were several torque sensors and four position sensors which enabled the robot to work in different kinds of control modes (position control, impedance control, admittance control). Fig. 1.12 showed its mechanical structure.

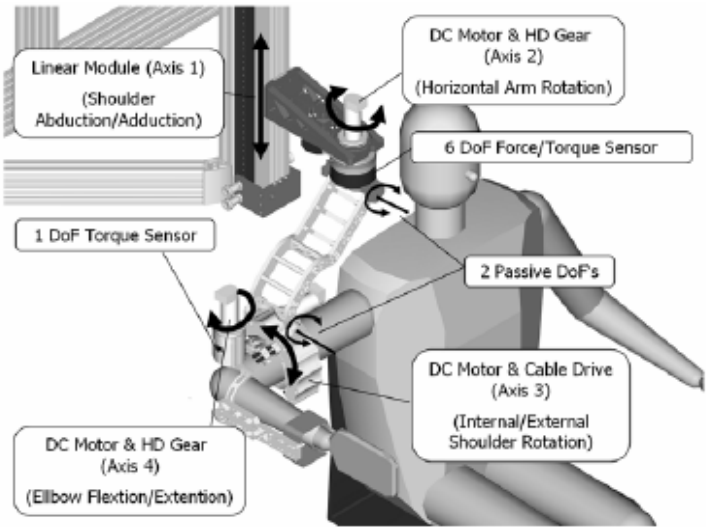

Fig. 1.12 Mechanical structure of the ARMin system (Nef et al., 2005).

Table 1.1 summarized the features of the above rehabilitation robotic systems.

Robot name	Active DOFs + (passive DOFs)	Number of patients that had used the system	Features/description	Advantages and disadvantages
Assisted Rehabilitation and Measurement (ARM) Guide (Reinkensmeyer et al., 1999; 2000; Kahn et al., 2001)	1+ (2)	Evaluation experiment: 4 Rehabilitation training: 3+7	Assistance in linear movements in horizontal plane and at varied degrees of elevation in vertical plane. Statically counterbalanced to eliminate gravitational load on arm.	Robot training is restricted to a linear path and, therefore, does not provide feedback assist to correct errors perpendicular to the movement trajectory. Can provide low impedance assistive therapy or resistive training.
Mirror Image Motion Enabler – MIME (Burgar et al., 2000; Lum et al., 1999; Lum et al., 2004)	6	Rehabilitation training: 13+21	Position controlled PUMA robot that provides passive, active-assisted, active-resisted and bimanual training in three-dimension space.	Less compliant to weak movement attempts during evaluation and treatment, thereby reducing its sensitivity as a measurement tool.

(Continued)

Robot name	Active DOFs + (passive DOFs)	Number of patients that had used the system	Features/description	Advantages and disadvantages
MIT-Manus (Krebs et al., 1998; 1999; 2000 Volpe et al., 2000; Aisen et al., 1997)	2	Rehabilitation training: >100	Low endpoint impedance Provides passive, active-assistive, active, and resistive training in horizontal plane.	Low intrinsic impedance enables precise measure of motor control and performance. Adaptive therapy algorithm automatically modifies assist provided by robot based on patient's motor abilities.
Bi-manu-tracking trainer (Hesse et al., 2003)	1	Rehabilitation training: 12	Position controlled robot that provides bilateral passive, active-assistance in two DOF	Bimanual mirror image training for wrist and elbow
Colombo's robotic systems (Colombo et al., 2005)	Wrist: 1 Shoulder and elbow: 2	Rehabilitation training: Wrist: 7 shoulder and elbow: 9	Admittance control which facilitates the patients to move it	Admittance control can reduce the inertia and the system can be used as measurement tool to evaluate the upper limb function with robot measured parameters.
MULOS (Johnson et al., 2001)	5	Unknown	Position controlled robot with five DOFs	Only continuous passive motion could be performed
Cozens's robot (Cozens 1999)	1	Assistive experiment: 10; Rehabilitation training: unknown	Assist feedback control scheme.	spasticity could be detected from acceleration and a ramp torque could be provided to help the elbow movement
Ju's robot (Ju et al. 2005)	2	Unknown	Force/position Hybrid fuzzy control	Linear and circular movements under predefined external force levels. A desired force could be applied a long the tangential direction of the movement. The trajectory is rigid.
ARMin (Riener et al., 2005; Nef et al., 2005)	4+(2)	Unknown	Semi-exoskeleton structure with six DOFs	A high number of DOFs allows a broad variety of movements related to activity of daily life. Impedance control and admittance control is under-developing

Table 1.1 Comparisons among rehabilitation robots for the upper limb. Active DOF: there is a motor to move the subject's arm actively in this DOF; passive DOF: no actuation is implemented in this DOF to move the subject's arm (Modified from Fasoli et al., 2004; Riener et al., 2005).

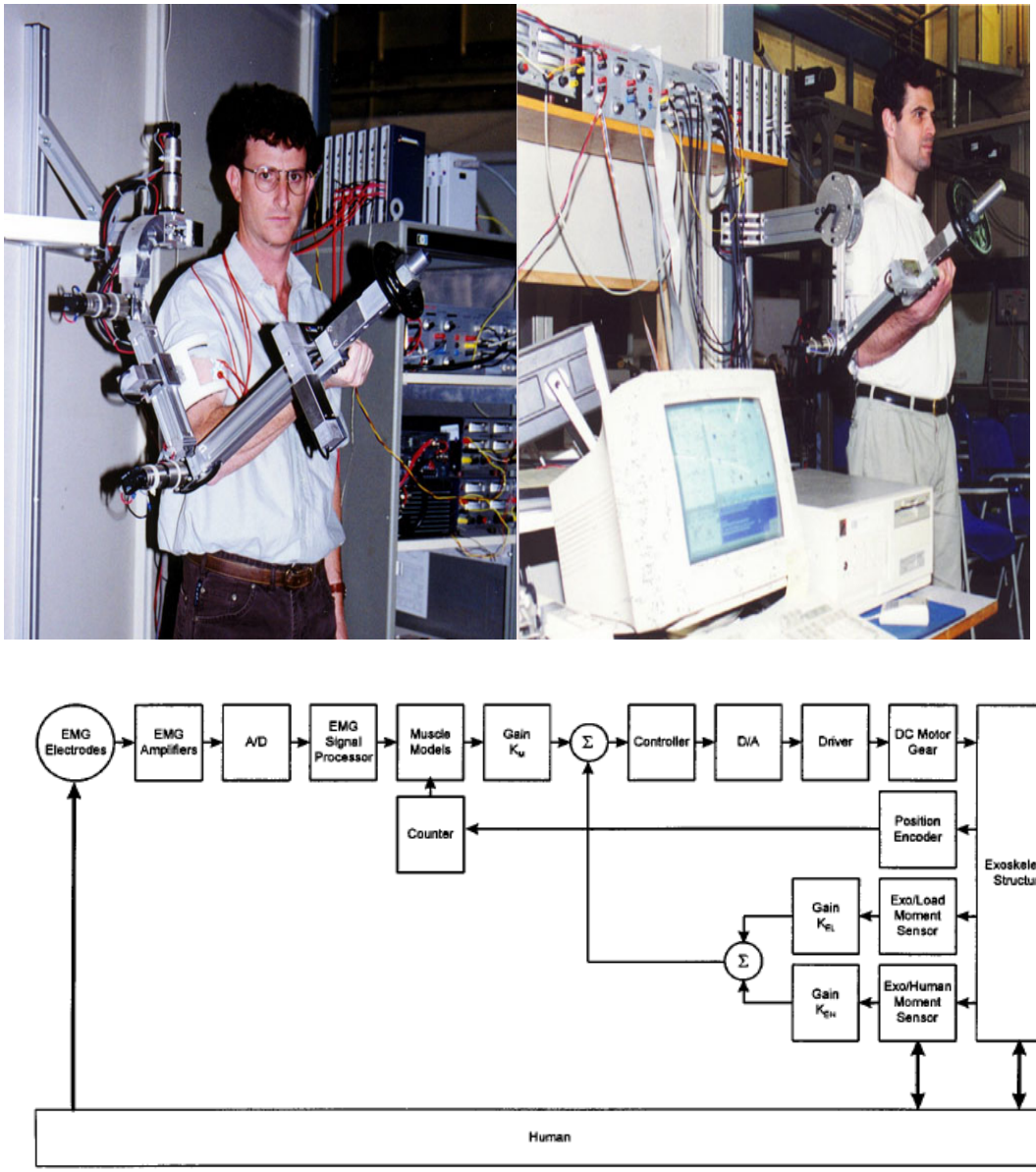

Fig. 1.13 Exoskeleton experimental systems-components and signal flow diagram (command signal gain-muscle model gain K_M, load moment gain-K_{EL}, and human-arm moment gain-K_{EH}) (Rosen et al., 2001).

1.3.7 Myoelectrically controlled exoskeleton

However, most of the rehabilitation robots only provided passive training on the affected arms of patients after stroke, or focused on a gentle compliant trajectory, following a specified task without any association with human intention. The robotic system which provided a highly accurate position control might generate excessive interaction forces when the subjects contradicted its pre-programmed trajectory.

In section 1.2.4, the rehabilitation devices with cognitive investment have been

applied in the FES systems. There are also many robotic devices that can assist the subjects to perform arm or leg movement with cognitive investment, although they are not directly used for rehabilitation treatment.

The exoskeleton system is a special robot system. The major difference between the exoskeleton system and other robot systems is that the exoskeleton robot is worn by the human operator as an orthotic device. Its joints and links correspond to those of the human joint. Many researchers have tried to integrate robots with human body in a more voluntary way which can be adopted in the rehabilitation process. An innovative exoskeleton system developed by Rosen et al. (2001), which had a human machine interface at the neuromuscular level, used EMG signals as the primary command signal to control the system. A Hill-type muscle model was built to estimate the muscle moment at the elbow joint. The moment estimated from the Hill-type model together with feedback moment measured at the human arm/exoskeleton and external load/exoskeleton interfaces made up of the control moment of the system (Fig. 1.13). Then the operator would feel a scaled-down version of the load and the remaining external load on the joint was carried by the exoskeleton. The system can be applied as a rehabilitation tool for automatic physiotherapy, which can help patients after stroke to move their affected arms with less effort with the assistance of the exoskeleton.

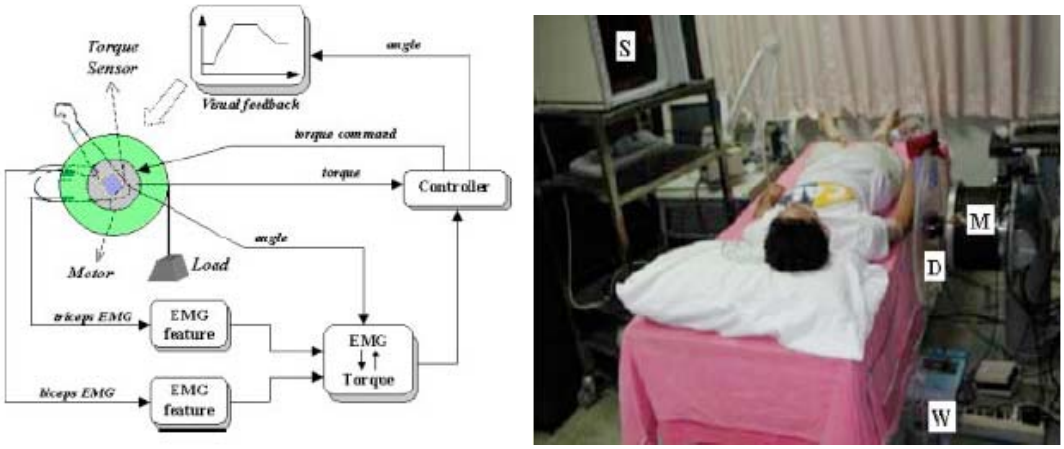

Fig. 1.14 Block diagram of the robotic system and the experimental setup (Cheng et al., 2003).

Cheng et al (2003) also reported an EMG-controlled robotic device which gave assisted torque for subjects after stroke to perform elbow tracking and reaching at vertical plane (Fig. 1.14). Processed EMG signals from biceps and triceps determined

the amplitude of the torque of the motor to apply through an adaptive filter. The system could assist the subjects to perform many tasks with less effort and no obvious deterioration of the movement performance was observed.

Lee et al developed a Hybrid assistive leg (HAL) to assist the motion of lower body by predicting the moment around joints with EMG signals. Fig. 1.10 showed the structure of how the system helped the subject to perform walking. Operator's intention can be detected from the EMG signals and the estimated torque around joint of the operator can be described as follows:

$$\tau_{virtual}(t) = K_f E_{fle}(t) - K_e E_{ext}(t) \tag{1.2}$$

where $\tau_{virtual}(t)$ is the estimated torque generated by the motor, K_f and K_e are the conversion factors from EMG to torque, and $E_{fle}(t)$ and $E_{ext}(t)$ are filtered EMG signal at flexor and extensor. In order to perform more effective assisting control of joint movement, the actuator can regulate the characteristics around its joints according to the motion. The lower thigh of the operator together with HAL system can be represented by an integrated pendulum model. The compensation torque generated by the actuator is determined as:

$$\tau_{com}(t) = (I - M)\frac{d^2\theta}{dt^2} + (D - B)\frac{d\theta}{dt} + K(\theta_0 - \theta) + C(\theta, \frac{d\theta}{dt}) \tag{1.3}$$

where I and D are the inertia and viscous coefficient around knee joint respectively, $C(\theta, \frac{d\theta}{dt})$ is a non-linear term including gravity and friction. M, B, K are the target values of inertia, viscous coefficient, elastic coefficient; θ_0 is the angle of joint in target posture.

Hence, virtual torque with impedance adjustment around knee joint was calculated as follows:

$$\tau_{sum} = \tau_{virtual} + \tau_{com} \tag{1.4}$$

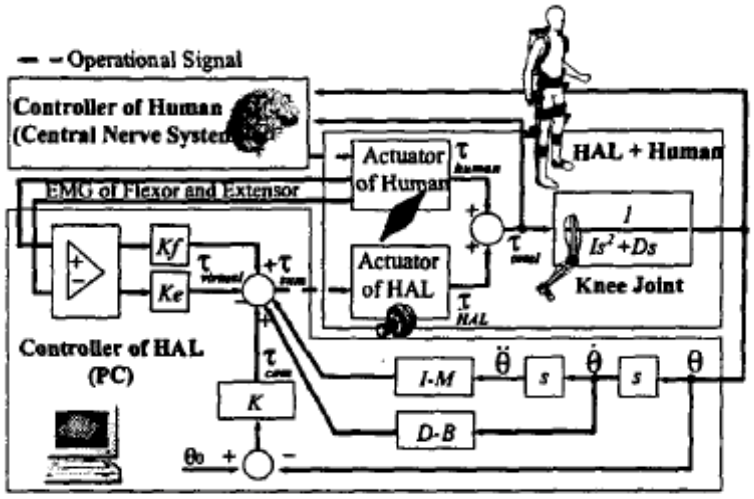

Fig. 1.15 Block diagram of virtual torque estimation and impedance adjustment around knee joint of HAL (Lee et al., 2002).

The systems in this part use the EMG signals as inputs to the control model. The design can help the subjects to perform the movement more easily or with a scale-down loading which is shared by the robot and without losing the natural control of the movement. The devices have potential applications for rehabilitation training and also give us some hints about the design of the rehabilitation robot system.

1.4 Musculoskeletal model

In order to treat the motion disorder of the subject after stroke, it is also important to know how the central nervous system (CNS) controls the muscle and conducts the movement. The control strategies employed by the CNS when controlling the limbs can be reflected from the responding EMG signals.

Fig. 1.16 shows the nervous system for the neuromusculoskeletal system and illustrates the control flow of voluntary movement. The control system for voluntary movement includes (Gonzalez et al., 2001):

1. Continuous flow of sensory information about the environment, position, and orientation of the body and limbs as well as the degree of contraction of the muscles.
2. Spinal cord
3. Descending systems of the brain stem

4. Pathways of the motor areas of the cerebral cortex

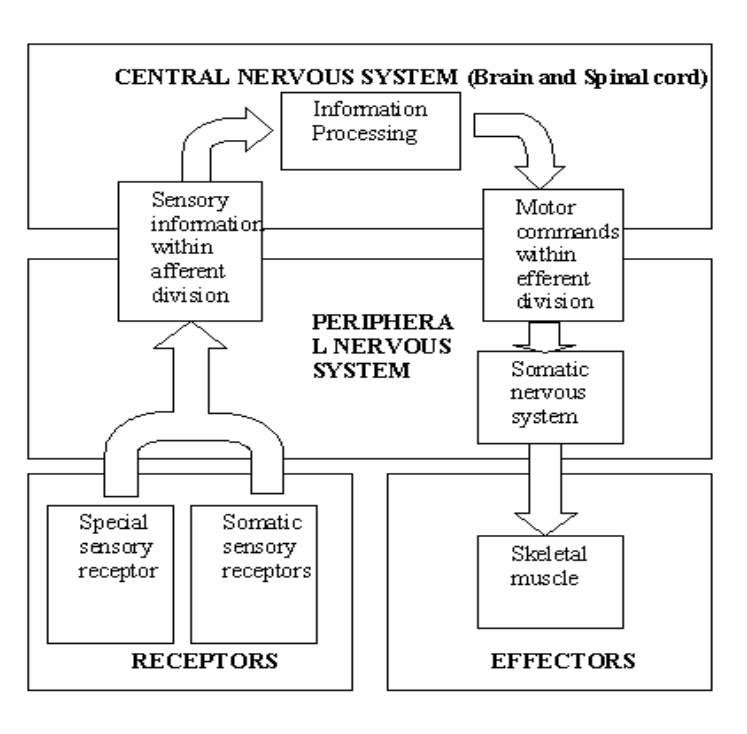

Fig. 1.16 Functional overview of the nervous system for the neuromusculoskeletal system (Martini, 1995)

Many researchers have investigated the relationship between the muscle activity and the EMG in neurophysiology and biomechanics. They used EMG signal to estimate force in a dynamic process. Misener et al. (1995) built a model to predict force production about the elbow using surface EMG signals. The model was for both static (isometric) and dynamic (constant velocity) concentric contractions about the elbow. Zhang used an adaptive filtering method to estimate the force on a cat's muscle (Zhang et al., 1997). Feng et al. (1999) built an EMG-driven musculoskeletal model to investigate the elbow flexion and extension. They also compared the results of the subjects without impairment and the subjects with spasticity. Among these models, the Hill-type model received wide acceptance to describe the muscle function during the movement.

1.4.1 Hill-type musculoskeletal model

Since Hill put forward the classical model about the muscle in 1938, the neurophysiology and biomechanics of neuromusculoskeletal systems have been investigated extensively to find the principles of human body movement generation

(Hill, 1938). Musculoskeletal models include how the CNS excites muscles, then subsequently develops forces and generates various movements. The muscle tendon model generates muscle force not only based on the muscle activation state but also based on musculotendon length and velocity, which are related to joint angle and angular velocity (Winters et al., 1988; Feng et al., 1999). Muscle force of previous state, which determines the tendon compliance, is also responsible for the muscle force at next stage (Zajac, 1989). Once all the muscle forces responsible for the joint movement are found, multiplying the muscle forces with respective muscle moment arms and summing the results can acquire joint torque. The mathematical integration of all the submodels can be used for describing how joint movements are generated from CNS command and what kinds of parameters are responsible for joint torque. EMG signals reflect the muscle activity, and EMG-force/torque relations have been studied in static and dynamic situations (Zhang et al., 1997; Misener et al., 1995). The EMG signals of the muscles are also often considered as the command signals of the CNS to drive the musculoskeletal system (Feng et al., 1999; Lloyd et al., 2003). Many models have been developed to explicitly and qualitatively describe the properties of the musculoskeletal system at different levels (Winters, 1990; Zajac et al., 1990). A generally accepted Hill-type neuromusculoskeletal system is composed of the following submodels step by step: muscle excitation contraction model, muscle tendon model, skeletal dynamic model (Zajac, 1989). Fig. 1.17 shows how the CNS system conducts a multi-joint lower limb movement based on the Hill-type model and how the movement affects the parameters of a muscle-tendon model.

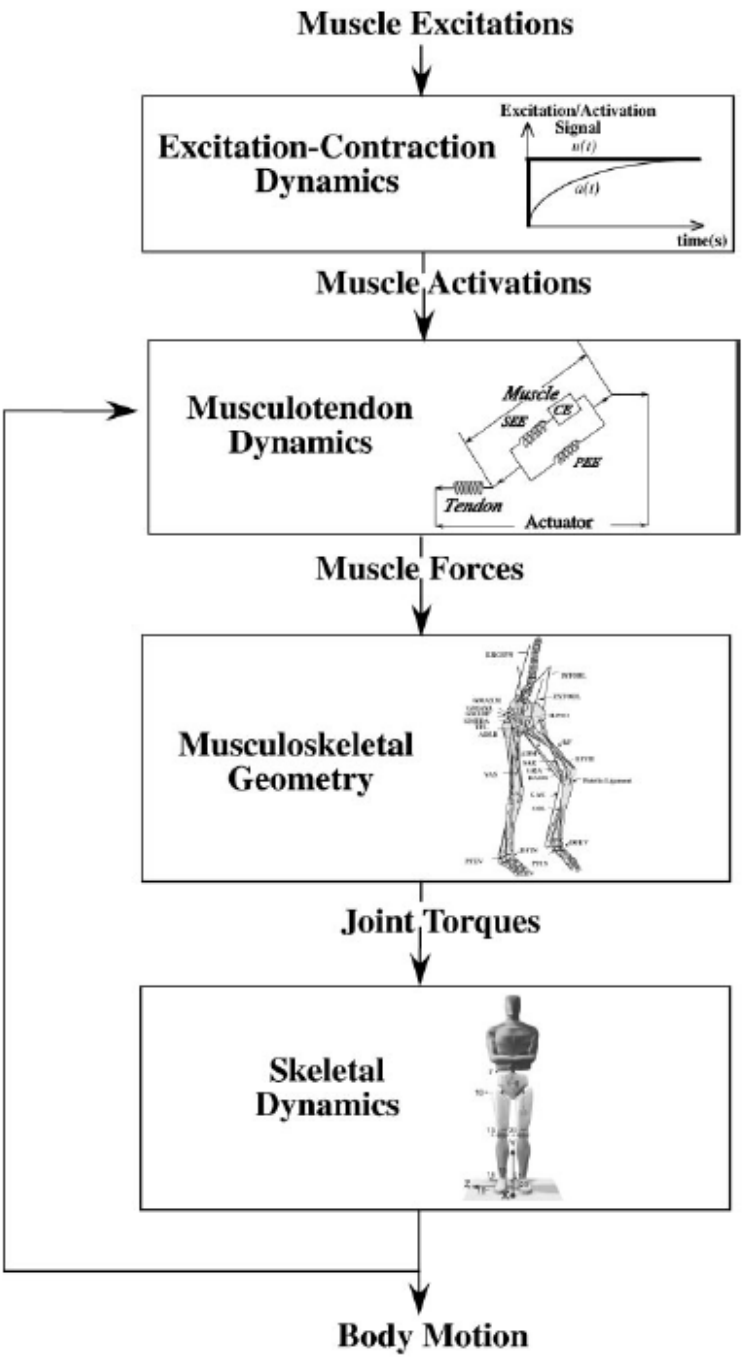

Fig 1.17 Diagram showing the components most commonly included in a multijoint model of movement. The insets show specific models of muscle excitation-contraction coupling, musculotendon actuation, muscle-path geometry, and the skeletons that were used to simulate jumping and walking (Pandy et al., 2001).

1.4.1.1 Muscle excitation contraction model

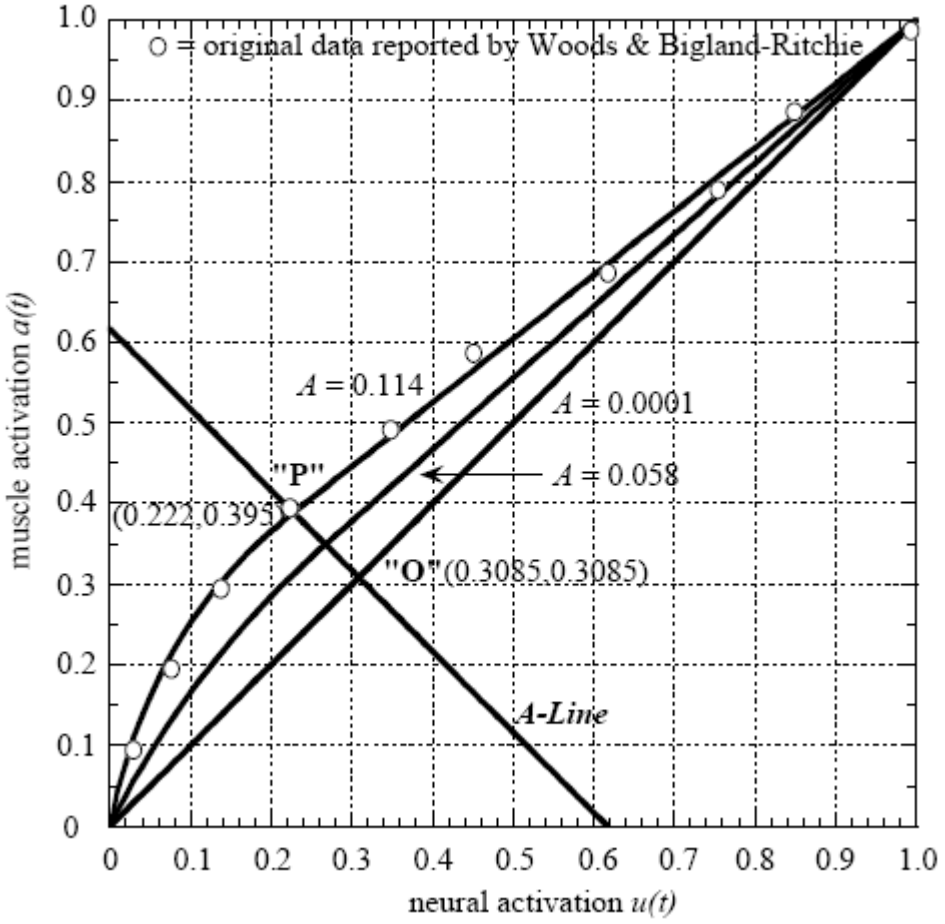

Fig. 1.18 Nonlinearization of neural activation, u(t), to muscle activation, a(t). The open circles represent data for the biceps reported by Woods and Bigland-Ritchie (1983). The path length from O to P (i.e., A) defines the degree of curvature. The piecewise curve for A=0.0001 approximates the line a =u: For A= 0.114; the resulting curve is very similar to the relationship reported by Woods and Bigland-Ritchie. (Manal et al., 2003)

From Fig. 1.18, a muscle excitation contraction model is used to estimate muscle active state based on CNS command. Since the EMG reflects the activity of muscle, the EMG signals that reflect the muscle activations, are often used as inputs to a musculoskeletal model. Conventionally, the band-pass filtered, rectified, and low-pass filtered EMG signals are directly used as muscle activations and inputted into the musculoskeletal model (Rosen et al. 1999). Hof and Berg (1981 a; b; c) developed an EMG-active state converter to process the normalized EMG signals to muscle activations. A nonlinear muscle excitation contraction model in some studies was also

used to estimate muscle activations (Lloyd et al., 2003; Manal et al., 2003): first, rectified, filtered and normalized EMG signal is transformed to neural activation $u(t)$ through a second-order recursive filter (Equation 1.5); then neural activation can be adjusted by a nonlinear relationship to muscle activation $a(t)$ (Equation 1.6).

$$u_j(t) = \beta_1 e(t-d) - \beta_2 u_j(t-1) - \beta_3 u_j(t-2), \tag{1.5}$$

$$a_j(t) = \frac{e^{Au_j(t)} - 1}{e^A - 1}, \tag{1.6}$$

where d is electromechanical delay, $\beta_1, \beta_2, \beta_3, A$ are activation parameters to change the EMG signal to the muscle activation. Fig. 1.18 shows the relationship between neural activation and muscle activation.

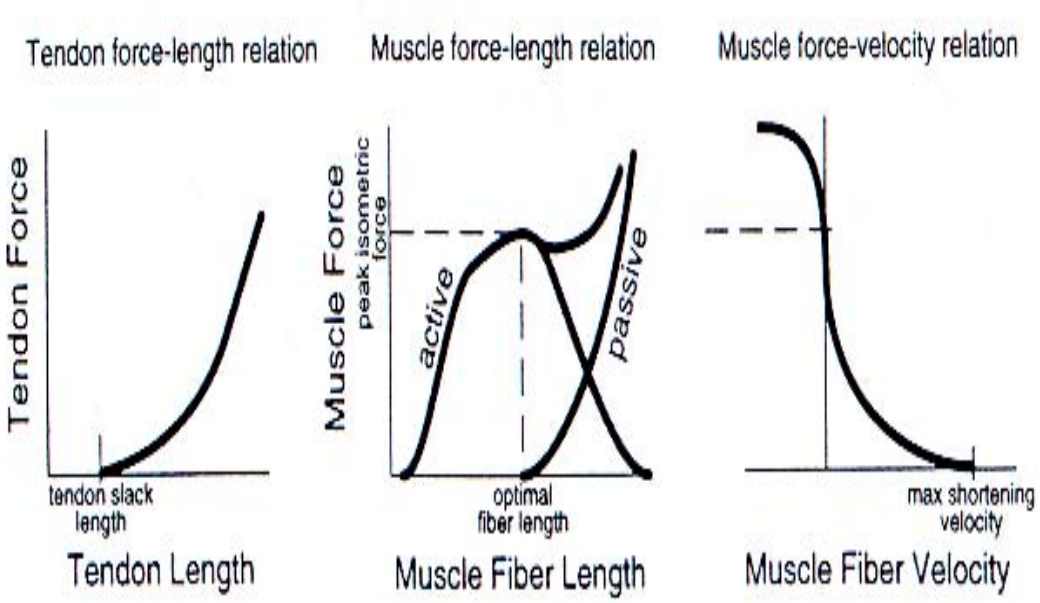

Fig. 1.19 (a) The force-length relationship of tendon (the left); (b) the active and passive force-length relationships of muscle (the middle); (c) the force-velocity relationship of muscle (the right). Tendon slack length is the length below which the tendon cannot exert any force. Optimal fibre length is the length where passive muscle force comes into play and active force component maximizes. Max shortening velocity is the velocity above which no active muscle force can exert (Delp et al., 1995).

1.4.1.2 Muscle tendon model

The Hill-type model describes muscle forces-generating properties, which can be represented by an active contractile element (CE) in parallel with a passive elastic element (PE) and then in series with tendon, a non-linear elastic element (Zajac, 1989; Komura et al., 2000). The force in the musculotenden unit is a function of these components.

$$F^{mt}(t) = F^{t} = F^{\max}[f(l_m) f(v_m) a(t) + f_p(l_m)]\cos\alpha \qquad (1.7)$$

where F_t is the tendon force, α is pennation angle, which is assumed to be constant during isometric contraction and is obtained from literature. $F^{\max}$ is the maximum isometric muscle force. $f(l), f(v)$ and $f_p(l)$ reflect the functions of the CE and PE element described in Fig. 1.19 (Delp et al., 1995).

1.4.1.3 Skeletal dynamic model

In the musculoskeletal modeling, accurate data on anatomical parameters such as muscle lengths (ML), moment arms (MA) are required to calculate muscle force and moment. The development of musculotendon force depends on both its length and its velocity and MA are needed when converting musculotendon force to moment about a joint. In order to decide the muscle lengths and movement arms, musculotendon path is needed, which defines the variations of muscle moment arms and musculotendon lengths across the joint range of motion (Winters and Stack, 1988). Murray et al. (2002) investigated how to scale the moment arm of elbow with upper extremity bone dimension. Pigeon et al. (1996) approximated MA/angle curves and ML/angle curves with polynomials from cadaver data. Moment arms were estimated using the tendon displacement method which involves computing the partial derivative of measured tendon displacement with respect to joint angle by An et al (An et al., 1984; Muarry et al., 1995; Heine et al 2003). The relationship can be shown in the following equation (1.8):

$$r(\theta) = \frac{\partial l^{mt}(\theta)}{\partial \theta} \qquad (1.8)$$

where θ is joint angle, $r(\theta)$ is the moment arm, and $l^{mt}(\theta)$ is musculotendon length. Delp et al. (1995) created a commercially available software package called SIMM

which could provide a generate framework that enabled users to develop, alter, and evaluate models of musculoskeletal structures.

1.4.2 Artificial neural network

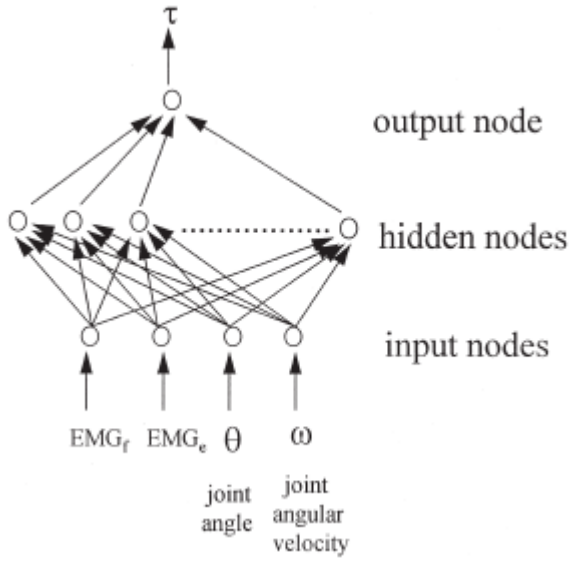

Fig. 1.20 The 3-layer ANN model to represent EMG-torque relations. EMG_f, EMG_e, θ, ω are the processed EMG from flexor and extensor, joint angle, and joint angular velocity, respectively (Luh et al., 1999).

Conventional methods (e.g. the Hill-type model) help to understand the inside physiological characteristics. However, these models made many assumptions on unknown nonlinear properties of the musculoskeletal and nervous system. Some subject-specific parameters of these models also cannot be measured directly. Optimization methods were often needed to estimate these parameters (Lloyd et al., 2003; Manal et al., 2002; Koo et al., 2005). The accuracy of the parameters and submodels limited the prediction accuracy. In recent years, artificial neural network (ANN) was often used to integrate the muscle activation dynamics model, muscle contraction dynamics model and muscle geometry model to estimate the kinematic EMG-force or EMG-torque relationship (Fig. 1.20) (Luh et al., 1999; Koike et al., 1995; Wang et al., 2000; Liu et al., 1999; Cheron et al., 1996). The ANN model could optimise its internal network to build the relationship between inputs and outputs parameters using a back propagation algorithm to learn all the training data. A back-

propagation through time ANN was proposed by Dipietro et al. (2003) to map the EMG signals of five selected muscles on arm kinematics of subjects performing three-dimensional unrestrained grasping movements. Rosen et al., compared the performance of Hill-type and neural network muscle models in terms of predicting the torque of elbow joint complex based on joint kinematics and neuromuscular activity during single-joint movements (Rosen et al., 1999). A time-delayed ANN was used by Au and Kirsch to predict the shoulder and elbow motions from the EMG signals in able-bodied and spinal cord injured subjects (Au et al., 2000). Wang et al. (2002) developed a three-layer feed-forward Neural Network model of muscle activations from EMG signals to predict joint torques. The success of these models indicates that ANN model is a promising technique to simulate the musculoskeletal model.

1.5 Evaluation of deficits after stroke

The damage in brain caused by stroke (motor cortex and neural pathways) often affects voluntary control. Impairments such as spasticity (Katz and Rymer, 1989; Ju et al., 2000), muscle weakness (Canning et al., 1999; Lum et al., 2004), increased reaction time (Chae et al., 2002b), cocontraction (Chae et al., 2002a; Kamper et al., 2001; Dewald et al., 1995; Hammond et al., 1988), contracture (Pandyan et al., 2003, O' Dwyer et al., 1996) and disordered movement organization (Takahashi et al., 2003) create deficits in motor control for patients after stroke.

In order to find better treatment strategies, it is necessary to evaluate the functional improvement in the upper limb during the rehabilitation training for subjects after stroke. The effectiveness of the device or the treatment strategy could be judged by the evaluations before and after the treatment. In this section, the impairment after stroke will be evaluated in the following four aspects: clinical scales, mechanical properties, kinematics and muscle activities.

1.5.1 Clinical scales

Clinical scales can be used as tools to evaluate patients after stroke, which are efficient, easy-to-use and economical. Based on the assessment goals, there are different kinds of clinical scales that focus on the stroke disabilities.

The two widely used scales for the measurements of disability/activities of daily living are the Barthel Index (Wade et al., 1988) and functional Independence Measure

(Keith et al., 1987). They are proposed as the standard index for clinical and research purposes.

In order to evaluate the mobility, the Rivermead Motor Assessment Gross Function scale was given by Lincoln et al. (1979). The Rivermead Mobility Index (RMI) was developed to document change in 15 items of functional ability by Collen et al. (1991). Lennon and Johnson (2000) proposed the modified RMI with eight items by using a six-point scoring system, which enhanced its sensitivity.

The Ashworth scale is a widely applied clinical tool for muscle tone assessment. The original Ashworth scale was a five-point ordinal scale for grading the resistance encountered during a passive movement of a limb through the range of motion to passively stretch specific muscle groups (Ashworth, 1964), and the modified Ashworth scale was extended with an additional grade to the original one to improve the sensitivity (Bohannon et al., 1986).

Another three clinical scales are often used for assessing motor function in patients with stroke: the Fugl-Meyer scale, the motor status scale (MSS) and the motor assessment scale (MAS). A full evaluation of Fugl-Meyer scale includes five different parts: (1) motor function of the upper extremity, (2) motor function of the lower extremity, (3) balance, (4) sensation, and (5) joint motion and joint pain. Each part can be used independently (Fugl-Meyer, et al., 1975; Trombly et al., 2002). The motor status scale (MSS) measures shoulder, elbow (maximum score = 40), wrist, hand and finger movements (maximum score = 42), and expands the measurement of upper extremity impairment and disability provided by the Fugl-Meyer score. The MSS is closely related to the FM and evaluates the complete range of motor functions of upper limb (Ferraro et al., 2002). The motor assessment scale (MAS) is another scale for measuring motor function (Poole et al., 1988). The MAS registers eight functional activities: turning in bed, sitting, standing up, walking, balance in sitting, activities of the upper arm, the wrist and the hand. Each item is scaled from 0 to 6 and the overall scores range between 0 and 48 (normal function).

The clinical scales provide semi-quantitative information, which lack temporal and inter-examiner reproducibility and suffer from a clustering effect in which patient scores tend to be graded in the middle range (Rymer et al., 1994). More quantitative methods might help to increase the scope and resolution of the functional impairment

after stroke, which is important to identify the characteristics related to stroke and to evaluate the effect of the treatment and to comprehend the mechanism that causes the change.

1.5.2 Evaluation of spasticity and joint mechanical properties

Spasticity is a motor disorder commonly observed in patients after cerebral palsy, brain injuries, spinal cord injuries, multiple sclerosis, and stroke. It is characterized by a velocity-dependent increase in tonic stretch reflexes with exaggerated tendon jerks (Lance, 1980). Spasticity can be caused by some types of damage to the nerve pathways that regulate muscles. Subjects with spasticity are often observed to have an increase in resistance to passive movement which interferes with the motor functions (Katz and Rymer, 1989). According to the concept of mechanical impedance, the internal characteristics of a musculo-articular system are expressed by inertial, elastic and viscous parameters (Winters et al., 1988), and it can therefore be hypothesized that inherent muscle and joint properties are modified by alterations induced by stroke or by immobilization after stroke. Quantitative measurements of these parameters are necessary and a great contribution to clinical rehabilitation evaluation and management.

Numerous biomechanical methods have been applied to obtain quantitative mechanical information about a muscle's stretch reflex. Three types of stretching methods are frequently used to measure the stretch reflex: the constant velocity stretch (Ju et al., 2000; Given et al., 1995; Mccrea et al., 2003; Schmit et al., 1999), the sinusoidal excitation (Cornu et al., 2001; Yeh et al., 2004) and the pendulum test (Feng et al., 1998; He et al., 1997; Lin et al., 1991; Lin et al., 2003).

Normally, constant velocity stretch is conducted when a relaxed joint is stretched at a constant angular velocity over a predetermined angular displacement and spastic hypertonia is quantified by the resistive torque generated by the stretched muscle. An on-line spasticity measurement system was designed by Ju et al. (2000), to measure the spasticity index and an appropriate verification process was applied to ensure the data validity. Pisano investigated a quantitative evaluation of muscle tone in patients after stroke with constant velocity stretch; they built a model and found the correlation of the biomechanical indices with conventional clinical scales and the neurophysiological measures (Pisano et al., 2000). Schmit et al. (1999) modeled the

reflex torque response of the spastic elbow flexors during constant velocity stretch with a simple musculoskeletal model, which was composed of the physiological cross-section areas, the moment arms, and the activation functions of biceps and brachioradialis.

Pendulum tests are often applied to investigate the characteristics of lower limb. He et al. (1997) combined a neuromuscular dynamic model with stretch reflex loop, based on the pendulum test of spasticity, to study the effect of specific parameters (stretch reflex gains, stretch reflex threshold, and muscle mechanical properties) to the knee trajectory. Lin et al. (2003) developed a comfortable device to facilitate the pendulum test on the upper limb; and a linear stiffness-damping model was also applied to quantify the parameters using optimization techniques. They found a significant larger damping coefficient and damping ratio of affected arms in comparison with those of unaffected arms and normal subjects.

Another widely used approach to measure the characteristics of limb is sinusoidal stretch, which is the response of a motor-driven sinusoidal displacement over a range of frequencies. Yeh et al. (2004) added the Sinusoidal perturbations (1–15 Hz, ± 3 deg, peak-to-peak harmonic angular displacement) to quantify the immediate effect of prolonged muscle stretch on the inhibition of ankle hypertonia in patients after stroke. After 30 minutes prolonged muscle stretch treatment, there was a significant decrease in elasticity and viscosity of the hypertonic muscles in subjects after stroke.

Investigations of intrinsic and reflex contribution of the mechanical properties of joint have also been conducted. Mechanical changes underlying spastic hypertonia were explored using a parallel cascade system identification technique to evaluate the relative contributions of intrinsic and reflex mechanisms to dynamic ankle stiffness in healthy subjects (controls) and spastic, spinal cord injured patients (Mirbagheri et al., 2000; 2001). Zhang et al. (1997) developed a nonlinear, time-delay, continuous-time, and dynamic model to identify intrinsic and reflex mechanical properties of the human elbow joint.

1.5.3 Kinematic analysis

Kinematic analysis of subjects after stroke was also an important tool to evaluate the motor disorder during voluntary movement. A number of invariant features of single-joint movements have been observed from the trajectories. The plan of movements

appears to be independent of the subjects, in which limb has symmetric, bell-shaped velocity profiles in single-joint movements.

Hogan (1984) proposed a principle underlying the selection of a movement trajectory by the CNS. The movement with maximum smoothness is most likely to be selected among all possible trajectories. Mathematically, minimization of the integral of mean squared jerk (the third time derivative of displacement) was used to describe the characteristic. Wiegner et al. (1985) investigated a seventh-order polynomial minimum-snap model which was an extension of the five order minimum-jerk model and was consistent with the physiological range of the rate of change of the torque. Mescheriakov et al. (1995) also proposed that the acceleration-time profile of the movement can be described by a linear combination of two Gaussian functions (positive for acceleration and negative for deceleration). Feng et al. (1997) investigated the spastic elbow movement in three-dimensional (3D) space. A significant increase in average jerk cost of spastic elbow was found in their research. Ju et al. (2002) also compared the integration of square jerk (ISJ) between normal subjects and subjects after stroke and they found that the ISJ of the affected arm was larger than that of unaffected arm and also larger than that of normal subjects. The above results showed the change of trajectory planning for subjects after stroke.

In 1954, the Information theory was employed to explain the human motor system by Fitts et al. (1954), who mathematically integrated speed, accuracy, amplitude of the movements and target size into a one-dimensional parameter to evaluate upper extremity tasks (equation 1.9 and 1.10):

$$I_d = -\log_2(W/2A) \tag{1.9}$$

$$I_p = -\frac{1}{t_m}\log_2(W/2A) \tag{1.10}$$

where A is the movement amplitude, W is the target width, and t_m is the target-to-target movement time. In addition, Yang et al. also applied Fitts' law to evaluate the upper limb target-reaching movements in 3-D dimension (Yang et al., 2002).

Haaland et al. (1988) used Fitts' law to investigate the effect of task complexity on movement ipsilateral to lesion in twenty controls and ten left hemisphere and nine right hemisphere patients after stroke; the left hemisphere group showed significant deficits found in wide target condition based on the Fitts' law indices.

McCrea et al. (2005) studied the stroke-induced changes to motor control of the affected arms of subjects after stroke. The study quantified the capacity of CNS transmitting motor commands by a linear relationship between movement time and task difficulty (Fitts' law) during a reaching task. They compared the affected arm of 20 persons after stroke with the non-dominant arm of ten healthy persons and found that there were significantly increases of Fitt's slope and intercept in the more affected arms of the group with strokes. Indirect, segmented, and positively skewed movement was found in the group with stroke, which could result in greater neuromotor noise.

A 3-D biomechanical model of the upper extremity was developed by Van Bogart et al. (2001) to provide a comprehensive method of assessing upper limb motion during performing tasks including exercises in reaching, grasping and releasing in patient after stroke.

However, these studies focused on motor execution and ignored sensory function, which was also an important source for the central nervous system to correct the movement. Trajectory-tracking was a useful tool to evaluate sensorimotor control function of upper limbs which couples both perception-action and motor execution. Furthermore, the trajectory-tracking provided a standard reference for the neuromusculoskeletal system to follow and to be corrected by the feedback across different subjects. Patten et al. (2001) evaluated the perceptual motor control in hemiparetic adults with an upper limb trajectory tracking task. In their study, subjects performed an elbow flexion-extension task against a low-resistance isotonic load at three speeds: 25, 45 and 65 deg/s from 10 deg extension to 75 deg flexion. They found a larger root mean square error (RMSE) between elbow trajectory and target from affected arms than that of unaffected arms and normal subjects. Ju et al 2001 also investigated the effect of external torque on the performance of tracking in normal people and patients after stroke; only elbow extension was studied and the characteristics of elbow flexion were not considered in their study.

1.5.4 EMG analysis

1.5.4.1 Introduction of electromyography

EMG is an electrical signal from a contracting muscle which reflects the neuromuscular activation (Basmajian et al., 1985). It is a very complicated signal,

which is comprised of many kinds of information: the activity of muscle, the activity of the descending upper motoneurons and the afferent activity emanating from a number of peripheral sensors. It can be affected by the anatomical and physiological properties of muscles, as well as the characteristics of the instrumentation and electrodes that are used to detect the signals. During voluntary contraction, a neural action potential propagating down a motoneuron activates all the muscle fibers that belong to the same motor unit. Each firing of the motoneuron triggers a depolarization of the muscle membrane at the neuromuscular junction, which causes a muscle fiber action potential that travels in both directions along the muscle fiber. These muscle fiber action potentials are referred as a motor unit action potential (MUAP), and EMG can be regarded as accumulation of a series of active MUAP trains detected by the electrode pair during muscle contraction. Since human motion is comprised of series of muscle contractions and EMG signals are the byproducts of the corresponding muscle contractions, EMG signals can reflect human's intention about the movement. Many models have been developed to find the relation between muscle contraction and force.

1.5.4.2 Relationship between EMG and force

EMG provides easy access to the physiological processes that cause the muscle to generate force and corresponding movement. However, the relationship between EMG and force / movement trajectory is complicated and affected by many features. Carlo analyzed the quantitative relationship between EMG amplitude and the muscle force of some muscles in isometric contraction (Fig. 1.21) (Carlo et al., 1995). It is generally agreed that when the EMG signal is sufficiently smoothed, the relationship is linear, but the linearity is different among different muscles.

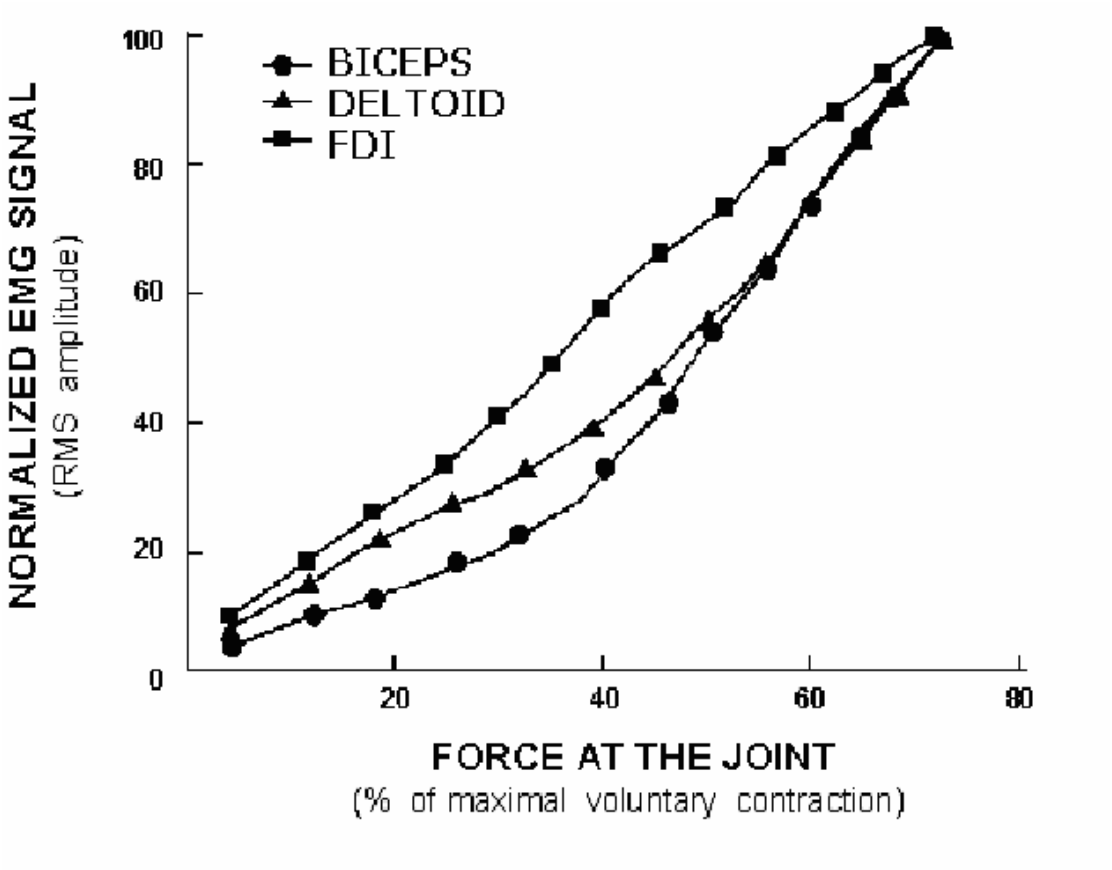

Fig. 1.21 Normalized EMG/Force signal relationship for biceps, deltoid and First Dorsal Interosseus (FDI). The data have been greatly smoothed, with a window width of 2 s (Carlo et al., 1995).

1.5.4.3 EMG analysis on patients after stroke

EMG and kinetic measures have been used as the primary tools in the study of movement, which provide an electrophysiological view of movement. The methods are also used to analyze the motion disorder after stroke.

Canning et al. (2000) investigated the abnormalities of muscle activation with low dexterity after stroke. They found excessive biceps muscle activation and decreased coupling of muscle activation to target motion. Weakness, slowness of muscle activation, excessive co-contraction, and spasticity can cause the abnormalities after stroke.

Chae et al. (2002a) recorded EMG activity of the paretic and nonparetic wrist flexors and extensors from 26 chronic stroke survivors during isometric wrist flexion and extension in order to find the relationship between poststroke upper limb muscle weakness, cocontraction**,** and clinical measures of upper limb motor impairment and

physical disability. In their research, they found that the strength of muscle contraction was significantly greater in the nonparetic limb; the degree of cocontraction was significantly greater in the paretic limb; muscle weakness and degree of cocontraction correlate significantly with motor impairment and physical disability in upper limb hemiplegia. They also found that delay in initiation and termination of muscle contraction was significantly prolonged in the paretic arm and the delay did not have significant correlation with motor impairment and physical disability (Chae et al., 2002b). Dickstein et al. (2004) found that EMG activity of rectus abdominis was significantly delayed in comparison to that of external oblique relative to the unaffected side in the patients and relative to the control subjects during voluntary trunk flexion.

Since functional connection between the motor cortex and muscle can be measured by electroencephalogram-electromyogram (EEG-EMG) coherence, Mima et al. (2001) used EEG and EMG of the hand, forearm, and biceps muscles to conduct three contraction tasks: (1) elbow flexion, (2) wrist extension, and (3) power grip on 6 patients with chronic subcortical stroke to evaluate the cortical control of EMG. They found that EEG-EMG coherence was localized over the contralateral sensorimotor area in all circumstances, and there was no significant coherence at the ipsilateral side. EEG-EMG coherence was significantly smaller on the affected side for the hand and forearm muscles but not for the biceps muscle.

1.6 Objectives of this study

We have reviewed the literatures about the mechanism underlying the neuro-rehabilitation, the current rehabilitation devices and approaches for stroke rehabilitation and function evaluations. From the previous studies, robotic systems have been widely applied for the neuro-rehabilitation to restore upper limb functions for subjects after stroke in this decade. The myoelectrically controlled robotic system has been developed since 2001 (Rosen et al., 2001; Cheng et al., 2003). However, Rosen et al. (2001) only applied the robotic system on normal subject to share the loading rather than on subjects after stroke. Cheng et al. (2003) had applied his system to provide the assistive torque for subjects after stroke. Although their system could improve the elbow torque capability of normal and stroke subject. It has not been reported that if such kind of device could help subject after stroke to improve range of

motion, and if such kind of device could be applied into robot-aided therapy in their studies. In order to find an effective way of robot-aided neuro-rehabilitation, myoelectrically controlled robotic system was investigated in this study, which might have the following advantages:

1. Continuous intention involvement into the physical exercise might assist to restore the damaged efferent motor output induced by stroke.
2. Using EMG signal to control the output torque might allow a natural control of the movement since EMG signal can be correlated to the torque developed by the muscles with respect to a joint.
3. It might allow seriously-affected subjects to perform voluntary movement with the robot's assistance; such patients might not generate movement to some directions but still retain measurable residue surface EMG signals from the affected muscles.

We hypothesized that this kind of robotic system might be beneficial to restore the upper limb function for subjects after stroke in a training program. The specific objectives of this study are described as follows:

1. To develop a robotic system including hardware and software for persons after stroke to perform rehabilitation training at the elbow joint
2. To develop a control strategy for the robotic system based on the EMG signals of the affected arm
3. To evaluate the feasibility and effectiveness of the robotic system in the rehabilitation training
4. To quantitatively evaluate the elbow control function in dynamic situations for subjects after stroke

CHAPTER 2 METHODS

2.1 Introduction

Robotic systems can be applied to restore the upper limb function for subjects after stroke, which has been supported by many researches (Colombo et al., 2005; Hesse et al., 2003; Hogan, et al., 1992; Reinkensmeyer et al., 1999; Lum et al., 1999). This study focused on designing an innovative rehabilitation robot which would be controlled by electromyographic (EMG) signals from the affected muscles to perform active rehabilitation training at the elbow joint. In order to realize this, several tasks were done. Firstly, the robotic system was designed and fabricated; its structure was introduced in section 2.2. Secondly, in order to use EMG signals to control the robotic system and to find a suitable control strategy for subjects after stroke, two control strategies were investigated for the robotic system: the recurrent artificial neural network (RANN) model and proportional control. A recurrent artificial neural network (RANN) model was developed and compared with the proportional control strategy. The recurrent artificial neural network was built and evaluated using the data from six subjects without impairment and three subjects after stroke, and the experimental setup was introduced in section 2.3. The proportional control with different combinations of the resistive load and EMG-torque gain was also investigated in an arm tracking experiment (elbow extension) on the affected arms of nine subjects after stroke in section 2.3. Thirdly, a quantitative method to monitor the elbow control function was developed. A sinusoidal arm tracking experiment and the evaluation parameters were described in section 2.4 to investigate the elbow control function of the affected and the unaffected arm in dynamic situations. Finally, a four-week rehabilitation training program was designed in section 2.5 to investigate the long-term training effect of the myoelectrically controlled robotic system in restoring the upper limb function of the subjects after stroke. Different kinds of evaluation methods to monitor the functional improvement in the affected arm of the subjects after stroke after the four-week rehabilitation training were also introduced in section 2.5. Fig. 2.1 shows the structure of the whole study.

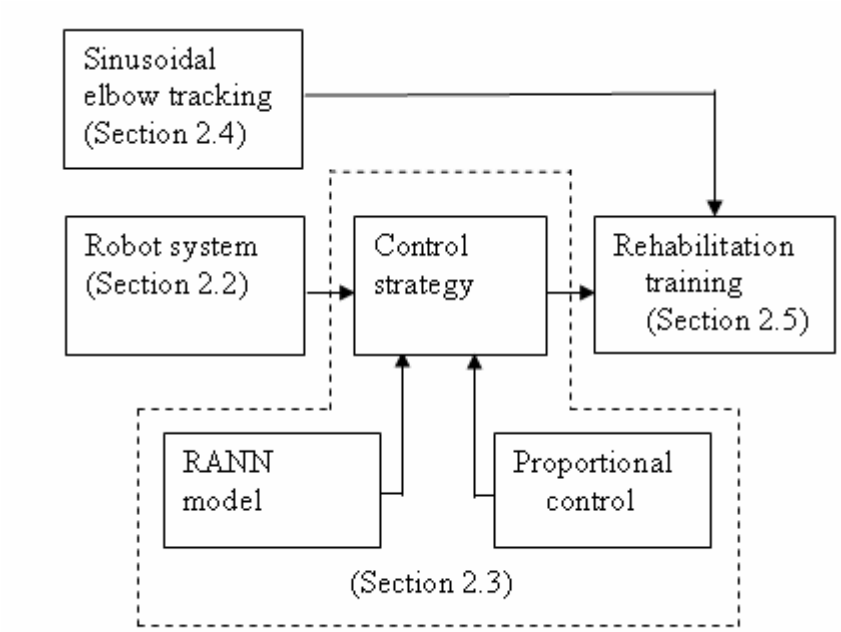

Fig. 2.1 Structure of this study

2.2 Robotic system

Different types of robotic devices had been introduced in section 1.3. The main objective of this part was to develop a robotic system controlled by EMG signals, which could be applied in the rehabilitation training for subjects after stroke. EMG signal was selected as the control signal because its advantages had been described in EMG controlled FES systems (Cauraugh et al., 2000; Chae et al., 1998) and exoskeletons (Rosen et al., 2001; Cheng et al., 2003), which could detect the subject's own intention and give corresponding assistance. The robotic system was also designed for functional evaluation since it could capture torque, kinematics and the EMG signals for on-line or off-line analysis. In this section, the hardware and software parts of the robotic system were introduced.

2.2.1 Hardware

According to the objective of the study, the mechanical part of a robotic manipulator with one-degree of freedom (DOF) was designed and fabricated for assisting the performance of elbow flexion and extension, and the mechanical structure was shown in Fig. 2.2 and Fig 2.3. The two layers of aluminum plates were connected by four aluminum pillars. The lower plate was fixed to a table. The direct drive (DDR) brushless AC servo motor (DM 1045B, YOKOGAWA, Japan) was fixed to the lower

plate by six small aluminum pillars. There were two custom-made connectors (Connector 1 and Connector 2) in this system. Connector 2 connected the motor and one end of a torque sensor (AKC-205, the 701th Institute of China Aerospace Science and Technology Corporation, China). The other end of the torque sensor was connected to a manipulandum by connector 1. The mechanical integration between the forearm and the manipulandum was obtained by an orthosis with semicircular cross section and straps were used to fix the forearm to the orthosis. There was a handle in the manipulandum that could be grasped by the subject during the movement. The upper arm was also fixed by a strap to a supporter mounted on the upper aluminum plate (Fig. 2.3). The orthosis and manipulandum could guide the forearm to rotate with an axis of rotation in line with the motor and the torque sensor. The torque sensor can measure the interaction torque between the manipulandum and the servo motor. Fig. 2.4 showed the system with a subject from different viewing directions.

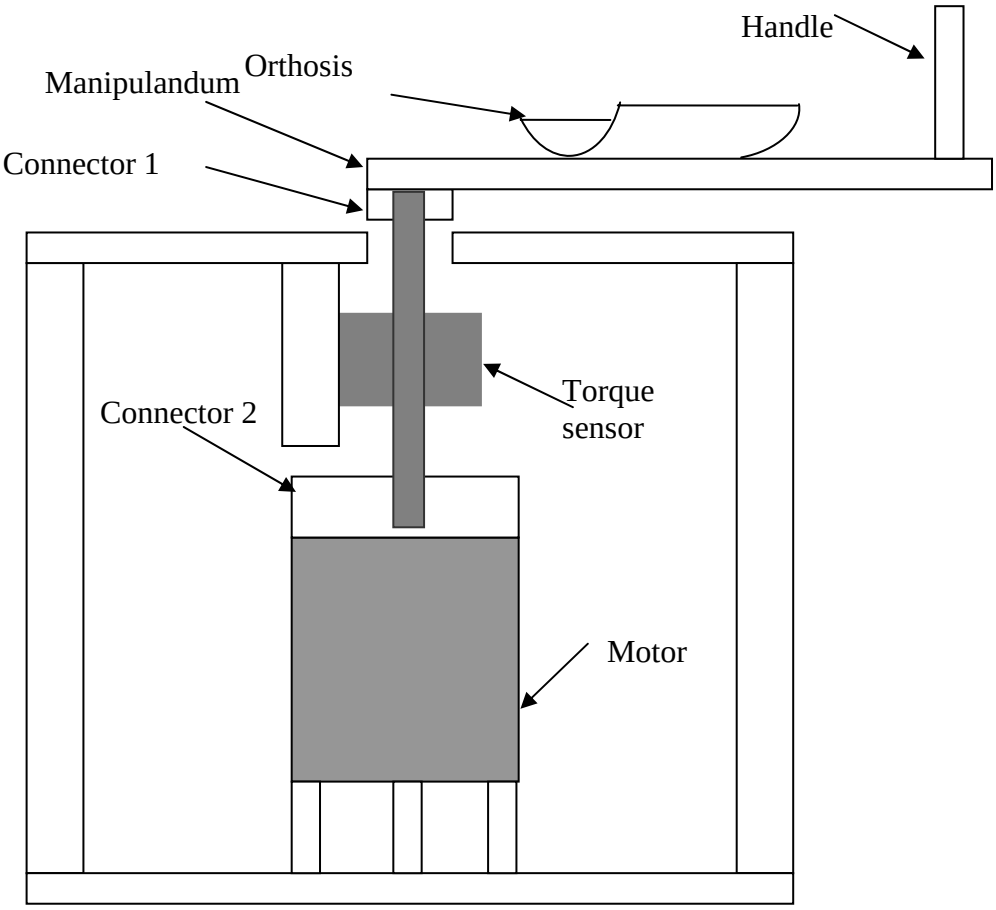

Fig. 2.2 Side view of the robotic system

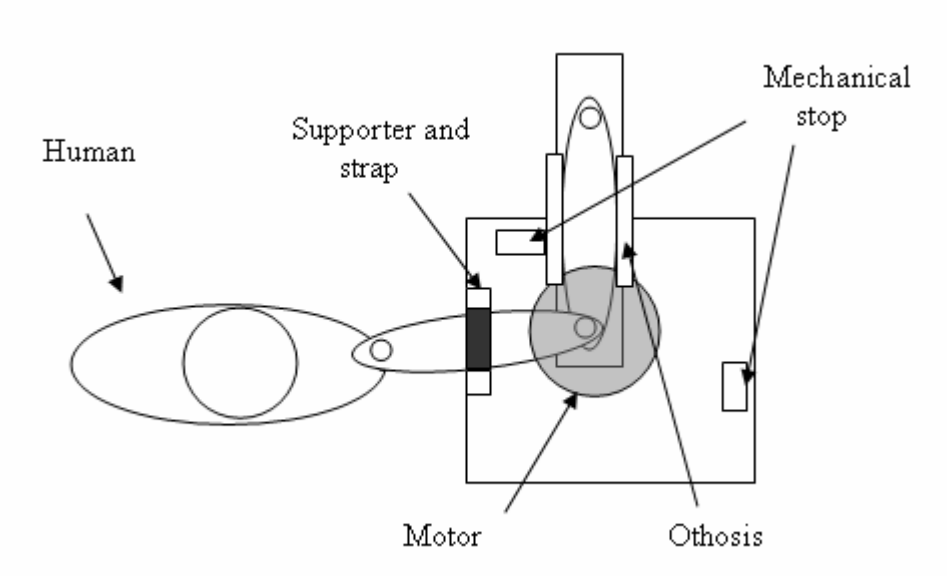

Fig. 2.3 Top view of the robotic system with a subject

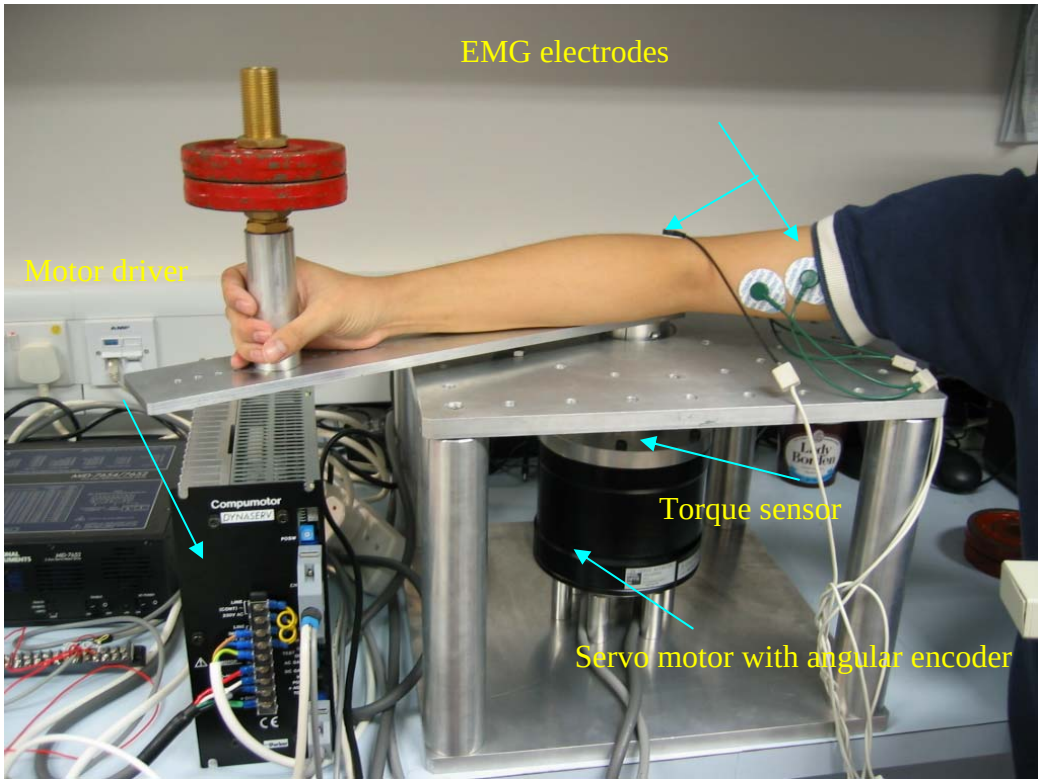

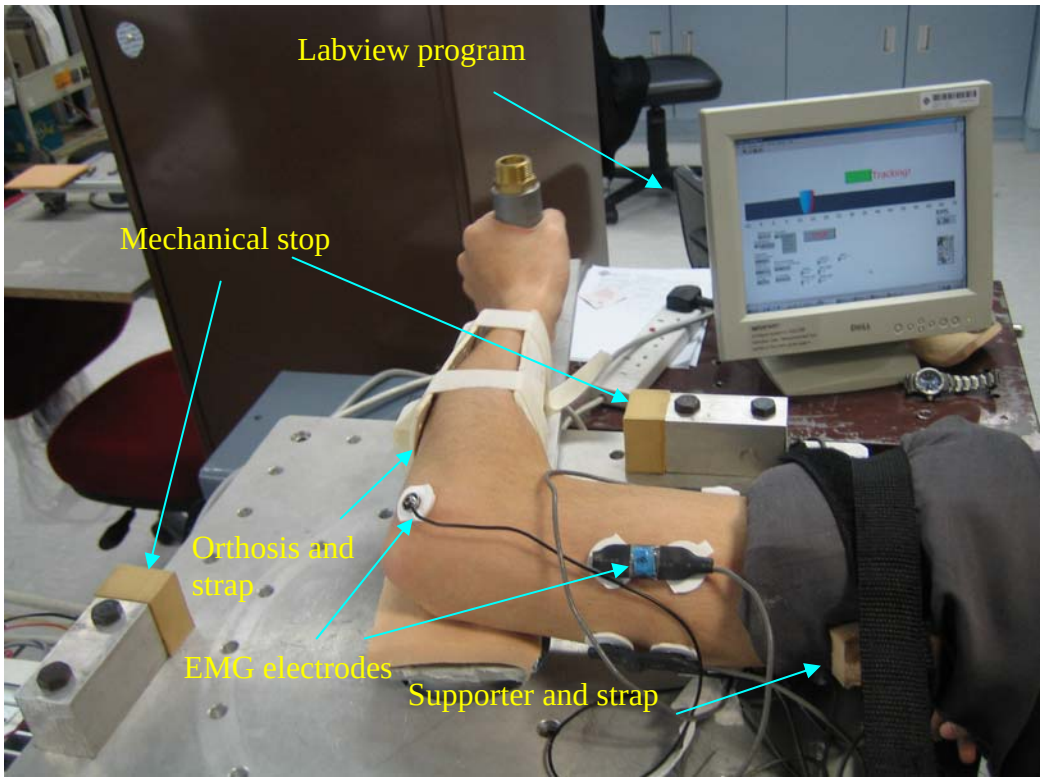

Fig. 2.4 Diagram of the robotic system

The DDR motor was driven by a servo driver (SD1045B, YOKOGAWA, Japan); it could rotate smoothly at a very low velocity (less than 2 rev /s) and had a flat velocity/torque curve with a high torque output (up to 48 Nm), which was suitable for the biomechanical application of a human's joint. An optical incremental shaft encoder was attached to the motor shaft and the practical encoder's resolution for measuring the joint angle could reach 655,360 lines/revolution, which provided the maximum accuracy of the measured joint angle up to 0.00055 deg. The servo motor could work in the following three different control modes:

1. In position control mode, motor positioning control was performed according to the command position sent from the higher-level motion controller card (PCI 7344, National instrument, USA). A proportional-integral-differential (PID) control algorithm was applied to make the output position equal to the target position based on the feedback of the digital encoder.
2. In velocity control mode, the rotating velocity of the motor was controlled by the command voltage (-10 v to +10 v) from the higher-level controller.
3. In torque control mode, the current which flowed through the motor was controlled by the input command analog voltage (-8.5 v to +8.5 v). There was no torque when the command voltage equaled zero and the maximum torque was produced when the command voltage equaled ± 8.5 v. The torque generated by the motor was almost linear with input analog voltage, which was calibrated in section 2.2.3.2.

In velocity control and torque control mode, the higher-level command signal was generated using Labview software through a DAQ card (PCI 6036E, National instrument, USA). The DAQ card has sixteen 16-bit analog inputs, two 16-bit analog outputs and two 24-bit counters.

For safety issues, three steps were taken to protect the subject during the experiments. Firstly, two mechanical stops were used to limit the rotation range of the motor, and they were shown in Fig. 2.3 and Fig. 2.4. Secondly, the software program would limit the torque to the preset range, and the operation would be stopped if the motor exceeded the range. The torque that the motor could generate ranged from -5 Nm to 5 Nm. Thirdly, an emergency stop could be used by the person who was in charge of the experiment to break the power supply to the servo motor.

2.2.2 Software and system architecture

In order to operate the robotic system for different purposes, three software programs were developed in Labview and were run on a PC-based platform to control the robotic system, which would be described in details in succeeding experiments. The architecture of the myoelectrically controlled robotic system was shown in Fig. 2.5. The inputs to the system were the EMG signals, the torque signal and the angle signal. The EMG signals and the torque signal were captured through the 16-bit analog inputs of the DAQ card and the angle signal was captured through the counter of the DAQ card. These signals were inputted to the computer, and then the control signals would be generated and outputted to the servo driver to control the servo motor through the 16-bit analog output of the DAQ card based on the control strategy. During real-time control of the system the data were stored into the hard disk for further analysis. Two computer screens were used, one was placed in front of the subject to provide guidance in the experiment and the other was for the operator to control the system.

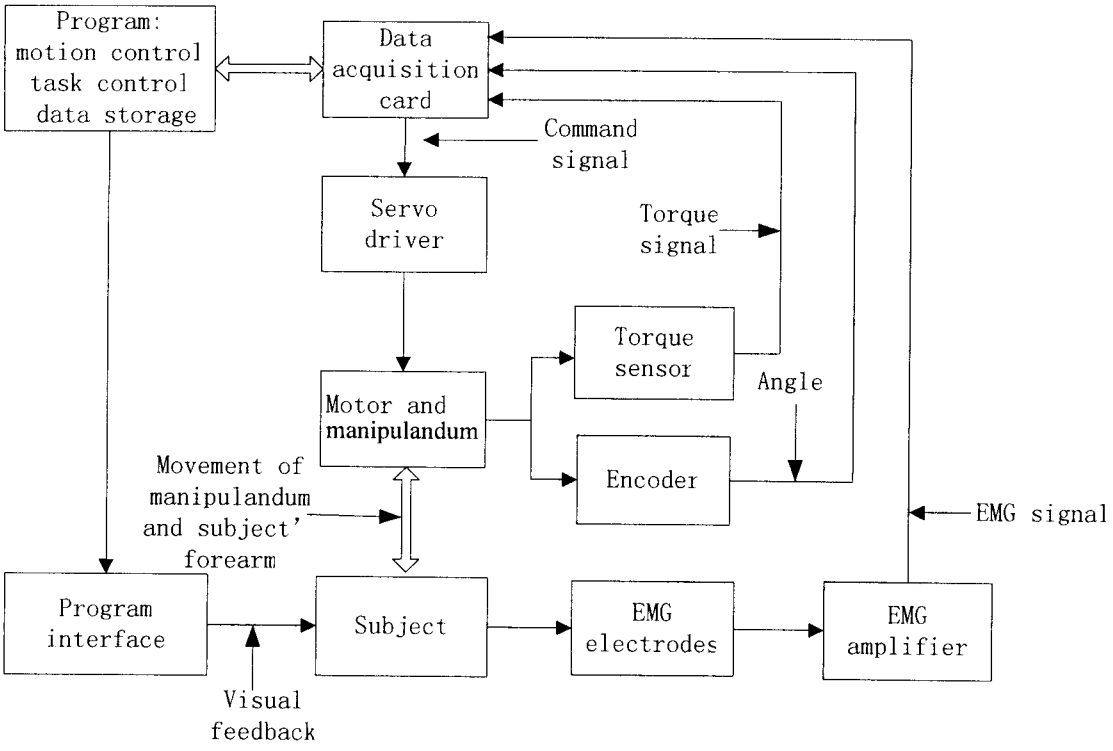

Fig. 2.5 Architecture of the myoelectrically controlled robotic system

2.2.3 System calibration

2.2.3.1 Calibration of the torque sensor

The accuracy of the torque sensor should be validated before the experiments. In order to calibrate the torque sensor, the robotic system was set to the vertical plane, and the system was changed to the position control mode. The command signal was to keep the manipulandum horizontally based on the PID control, and the torque was measured by the torque sensor. Fig. 2.6 showed the relationship between the measured torque by the torque sensor and the calculated torque that was based on the mass of the load and the moment arm in equation (2.1):

$$T=T_0+D*M \qquad (2.1)$$

where T_0 was the torque of the manipulandum, D was the moment arm of the load from the rotation axis and M was the mass of the load. Twelve points were calculated with the combinations of four different loads (1, 2, 3 and 4 kg) and three different moment arms (0.265m, 0.305m, and 0.345m). Fig. 2.6 showed that there was a good linearity between the measured torque and the calculated torque (R=0.9974).

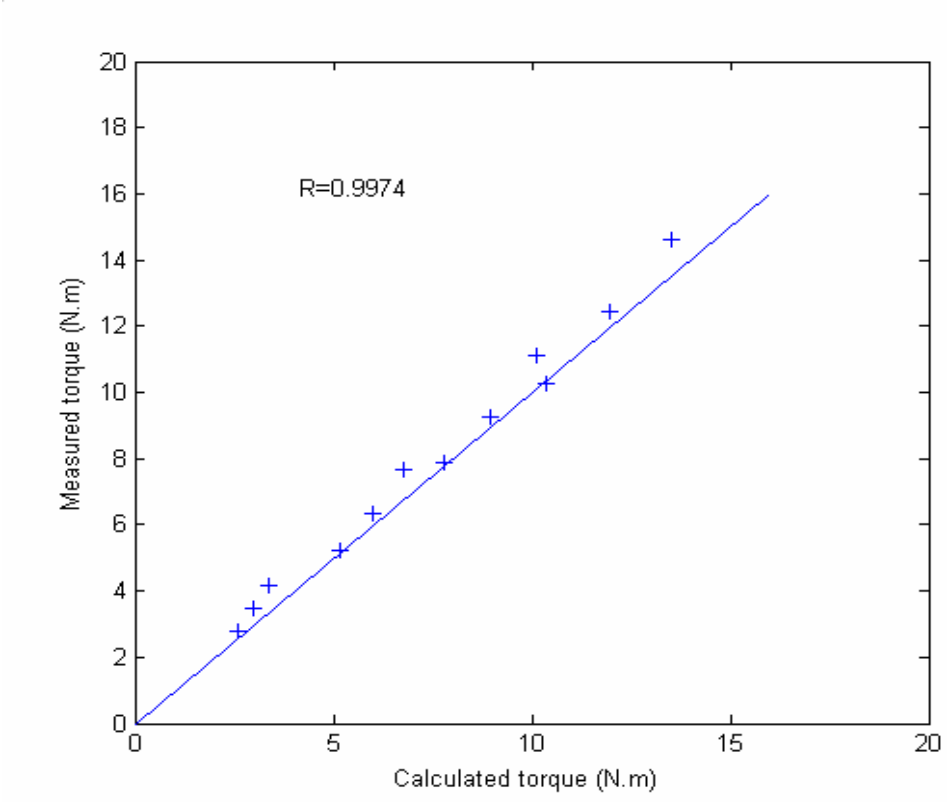

Fig. 2.6 Calibration of the torque sensor and motor

2.2.3.2 Calibration of the motor in the torque mode

After calibrating the torque sensor, the relationship between the analog input and the output torque of the motor was also calibrated. This calibration test was performed with the manipulandum in the horizontal plane. The system was in the torque control mode, and the manipulandum was fixed by the two mechanical stops. The torque that was applied from the motor to the manipulandum could be measured by the torque sensor. Different analog inputs (from 0 to 2v with an increment of 0.1v) to the motor were generated with a Labview program through the DAQ card. The results were shown in Fig. 2.7. There was a good linear relationship between input voltage and the measured torque by the torque sensor (R=0.9987). The line did not pass through the origin which was due to the initial friction torque of the motor. The maximum static friction torque (T_f) of the motor could be calculated based on the linear equation when the analog input equaled to zero (T_f =-1.687 Nm).

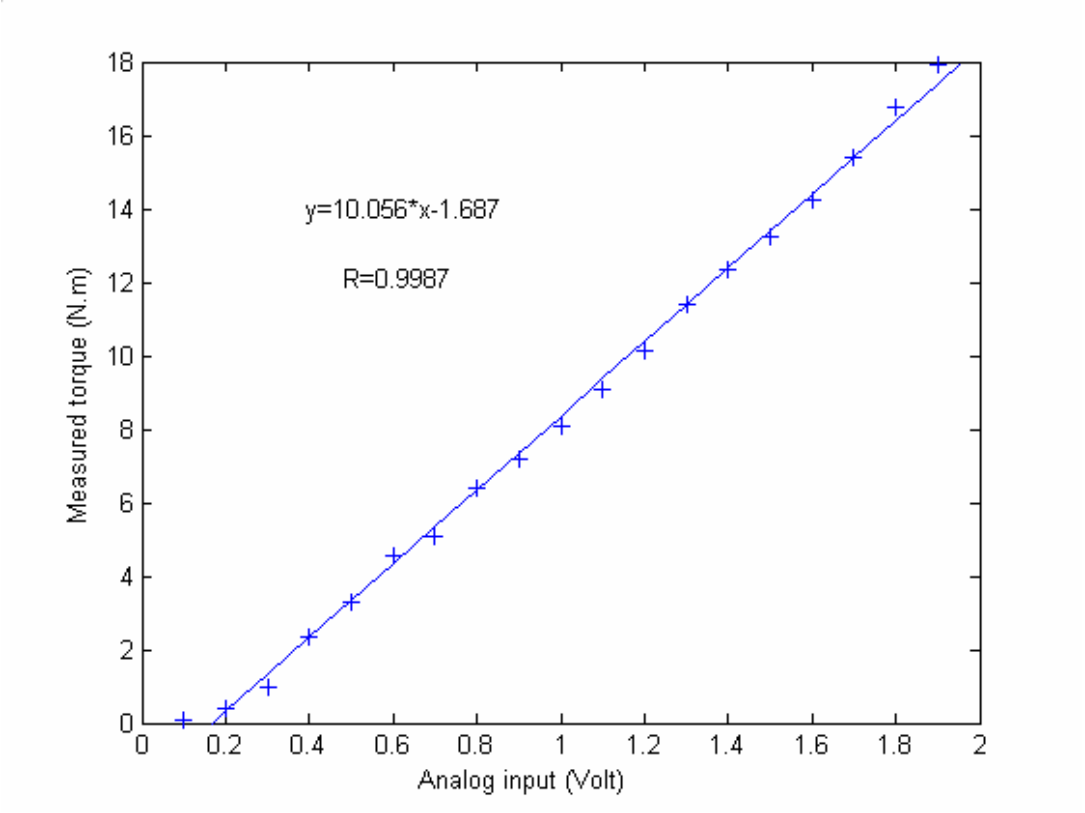

Fig. 2.7 Calibration of the motor in the torque mode.

2.3 Control strategy

In order to find a control strategy for the robotic system in the rehabilitation training, two control strategies were investigated in this study: the recurrent artificial neural network (RANN) and proportional control.

2.3.1 Recurrent artificial neural network model (RANN)

2.3.1.1 RANN model for subjects without impairment

Section 1.4.2 shows that ANN models are promising techniques to simulate the musculoskeletal model, but few of these models have been used to investigate the EMG-torque relationship under a dynamic situation. In this study, a three-layer RANN model (Fig. 2.9) was built. The inputs and output were similar to the Hill-type model in Fig. 2.8 to describe the musculoskeletal function in voluntary dynamic situations. The special feature of the RANN model was that the feedback from a previous stage was used as the input for the next stage. The EMG signals from selected muscles were used as inputs to reflect the central nervous system (CNS) command signal; the angle and angular velocity of the elbow joint were used as inputs to reflect elbow geometry parameters, and the feedback from the output torque was used as input to reflect the previous state of the muscles around the elbow joint. This feedback was applied to simulate the muscle characteristic. The muscle force of the previous stage determined the tendon compliance and it would affect the force at the next stage (Zajac, 1989). The specific goal of this part of the study was to evaluate the performance of the RANN model using the EMG signals recorded from three selected muscles together with the kinematics information to predict the joint torque of the elbow when performing voluntary arm movement in the horizontal plane. Moreover, the effect of using kinematics information on the RANN model was studied by comparing the model with and without kinematics inputs.

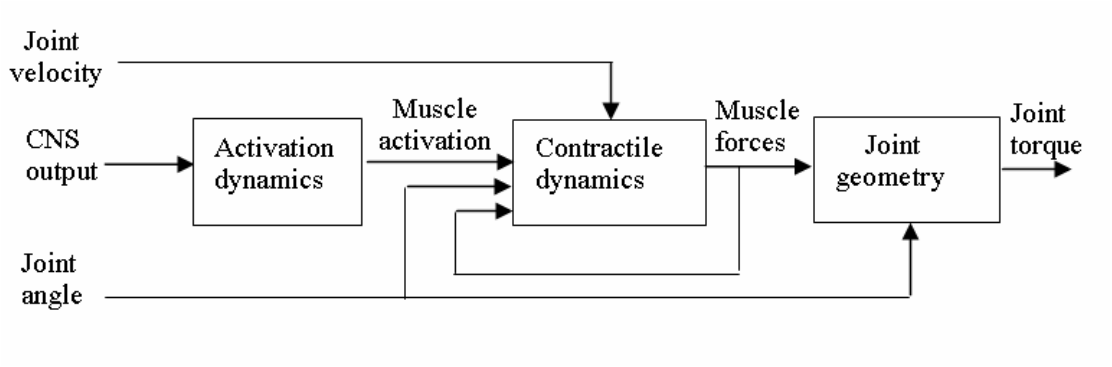

Fig. 2.8 Block diagram of the musculoskeletal model. A classical Hill-type model was divided into three parts to describe the relationship from CNS input to the body movement: the activation dynamics model, the contractile dynamics model and joint geometry model.

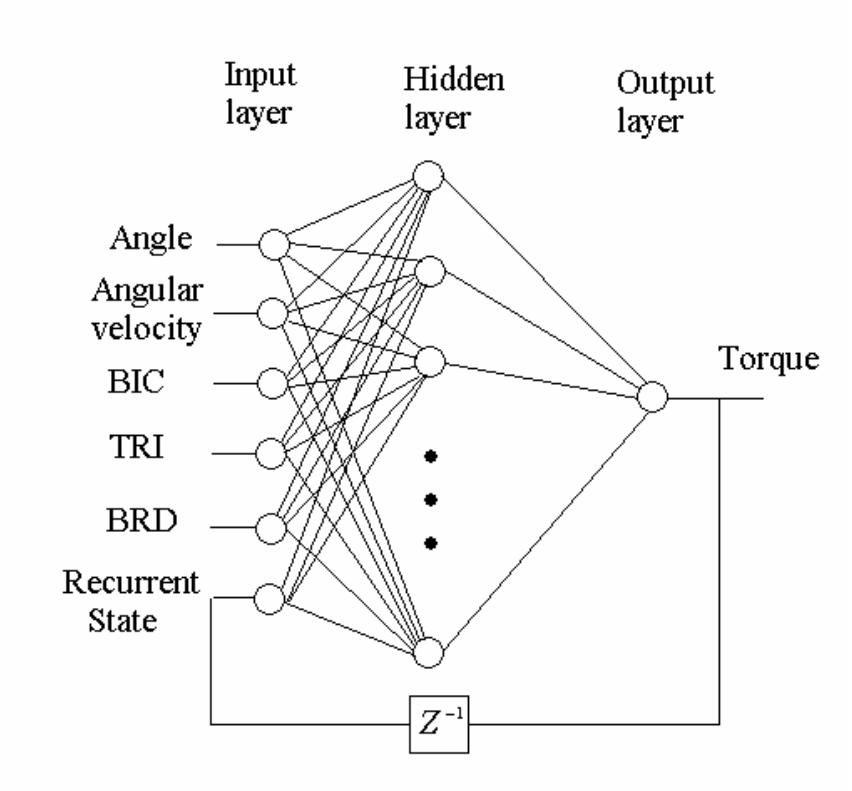

Fig. 2.9 Structure of the recurrent artificial neural network (RANN) model. The six input nodes consisted of normalized EMG signals from biceps brachii (BIC), triceps brachii (TRI), brachioradialis (BRD), angle, and angular velocity and a recurrent torque feedback. The output node was the normalized joint torque about the elbow complex.

(1) Experimental procedures

Six healthy subjects (male, 24-30 years of age) without any history of neuromuscular disorder were recruited in this study. Before the test, all subjects were introduced to the experimental protocol and gave their informed consents (Appendix III). Fig. 2.10 showed the experimental setup. In the experiment, the subject was asked to sit beside the table. The height of the table was adjusted to rest the arm in the horizontal plane with the same height of the shoulder, and the shoulder was in 90 deg abduction and 45 deg horizontal flexion. A strap was used to fix the upper arm to a supporter on the table. The forearm was attached to a custom-made manipulandum by an orthosis fixed on the manipulandum with an axis of rotation in line with the elbow joint. The manipulandum was used to support the forearm and the subject could flex and extend frictionlessly along the elbow joint. The aluminum manipulandum was light in weight in order not to affect the voluntary arm movement. There was a handle in the manipulandum that could be grasped by the subject during the movement. Then the subjects were instructed to perform reciprocal elbow flexion/extension between full extension (0 deg) and 90 deg flexion at different speeds which were guided by the sound of a metronome. The metronome was used to guide the kinematics trajectory of the movement. The subjects were asked to finish an elbow flexion or elbow extension within the time interval of two metronome beeps. The elbow should be either in the full extension position or in the 90 deg flexion position when the beep sound was heard. The subjects were instructed to move smoothly across the range and not to pause at the two ends. The frequencies of the metronome were set at 0.67 Hz and 1 Hz and the corresponding average angular velocities of the elbow were 60 deg/s and 90 deg/s respectively. Three different loads mounted on the top of the handle (0, 1 kg and 2 kg) were tested at these two frequencies. Each subject accomplished these 3×2 experimental trials twice which were structured in two blocks; each trial lasted for 30 seconds. The first block of trials was used as the training set and the second block of trials was used as the test set. There was at least a one-minute rest time between trials in order to minimize the effect of fatigue. An additional experiment was conducted on one subject (subject C) after these two blocks of trials. The subject was asked to perform reciprocal elbow flexion/extension between 0 deg and 90 deg freely without any guidance of the metronome. The trial was also used to validate the RANN model trained with the first block of data. The angular displacement of the elbow joint was

captured by a flexible electrogoniometer (Penny & Giles, UK). A tele-EMG system (Noraxon, USA) with a bandwidth of 10-500 Hz per channel was used to capture and amplify the surface EMG signals from three selected muscles: biceps brachii, medial triceps brachii and brachioradialis, which were the muscle groups that mainly contributed to the movements of elbow flexion and elbow extension. The surface EMG signals were captured with Ag/AgCl surface electrodes (Blue Sensor, Medicotest, Denmark). All Ag/AgCl electrodes were placed in bipolar configuration with a 2 cm space between the centers of the electrodes. The positions of the surface EMG electrodes were chosen as suggested by Cram et al. (1998). The surface EMG signals and angular signal were recorded simultaneously at a sampling frequency of 1000 Hz and were stored via a 16-channel A-D converter for off-line analysis (DT2821, Data Translation, USA).

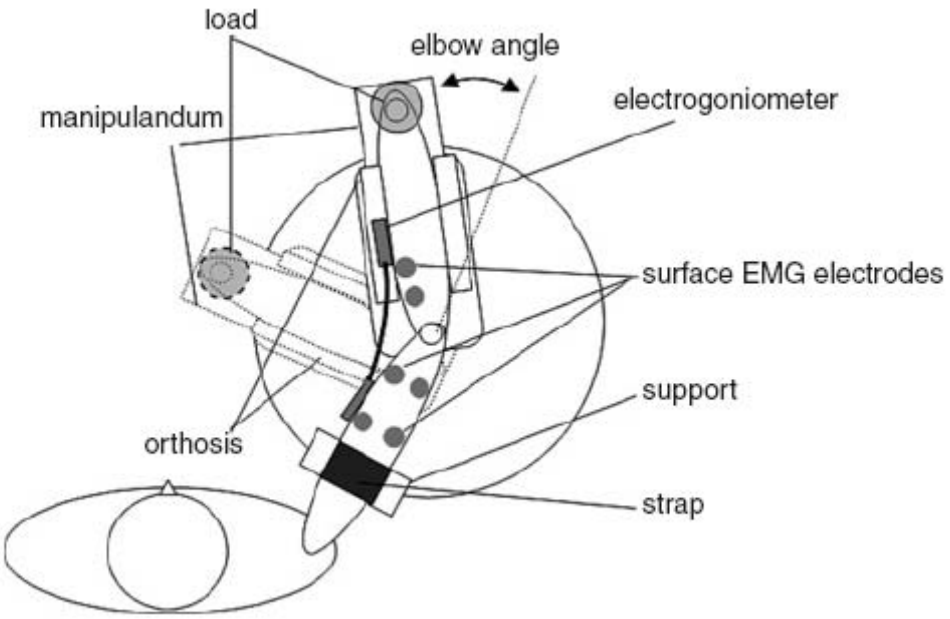

Fig. 2.10 Experimental setup. The experimental setup showed the EMG electrodes on the biceps, triceps, and brachioradialis, the placement of the electrogoniometer and the definition of elbow angle.

(2) Data processing

The angular signals were low-pass filtered using a 4^{th} order Butterworth digital filter with a cut-off frequency of 3 Hz. The surface EMG signals were band-pass filtered using the same digital filter with bandwidths of 10-500 Hz; then they were full-wave

rectified and low-pass filtered with a cut-off frequency of 3 Hz. The angular velocity was calculated from the first derivatives of the angle and the angular acceleration was the second-order derivatives of the angle. The angular acceleration was used to calculate the expected torque. The Matlab signal processing toolbox was used to process the data. All the data were digitally resampled at 100 Hz before they were inputted into the ANN model. In order to avoid zero or extremely large values, all the inputs and output were scaled to 0.1-0.9 using a linear scale method. Table 2.1 showed the references of the normalization criteria (Luh et al., 1999).

	Normalized to 0.1	Normalized to 0.9
EMG of Biceps brachii	At rest	Biceps EMG amplitude of MIVF
EMG of Triceps brachii	At rest	Triceps EMG amplitude of MIVE
Brachioradialis	At rest	Brachioradialis EMG amplitude of MIVF
Joint angle	0 deg	90 deg
Joint angular velocity	Max. extension velocity	Max. flexion velocity
Joint torque	Max. extension torque	Max. flexion torque

Table 2.1 Normalization criteria for input and output of normal subjects before training. The movement of flexion was assigned to be positive and the movement of extension was assigned to be negative. MIVF=maximum isometric voluntary flexion; MIVE=maximum isometric voluntary extension. The MIVF and MIVE were performed when the elbow joint was at 90 deg.

(3) Inverse dynamic model

The following nonlinear differential equation describes the joint movement with manipulandum and loads:

$$T_1 = I \cdot \frac{d^2\theta}{dt^2} + B \cdot \frac{d\theta}{dt} \qquad (2.2)$$

where θ was the joint angle, B was the viscosity coefficient of the tissue, which was assumed to be zero in this study, and I was the moment of inertia of subject's forearm,

hand, the manipulandum and the loads. For one DOF of movement of the forearm, I could be assumed to be constant, and Table 2.2 summarized the moment of inertia of each subject based on the subject-specific anthropometric parameters (Winter et al., 1990). Then the expected torque of the elbow joint during voluntary horizontal movement could be calculated from this inverse dynamic model by multiplying angular acceleration with moment of inertia (Gregor et al., 1991; Riener et al., 1997). No external forces were expected from the system, and the elbow movement could be performed freely along the axis.

Subject	A	B	C	D	E	F
Body weight (kg)	61	69	66	70	64	67
Forearm length (cm)	24	25.5	24.5	24.5	22.5	23
MOI when with a 0-kg load ($kg.m^2$)	0.079	0.094	0.086	0.090	0.075	0.079
MOI when with a 1-kg load ($kg.m^2$)	0.198	0.213	0.205	0.209	0.194	0.198
MOI when with a 2-kg load ($kg.m^2$)	0.317	0.332	0.324	0.328	0.313	0.317

Table 2.2 Anthropometric parameters and the summed moment of inertia (MOI) of subject's forearm, hand, the manipulandum and different loads.

(4) RANN model with EMG and kinematics inputs

A three-layer RANN model was chosen to map the input EMG signals and the expected torque (Fig. 2.9). The normalized EMG magnitudes of biceps brachii, triceps brachii, brachioradialis, angle, angular velocity, together with a recurrent feedback torque, formed six input nodes. The output node was the normalized joint torque at the elbow joint. The criterion to choose the number of hidden units was described in section 2.3.1.1-(6). The activation functions of the input and output nodes were linear, and the activation function of the hidden nodes was tangential-sigmoid defined by equation (2.3) and equation (2.4).

$$net_i = \sum_j a_j \omega_{ij} + bias_i \tag{2.3}$$

$$\text{TanSig} = \frac{e^{net_i} - e^{-net_i}}{e^{net_i} + e^{-net_i}} \tag{2.4}$$

where net_i was the net input to neuron, sum of multiplying each input signal a_j by the corresponding connection weight ω_{ij} and variable bias term $bias_i$. The initial connection weights were random values. The error could be improved by means of the back-propagation training method. Among many variations of the back-propagation training methods, the Levenberg-Marquardt algorithm was selected for its fastest convergences for medium sized neural networks until a few hundred neurons (Gurbuz et al., 2003). The Levenberg-Marquardt algorithm could be described by the following equation:

$$\Delta\omega = (J^T J + \mu I)^{-1}.J^T e \qquad (2.5)$$

where ω was a vector of weights and biases, J was the Jacobian matrix that contains the first derivatives of the network errors with respect to weights and biases, e was a vector of network errors, I was the identity matrix and μ was a scale. The default setting of μ was 0.01 before training. The Matlab neural network toolbox was used to train and test all the data. (Mathwork, USA)

The sum square error (SSE) and the root mean square error (RMSE) were used to reflect the performance of the model:

$$SSE = \sum_{i=1}^{N} (x(i) - y(i))^2 \qquad (2.6)$$

$$RMSE = \sqrt{\frac{SSE}{N}} \qquad (2.7)$$

where, x(i) was the predicted torque based on the RANN model, y(i) was the expected torque deduced from the inverse dynamic model and N was the number of samples.

The cross-correlation coefficient between the predicted torque and the expected torque was also used to reflect the performance of the model which is as follows (equation 2.8):

$$R = \frac{\sum_{i=1}^{N} x(i)y^*(i)}{[\sum_{i=1}^{N} x(i)^2 \sum_{n=1}^{N} y(i)^2]^{1/2}} \qquad (2.8)$$

All data from different frequencies (0.67 Hz, 1 Hz) and different loads (0 kg, 1 kg and 2 kg) were trained in a RANN model for each subject, then the RANN model of each subject was analyzed with the test data, respectively.

(5) RANN model with only EMG inputs

In addition to the RANN model described in section 2.3.1.1-(4), another three-layer recurrent network with only three EMG inputs (the normalized EMG of biceps brachii, triceps brachii and brachioradialis) and recurrent feedback was built to compare the performances of the models with and without the kinematics inputs. The other parts of the model were the same with the model in section 2.3.1.1-(4), and the model used the same training data and test data. The paired t-test (two-tail test) was used to statistically compare the RMSE from these two models. The level of significance was set at 0.05 for all statistical tests.

(6) Network structure and number of iterations

The number of hidden nodes was investigated to achieve the best performance. Fig. 2.11 showed the RMSE of the training data and the test data set by varying the number of hidden nodes and initial connection weights from the data of subject C. For each model with the same number of hidden nodes, it was trained ten times with different random initial conditions. The average RMSE from different initial conditions was shown in Fig. 2.11. In the training data, the mean RMSE decreased as the hidden nodes increased. When the model was evaluated by the test data, there was a decrease in the mean RMSE at the initial stage and when the number of hidden nodes was further increased, the mean RMSE increased and the fluctuation of RMSE also increased. The minimum RMSE of the test data was located where the hidden nodes varied from 5 to 10. The number of hidden nodes was chosen to be seven across all subjects. The number of training iterations was also a factor that affected the results. Fig. 2.12 showed the relationship between the iteration number and the RMSE of the training and the test data. Many investigators used a fixed number of iterations (Rosen et al., 1999; Liu et al., 1999; Koike et al., 1995) for training and their stopping criterion might cause the system to stay in a local minimum and might decrease the robustness with too many iterations. As shown in Fig. 2.12, although the RMSE of the training set decreased with the increase in the iteration number, the error of the test set increased. In order to avoid this situation, the training should be stopped, if there was

not much improvement in the error. In this study, the stop criterion for each RANN model was trained until the SSE between the expected torque and the predicted torque changed by less than 0.5% over 50 consecutive iterations.

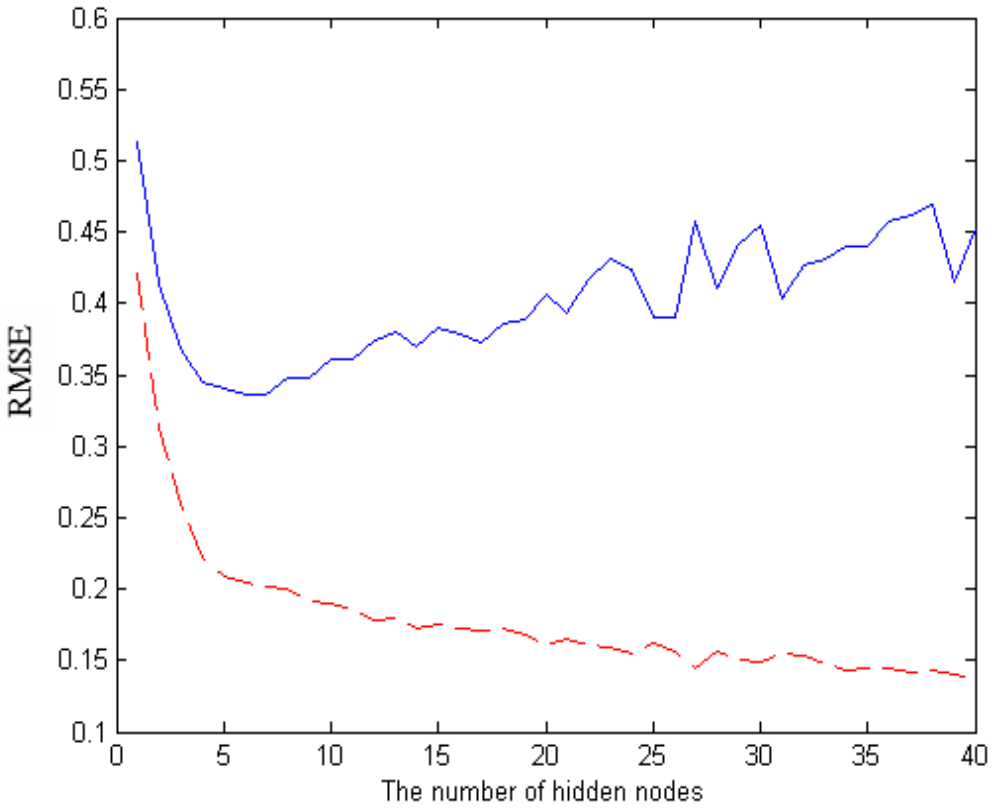

Fig. 2.11 The relationship between network complexity and the error of the network. The solid curve was the average RMSE from test set and the dashed line was the average RMSE from training set.

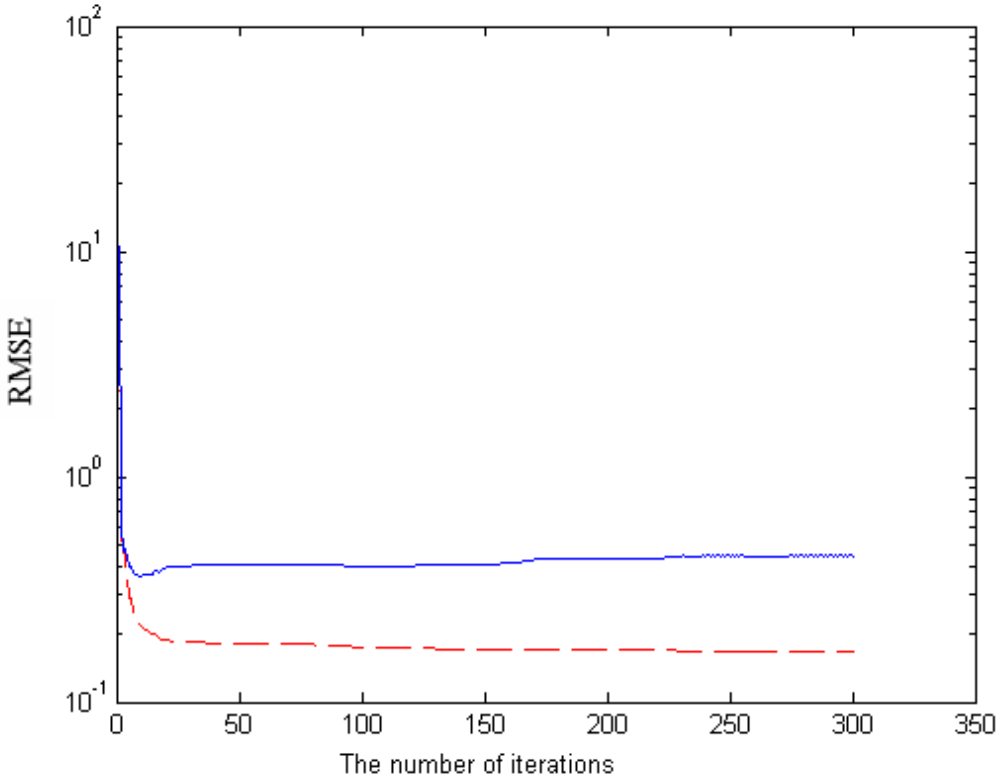

Fig. 2.12 The relationship between the RMSE of the network and the number of iterations in training. The solid line was calculated from test set and the dashed line was calculated from training set.

2.3.1.2 RANN model for subjects after stroke

(1) Experimental setup

After the experiment on normal subjects, three subjects after stroke were also recruited to evaluate the RANN model. Table 2.3 showed the clinical data from the three subjects and Fig. 2.13 showed the experimental setup. In the experiment, the subjects were instructed to sit beside the table with the manipulandum. A strap was used to fix the upper arm to a supporter on the table. The height of the table was adjusted to rest the arm in the horizontal plane with the same height as that of the shoulder, and the shoulder was in 90 deg abduction and 45 deg horizontal flexion. The forearm was attached to a manipulandum with the axis of rotation in line with the elbow joint. The manipulandum was used to support the forearm. The rotation axis was connected with a ball bearing, and the friction torque along the rotation axis could be ignored. The manipulandum was made of aluminum and weighed about 400 g. It was designed to minimize the inertial effect from the manipulandum during the

voluntary arm movement. A computer screen was placed in front of the subjects, which displayed both the target and the actual elbow joint angle. The subjects were instructed to initially set the elbow at 30 deg flexion, since many subjects after stroke often had difficulty moving to the fully extended position. After a random delay generated by the Labview software which ranged from 2 to 5 sec, the indicator light in the middle of the screen turned green, and the target pointer began to move along the horizontal line in a sinusoidal trajectory between 30 deg and 90 deg for 36 seconds. The subjects were instructed to try their best to follow the moving target pointer by controlling their elbow angle. The actual elbow angle was also displayed in another pointer as the real-time feedback. Before the test, three warm-up trials at 30 deg/s were arranged for the subjects to get familiar with the experiment. Then each subject was administered 18 trials structured in three blocks. Each block consisted of six trials with different velocities (10, 20, 30, 40, 50 and 60 deg/s) which were arranged in a random sequence. The subjects had a 30-s and five-minute rest time between each trial and between each block, respectively. For the three subjects, the task was performed on both the affected and the unaffected arms. The angular displacement of the elbow joint was captured by a flexible electrogoniometer (Penny & Giles, UK), which was attached to the manipulandum. A tele-EMG system (Noraxon, USA) with a bandwidth of 10-500 Hz per channel was used to capture and amplify the surface EMG signals from three selected muscles: biceps brachii, medial triceps brachii and brachioradialis, which were the muscle groups that mainly contributed to the movements of elbow flexion and elbow extension. The surface EMG signals were captured with Ag/AgCl surface electrodes (Noraxon, USA). All Ag/AgCl electrodes were placed in bipolar configuration with a 2 cm space between the centers of the electrodes. The angle signal and EMG signals from the biceps brachii, medial triceps brachii and brachioradialis were recorded simultaneously at a sampling velocity of 1000 Hz and were stored in a PC via a 16-channel A-D converter for off-line analysis (PCI 6036E, National instrument, Texas, USA). The model structure, training criteria and data processing were the same as those for the normal subjects as described in section 2.3.1.1-(2). The data from all the six velocities were used for training the RANN model. Since no external load was added during the movement and the moment of inertia of the forearm and the hand was assumed to be constant, the joint torque could be proportional to the acceleration of the movement throughout the whole experiment (equation 2.9).

$$T = I * \alpha \qquad (2.9)$$

Where T was the torque generated by the muscle group around the elbow joint, I was the moment of inertia of the subject's forearm, hand and the manipulandum and α was the angular acceleration. Therefore, the output of the RANN was simply replaced by the angular acceleration of the elbow. Table 2.4 showed the modified normalization criteria for subjects after stroke.

Subject	Age/ (Sex)	Lesion side	Years after stroke	Modified Ashworth scale
A	39 (M)	R	11 yrs	2
B	46(M)	R	5 yrs	1+
C	46 (F)	L	2 yrs	1

Table 2.3 Clinical data from the subjects after stroke for the RANN model.

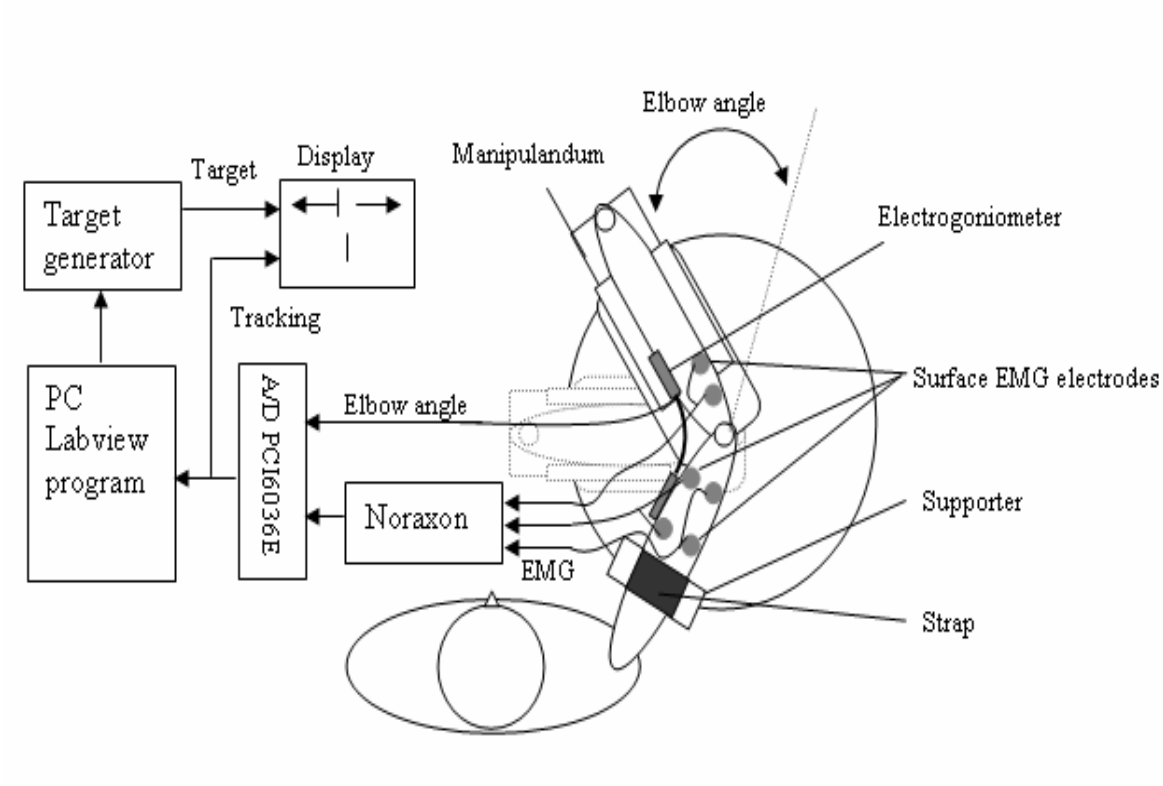

Fig. 2.13 Block diagram of experimental setup

	Normalized to 0.1	Normalized to 0.9
EMG of Biceps brachii	At rest	Max Biceps EMG amplitude
EMG of Triceps brachii	At rest	Max Triceps EMG amplitude
Brachioradialis	At rest	Max Brachioradialis EMG amplitude
Joint angle	30 deg	90 deg
Joint angular velocity	Max. extension velocity	Max. flexion velocity
Joint angular acceleration	Max. extension acceleration	Max. flexion acceleration

Table 2.4 Normalization criteria for input and output before training for subjects after stroke (The movement of flexion was assigned to be positive and the movement of extension was assigned to be negative).

(2) Calibration of the electrogoniometer

In order to ensure that the electrogoniometer could measure the elbow angle accurately during the horizontal movement, a calibration test was conducted before the experiment. Fig. 2.14 showed the results from the electrogoniometer and the angle measured by a protractor. The high cross-correlation (R=0.9997) between the angle measured by the protractor and that calculated by the electrogoniometer showed that the electrogoniometer could be mounted on the manipulandum to measure the elbow angle. The angle was calculated from the following linear equation:

$$Angle=K*(X-X_{offset}) \quad (2.10)$$

where X was the analog voltage measured from the electrogoniometer, K equaled 88.26 deg/v, which reflected the characteristic of the electrogoniometer. X_{offset} was the offset voltage, which was determined each time before the experiment.

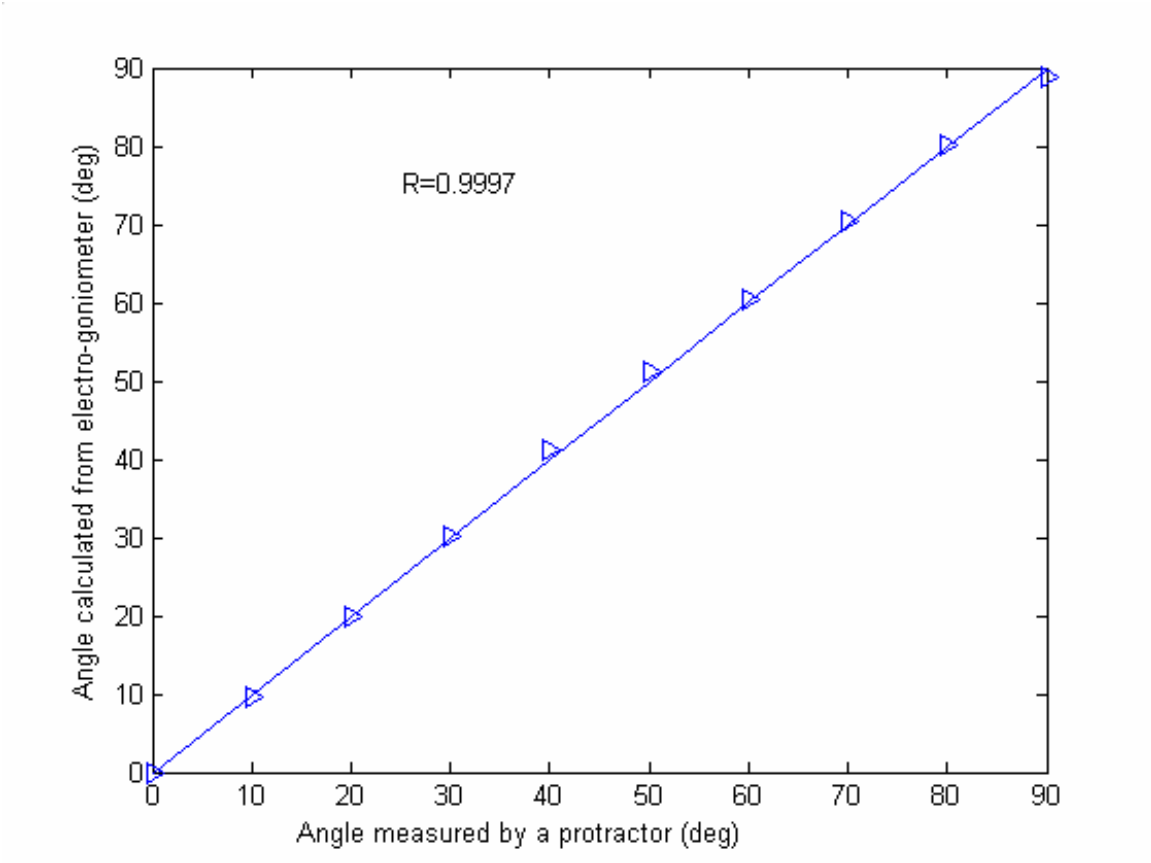

Fig. 2.14 Calibration of the electrogoniometer. In the figure, the x coordination was the angle measured by a protractor from 0 deg to 90 deg with a 10 deg increment, and the y coordination was the angle calculated from electrogonoimeter.

2.3.2 Robotic system using proportional myoelectric control

2.3.2.1 EMG signal processing procedures

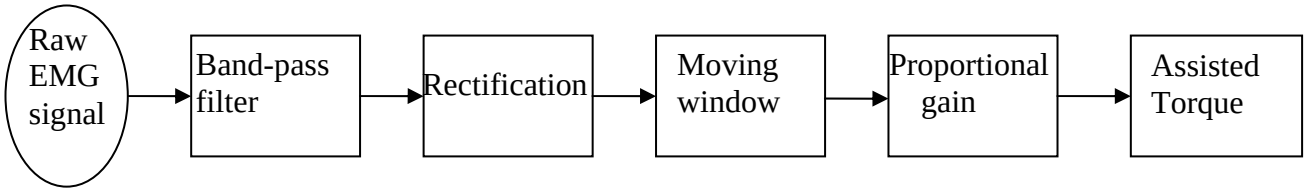

Fig. 2.15 Procedures for estimating the output torque from the EMG signal.

Proportional control is an alternative method for the robotic system. Fig. 2.15 showed the control flow which started with the raw EMG signal. Before sampling, the signals were amplified with a gain of 1000 and were band-pass filtered in 10-400 Hz. The EMG signals were all sampled at 1000 Hz. Then the EMG signals were full-wave rectified and calculated with a moving window (100 ms). Electromechanical delay, which exited between the EMG signals and the mechanical torque generated by the muscle, was assumed to be 50 ms in the literature (Koo et al., 2005). The moving window could also cause a delay of 50 ms to the processed EMG signals in real time, which would cause the synchronization between the torque generated by the motor and the torque generated by the muscle.

The processed EMG signals w_j were then normalized to the range 0-1 for $NEMG_j$ as follows:

$$NEMG_j = \frac{w_j - w_r}{w_{mvc} - w_r} \tag{2.11}$$

where w_r was the amplitude of processed EMG signal at rest, and w_{mvc} was maximal amplitude of the processed EMG signal during maximum voluntary contraction (MVC). The assistive torque T_m was estimated based on the normalized EMG signals:

$$T_m = G * T_{mvc} * NEMG_j \tag{2.12}$$

where G was the EMG-torque gain and T_{mvc} was the torque during the MVC. Then the summed torque T_{sum} the motor would generate could be shown in the following equation:

$$T_{sum} = T_m - T_{resist} \tag{2.13}$$

where T_{resist} was the constant resistive torque applied to the motor based on the maximum voluntary contraction at the elbow joint.

2.3.2.2 Selection of the control signal

Proportional control would be evaluated on the subjects after stroke in this part of the study. The first objective was to find the suitable muscle as the source of the control signal. The muscle groups from the affected elbow could be different from those in subjects without impairment, and this characteristic could affect the performance of the control system.

Elbow contracture could be commonly found in subjects after stroke (O'Dwyer et al., 1996; Williams, 1988), which required them to exert additional effort to counteract the passive torque generated by the stiff and shortened muscles during movement within the available range. Koo et al. (2003) reported the position-dependent joint weakness of elbow extensors which might be due to the reduced activation of the extensors at an extended place. Moreover, it was also found that muscle cocontraction occurred in subjects after stroke which reflected impairment in the ability to inhibit the flexor during elbow extension (McLellan et al., 1985; Canning et al., 2000). Spasticity was also a factor that might affect elbow extension (Mccrea et al., 2003; Schmit et al., 1999; Cozens, 1999). These findings showed that subjects after stroke had difficulties in performing elbow extension and involuntary torque generated by the biceps would affect the movement. Therefore, the elbow flexors were not used as control signal during elbow extension to minimize the effect of abnormal firing pattern to the movement; the EMG signal from medial triceps brachii of the affected arm was used as the control signal for the proportional control of the robotic system.

In this experiment, effects of the resistive loads and the EMG-torque gains on the motion performance of the affected arm with the myoelectrically controlled robotic system were evaluated in a tracking experiment. The effects of the resistive loads were investigated, as the resistance training was reported to be beneficial for subjects after stroke in developing muscle strength (Weiss et al., 2000; Morris et al., 2004; Ouellette et al., 2004).

2.3.2.3 Experiment protocol

A four-channel EMG system (HTI, polyu, HK) with a bandwidth of 10-400 Hz per channel was used to capture and amplify the EMG signals from the selected muscles: biceps brachii and medial triceps brachii. These two muscles mainly contributed to the movements of elbow flexion and extension. During elbow extension, the robotic system would provide an external extension torque to assist the subject’s affected elbow joint, which was in proportion to the amplitude of the processed EMG signal of the medial triceps brachii. The surface EMG signals were captured by pre-gelled Ag/AgCl surface electrodes (Noraxon, USA). All Ag/AgCl electrodes were placed in a bipolar configuration with a 3 cm space between the centers of the electrodes. An additional reference electrode was placed distant lateral of the elbow on the bony part.

The torque between the manipulandum and the motor was measured by the torque sensor during the movement and the elbow joint angle could be measured from the encoder.

Nine subjects with stroke were recruited in this part of the study. The mean age of subjects was 46 ± 10 years ranging from 26 to 59 years. The criteria for recruiting the subjects included the following: (1) there should be at least six months after unilateral stroke, (2) the subjects should not have visuospatial, cognitive or attention deficits which would prevent them from following the instructions or performing the experimental procedures, (3) the subjects should have measurable EMG signal from medial triceps brachii (the processed EMG signal after the moving window should at least be twice larger than that at rest). Eight of them could not fully extend their elbow, and only one subject (Subject D) could fully extend her elbow in the horizontal plane. All the subjects had sufficient strength to complete the flexion movement back to 90 deg elbow flexion when their affected elbows were passively positioned at 30 deg elbow flexion. Before the experiment, all the subjects were introduced to the experiment procedures and were asked to sign the consent forms (Appendix III).

During the experiment, the subjects were asked to sit beside the system. A strap was used to fix the affected upper arm to a supporter in the horizontal plane and the shoulder was in 90 deg abduction. The affected forearm was attached to the manipulandum, and the subject was asked to grasp the handle of the manipulandum with the hand. The orthosis and strap were used to fix the forearm. The subject could voluntarily move the manipulandum to perform elbow flexion, and elbow extension in the horizontal plane. A screen was placed in front of the subject to provide guidance, and all the subjects were instructed to complete the following tasks:

1) The MIVE and MIVF torques were measured for the affected elbow flexors and extensors when the elbow was positioned at 90 deg in the horizontal plane, which were used to define the level of resistive torque generated by the motor for each subject. The EMG signals during MIVE and MIVF were also captured to normalize the EMG signals of the biceps and the triceps. Three trials were performed and the maximum values were used for the torque and the EMG signals. The motor system was in the position control mode as a dynamometer. The program interface that was used for measuring the MIVE and MIVF torques was shown in Fig 2.16. When the indicator light in the middle of the screen turned red,

the subject was instructed to perform MIVE or MIVF for 5 sec. The real-time value of the elbow torque was showed from a pointer. The raw EMG signals from the biceps and the medial triceps and the torque signal were recorded at a sampling frequency of 1000 Hz by the DAQ card (PCI 6036E, National instrument, USA) for off-line analysis.

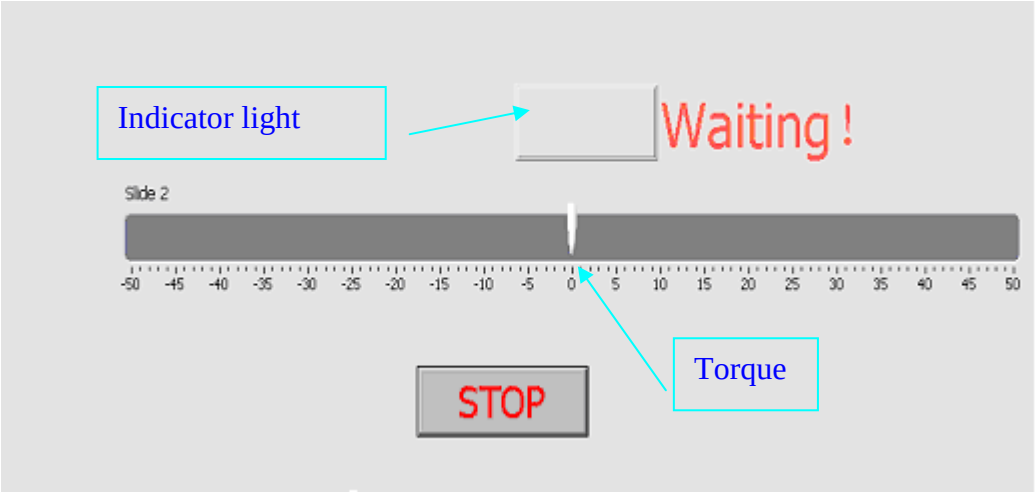

Fig. 2.16 The Labview interface for torque measurement.

2) After being measured the MIVE and MIVF torques, the subjects were instructed to perform the arm tracking test which began with the elbow at 90 deg. The Labview program provided visual guidance for the task. After a delay of 3 sec, the indicator light in the middle of the screen turned green to instruct the subjects to start to follow the target pointer by extending his/her forearm and the target pointer would move from 90 deg to 0 deg at a constant speed of 10 deg/s. Both the target and the actual elbow joint trajectories were displayed as two pointers on the screen as a real-time visual feedback; the subjects could correct the elbow movements to match the target pointer. The myoelectrically controlled robotic system would generate a torque which was calculated from equations (2.11), (2.12) and (2.13) in section 2.3.2.1 to assist or resist the elbow movement. Four gains (G=0%, 50%, 100%, 150%) and three resistive loads (T_{resist}=0% MIVE, 10% MIVE, 20% MIVE) were applied when the subject performed the elbow tracking task from 90 deg to 0 deg. Each subject would complete these 3×4 experimental trials for three times. The RMSE between the target angle and the subject's elbow angle would be displayed on the panel to provide the subject an index of his/her

performance after each trial. The smaller the RMSE value meant the better the performance in tracking the target. Fig. 2.17 showed the interface of this task. The red pointer showed the angle of the elbow and the blue pointer showed the target trajectory. The raw EMG signals of the biceps, medial triceps and torque were recorded at a sampling frequency of 1000 Hz and the elbow angle and target signal were recorded at a sampling frequency of 100 Hz by the DAQ card (PCI 6036E, National instrument, USA) for off-line analysis.

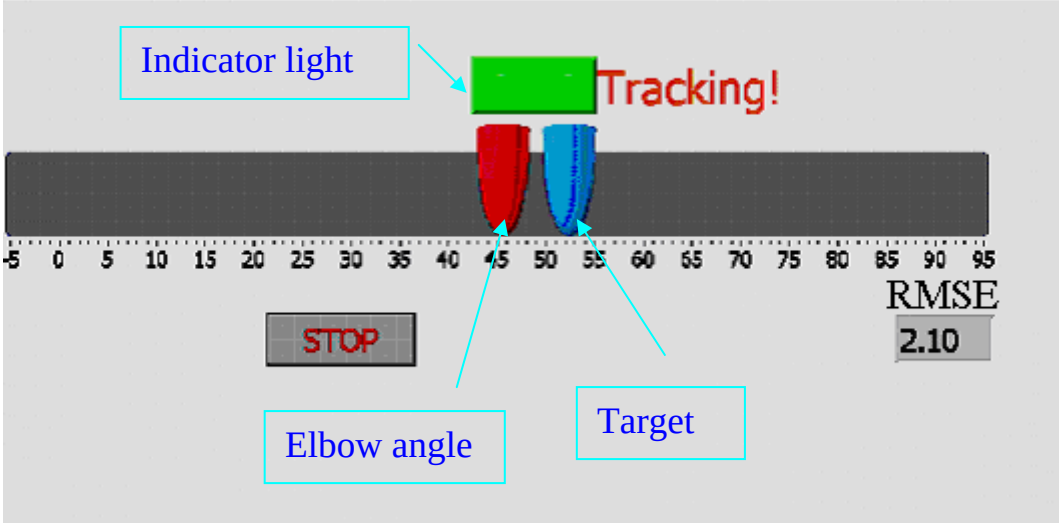

Fig. 2.17 The Labview interface for tracking with the myoelectrically controlled robotic system.

2.3.2.4 Off-line data analysis

The angular signals were low-pass filtered using a 4th order Butterworth digital filter with a cut-off frequency of 5 Hz. The surface EMG signals were band-pass filtered using the same digital filter with bandwidths of 10-400 Hz; then full wave rectified, and low pass filtered with a cut-off frequency of 3 Hz. The normalized EMG (NEMG) was used for further analysis after the processed EMG signal was normalized with the processed EMG signal measured at the MVC. In order to investigate the performance of the subjects with the myoelectrically controlled robotic system, different combinations of EMG-torque gain and resistive torque were applied to the subjects. Five parameters were used as indices to reflect the performance of the movement: (1) RMSE between the actual elbow angle and the target angle, (2) RMSJ of the trajectory, (3) extension range, which can be defined as the maximum angular

displacement of the elbow during elbow extension from 90 deg, (4) the normalized EMG (NEMG) signal of biceps and (5) the NEMG signal of triceps.

Two-way analysis of variance (ANOVA) with repeated measures was used to analyze the effects of gain and resisted load on all five parameters. The significant level was set at 0.05. All statistical work was performed with SPSS.

2.4 Functional evaluation using the elbow tracking system

2.4.1 Experimental setup for the sinusoidal elbow tracking

The main objective of this part was to systematically evaluate the elbow control ability of subjects after stroke during the voluntary elbow tracking task, which coupled the sensory and motor functions of the neuromusculoskeletal system in order to comprehensively understand the motor disorder caused by stroke. A sinusoidal tracking trajectory was designed, because the velocity profile was similar to the bell-shaped velocity profile, an independent characteristic in single-joint movement of human. The differences between the affected and unaffected arms were analyzed at six different tracking velocities (10, 20, 30, 40, 50 and 60 deg/s) according to the following parameters: the RMSE between the actual elbow angle and the target angle, root mean square jerk (RMSJ) and response delay (RD).

Nine subjects (seven males and two females) after stroke were recruited in this study. The mean age of the subjects was 45 ± 11 years and the range was from 21 to 57 years. Table 2.5 summarized the basic clinical information and the modified Ashworth scale of all the subjects. The subject selection criteria included: (1) hemiparesis resulting from a single unilateral lesion of the brain with onset at least six months before data collection; (2) sufficient active elbow range of motion (ROM) (30 deg-90 deg) on the affected arm; and (3) subjects should not have visuospatial, cognitive or attention deficits which would prevent them from following the instructions or performing the experimental procedures. This study was reviewed and approved by the human ethical committee of the Hong Kong Polytechnic University. Before the test, all the subjects were introduced to the experimental protocol and gave their informed consent following the ethical procedures (Appendix III). The experimental setup and procedures were the same with those of the experiment in section 2.3.1.2. Only the angle signal was captured and analyzed by an electrogoniometer attached to the manipulandum.

Subject	Age/ (Sex)	Lesion side	Years after stroke	Modified Ashworth scale
A	39 (M)	R	11 yrs	2
B	46(M)	R	5 yrs	1+
C	46 (F)	L	2 yrs	1
D	51 (F)	L	1 yr	1+
E	57 (M)	R	3 yrs	1
F	40 (M)	R	4 yrs	2
G	21 (M)	R	9 yrs	1+
H	49 (M)	L	1 yrs	1+
I	57 (M)	R	13 yrs	3

Table 2.5 Clinical data from the subjects after stroke. Modified Ashworth scale: 0 = no increase in tone; 1 = slight increase in muscle tone; 1+ = slight increase in muscle tone, manifested by a catch, followed by minimal resistance throughout the remainder; 2 = more marked increase in muscle tone through most of ROM, but affected part move easily; 3 = considerable increase in muscle tone, passive movement difficult; 4 = affected part rigid.

2.4.2 Data analysis

2.4.2.1 Performance indices

The angular signals from the elbow joint were low-pass filtered using a 4^{th} order zero-phase Butterworth digital filter with a cut-off frequency of 5 Hz, because the majority of the power of the angle signal was below 5 Hz from spectral analysis. The angular velocity was calculated from the first derivatives of the angle, and the angular acceleration was the second-order derivatives of the angle. All the data analysis was carried out using the Matlab signal processing toolbox (Mathworks, USA). The three indices: the RMSE, RMSJ and response delay were used to evaluate the voluntary tracking performance of all subjects.

1) The RMSE evaluated the voluntary tracking performance of all subjects.

$$\text{RMSE}=\sqrt{\frac{1}{N}\sum(\theta_0(i)-\theta(i))^2} \tag{2.14}$$

where $\theta_0(i)$ was the target elbow angle at i[th] sampling instant and $\theta(i)$ was the actual elbow angle at i[th] sampling. N was the total number of samples.

2) The RMSJ measured the smoothness of the movement which could be expressed in the following equation:

$$\text{RMSJ}=\sqrt{\frac{1}{N}\sum J(i)^2} \tag{2.15}$$

where J(i) was jerk of elbow movement at i[th] sampling instant which could be calculated from the third derivatives of the angle, and N was the total number of samples.

3) Response delay

The RD was used to describe the time interval between the trajectory of the actual elbow and the trajectory of the target, which was quantified by the temporal shift (t) that maximized the following normalized cross-correlation function (Vint et al., 2000):

$$R_{xy}(\tau)=\frac{\int_{-T}^{T}x(t)y(t+\tau)dt}{R_{xx}R_{yy}} \tag{2.16}$$

where R_{xy} was the value of the cross-correlation between the target trajectory and the actual trajectory at any time shift τ. T was the length of the records, which equaled to the length of one cycle for each velocity in this experiment; x and y were the target and actual elbow angle in time domain; $d\tau$ was the interval between the adjacent time shifts and its resolution was 0.001s; R_{xx} and R_{yy} were the maximum values of the auto-correlations of the target and actual angle trajectories respectively, which were defined at τ = 0. The cross-correlation technique was adopted to calculate the RD, which avoided the subjective criteria for defining the onset of actual trajectory.

2.4.2.2 Statistical analysis

A two-way ANOVA with repeated measures was applied to statistically analyze the above three parameters (RMSE, RMSJ and RD), which comprised of two main

factors: side (affected arms or unaffected arms) and tracking velocity (10, 20, 30, 40, 50 and 60 deg/s). The statistical model was used to analyze the main effects of side and tracking velocity, as well as the side-by-velocity interaction on the RMSE, RMSJ and RD. The paired t-test (two-tail test) was performed to test the difference between the affected and the unaffected arms under the same velocity in terms of the RMSE, RMSJ and RD. The significant level was set at 0.05. All statistical work was performed with SPSS 12. (SPSS Inc., Chicago, Illinois, USA)

2.5 Effect of the training using the myoelectrically controlled robot

The myoelectrically controlled system could facilitate the elbow movement based on the results from the experiment in section 2.3.2. The long-term training effect of the system on the affected arms of subjects after stroke was investigated. The features of this system were as follows:

1. Robotic system which could provide assistive and resistive torque on the elbow joint of the subject during the movement
2. Myoelectric control which could facilitate cognitive investment
3. Virtual feedback and tracking program which could provide real-time visual feedback to the subject

2.5.1 Experimental setup

Subject	Age/ (Sex)	Lesion side	Years after stroke
A	39 (M)	R	11 yrs
B	49 (M)	L	1 yrs
C	57 (M)	R	13 yrs

Table 2.6 Clinical data from the subjects after stroke for the rehabilitation training.

Three male subjects after chronic stroke were recruited in this four-week training program. The training program was conducted five times a week for four weeks. Table 2.6 summarized the basic clinical information from these subjects. The criteria for recruiting the subjects were the same with those described in section 2.3.2.3. All

the subjects could not fully extend their forearm in the horizontal plane before they were recruited for the training. Subject A and subject B could walk without a walking aid while subject C required a crutch when walking. Before the experiment, all the subjects were made to understand the experimental procedures and duration, and they signed the consent forms (Appendix III).

During each training session, the experimental setup used was similar to the procedures described in section 2.3.2.3. The subjects were instructed to complete the following tasks:

1. The torque measurements during the MIVE and MIVF were the same as the first task in section 2.3.2.3.

2. After the torque measurements, the subjects were asked to perform a repetitive arm tracking test which began with the elbow at 90 deg. The Labview program provided visual guidance which was shown in Fig. 2.18. In each trial, after a 3-sec delay from the beginning of the program, the indicator light in the middle of the screen turned green to instruct the subject to start following the target. First, the target would move from 90 deg to 0 deg at a constant speed of 10 deg/s, and the subject extended his/her affected elbow with the myoelectrically controlled system; then the target pointer would pause at 0 deg for 3 seconds; then the target pointer would come back from 0 deg to 90 deg at a constant speed of 10 deg/s to complete one cycle, and the subject flexed his/her affected elbow with the myoelectrically controlled system back to 90 deg. Five cycles were conducted in each trial, and it took 2 min to complete one trial. The LCD monitor in front of the subjects displayed both the target (blue pointer in Fig. 2.18) angle and the actual elbow joint angle (red pointer in Fig. 2.18) with the two pointers. The subjects could correct the elbow movement to match the target pointer with this real-time visual feedback. During the elbow extension, the robotic system would generate an assistive torque which was proportional to the amplitude of the processed triceps EMG signal (section 2.3.2.1) to assist elbow movement together with a constant resistive torque which was a percentage of the MIVE torque. During the elbow flexion, there was only a constant resistive torque which was a percentage of the MIVF torque and no assistive torque was applied. This was because that elbow flexion could be more easily performed than elbow extension in the affected arm of subjects after stroke. They could flex

back to 90 deg if passively positioned to an extended position. The percentages of resistance for extension and flexion were the same. Fig. 2.19 showed the relationship among target angle, the gain and resistive load during a cycle. If the subject could not extend his forearm to follow the target pointer because of cocontraction, contracture, spasticity of the biceps or weakness of the triceps muscle, he would be suggested to stop at the largest extended position and wait for the target pointer to come back so that he could follow it again. The program provided real-time information on the number of completed cycles, and the RMSE between the target angle and the actual elbow angle was also displayed on the screen after each trial. A lower RMSE value indicated a better tracking performance. The subject would try to minimize the RMSE value during the training. The raw EMG signals of the biceps and the medial triceps were recorded at a sampling frequency of 1000 Hz, and the elbow angle and target signal were recorded at a sampling frequency of 100 Hz by the DAQ card (PCI 6036E, National instrument, USA) for off-line analysis. The angular signals were low-pass filtered using a 4^{th} order Butterworth digital filter with a cut-off frequency of 5 Hz, and the surface EMG signals were band-pass filtered using the same digital filter with bandwidths of 10-400 Hz. Then they were full-wave rectified and low-pass filtered with a cut-off frequency of 3 Hz. The normalized EMG (NEMG) was the processed EMG signals divided by the amplitude of the processed EMG signal measured at MVC.

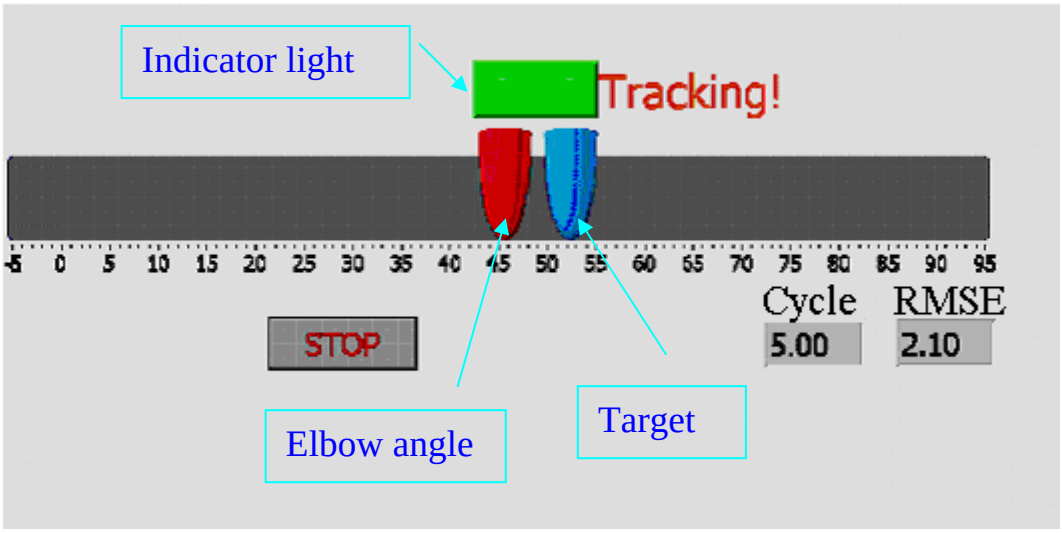

Fig. 2.18 The Labview interface used in the rehabilitation training.

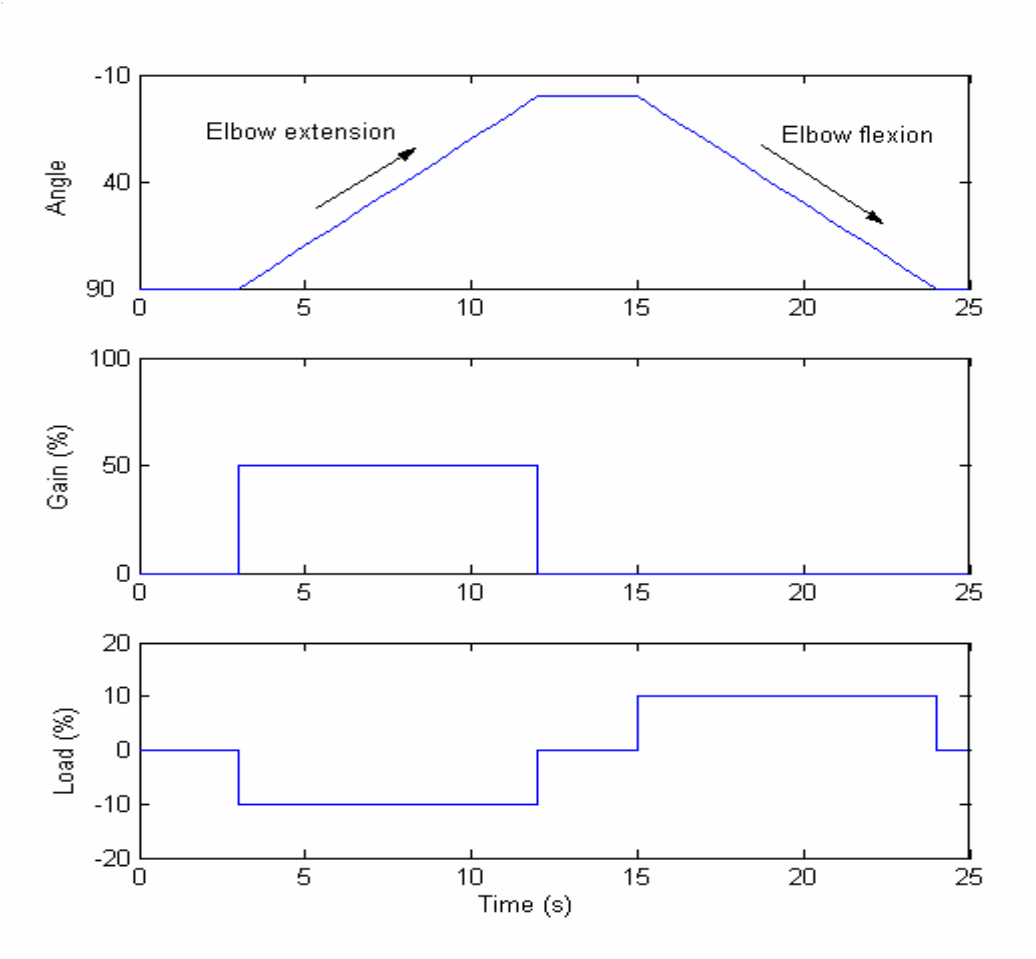

Fig. 2.19 The target angle, gain and resistive load in one cycle. The negative value was the resistive load during flexion and the positive value was the resistive load during extension.

In a trial, the resistive load and the EMG-torque gain were constants. There were 18 trials in the training session with different combinations of the gain and the load (Fig. 2.20). There was a one-minute resting period after each trial, and the total time for one session together with the evaluation trial described in section 2.5.2 was about 120 minutes.

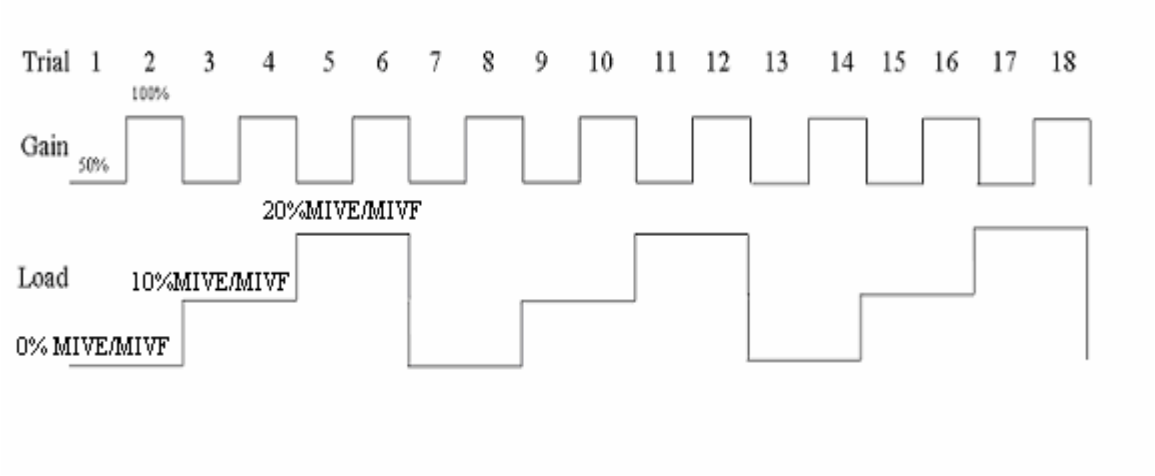

Fig. 2.20 Experiment protocol for each session of rehabilitation training. The number on the top of the figure showed the sequence of the trials. The EMG-torque gains were provided at two levels (50% and 100%). The resistive loads during elbow extension and elbow flexion were provided at three levels (0%, 10% and 20%).

2.5.2 Evaluation procedures

1) Clinical scales

Clinical scales were used to evaluate the upper limb functions before and after the four-week training. These scales included the Fugl-Meyer (range 0-66) (Appendix I) (Trombly et al., 2002) for the evaluation of motor function and the modified Ashworth scale (range 0-4) (Bohannon et al., 1986) for the muscle tone at the elbow joint.

2) Robot-measured parameters

Before each training session, the robotic system could be used as a dynamometer to measure the MIVF and MIVE torques when the elbow joint was at 90 deg. These two parameters were used to reflect the muscle strength during the rehabilitation training. Moreover, each subject was then asked to perform an evaluation trial without any

assistive and resistive torque from the robotic system. The tracking for the target pointer was the same as that in other trials in section 2.5.1. Five cycles of extension and flexion would be used for evaluation. The RMSE between the elbow angle and the target angle was used as a performance indicator for tracking.

3) The sinusoidal elbow tracking experiment

The elbow tracking experiment which was described in section 2.4 was also used to evaluate the elbow control function of the three subjects. The experiment was conducted twice; one day before and after the training. The parameters used to evaluate the functional improvement in the affected arm were the RMSE, RMSJ and RD, which had been described in section 2.4.

4) Subjective evaluation questionnaire

After finishing the last session of the rehabilitation training, all the subjects were asked to complete a questionnaire (Appendix II) about the system and the training protocol, which would be important for further development and improvement of the system and the training protocol in the future.

CHAPTER 3 RESULTS

3.1 Recurrent artificial neural network model

3.1.1 Recurrent artificial neural network model for normal subjects

After determining the structure and iteration criteria of the recurrent artificial neural network (RANN) model, the model was used in the experimental trials. The normalized input data recorded during a typical experimental trial were illustrated in Fig. 3.1. The subject moved with a 1-kg load on the top of the handle and was guided by a metronome at the frequency of 1 Hz in this trial. The processed normalized EMG signal of the biceps seemed to display less modulation in comparison to those of the triceps and the brachioradialis. There were two reasons which could explain this phenomenon. Firstly, the maximum flexion torque was often larger than the maximum extension torque at the elbow joint. Thus after normalization, the amplitude of the biceps EMG was less than that of the triceps if they represented the same amount of torque. Secondly, several muscles around the elbow joint could generate elbow flexion torque. The figure showed that the brachioradialis also contributed to part of the flexion torque for this movement.

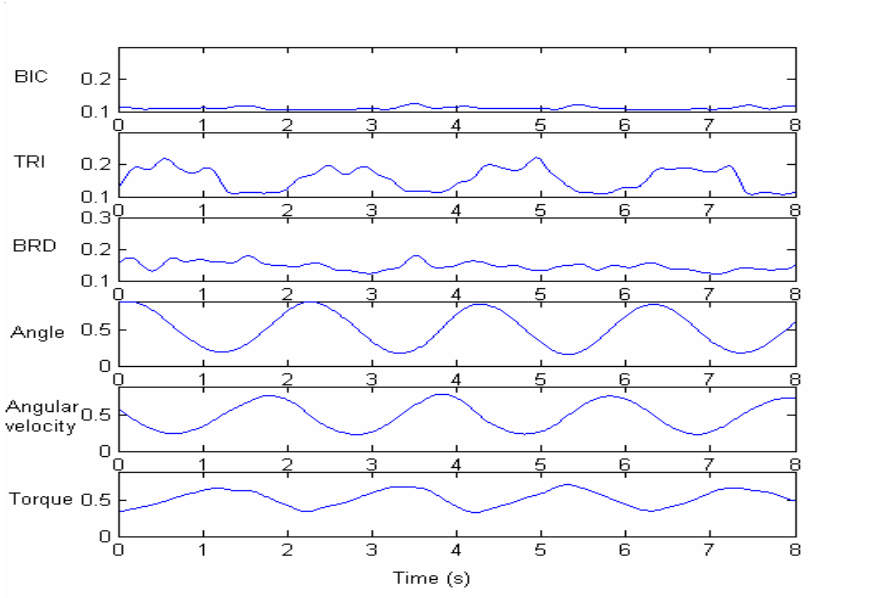

Fig. 3.1 Experimental data recorded during a single trial in which the subject performed elbow flexion and elbow extension with a 1-kg load on the top of the handle and guided by a metronome at the frequency of 1 Hz. BIC=the normalized EMG magnitudes of biceps brachii; TRI=the normalized EMG magnitudes of triceps brachii; BRD=the normalized EMG magnitudes of brachioradialis; Torque= expected torque in this trial.

Subject	Range (N.m)	Training set			Test set		
		RMSE (N.m)	Relative error	R	RMSE (N.m)	Relative error	R
A	6.85	0.17	2.48%	0.98	0.31	4.53%	0.92
B	6.36	0.22	3.46%	0.96	0.45	7.08%	0.95
C	7.08	0.15	2.12%	0.98	0.36	5.08%	0.92
D	4.92	0.14	2.85%	0.96	0.29	5.89%	0.94
E	6.32	0.18	2.85%	0.97	0.30	4.70%	0.90
F	4.26	0.14	3.29%	0.95	0.36	8.45%	0.87
Mean	5.96	0.17	2.84%	0.97	0.35	5.96%	0.92
Standard deviation	1.12	0.03	0.50%	0.01	0.06	1.54%	0.03

Table 3.1 Absolute RMSE, relative error of the RANN predictions and the cross-correlation coefficient between the expected value and the predicted value across all the subjects using the RANN model with EMG and kinematic inputs. (Torque range= Max. flexion torque-Max. extension torque, average relative error=RMSE/average range; R=cross-correlation coefficient)

3.1.1.1 RANN model with the EMG and kinematic inputs

The surface EMG signals of the three muscles, together with elbow angle and angular velocity, were used to predict the elbow torque when performing voluntary elbow flexion and elbow extension. Fig. 3.2 (a, b, and c) showed a typical predicted torque with different loads from a subject when the frequency of the guided sound was 0.67 Hz. Fig. 3.2 (d, e, and f) showed the predicted torque with different loads at a higher speed from the subject. The frequency of the guided sound was 1 Hz. Table 3.1 summarized the results which included the root mean square error (RMSE), the range of the predicted torque, the relative error, and the cross-correlation coefficient between the expected value and the predicted value. The relative error was computed by dividing the RMSE by the range of the torque, and the range was computed by evaluating the difference between the maximum and the minimum predicted torque from each subject. From Table 3.1, the RMSE between the expected torque and the predicted torque of the model with EMG and the joint kinematics inputs in the training and test data were 0.17±0.03 Nm and 0.35±0.06 Nm, respectively. The

average relative errors were 2.84±0.50% in the training data, and 5.96±1.54% in the test data. The average cross-correlation coefficients were 0.97±0.01 in the training data, and 0.92±0.03 in the test data.

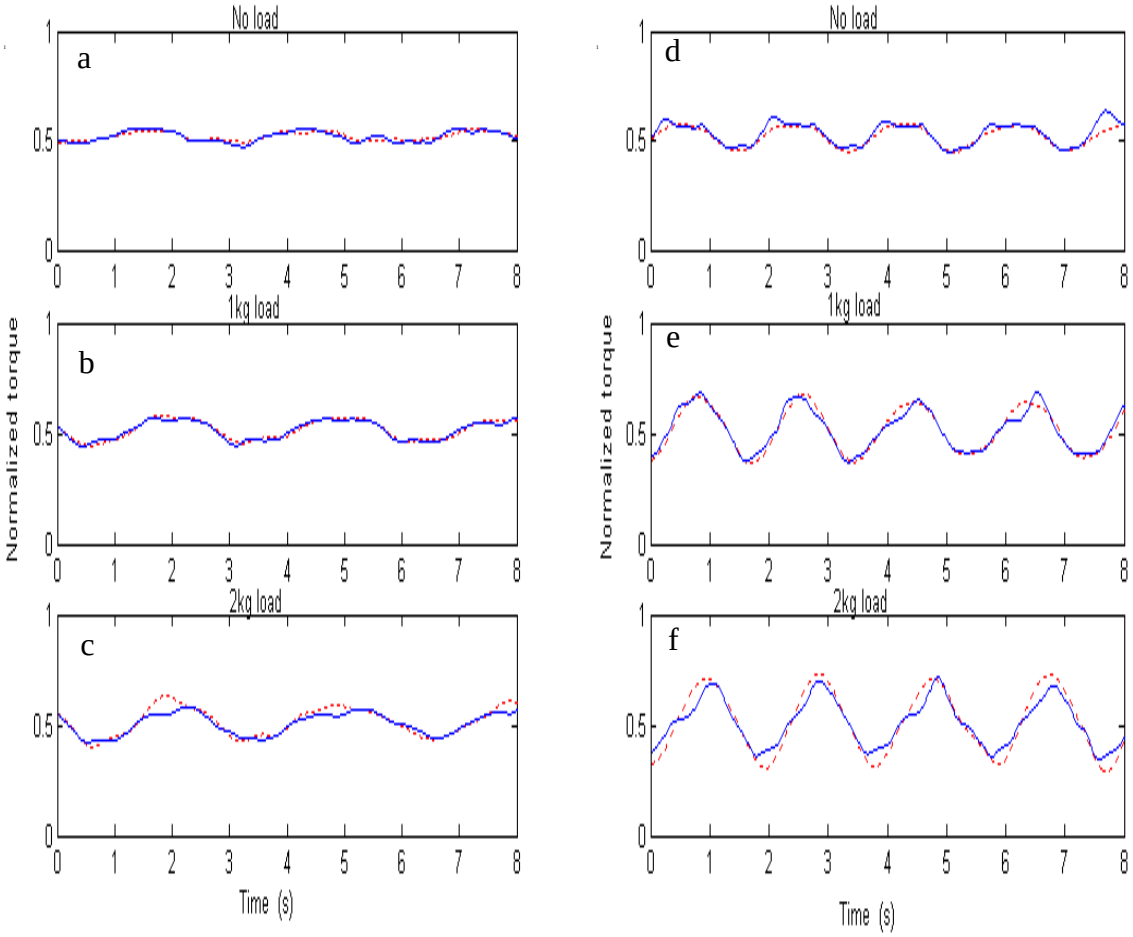

Fig. 3.2 Comparison of the predicted joint torque and the expected torque from the test results of the model with EMG and kinematic inputs. The solid curves were the predicted results from RANN model and the dashed lines were the expected torque calculated from the inverse dynamic model. The frequency of guided sound of a, b, c was 0.67 Hz and the frequency of guided sound of d, e, f was 1 Hz; a, d showed the data with no load; the data with a 1-kg load were showed in b, e; c, f showed the data with a 2-kg load.

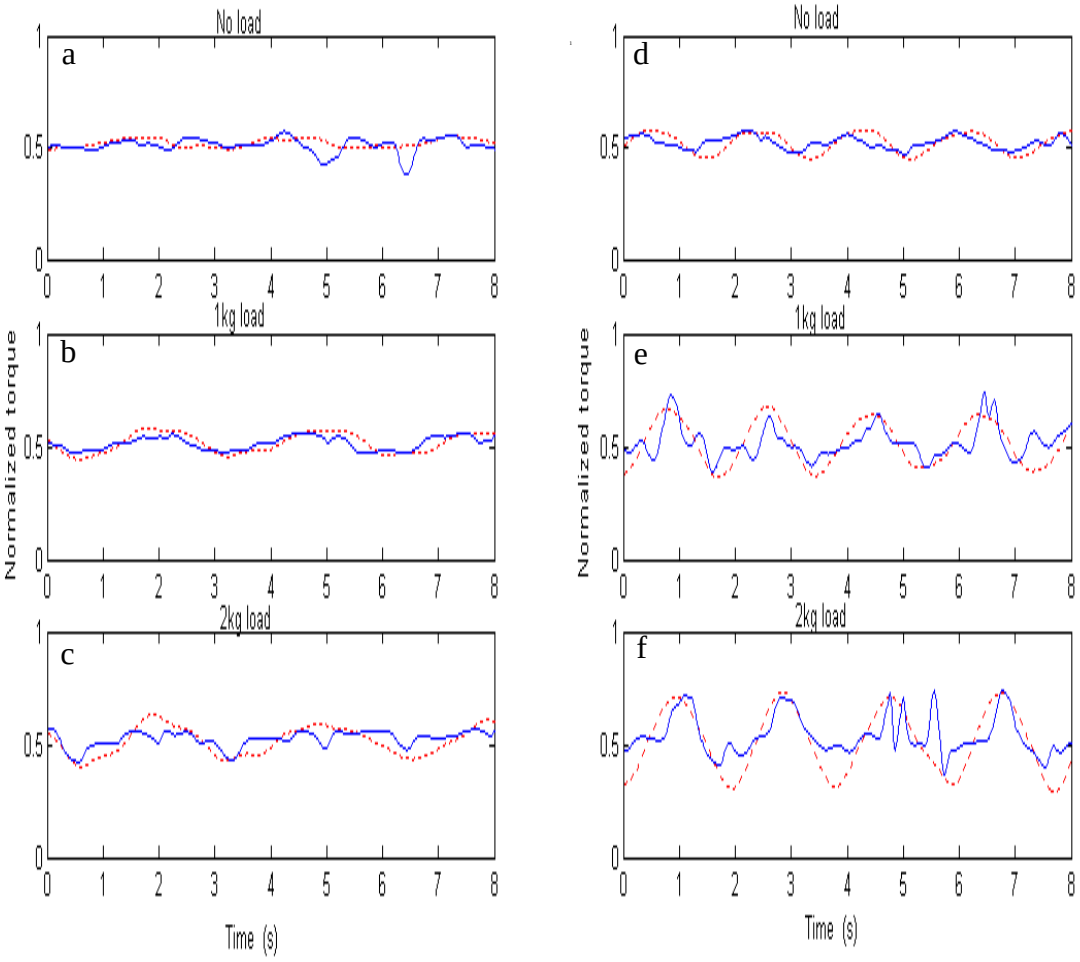

Fig. 3.3 Comparison of the predicted joint torque and the expected torque from the test results of the model with only EMG inputs. The solid curves were predicted results from RANN model and the dashed lines were the expected torque calculated from the inverse dynamic model. The frequency of guided sound of a, b, c was 0.67 Hz and the frequency of guided sound of d, e, f was 1 Hz; a, d showed the data with no load; b, e showed the data with a 1-kg load; c, f showed the data with a 2-kg load.

3.1.1.2 RANN model with only EMG inputs

Table 3.2 showed the RMSE, the range of the predicted torque, the relative error of the elbow torque and the cross-correlation coefficient between the expected value and the predicted value of the model with only EMG inputs. From Table 3.2, the RMSE value between the expected torque and the predicted torque in the training and test data were 0.57±0.07 Nm and 0.73±0.11 Nm, respectively, and the average relative errors were 9.72±1.72% in the training data, and 12.42±2.01% in the test data. The average cross-correlation coefficients were 0.68±0.16 in the training data, and 0.60±0.11 in the test data. Fig. 3.3 (a, b, and c) showed a typical predicted torque with different loads at a low velocity from a subject (the frequency of the guided sound was 0.67 Hz). Fig. 3.3 (d, e, and f) showed the predicted torque with different loads at a higher velocity from this subject (the frequency of the guided sound was 1 Hz). For all six subjects, the output of the model with EMG and kinematic inputs had higher accuracy than that obtained by only using the EMG signals as inputs. For both the training data and the test data, the RMSE of the RANN model with only the EMG inputs was significantly larger than that of the RANN model with EMG and kinematic inputs, and the cross-correlation coefficient of the RANN model with only the EMG inputs was significantly less than that of the RANN model with EMG and kinematic inputs ($p<0.01$).

Subject	Range (N.m)	Training set			Test set		
		RMSE (N.m)	Relative error	R	RMSE (N.m)	Relative error	R
A	6.85	0.49	7.15%	0.89	0.80	11.68%	0.66
B	6.36	0.59	9.27%	0.68	0.75	11.79%	0.60
C	7.08	0.65	9.18%	0.73	0.80	11.30%	0.68
D	4.92	0.50	10.16%	0.41	0.52	10.56%	0.40
E	6.32	0.64	10.12%	0.72	0.82	12.97%	0.71
F	4.26	0.53	12.44%	0.65	0.69	16.20%	0.56
Mean	5.96	0.57	9.72%	0.68	0.73	12.42%	0.60
Standard deviation	1.12	0.07	1.72%	0.16	0.11	2.01%	0.11

Table 3.2 Absolute RMSE, relative error of the RANN predictions and cross-correlation coefficients between the expected value and the predicted value across all the subjects using the RANN model with only EMG inputs. (Torque range= Max. flexion torque-Max extension torque, average relative error=RMSE /average range; R= cross-correlation coefficient)

3.1.1.3 Movement without the guidance of metronome

Subject C also performed an additional movement in order to validate if the model with EMG and kinematic inputs was robust enough to estimate the output torque of the movement beyond the guided frequencies. The trials which were used to train the RANN model with EMG and kinematic inputs were the same as the former models, and then the trained RANN model was applied to estimate the movement without the guidance of a metronome. Different kinds of loads were also applied to the forearm during the movements. Fig. 3.4 showed the results of the predicted torque of the model and the expected torque with 0-kg, 1-kg and 2-kg loads. The trained RANN model could also have a good prediction without the guidance of a metronome. The RMSE values between the expected torque and the predicted torque of the movement with 0-kg, 1-kg and 2-kg loads were 0.4290, 0.4308 and 0.9030 Nm, respectively. The torque range was 10.67 Nm, and the relative errors of this test were 4.02%, 4.03%, and 8.47%, respectively. The cross-correlation coefficients between the predicted torque and the expected torque of the movement with 0-kg, 1-kg and 2-kg loads were 0.89, 0.93, and 0.96, respectively. The relative errors and the cross-correlation coefficients were comparable with the predicted data within the guided frequencies.

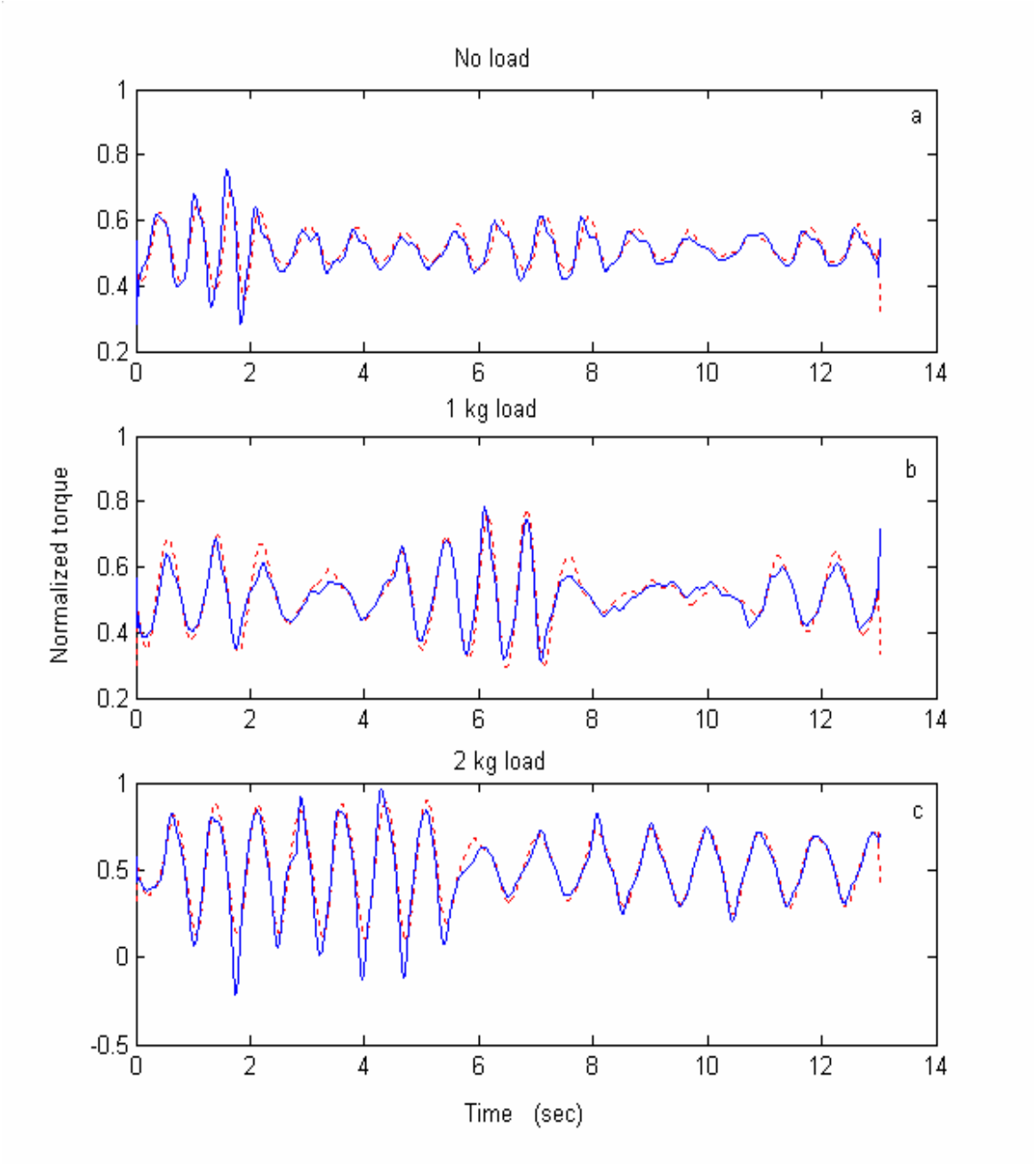

Fig. 3.4 Comparison of the actual joint torque and the predicted torque from the test results of the model with kinematics and EMG inputs. The solid curves were the predicted results from the RANN model and the dashed line was the expected torque calculated from the inverse dynamic model. The subject was asked to perform an arbitrary movement without the guidance of the metronome and with different kinds of loads (0 kg 1 kg, and 2 kg).

3.1.2 RANN model for subjects after stroke

The RANN model was also evaluated on subjects after stroke. The structure of the RANN model was the same with that used for the normal subjects. Table 3.3 showed the RMSE, the range of the predicted acceleration, the relative error of acceleration and the cross-correlation coefficient between the expected value and the predicted value of the model with EMG and kinematic inputs. Fig. 3.5 plotted the test results of the predicted acceleration from the RANN model and the expected acceleration at different velocities (a: 10 deg/s, b: 20 deg/s, c: 30 deg/s, d: 40 deg/s, e: 50 deg/s, and f: 60 deg/s). The relative errors of this test were 12.49%, 11.67%, and 8.29%, which were larger than the results from the normal subjects. The average cross-correlation coefficients were 0.72±0.10 in the training data, and 0.41±0.07 in the test data.

Subject	Range(deg/s^2)	Training set			Test set		
		RMSE (deg/s^2)	Relative error	R	RMSE (deg/s^2)	Relative error	R
A	1539.4	112.2	7.29%	0.69	192.3	12.49%	0.37
B	1471.0	96.9	6.59%	0.83	171.7	11.67%	0.49
C	1534.4	123.9	8.88%	0.65	127.2	8.29%	0.38
Mean	1514.9	111.0	7.59%	0.72	163.7	10.82%	0.41
Standard deviation	38.12	13.54	1.17%	0.10	33.27	2.23%	0.07

Table 3.3 Absolute RMSE, relative error of the RANN predictions and cross-correlation coefficient between the expected value and the predicted value across all the subjects after stroke using the RANN model with EMG and kinematic inputs. (Range= Max. flexion acceleration- Max extension acceleration, average relative error=RMSE /average range; R=cross-correlation coefficient)

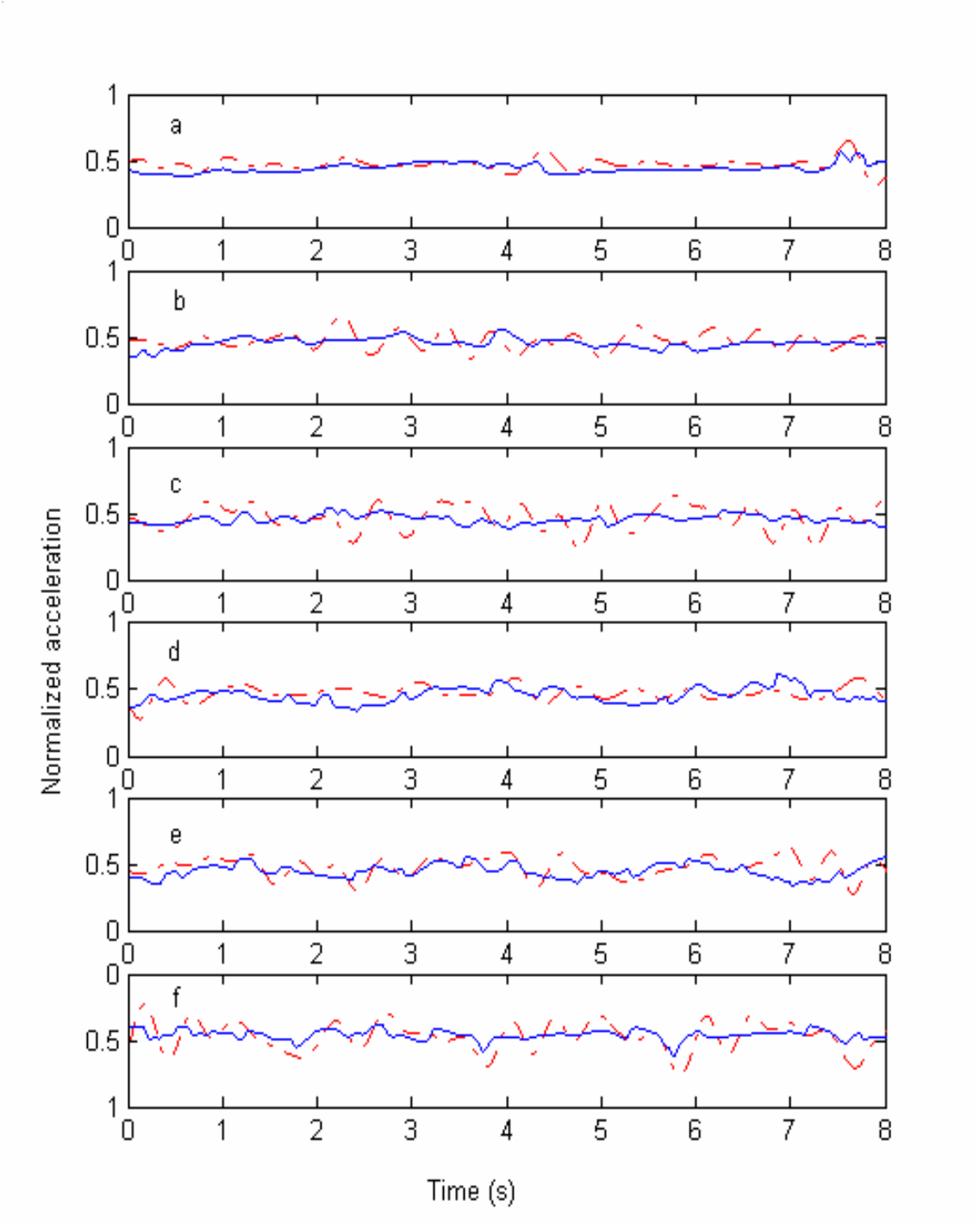

Fig. 3.5 Comparison of the actual acceleration and the expected acceleration from the test result of the model with kinematics and EMG inputs. The solid curve was the predicted result from RANN model and the dashed line was the expected acceleration (a: 10 deg/s, b: 20 deg/s, c: 30 deg/s, d: 40 deg/s, e: 50 deg/s, and f: 60 deg/s).

3.2 Myoelectric control of the robotic system

A myoelectrically controlled robotic system was evaluated on subjects after stroke. The control strategy was based on the proportional control, since the EMG was related to the muscle torque and could provide reliable control. The effects of the system with different combinations of the EMG-torque gain and resistive load on the movement performance were investigated. Nine subjects after stroke participated in the test which could be divided into two categories depending on their elbow extension ranges. The moderate group was composed of six subjects who had an extension range larger than 30 deg, while the severe group was composed of three subjects who could not extend their elbow to a more extended position that 60 deg (the extension range was less than 30 deg) without the assistance of the robotic system. Different combinations of load and gain were applied to the moderate group and only different gains were applied to the severe group. No load was applied to the severe group, since they had difficulty in extending their elbows even without the load. Table 3.4 summarized the clinical data together with the MIVE and MIVF torques and voluntary extension range of all the subjects after stroke. The MIVE and MIVF torques of these subjects were measured by the torque sensor in the robotic system which worked in the position mode as a dynamometer. The mean MIVE and MIVF torques for all the subjects were 7.31±6.66 Nm and 13.63±5.22 Nm, respectively, which were measured when the elbow was at 90 deg. If the subject could not generate any torque, or the torque was generated in the direction opposite of the intended direction, then the MIVE or MIVF torque was assumed to be zero in the calculation. Two of the severely affected subjects could not generate any extension torque when the elbow was at 90 deg.

Subject	Age/ (Sex)	Lesion side	Years after stroke	Ashworth scale	MIVE torque (N.m)	MIVF torque (N.m)	Level	Extension range (deg)
A	52(M)	L	6 yrs	2	18.8	17.0	moderate	35.2
B	46 (M)	R	5 yrs	1+	10	17.2	moderate	52.0
C	42(M)	L	3 yrs	2	0.6	19.4	severe	16.3
D	46 (F)	L	2 yrs	1	7.2	9.6	moderate	86.9
E	49 (M)	L	1 yrs	1+	8.6	13.1	moderate	51.3
F	53 (F)	R	8 yrs	1+	5.6	10.1	moderate	49.8
G	39 (M)	R	11 yrs	1+	15.0	21.6	moderate	72.8
H	26(M)	R	3 yrs	3	NA	8.6	Severe	0
I	55(F)	L	1 yrs	1	NA	5.3	Severe	0

Table 3.4 Clinical data together with the MIVE torque, MIVF torque and the voluntary extension range of all the subjects after stroke. NA: subject could not generate any torque or generate a torque in the direction opposite of the intended direction.

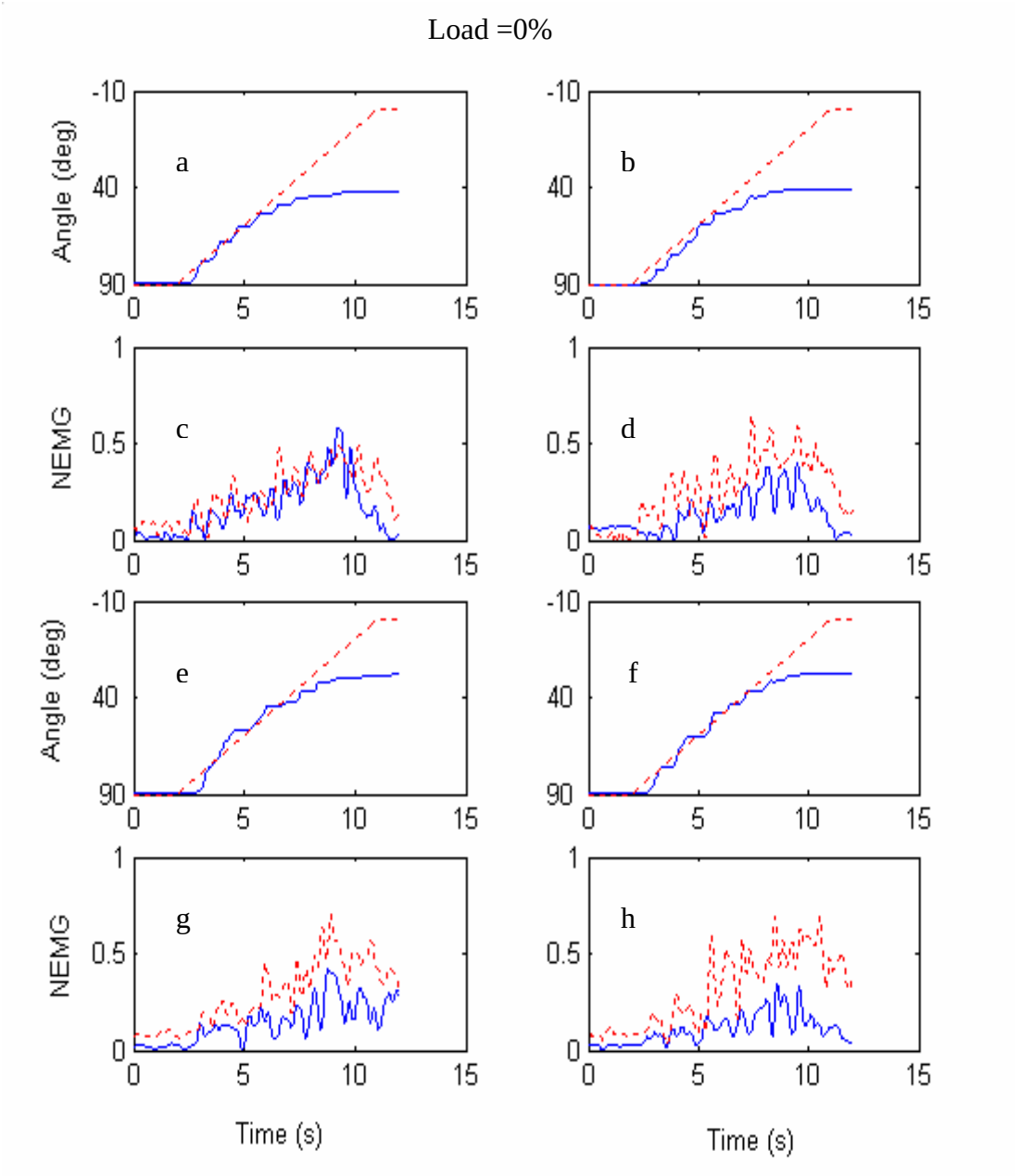

Fig. 3.6 The elbow trajectories and the NEMG signals of a moderately affected subject during the voluntary elbow tracking at a velocity of 10 deg/s when the load was equal to 0%. The dotted lines in a, b, e, f were the target trajectories; the solid lines in a, b, e, f were the elbow trajectories; the dotted lines in c, d, g, h were the NEMG of biceps; the solid lines in c, d, g, h were the NEMG of triceps (a and c: gain=0%, b and d: gain=50%, e and g: gain=100%, f and h: gain=150%).

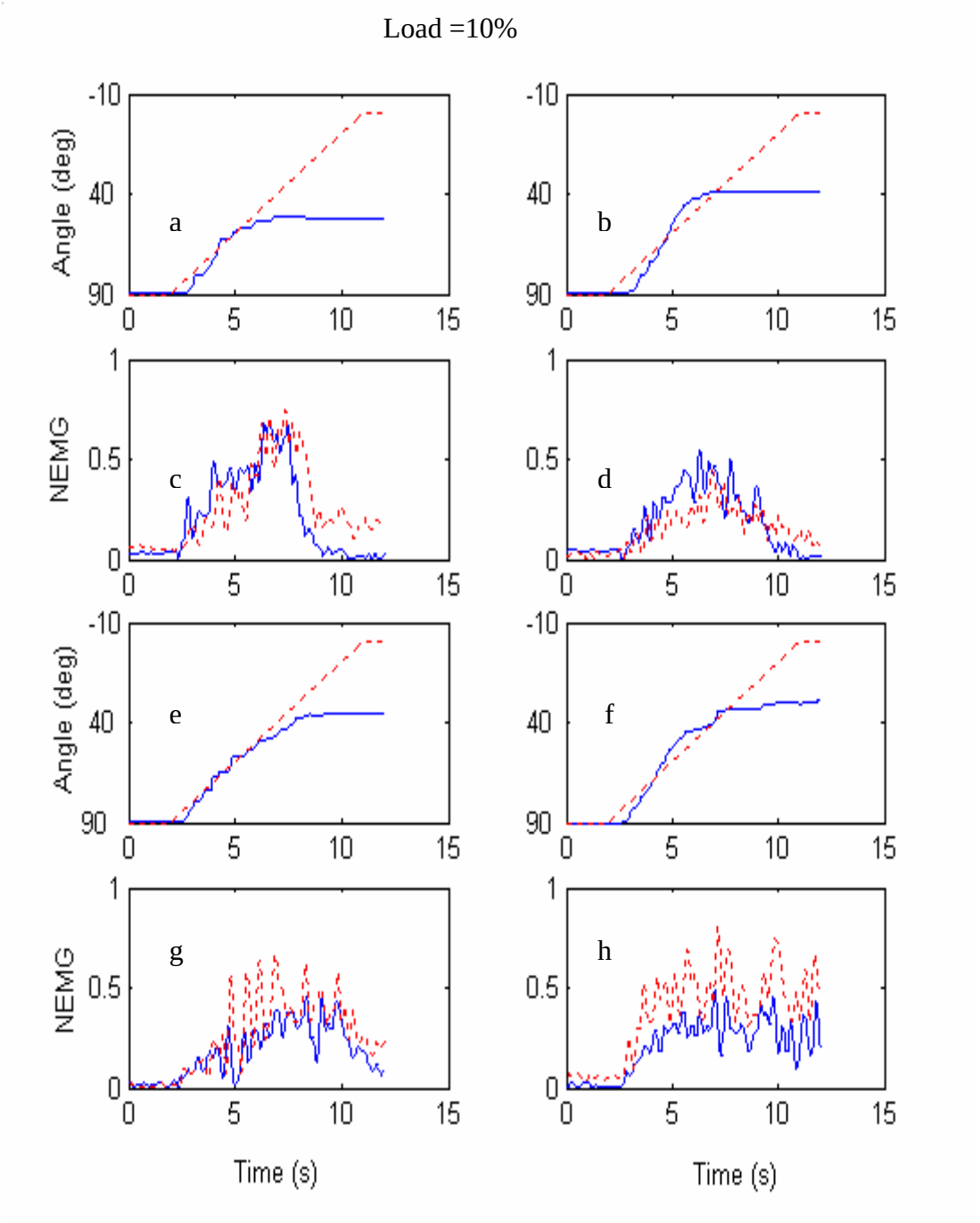

Fig. 3.7 The elbow trajectories and the NEMG signals of a moderately affected subject during the voluntary elbow tracking at a velocity of 10 deg/s when the load was equal to 10%. The dotted lines in a, b, e, f were target trajectories; the solid lines in a, b, e, f were the elbow trajectories; the dotted lines in c, d, g, h were NEMG of biceps; the solid lines in c, d, g, h were NEMG of triceps (a and c: gain=0%, b and d: gain=50%, e and g: gain=100%, f and h: gain=150%).

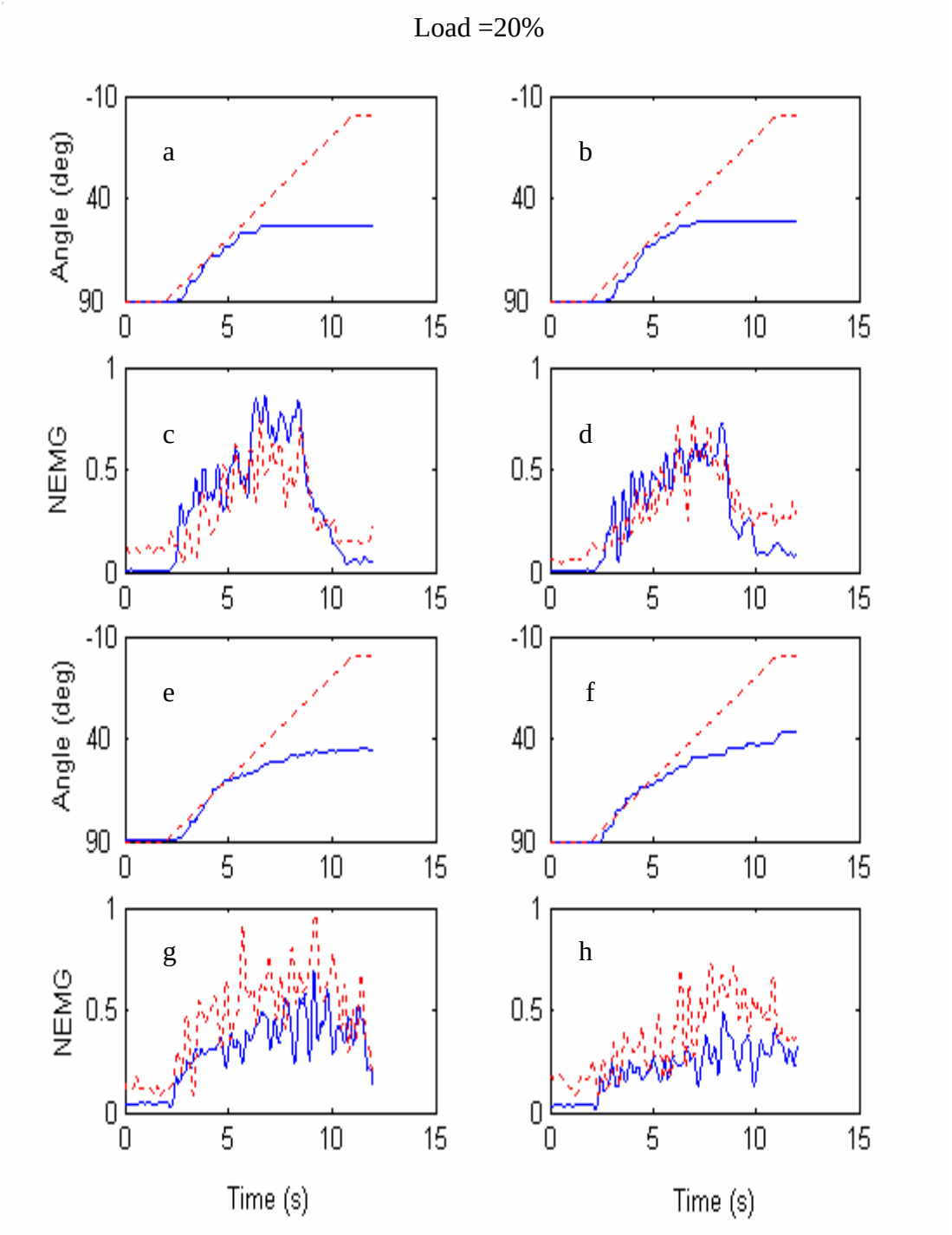

Fig. 3.8 The elbow trajectories and the NEMG singals of a moderately affected subject during the voluntary elbow tracking at a velocity of 10 deg/s when the load was equal to 20%. The dotted lines in a, b, e, f were target trajectories; the solid lines in a, b, e, f were the elbow trajectories; the dotted lines in c, d, g, h were NEMG of biceps; the solid lines in c, d, g, h were NEMG of triceps (a and c: gain=0%, b and d: gain=50%, e and g: gain=100%, f and h: gain=150%).

3.2.1 Results of the moderate group

Fig. 3.6-3.8 plotted the trajectories and EMG activations of a moderately affected subject after stroke at different combinations of resistive loads (0%, 10%, and 20% MIVE) and gains (0%, 50%, 100% and 150%). From Fig. 3.6-3.8, results showed that the subject after stroke had difficulty in extending his/her elbow without any assistance, but with the assistance from the robotic system, a larger extension range could be achieved. With the increase in the gain, there was a decrease in the amplitude of the normalized triceps signal, and with increase in the load, there was an increase in the amplitude of the normalized triceps signal. For the biceps EMG signals, no obvious trend was observed with the changes in the gain and load. The results of movement performance were analyzed in terms of the extension range, RMSE between the actual elbow angle and the target trajectory, root mean square jerk (RMSJ), the normalized EMG (NEMG) signals of biceps and triceps.

3.2.1.1 Extension range

Fig. 3.9 plotted the group mean extension range of the moderate group against different gains and loads. The extension range increased with the increase in the gain. All three loading conditions had a similar trend. The maximum mean extension range was 63 deg which was generated when the gain equaled 150% and the load equaled zero. The two–way analysis of variance (ANOVA) with repeated measures showed that there was a significant main effect of the gain on the extension range ($P<0.001$), but no significant main effect of the load was found on the extension range ($P=0.948$), and there was also no significant gain-by-load interaction ($P=0.248$). The pairwise comparisons of extension range among different combinations of the gain showed that there were significant differences of extension range in all the pairwise comparisons except for the comparison between 100% and 150% of the gain, which showed that with the assistance of the robotic system, subjects after stroke could reach a more extended position (Table 3.6).

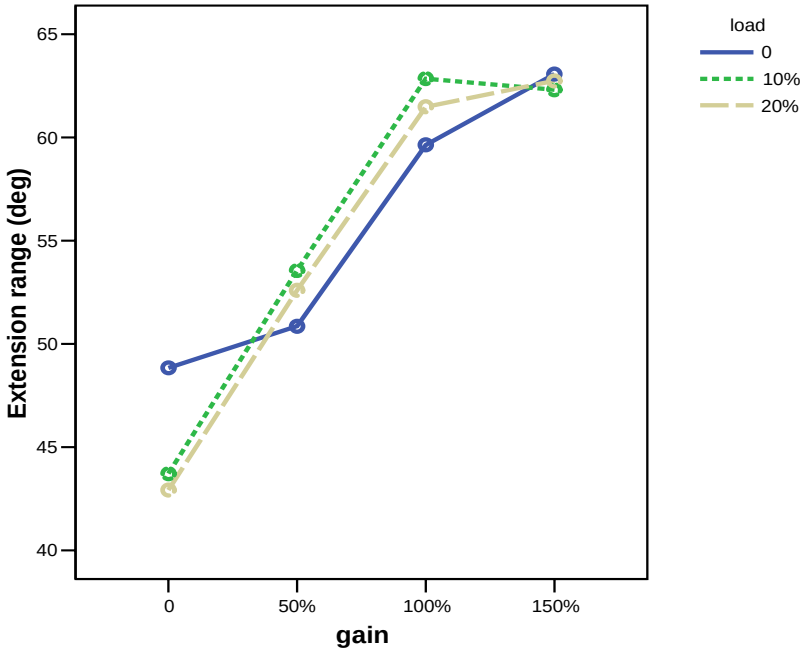

Fig. 3.9 Comparison of the group mean extension range at four different gains among three different loads.

	Load	0 %	10%	20%
RMSE	0	-----	NS	**
	10 %		-----	**
	20%			-----
RMSJ	0	-----	*	*
	10 %		-----	NS
	20%			-----
TRI	0	-----	*	*
	10 %		-----	*
	20%			-----

Table 3.5 Pairwise comparisons of the RMSJ, RMSE and the NEMG of triceps (TRI) among different loads for moderate group. Two-way ANOVA with repeated measures was used for the pairwise comparisons. (*: P<0.05; **: P<0.01; NS: P>0.05)

	Gain	0	50 %	100%	150%
extension range	0	------	*	*	*
	50 %		-----	*	*
	100%			-----	NS
	150 %				-----
RMSE	0	------	NS	*	NS
	50 %		-----	NS	NS
	100%			-----	NS
	150 %				-----
RMSJ	0	------	*	**	**
	50 %		-----	**	**
	100%			-----	*
	150 %				-----
TRI	0	------	*	*	*
	50 %		-----	*	**
	100%			-----	*
	150 %				-----

Table 3.6 Pairwise comparisons of the extension range, RMSJ, RMSE and the NEMG of triceps (TRI) among different gains for moderate group. Two–way ANOVA with repeated measures was used for the pairwise comparisons. (*: $P<0.05$; **: $P<0.01$; NS: $P>0.05$)

3.2.1.2 Performance indices

In order to evaluate the movement performance, the RMSE between the target and the elbow angle, the RMSJ of the elbow trajectory and the NEMG of the biceps and the triceps were analyzed on the moderately affected subjects after stroke when the elbow angle was within 90-60 deg, since most of these subjects could reach a more extended position than 60 deg under all the combinations of gains and loads. The data for one subject were excluded from the analysis since he could not reach 60 deg under some combinations.

Fig. 3.10 plotted the group mean RMSE of the subjects against the different gains and loads. The two–way repeated ANOVA showed that there was a significant main effect

of the gain and load on the RMSE ($P<0.05$), but no significant gain-by-load interaction on the RMSE was found ($P=0.073$). The pairwise comparisons of the RMSE among different gains showed that there was a significant difference in the RMSE between 0% and 100% of the gain ($P<0.05$), while no significant differences in the other pairwise comparisons could be observed (Table 3.6). The pairwise comparisons of the RMSE among different loads showed that there was no significant difference in the RMSE between 0% and 10% of the load and there were significant differences in the other pairwise comparisons ($P<0.01$, Table 3.5). The results showed that it seemed more difficult for subjects to control their elbows with the increase in the load, while the increase in the gain did not cause the deterioration in the control of elbow.

Fig. 3.11 plotted the group mean RMSJ of the subjects at the different gains and loads. The RMSJ increased with the increase in the gain. The RMSJ also increased with the increase in the load. The two-way repeated ANOVA showed that there was a significant main effect of the gain and load on the RMSJ ($P<0.01$ and $P<0.001$, respectively), but there was no significant effect of gain by load interaction on the RMSJ ($P=0.148$). The pairwise comparisons of the RMSJ among different gains showed that there was a significant difference in all the pairwise comparisons (Table 3.6). The pairwise comparisons of the RMSJ among different loads showed that there was no significant difference of the RMSJ between 10% and 20% of the load and there was a significant difference in other pairwise comparisons ($P<0.05$, Table 3.5). The significant increase in the RMSJ reflected that the trajectory was less smooth with the increase in the gain and the load.

Fig. 3.12 plotted the group mean NEMG of biceps with the different gains and loads. The two-way repeated ANOVA showed that there was no significant main effect of the gain and load on the NEMG of biceps ($P>0.05$), and there was also no significant effect of gain-by-load interaction on the NEMG of biceps ($P=0.261$).

Fig. 3.13 plotted the group mean NEMG of triceps with different gains and loads. With the increase in the gain, the NEMG of triceps decreased, and the NEMG of triceps also increased with the increase in the load. The two-way repeated ANOVA showed that there was a significant main effect of the gain and load on the NEMG of triceps ($P<0.001$), and that there was no significant gain-by-load interaction on the NEMG of triceps ($P>0.05$). From Tables 3.5 and 3.6, there was a significant

difference in all the pairwise comparisons of the NEMG of triceps among different gains and loads. The significant decrease of the NEMG of triceps with the increase in the gain reflected that less effort is needed for subjects after stroke to perform elbow extension with a larger gain, and the significant increase in the NEMG of triceps with the increase in the load reflected that more effort was needed for subjects after stroke to perform elbow extension with a larger load.

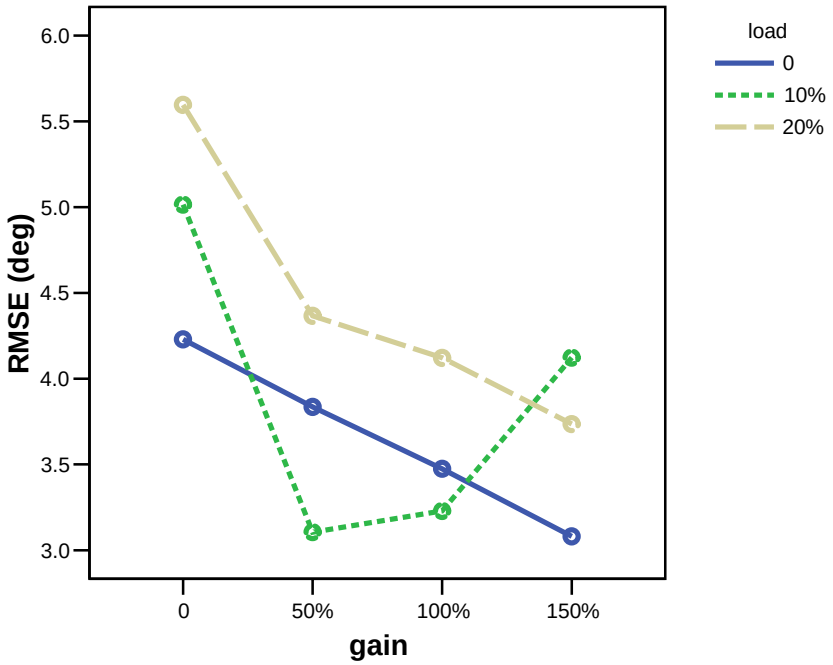

Fig. 3.10 Comparison of the group mean RMSE at four different gains among three different loads.

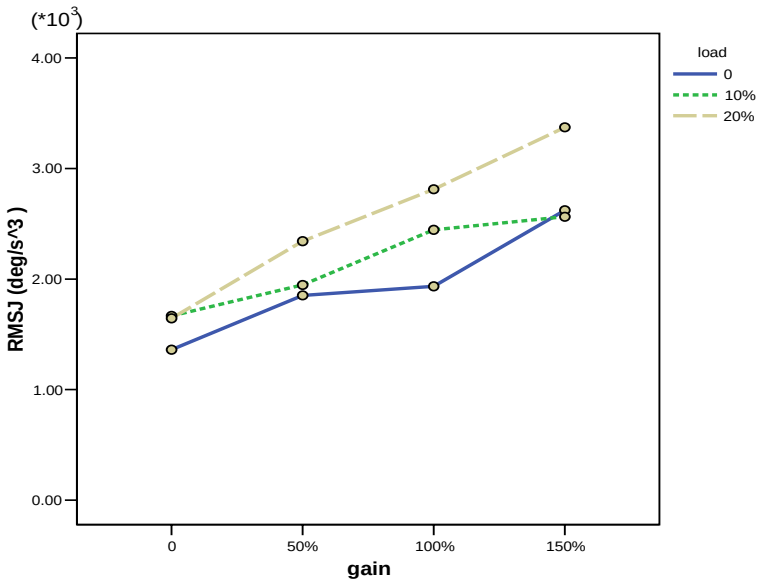

Fig. 3.11 Comparison of the group mean RMSJ at four different gains among three different loads.

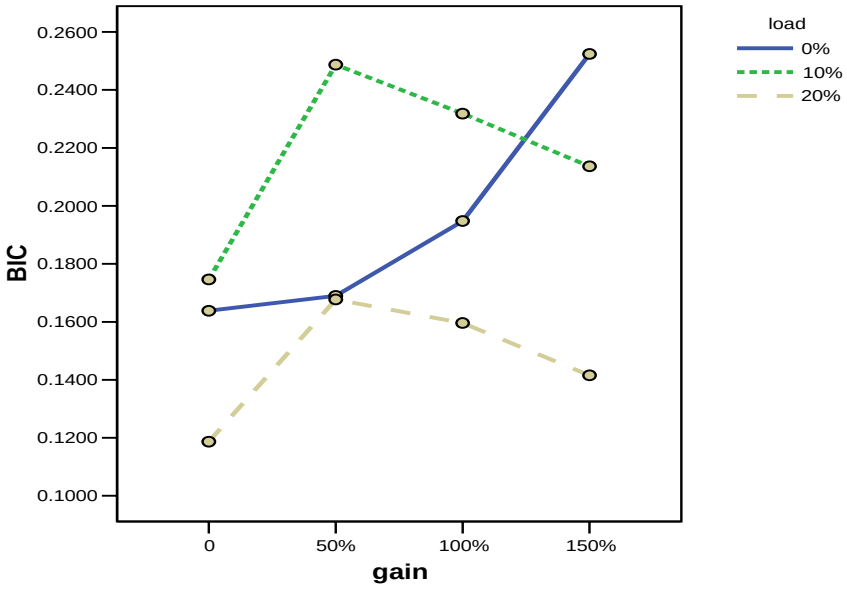

Fig. 3.12 Comparison of the group mean NEMG of biceps at four different gains among three different loads.

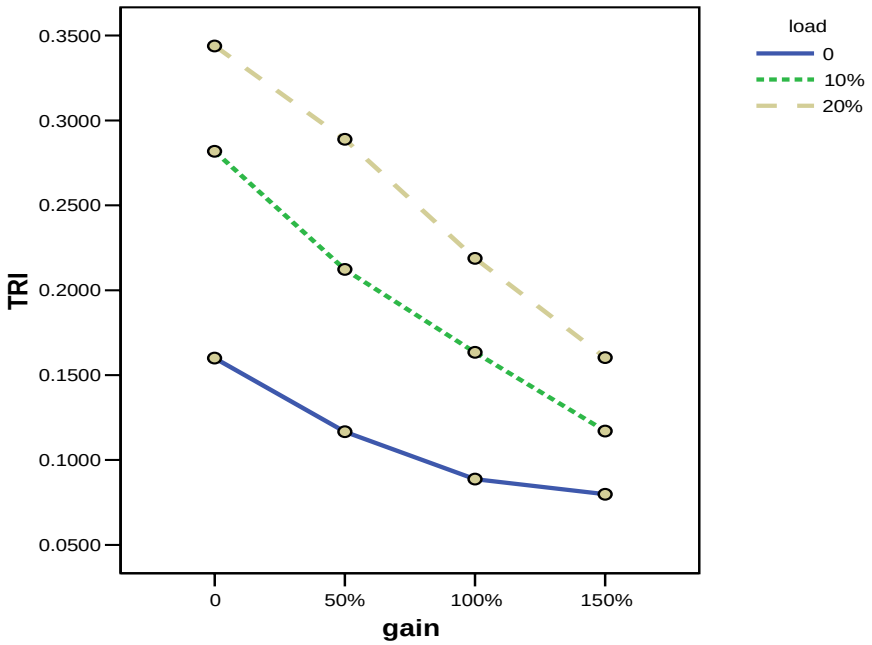

Fig. 3.13 Comparison of the group mean NEMG of triceps at four different gains among three different loads.

3.2.2 Results of severely affected subjects

The arm tracking test with the assistance of the myoelectrically controlled robotic system was also conducted on three severely affected subjects after stroke. No load was added to the elbow during the movement of the three severely affected subjects. Fig. 3.14 plotted the tracking trajectories of subject C when the gain was equaled to 0% and 150%. There was an increase of 7 deg in the extension range when the gain was 150% in comparison to that without the help of the system (gain=0%). The other two subjects could not extend their elbow by themselves without the help of the robotic system; with the assistance of the robotic system, the two subjects could manipulate their elbows to track the target with an extension range of 7 deg and 44 deg, respectively.

In section 3.2, the performance of the myoelectrically controlled robotic system was investigated when helping different levels of subjects after stroke to perform the arm tracking test during the elbow extension. Another objective of this experiment was to find suitable setting parameters for the rehabilitation training at the next stage. From

the results, when the gain was equaled to 150%, there was no further improvement in the RMSE and the extension range (Fig. 3.9 and Fig. 3.10). Therefore, 150% of the gain was not selected for the rehabilitation training at next stage.

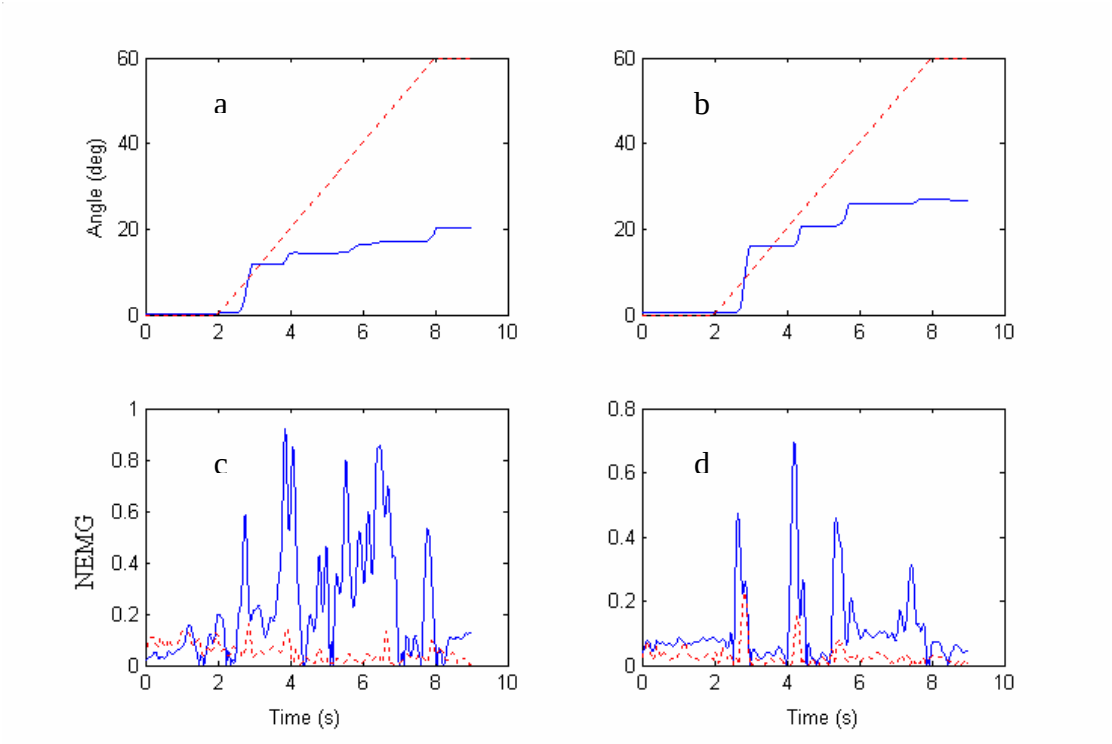

Fig. 3.14 The elbow trajectory and the NEMG signals of biceps and triceps from a severely affected subject during the voluntary elbow tracking at a velocity of 10 deg/s. The left column was the movement when load was equal to 0% and gain was equal to 0%, the right column was the movement when the load was equal to 0% and the gain was equal to 150%; the dotted lines in a and b were the target trajectories; the dotted lines in c and d were the NEMG of biceps; the solid lines in c and d were the NEMG of triceps.

3.3 Functional evaluation using the elbow tracking system

In this section, the tracking experiment was designed to quantitatively compare the difference between the affected and the unaffected arms of subjects after stroke in dynamic situations. Fig. 3.15 showed the actual elbow trajectories of the unaffected and the affected arm of a subject after stroke in the three trials at the six tracking velocities. The target trajectories at the six tracking velocities were also shown in this

figure as references. Results showed that the trajectories of the unaffected arm seemed smoother than that of the affected arm. In addition, a longer delay was observed in initiation of the movement of the affected arm than that of the unaffected arm at the velocities of 30, 40, 50 and 60 deg/s. Fig. 3.16 showed the elbow angular trajectory, velocity, acceleration and jerk of the affected and the unaffected arm of a subject after stroke at the velocity of 40 deg/s. The results showed that the trajectory from the unaffected arm was smoother than that from the affected arm, which could be shown from the angular velocity, angular acceleration and jerk.

3.3.1 Root mean square error

Fig. 3.17 showed the comparisons of the group mean RMSE between the affected and the unaffected arms against the angular velocity. The mean RMSE values of the unaffected arms were 2.56±0.74, 3.89±1.21, 5.27±2.01, 6.65±2.77, 8.48±4.15, and 11.05±5.03 deg from 10 deg/s to 60 deg/s, respectively; while the RMSE values of the affected arms were 3.75±1.09, 6.17±1.86, 8.54±2.95, 10.43±3.53, 12.23±4.12, and 15.53±5.81 deg from 10 deg/s to 60 deg/s, respectively. There was a monotonic increase in the RMSE for both the affected and the unaffected arms when the tracking velocity increased. The standard deviation also increased with the tracking velocity. The two-way ANOVA with repeated measures showed significant effects of both the side and angular velocity on the RMSE ($P<0.001$). The average RMSE from the affected arms was significantly larger than that from the unaffected arms and there was a significant side-by-velocity interaction ($P<0.01$). The paired t-test comparisons showed that there was a significant increase in the RMSE of the affected arms as compared to those of the unaffected arms at all the velocities ($P<0.05$).

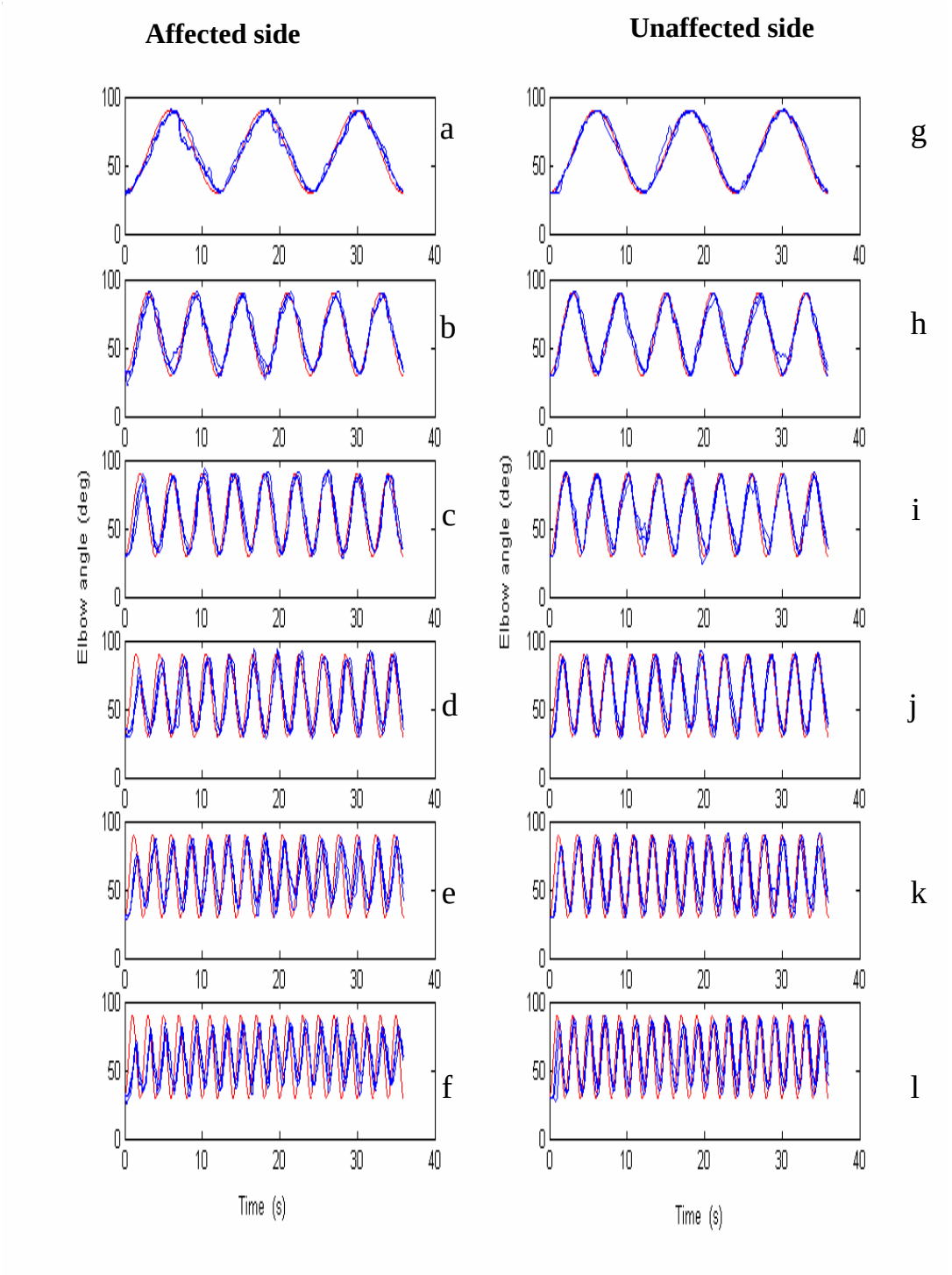

Fig. 3.15 The target (dotted line) and three actual elbow trajectories (solid line) of the affected arm (a, b, c, d, e, and f), and the unaffected arm (g, h, i, j, k, and l) of a stroke subject during the voluntary elbow tracking at different velocities (a, g: 10 deg/s, b, h: 20 deg/s, c, i: 30 deg/s, d, j: 40 deg/s, e, k: 50 deg/s, and f, l: 60 deg/s).

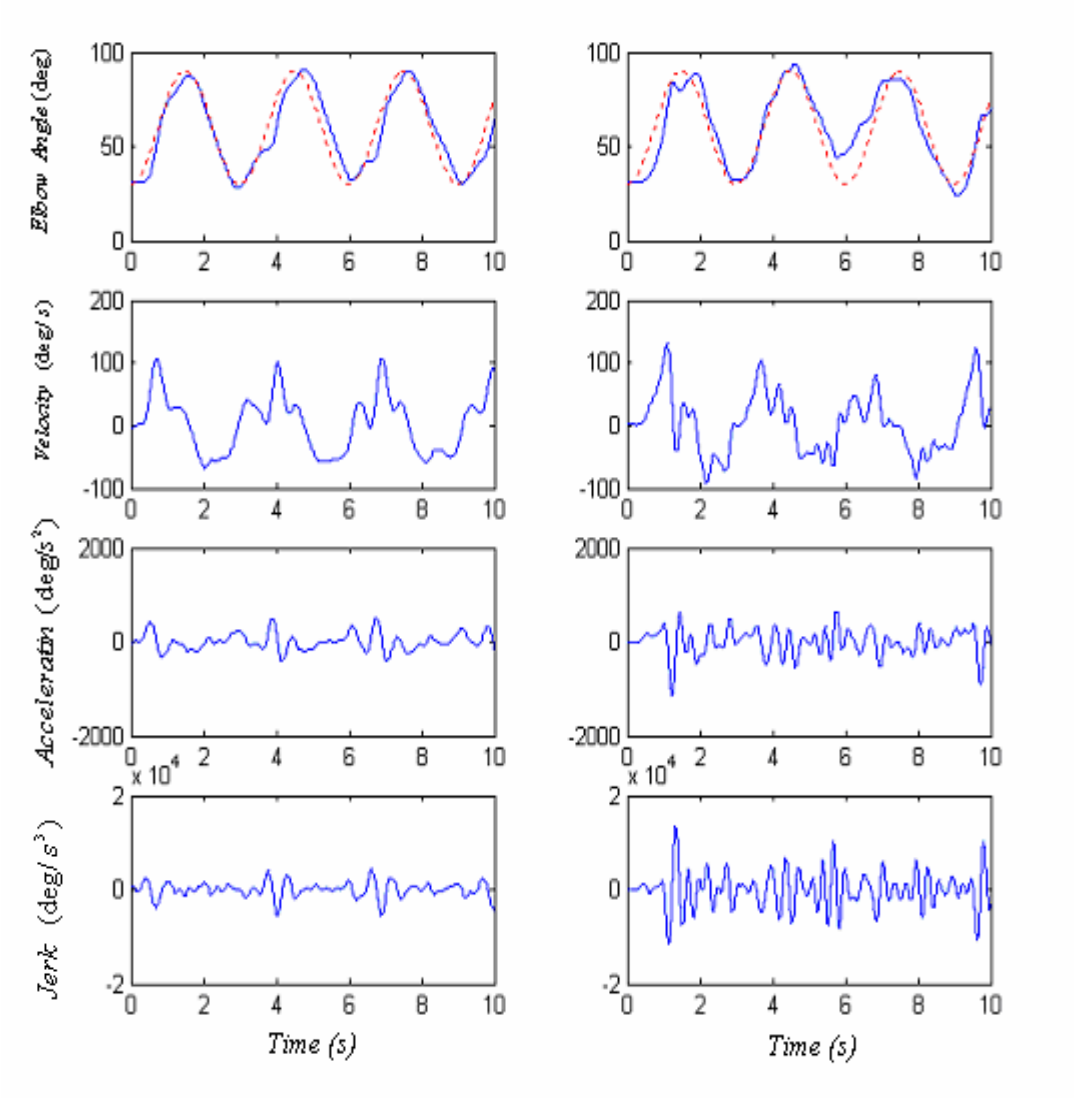

Fig. 3.16 The elbow angle (solid line), angular velocity, angular acceleration and jerk (the third derivatives of the angle) between the unaffected arm (left column), and the affected arm (right column) of a subject after stroke during the voluntary elbow tracking at the velocity of 40 deg/s. The dotted line is the target angle.

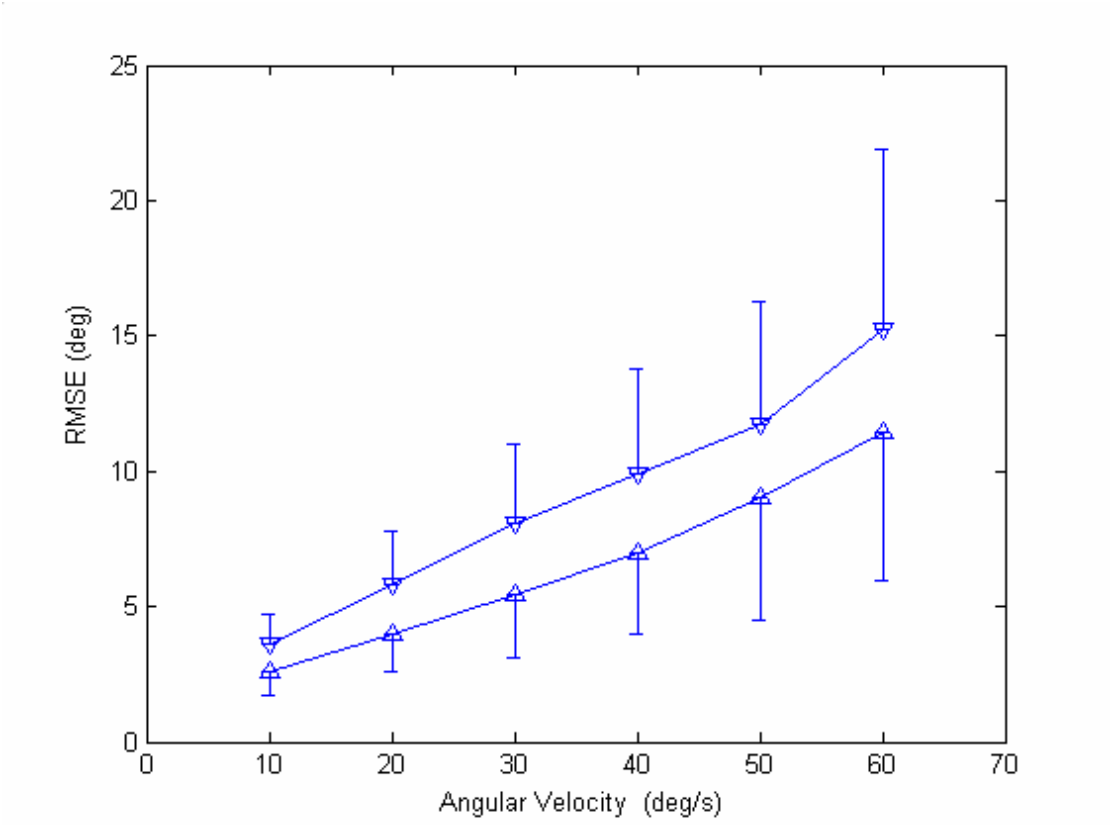

Fig. 3.17 Comparison between the RMSE of the affected (∇) and unaffected (Δ) arm and at six velocities (10, 20, 30, 40, 50 and 60 deg/s) during the elbow tracking movement. Vertical bars indicate standard deviation.

3.3.2 Root mean square jerk

Fig. 3.18 summarized the results of the group mean RMSJ at different velocities. The group mean RMSJ of the unaffected arms were 542±243, 786±286, 1090±429, 1349±469, 1665±637, and 2066±789 deg/s^3 from 10 deg/s to 60 deg/s, respectively, while the group mean RMSJ of the affected arms were 1211±406, 2074±880, 2630±1121, 3101±1293, 3826±1491, and 4223± 1879 deg/s^3 from 10 deg/s to 60 deg/s, respectively. Fig. 3.18 showed that there was a monotonic increase in the RMSJ for both the affected and the unaffected arms with the increase in tracking velocity. The standard deviation also increased with the tracking velocity. The RMSJ from the affected arms was significantly larger than that from the unaffected arms ($P<0.01$). The ANOVA also showed a significant effect of the tracking velocity on the RMSJ ($P<0.001$), and a significant side-by-velocity interaction ($P<0.01$). There was a significant increase in the RMSJ of the affected arms as compared to that of the unaffected arms at all six velocities based on the paired t-test ($P<0.05$), which

reflected the trajectory of the affected arms was less smooth than that of the unaffected arms.

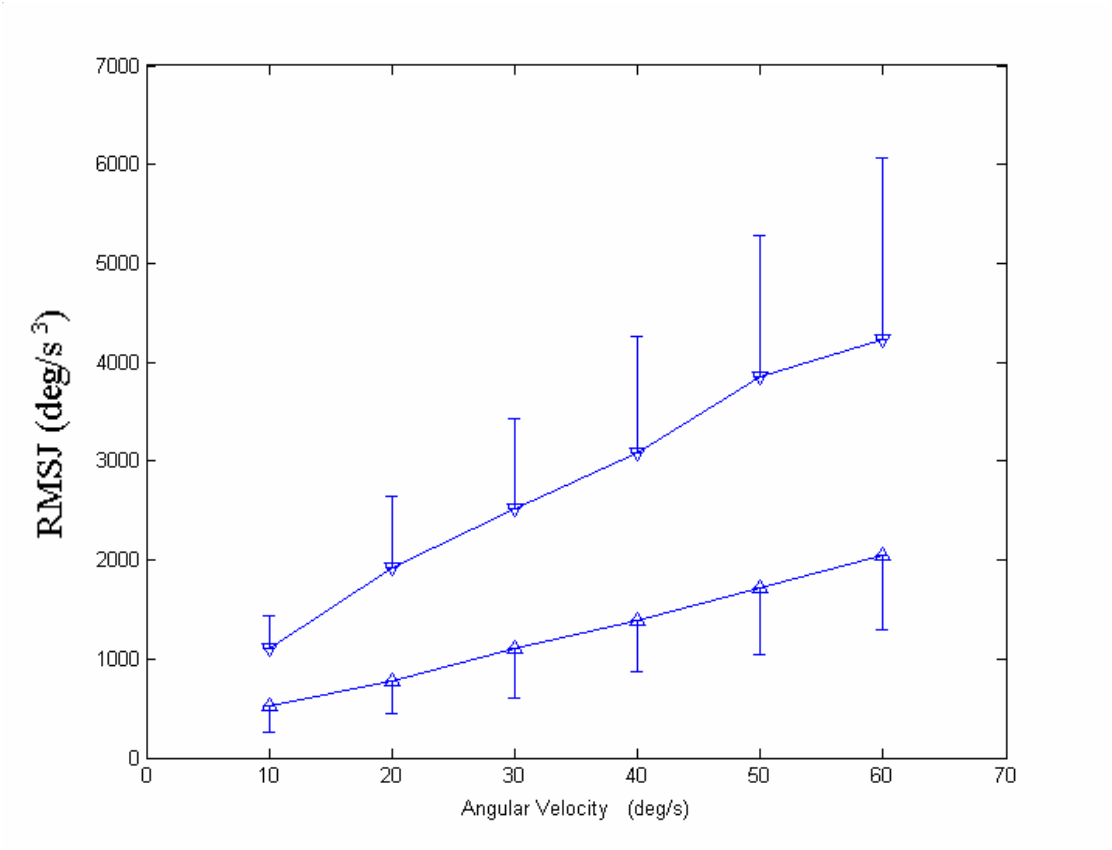

Fig. 3.18 Comparison between the RMSJ of the affected (∇) and unaffected (Δ) arm and at six velocities (10, 20, 30, 40, 50 and 60 deg/s) during the elbow tracking movement. Vertical bars indicate standard deviation.

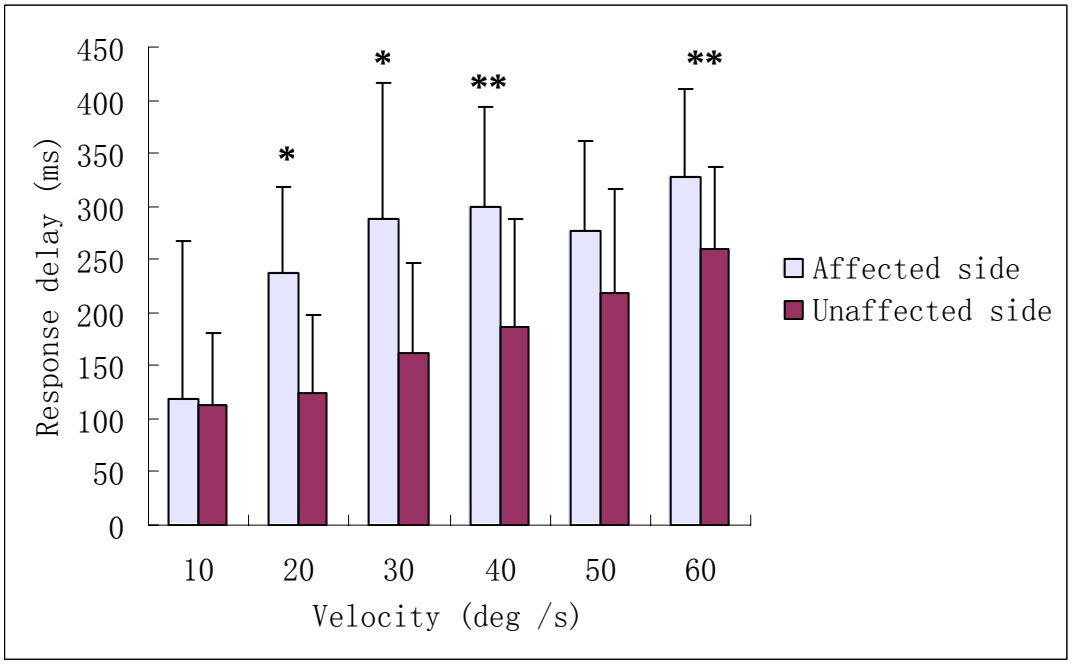

Fig. 3.19 Comparison between the response delay of the affected (∇) and unaffected (Δ) arm and at six velocities (10, 20, 30, 40, 50 and 60 deg/s) during the elbow tracking movement. Vertical bars indicate standard deviation (* $p<0.05$, ** $p<0.01$).

3.3.3 Response delay (RD)

The RD from all trials for both the affected arms and the unaffected arms were ranged from -195 to +495 ms and from 23 to 412 ms, respectively. The negative value implied that the phase of the actual elbow angle leaded the phase of the target angle. The average RD of unaffected arm were 114 ±65, 124±73, 161±85, 186±102, 218±98, and 260±78 ms from 10 degree/s to 60 degree/s respectively, while the RD of the affected arm were 118±148**,** 236±81, 288±128**,** 300±95, 276±86, and 328±83 ms from 10 degree/s to 60 degree/s, respectively. Fig. 3.19 showed the comparison between the affected and the unaffected arms at different tracking velocities. There was an increase in the RD for unaffected arms with the increase in the tracking velocity. In the affected arm at low velocity (10-30 deg/s), the RD had a larger variation among subjects, which could be reflected by the standard deviation. The actual elbow trajectory lagged behind the target trajectory in most of the trials, but there were three trials from two subjects in which the elbow trajectory led the target trajectory at the velocity of 10 deg/s. The two-way ANOVA with repeated measures showed that there

was a significant difference between the affected arms and the unaffected arms ($P<0.01$). The average RD of the affected arms was significantly longer than that of the unaffected arms. A significant side-by-velocity interaction was found on the RD ($P<0.05$). There were significant increases in RD of the affected arm in comparison to the unaffected arm at the velocities of 20, 30, 40 and 60 deg/s ($P<0.05$ for 20 and 30 deg/s; $P<0.01$ for 40 and 60 deg/s) based on the paired t-test. For other velocities at 10 and 50 deg/s, there were no significant differences between the affected and the unaffected arms ($P=0.72$ and $P=0.06$, respectively).

3.3.4 Relationships between the modified Ashworth scale and kinematic parameters

After analyzing the difference between the affected and unaffected arms in terms of the three parameters, RMSE, RMSJ, and RD, the relationships between these parameters and the modified Ashworth scale were also investigated. For purposes of numerical calculation, 1.5 was assigned to '1+' on the modified Ashworth scale. The Modified Ashworth scale was not significantly correlated, with the RMSE and the response delay at six velocities ($R=-0.04$-0.07, and -0.35-0.24, respectively, $P>0.05$, Fig. 3.20-3.21). The modified Ashworth scale was significantly correlated with the RMSJ when the velocities were at 10, 20, 30, 40, and 60 deg/s ($P<0.05$, $R=0.67$-0.83), and there was no significant correlation when the velocity was at 50 deg/s ($R=0.63$, $P=0.07$) (Fig. 3.22). The angular velocities at 20 and 30 deg/s had the highest correlation coefficients, which were 0.83 and 0.80 respectively. When the tracking velocity increased, this relationship was not as obvious as that at lower velocity. The results suggested that the muscle tone affected the smoothness of the trajectory during voluntary movement.

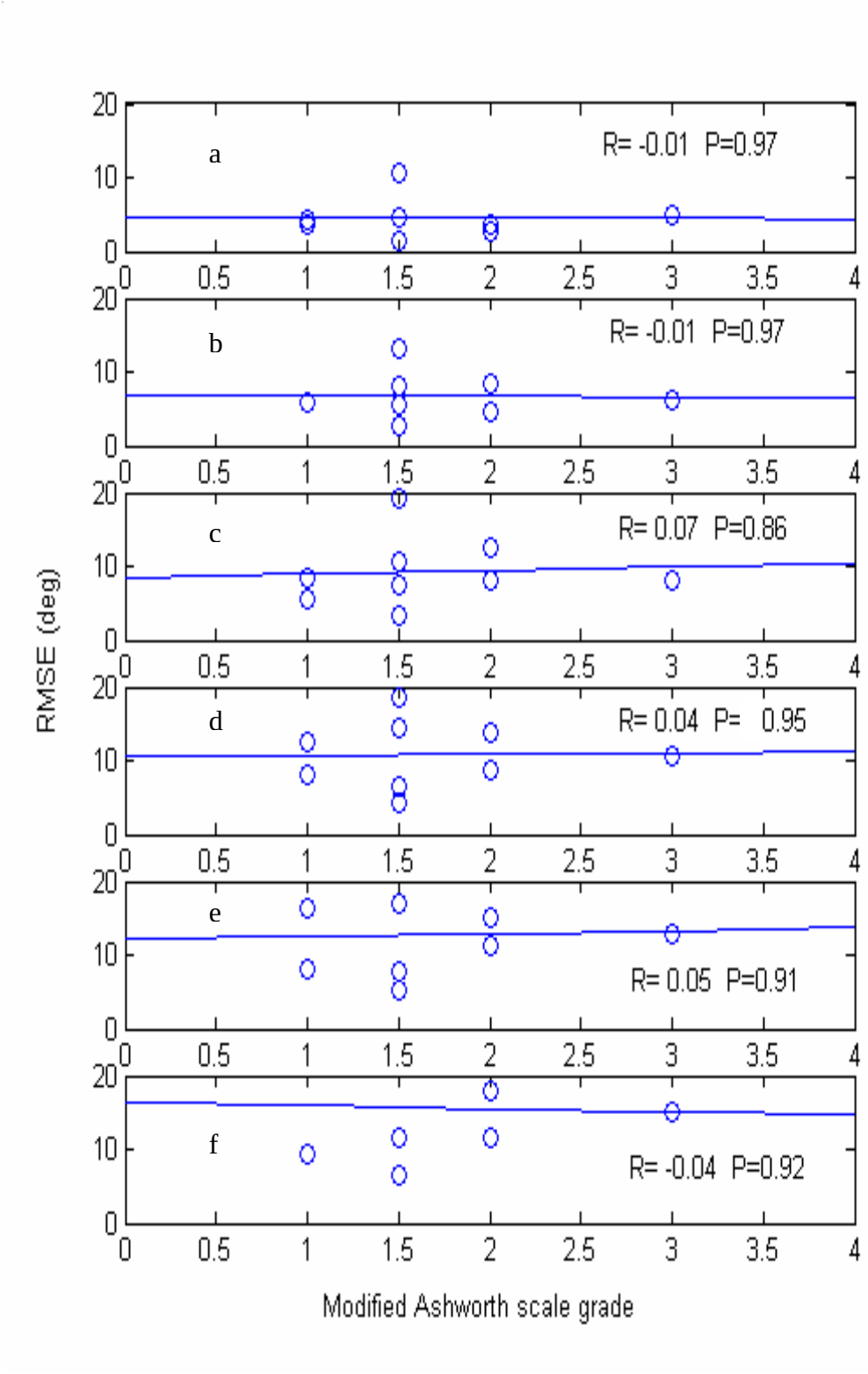

Fig. 3.20 Scatterplots of the modified Ashworth scale and the RMSE of the affected arm during the elbow tracking movement at different velocities (a: 10 deg/s, b: 20 deg/s, c: 30 deg/s, d: 40 deg/s, e: 50 deg/s, and f: 60 deg/s). Solid lines were the linear regressions noted with the correlation coefficients, R, and the probability for confidence.

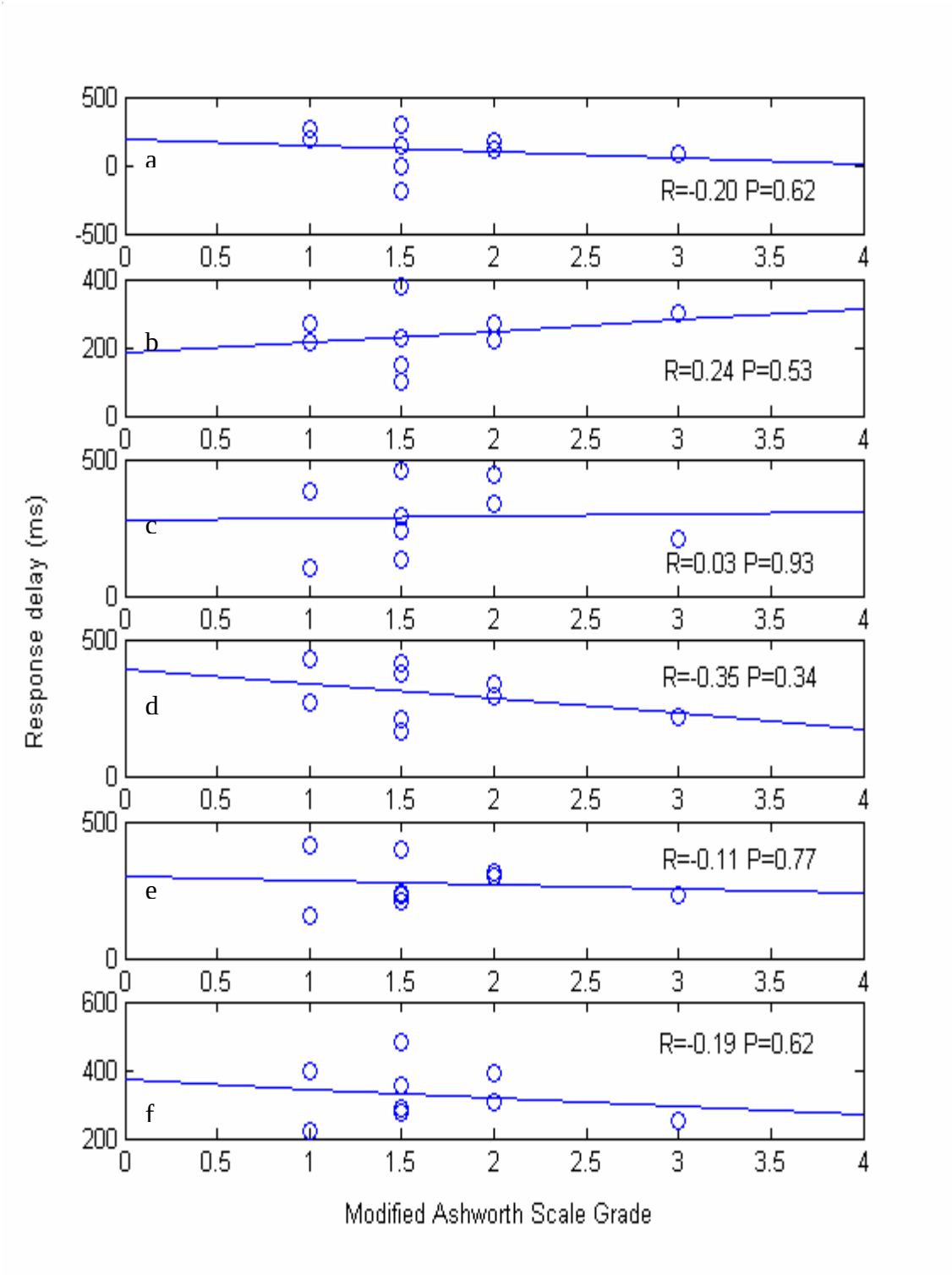

Fig. 3.21 Scatterplots of the modified Ashworth scale and the RD of the affected arm during the elbow tracking movement at different velocities (a: 10 deg/s, b: 20 deg/s, c: 30 deg/s, d: 40 deg/s, e: 50 deg/s, and f: 60 deg/s). Solid lines were the linear regressions noted with the correlation coefficients, R, and the probability for confidence.

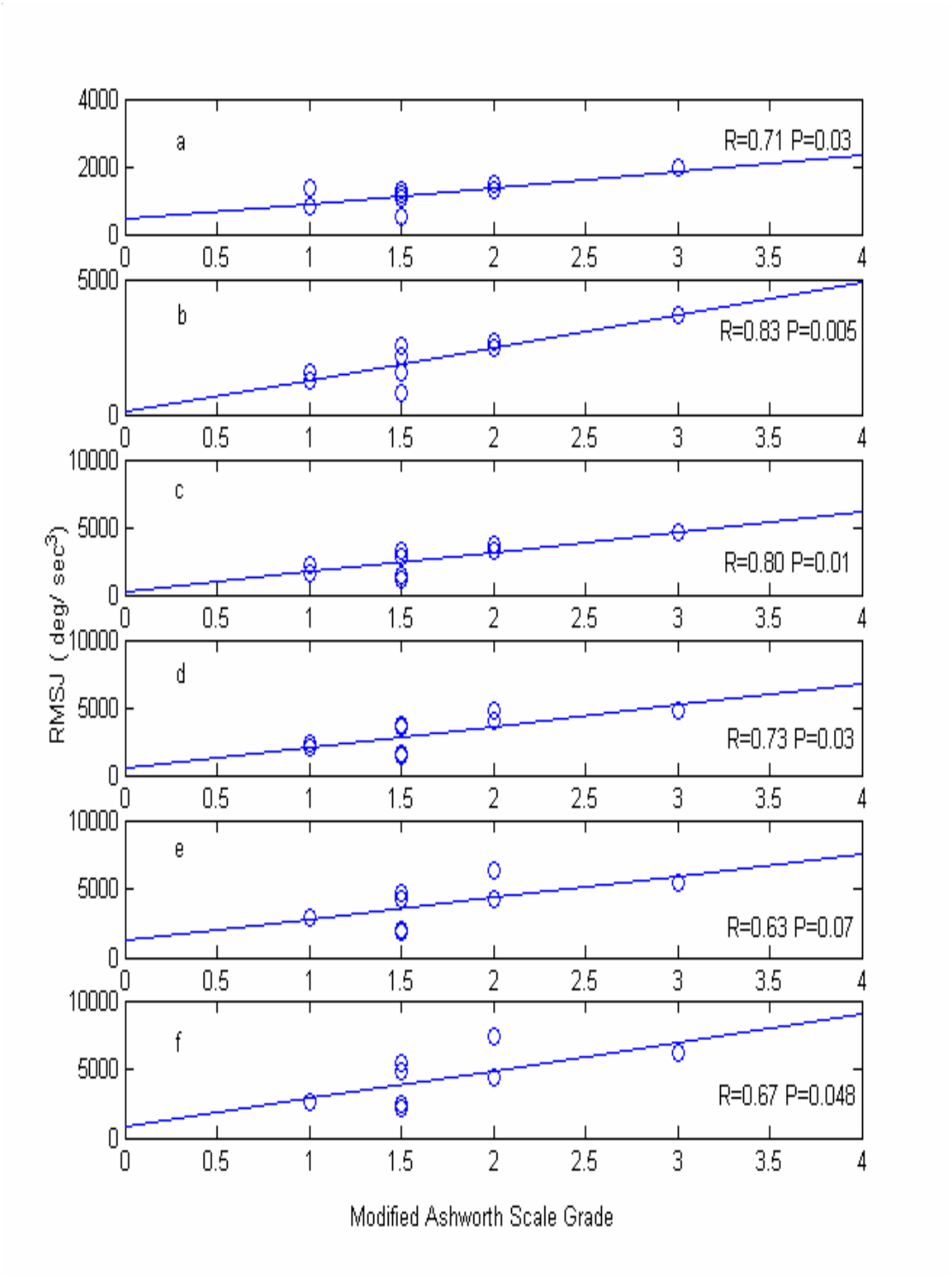

Fig. 3.22 Scatterplots of the modified Ashworth scale and the RMSJ of the affected arm during the elbow tracking movement at different velocities (a: 10 deg/s, b: 20 deg/s, c: 30 deg/s, d: 40 deg/s, e: 50 deg/s, and f: 60 deg/s). Solid lines were the linear regressions noted with the correlation coefficients, R, and the probability for confidence.

3.3.5 Range of motion

In the experiment, we also found that there were often overshoots in the unaffected arm at two end points (30 deg and 90 deg). However, the subjects sometimes could not reach the two end points especially at higher velocities in the affected arm. The range of motion of each cycle was its maximum tracking angle subtracted by its minimum tracking angle, and the range of motion of the whole trial was the mean range of motion of all the cycles. Fig. 3.23 plotted the comparison between the group mean range of motion of the unaffected arms and that of the affected arms at six velocities (10, 20, 30, 40, 50 and 60 deg/s). There was no significant effect of the velocity on the range of motion for the unaffected arm but there was significant effect for the affected arm based on the one-way ANOVA with repeated measures ($P<0.01$). The two-way ANOVA with repeated measures showed that the range of motion of unaffected arms was significantly larger than that of affected arms ($P<0.01$). The range of motion decreased with the increase in the tracking velocity.

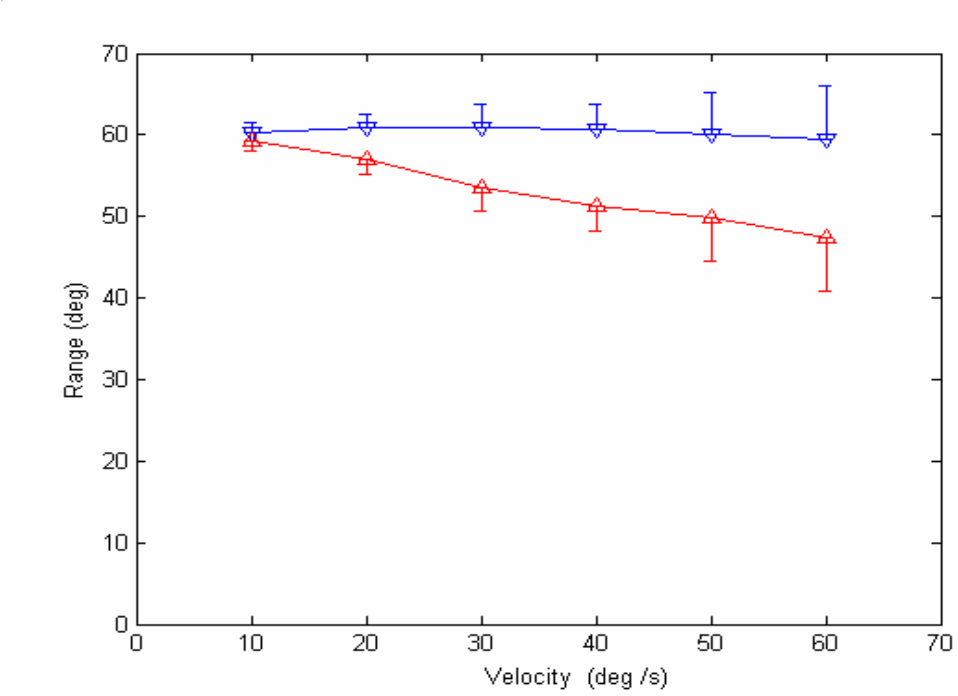

Fig. 3.23 Comparison between the average range of motion of the affected (Δ) and unaffected arm (∇) at six velocities (10, 20, 30, 40, 50, and 60 deg/s) during thee elbow tracking movement. Vertical bars indicate standard deviation.

3.4 Effect of the training using the myoelectrically controlled robot

After evaluating the assistive effect of the myoelectrically controlled robotic system, the effect of this system on restoring the upper limb functions of three subjects after stroke was investigated in a four-week training program. The results showed an obvious improvement in the extension range for all the subjects (Table 3.7). The extension range of Subject A and subject C increased from 66.8 deg to 90 deg and from 62.5 to 90 deg, respectively, after the four-week rehabilitation training, while the extension range of subject B also had a improvement from 51.3 deg to 82.7 deg. Based on the definition of the extension range in section 2.3.2.4, 90 deg of the extension range meant that the subject could reach the fully extended position.

3.4.1 Clinical scales

There were increases of 3, 7, and 2 in the Fugl-Meyer scores for the subjects A, B, and C, respectively, which reflected an improvement of the upper limb function (Table 3.7). The modified Ashworth scale decreased for the three subjects after the four-week training which reflected the improvement of muscle tone in the affected elbows.

Subject	Ashworth scale (Maximum score=4)		Fugl-Meyer (Maximum score=66)		Extension range (Maximum= 90 deg)	
	Pre-training	Post-training	Pre-training	Post-training	Pre-training	Post-training
A	1+	1	20	23	66.8	90
B	1+	1	15	22	51.3	82.7
C	3	1+	19	21	62.5	90

Table 3.7 Clinical assessment scores and the extension range of the three subjects before and after the four-week rehabilitation training.

3.4.2 Muscle strength

The torque signals measured by the robotic system were also used to evaluate the improvement in muscle strength during the rehabilitation training. The MIVE and MIVF torques were shown in Fig. 3.24 and Table 3.8 when the affected elbow was at 90 deg. Increases in the MIVE and MIVF torques for all three subjects were found during the rehabilitation training. The increases in the MIVE torque were 152%, 297% and 70%; and 23%, 193% and 74% in the MIVF torque for subject A, B, and C, respectively, which showed that the myoelectrically controlled robotic system had a positive effect in developing muscle strength. From Fig. 3.24, it could be seen that there was a large variation in the MIVE and MIVF torques especially at the beginning of the rehabilitation training, which reflected the poor control of the affected arm. After about 10 days' training, increases in both the MIVE and MIVF torques in all three subjects were observed and the variations in the measurement were improved. The MIVE and MIVF torques continued to increase until the end of the training.

Subject	MIVE torque (N.m)		MIVF torque (N.m)	
	First session	Last session	First session	Last session
A	14.5	36.6	21.0	25.8
B	6.2	24.6	8.6	25.2
C	17.6	30.0	14.4	25.1

Table 3.8 The MIVE and MIVF torques of the three subjects before and after the four-week rehabilitation training.

3.4.3 Robot measured parameters

The robotic system could be used to evaluate the upper limb function in an evaluation trial which was conducted in each session. In the evaluation trial, the robotic system was used to capture the EMG and kinematic data, which did not provide any assistive or resistive torque to the subject. Fig. 3.25 showed the trajectory and the NEMG of biceps and triceps from an evaluation trial. Fig. 3.26-3.28 plotted the elbow trajectory and the NEMG of the biceps and the triceps at different gains and loads. There was an

increase in the NEMG of the biceps with the increase in the load which could be shown in Fig. 3.26-3.28.

Fig. 3.29 compared the trajectories of the elbow at different gains and resistive torques with the trajectory without the assistance of the robotic system. It was shown that there was a larger extension range with the assistance of the robotic system in the earlier sessions. Fig 3.30 plotted the elbow trajectories of the evaluation trial of subject C in different weeks during the voluntary elbow tracking test. With the processing of the rehabilitation training, we could found a continuously increase in the active range of elbow extension in the evaluation trial (Fig. 3.30). The RMSE between the target angle and the actual elbow angle in the evaluation trial of 20 consecutive sessions were presented in Fig. 3.31. From this figure, the RMSE dropped abruptly during the first half of the training sessions, and the changes were not that much during the last several sessions.

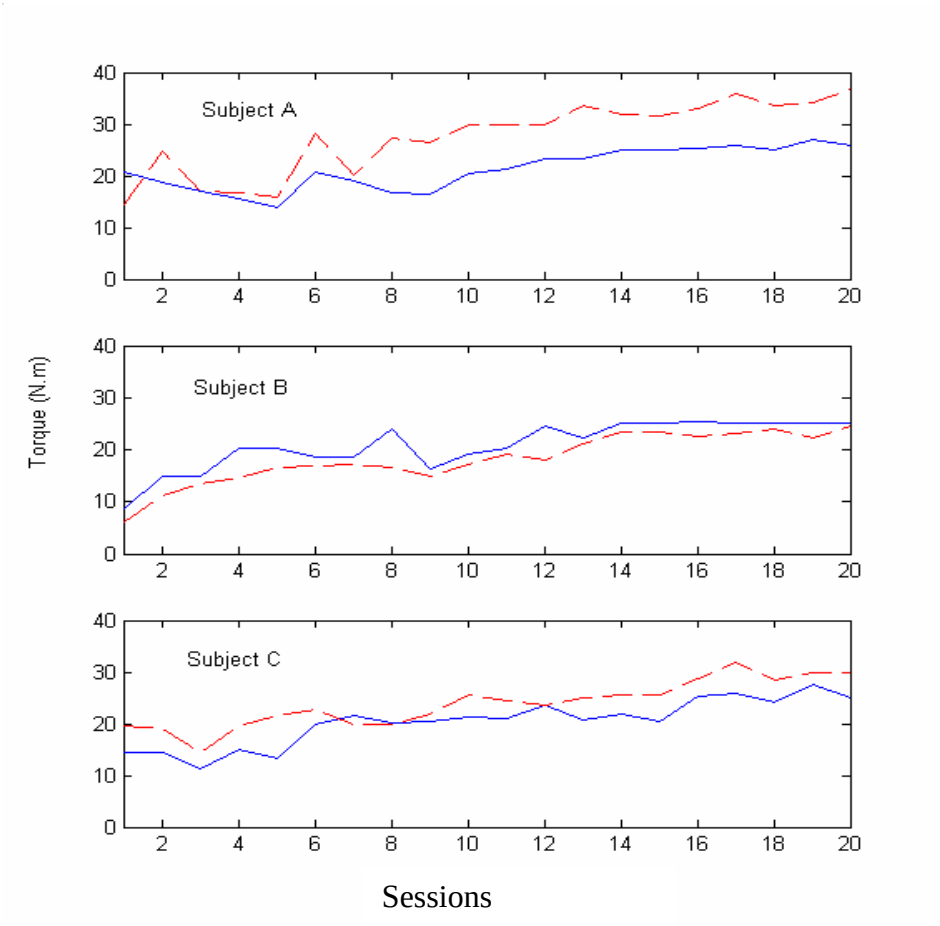

Fig. 3.24 The MIVE torque (dashed line) and MIVF torque (solid line) of three subjects in the 20 consecutive sessions.

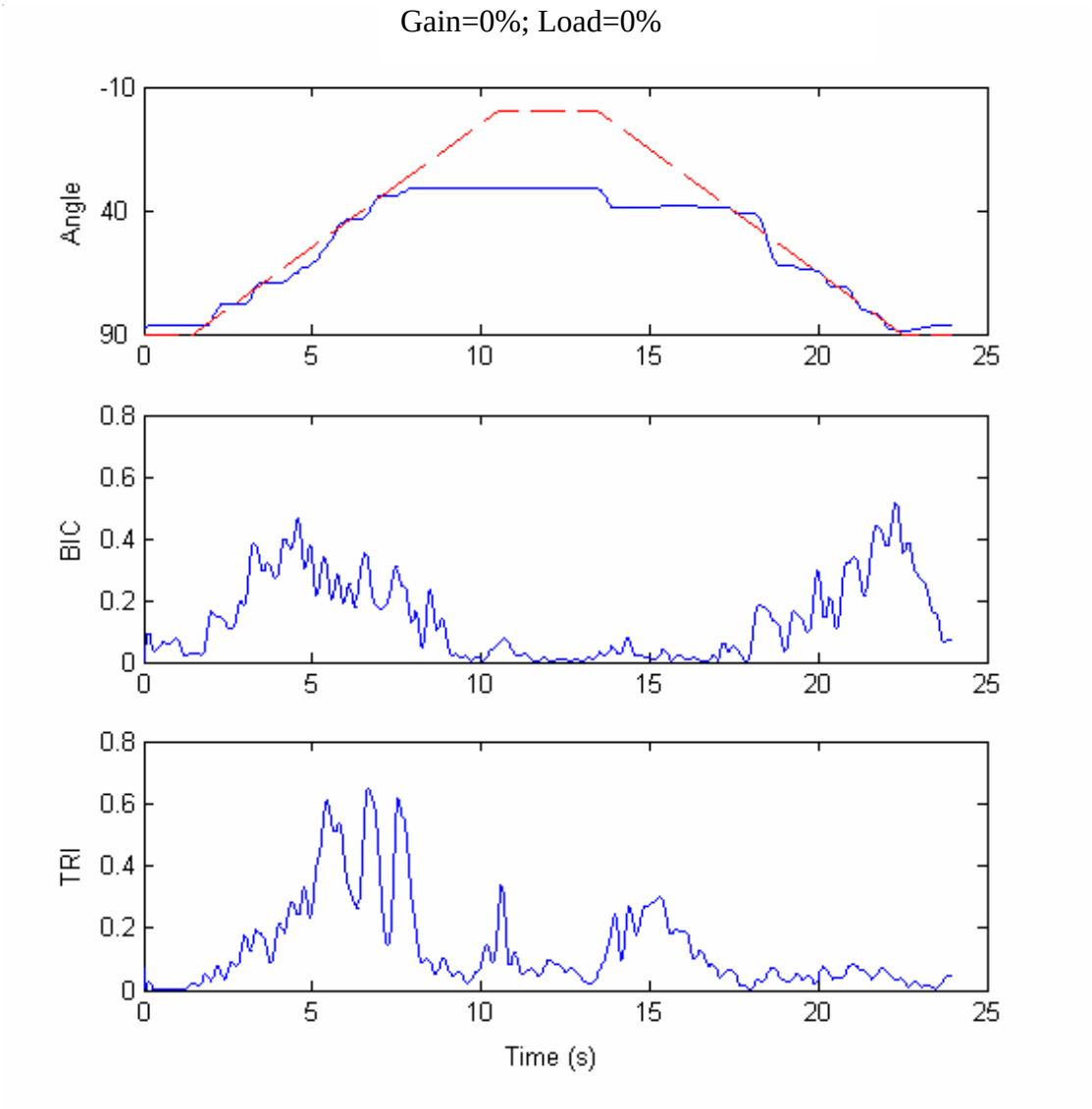

Fig. 3.25 The elbow trajectory (solid line) and the NEMG signals of biceps and triceps of subject C during the voluntary elbow tracking at a velocity of 10 deg/s when the load was equaled to 0% and the gain was equaled to 0%. The dashed line was the target trajectory (BIC: NEMG of biceps; TRI: NEMG of triceps).

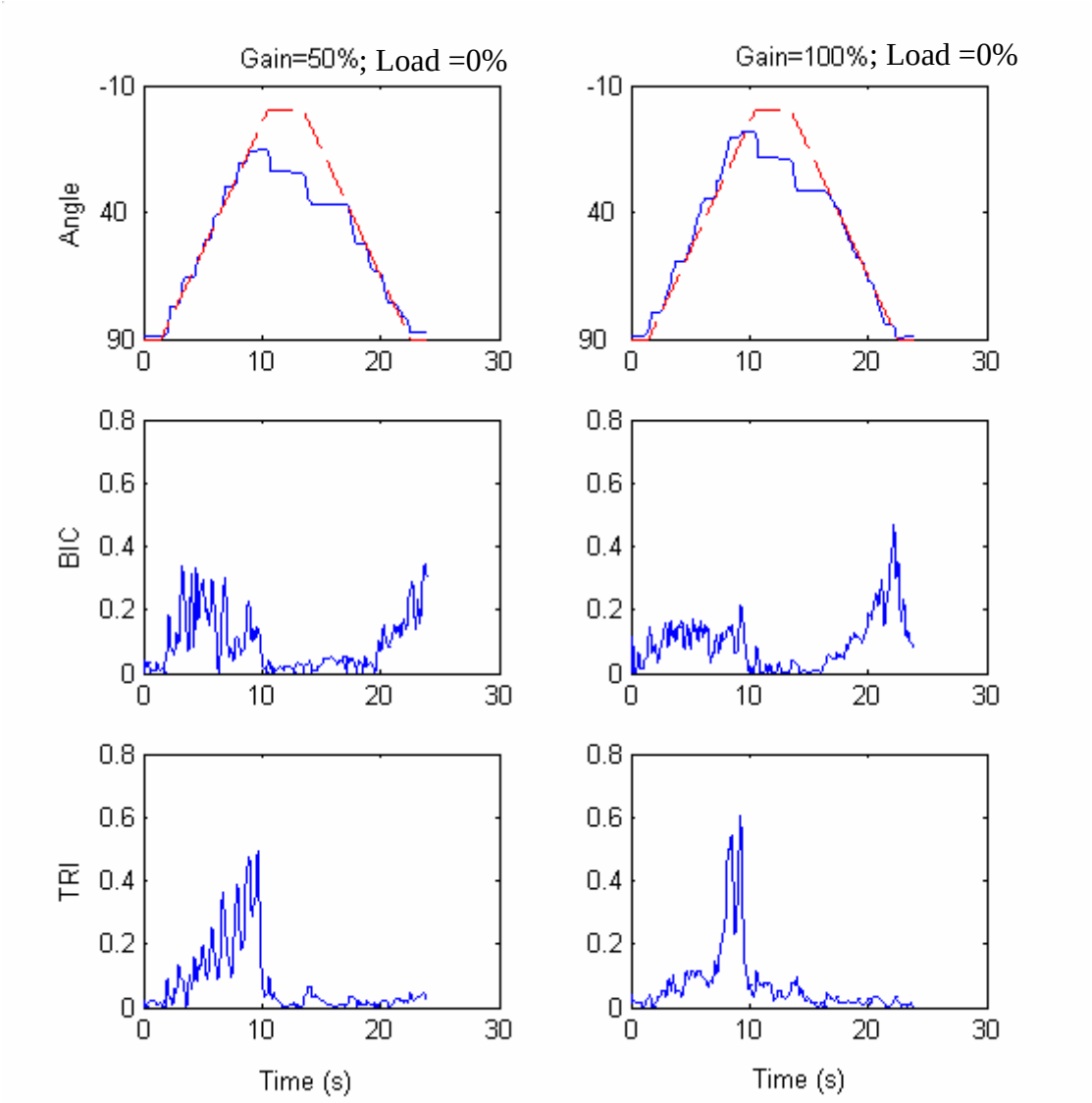

Fig. 3.26 The elbow trajectories (solid line) and the NEMG signals of biceps and triceps of subject C during the voluntary elbow tracking at a velocity of 10 deg/s when the load was equaled to 0%. The dashed line was the target trajectory (left column: gain=50%; right column: gain=100%; BIC: NEMG of biceps; TRI: NEMG of triceps).

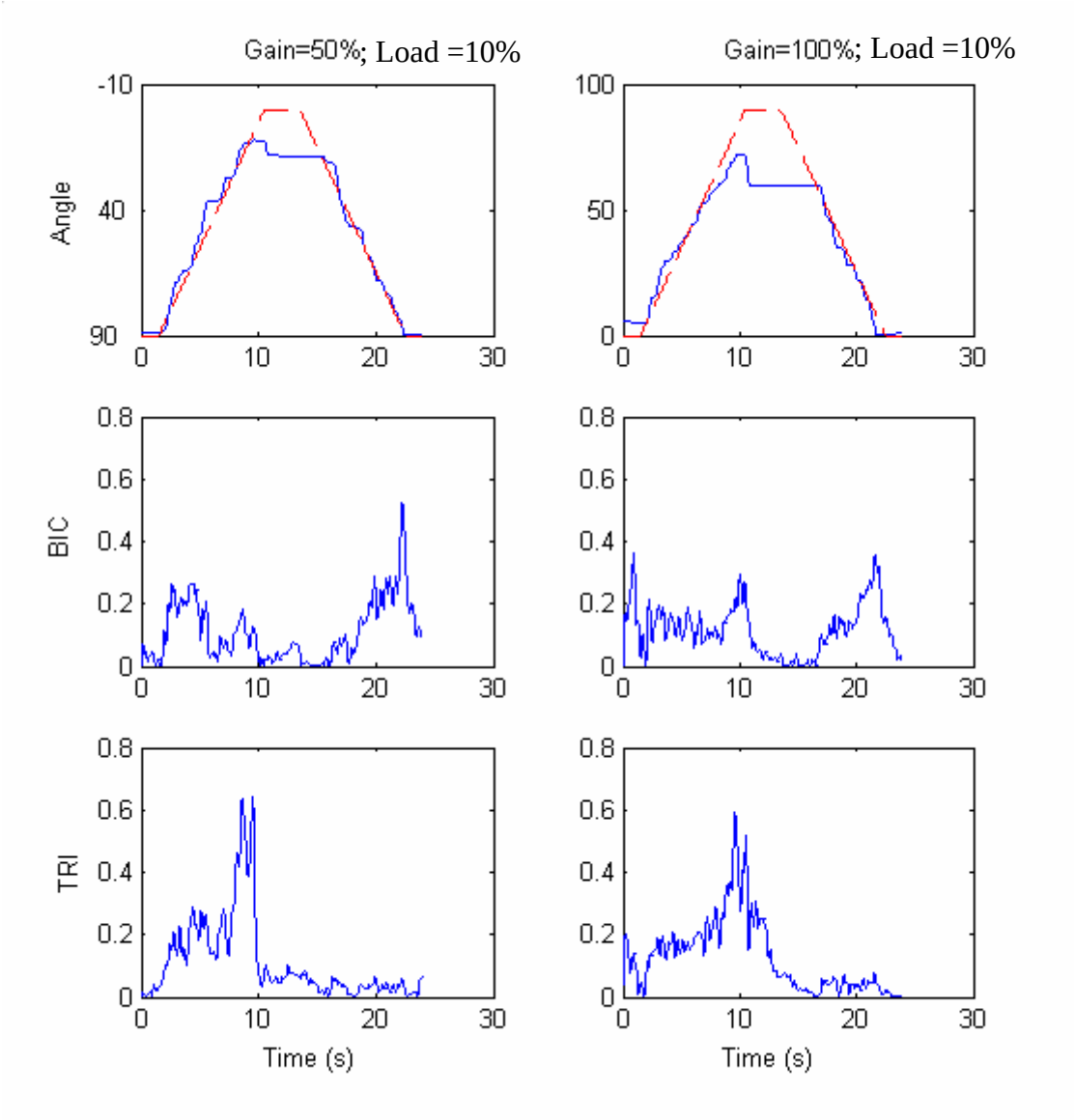

Fig. 3.27 The elbow trajectories (solid line) and the NEMG signals of biceps and triceps of subject C during the voluntary elbow tracking at a velocity of 10 deg/s when the load was equaled to 10%. The dashed line was the target trajectory (left column: gain=50%; right column: gain=100%; BIC: NEMG of biceps; TRI: NEMG of triceps).

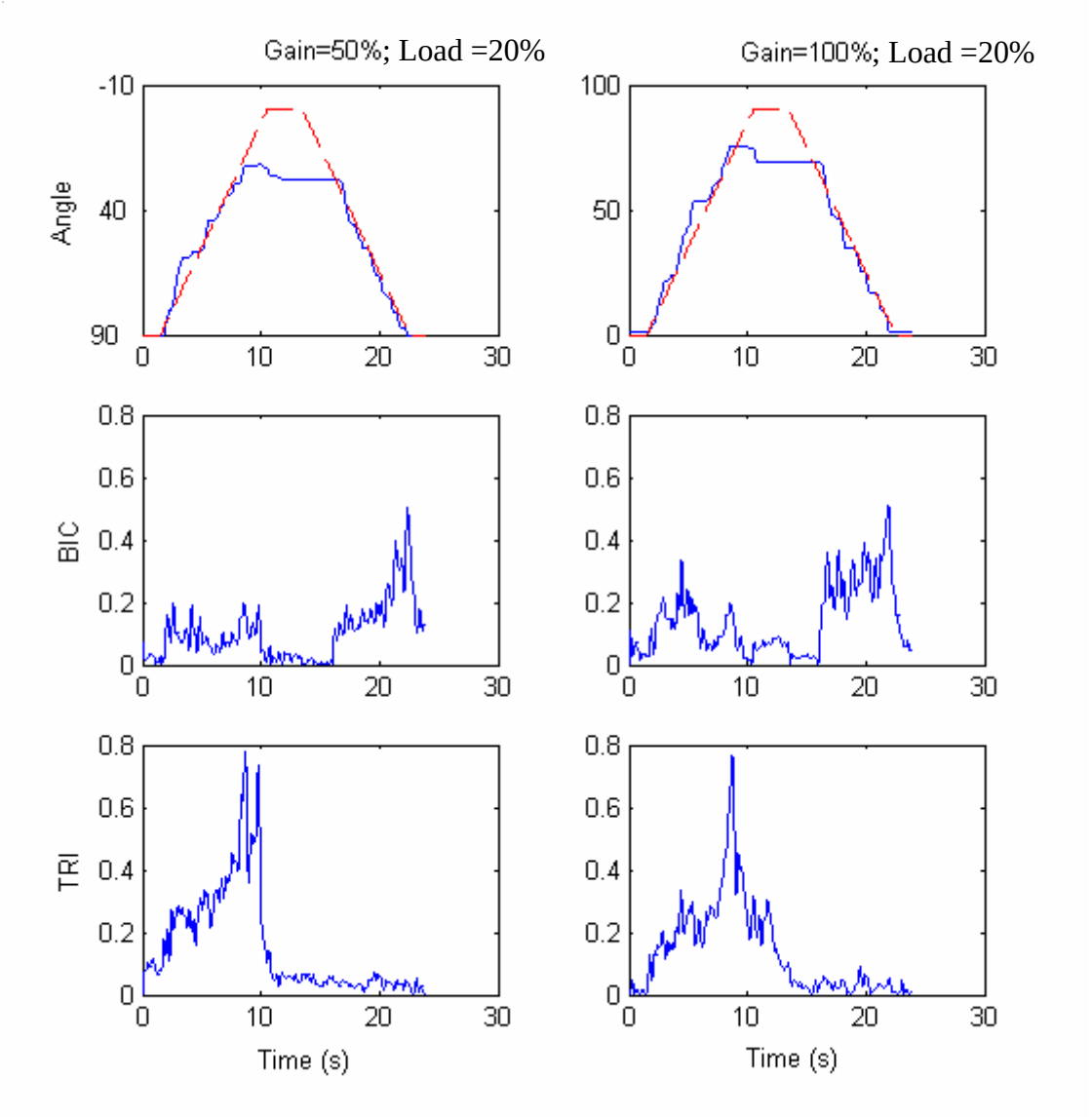

Fig. 3.28 The elbow trajectories (solid line) and the NEMG signals of biceps and triceps of subject C during the voluntary elbow tracking at a velocity of 10 deg/s when the load was equaled to 20%. The dashed line was the target trajectory (left column: gain=50%; right column: gain=100%; BIC: NEMG of biceps; TRI: NEMG of triceps).

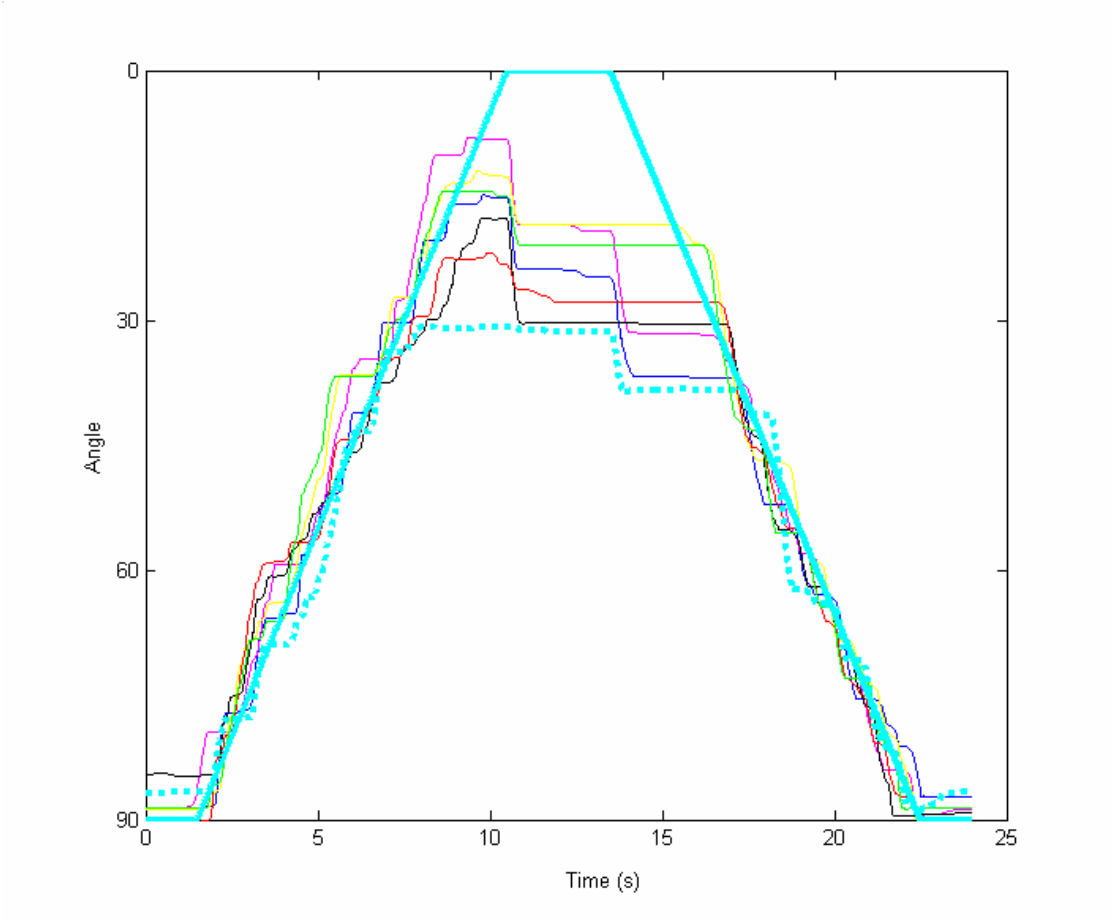

Fig. 3.29 The trajectories of subject C with and without the assistance from the robotic system during the voluntary elbow tracking at a velocity of 10 deg/s (bold solid line: the target trajectory; bold dotted line: gain=0%, load =0%; blue line: gain=50%, load=0%; magenta line: gain=100%, load=0%; yellow line: gain=50%, load=10%; black line: gain=100%, load=10%; red line: gain=50%, load=20%; green line: gain=100%, load=20%).

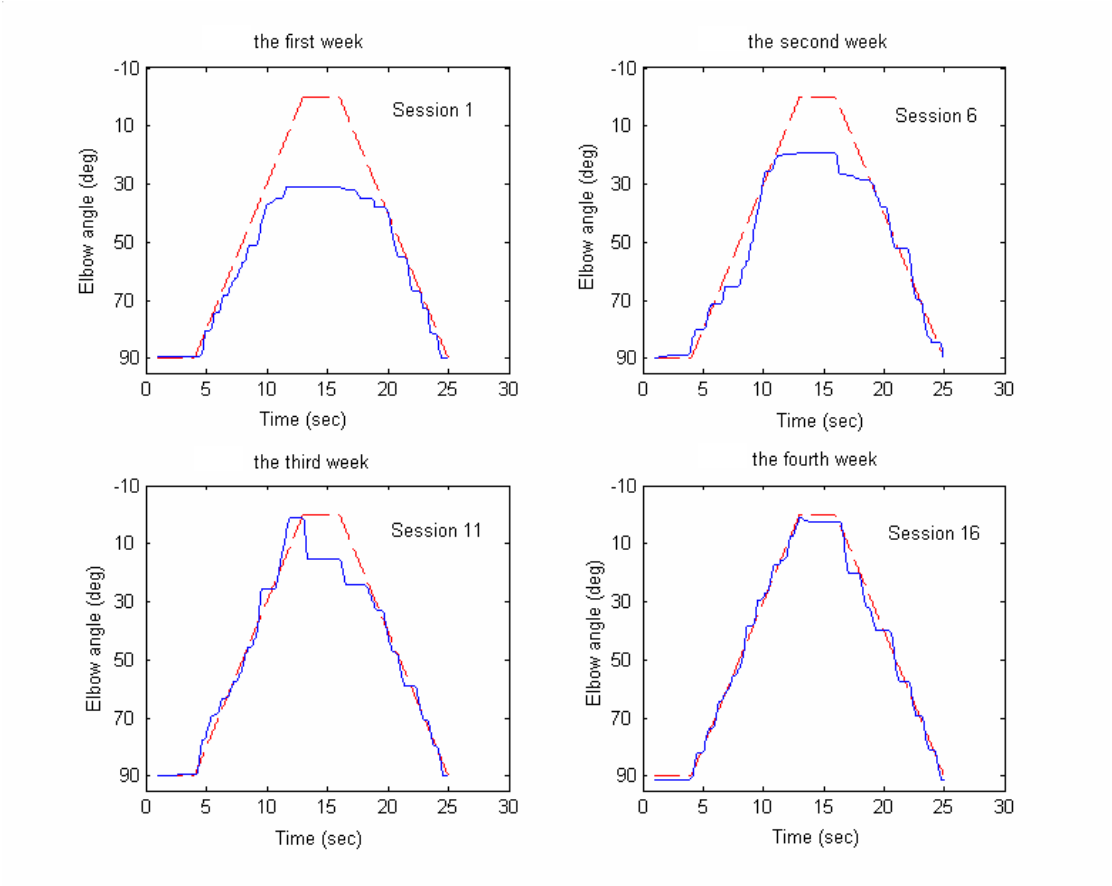

Fig. 3.30 The elbow trajectories (solid line) of the evaluation trial of subject C in different weeks during the voluntary elbow tracking at a velocity of 10 deg/s. The dashed line was the target trajectory.

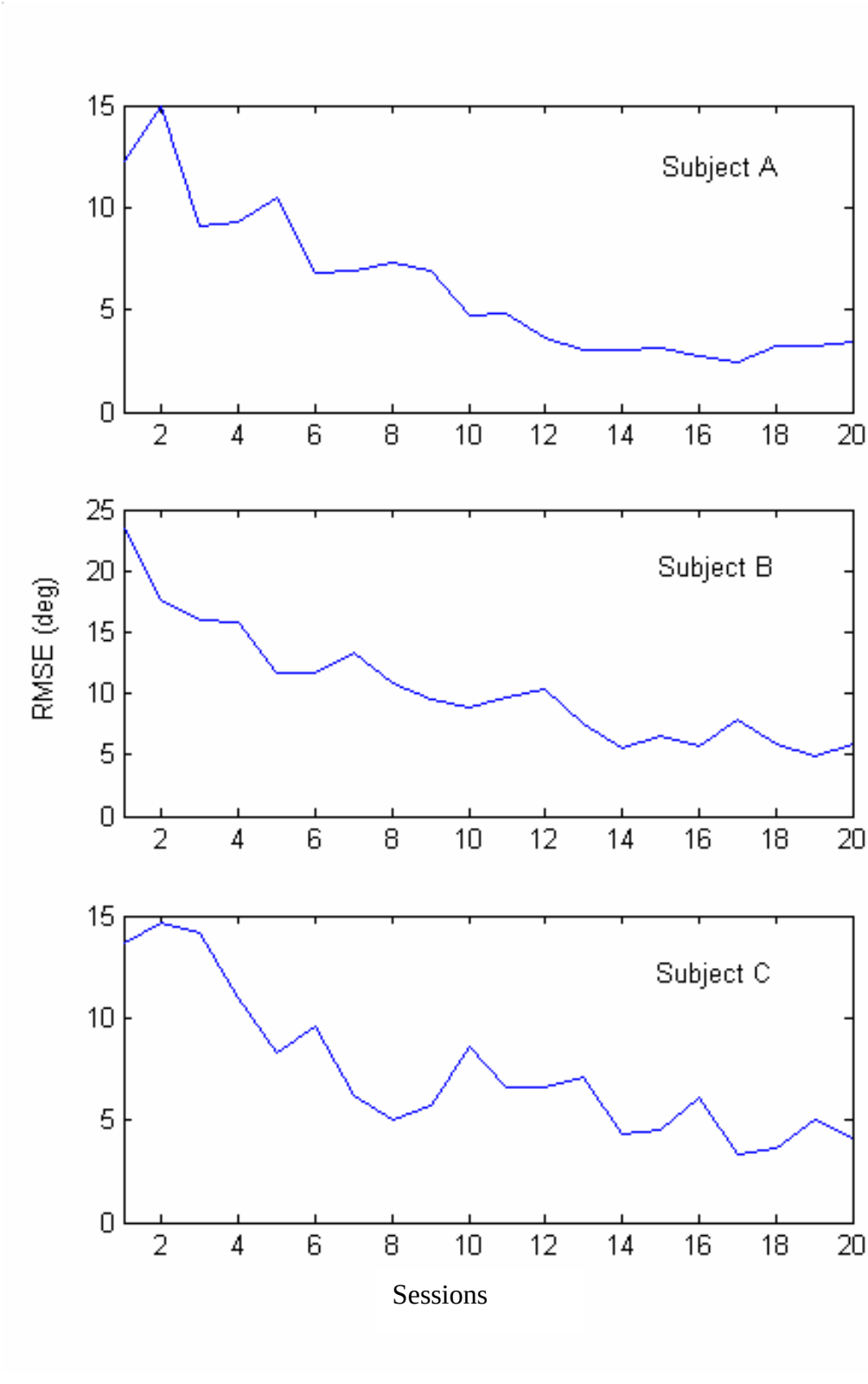

Fig. 3.31 The RMSE between the target trajectory and the actual elbow trajectory of the evaluation trial in the 20 consecutive sessions.

3.4.4 Sinusoidal elbow tracking test

Besides the daily evaluation trial before the rehabilitation training in each session, the sinusoidal elbow tracking experiment which was described in section 2.4 was also conducted on the three subjects before and after the four-week rehabilitation training in order to evaluate the functional improvement in the affected and the unaffected arm. Fig 3.32-3.34 presented the tracking trajectories of the affected arm of the subjects before and after the four-week rehabilitation training at six tracking velocities. The results showed that the trajectories were close to the target trajectory at lower velocities both before and after the training (10 deg/s and 20 deg/s). When the tracking velocities increased, it became harder for the subjects to follow the target, and they could not reach the two end points (30 deg and 90 deg) before the four-week training. After the four-week training, the trajectories were closer to the target trajectory than before. Fig. 3.35-3.37 plotted the RMSE of the affected and unaffected arms before and after the four-week rehabilitation training at six velocities. The results showed that there was an improvement in all three subjects in both their affected and unaffected arm at all the velocities. However, the performance of the affected arms was still not as good as that of the unaffected arms after the four-week training. Fig. 3.38-3.40 plotted the RMSJ of the affected arms and the unaffected arms for the three subjects before and after the four-week rehabilitation training at six velocities. From the figures, we found that there was a decrease in the RMSJ of the affected arms after the four-week rehabilitation training for subject A and subject B when the velocities were at 10 and 20 deg/s and for subject C when the velocities were at 10, 20 and 30 deg/s. The RMSJ was larger after training when the velocities increased to higher values for all the three subjects. For the unaffected arm, there was a slight decrease in RMSJ at almost all the velocities. The reason for the better performance at lower velocities was that the subjects could reach the two ends before and after the rehabilitation training. After the four-week training, the performance improved and resulted in a lower RMSJ value. However, when the tracking velocities increased, these subjects could not reach the two ends before the training and the range of motion improved after the training. Therefore, the trajectory after the training had larger amplitudes than those before the training at these higher velocities which caused an increase in the RMSJ at these velocities after rehabilitation training.

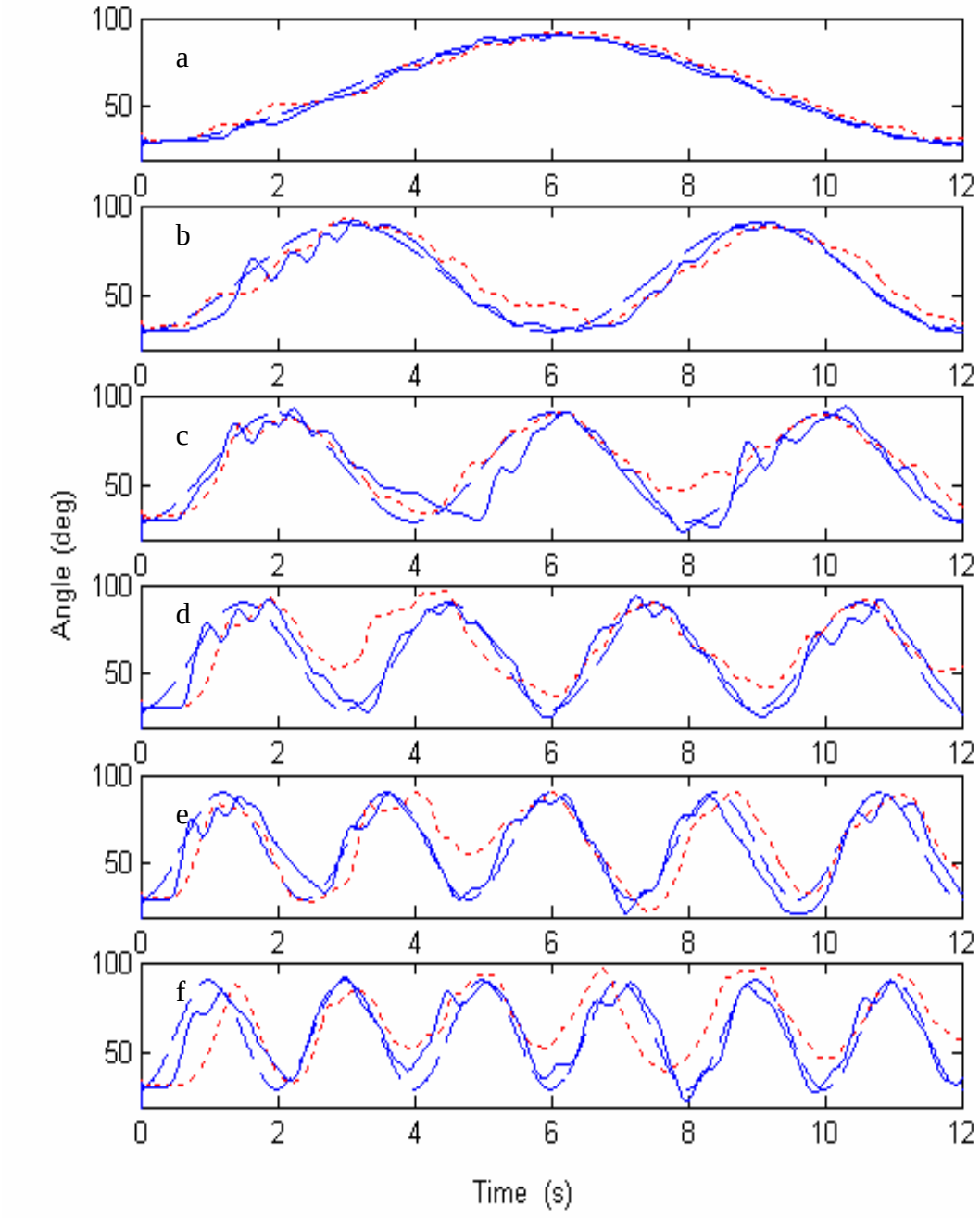

Fig. 3.32 The trajectories for the affected arm of subject A before (dotted line) and after (solid line) the four-week training during the voluntary elbow tracking at six velocities (a: 10 deg/s, b: 20 deg/s, c: 30 deg/s, d: 40 deg/s, e: 50 deg/s, and f: 60 deg/s). The dashed line was the target trajectory.

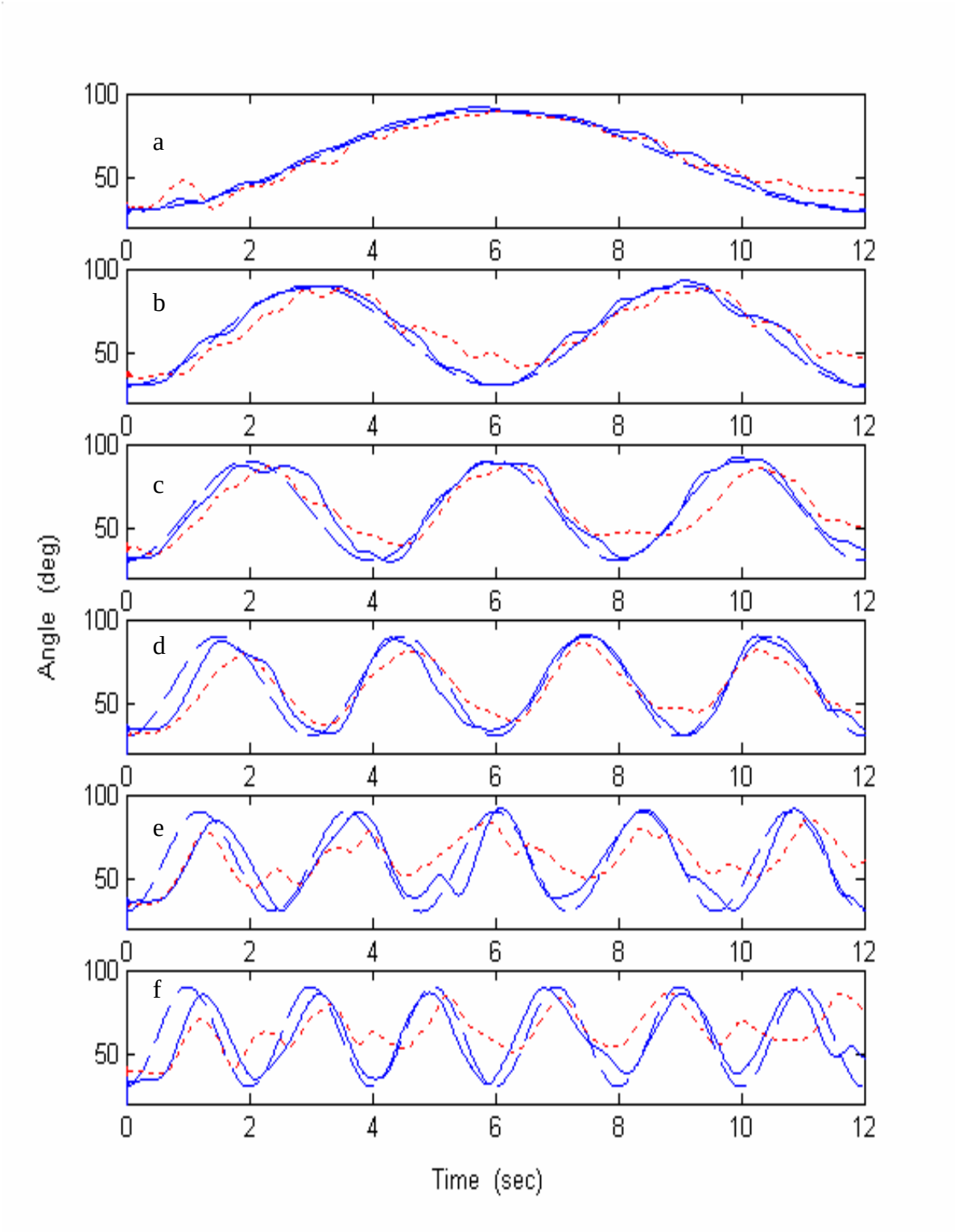

Fig. 3.33 The trajectories for the affected arm of subject B before (dotted line) and after (solid line) the four-week training during the voluntary elbow tracking at six velocities (a: 10 deg/s, b: 20 deg/s, c: 30 deg/s, d: 40 deg/s, e: 50 deg/s, and f: 60 deg/s). The dashed line was the target trajectory.

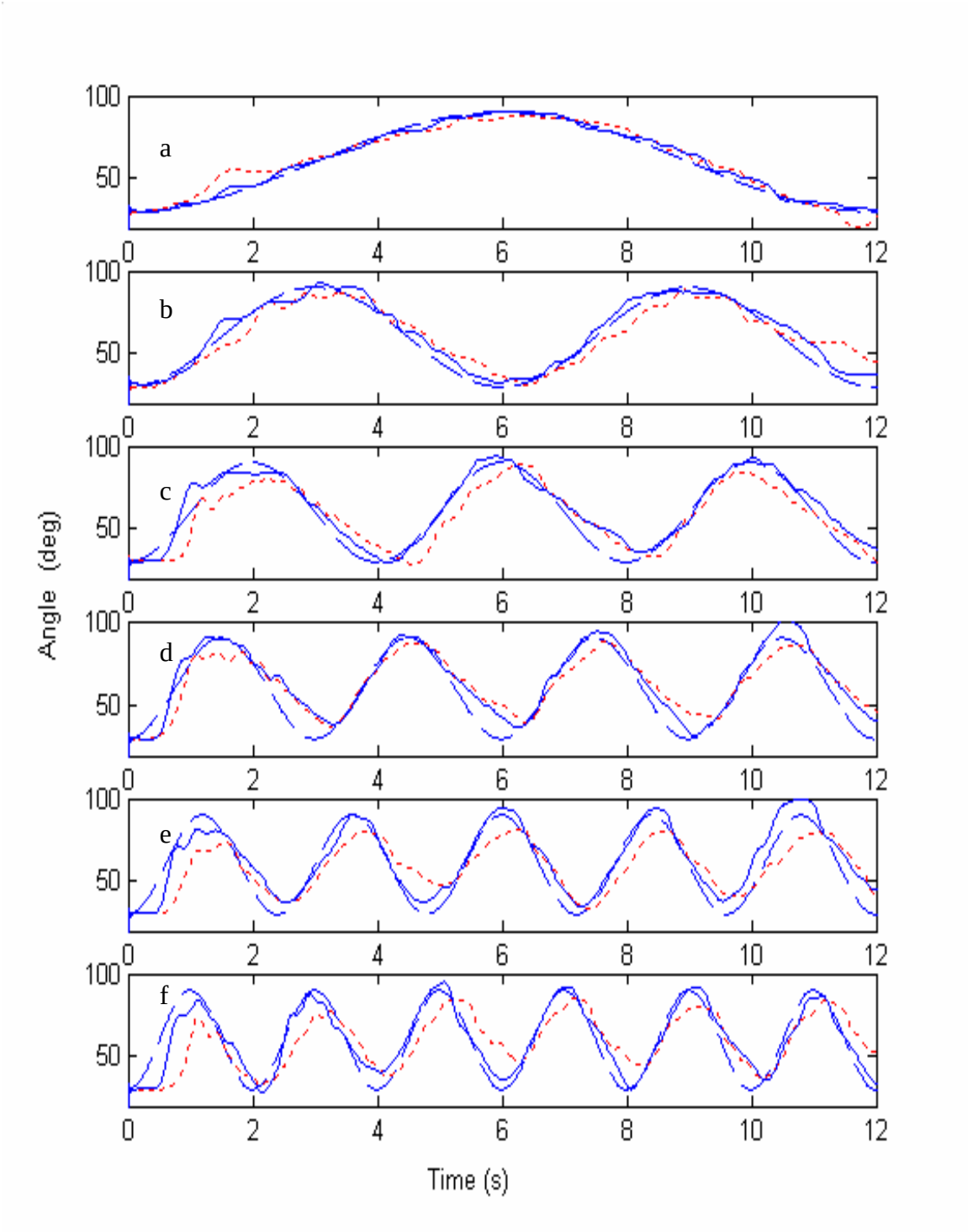

Fig. 3.34 The trajectories for the affected arm of subject C before (dotted line) and after (solid line) the four-week training during the voluntary elbow tracking at six velocities (a: 10 deg/s, b: 20 deg/s, c: 30 deg/s, d: 40 deg/s, e: 50 deg/s, and f: 60 deg/s). The dashed line was the target trajectory.

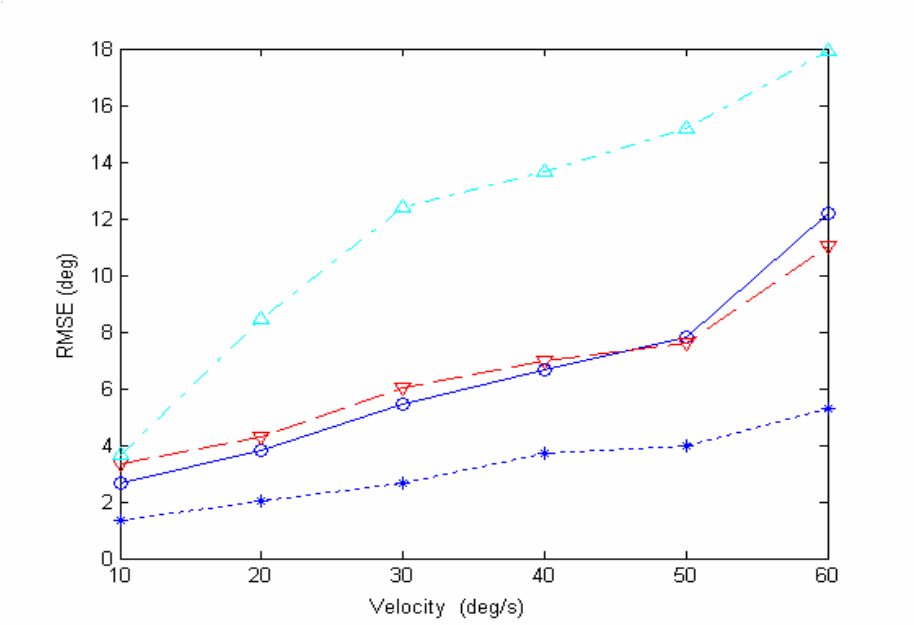

Fig. 3.35 Comparison between the RMSE of the unaffected arm (O) and the affected arm (Δ) before the four-week training, and the RMSE of the unaffected arm (*) and the affected arm (∇) after the four-week training at six velocities (10, 20, 30, 40, 50 and 60 deg/s) during the elbow tracking movement of subject A.

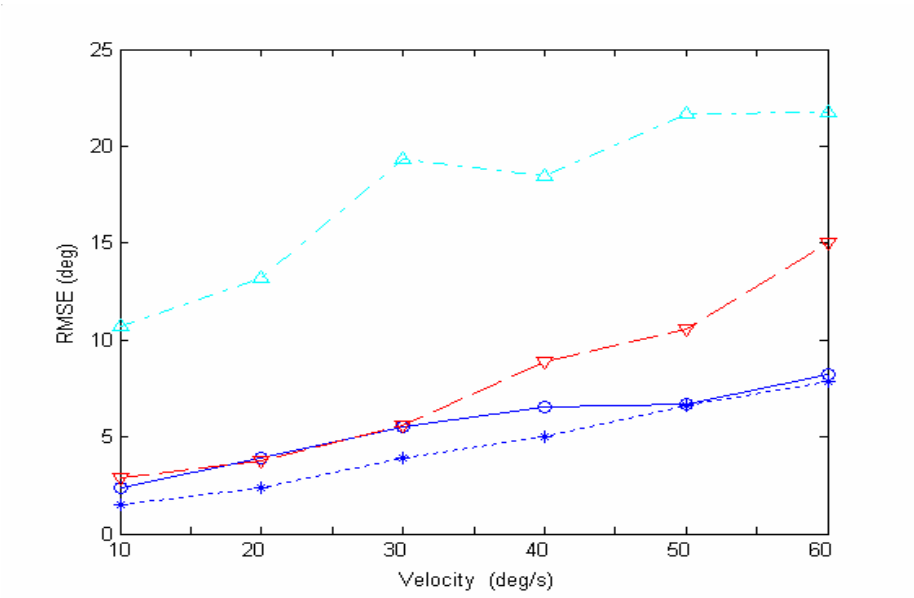

Fig. 3.36 Comparison between the RMSE of the unaffected arm (O) and the affected arm (Δ) before the four-week training, and the RMSE of the unaffected arm (*) and the affected arm (∇) after the four-week training at six velocities (10, 20, 30, 40, 50 and 60 deg/s) during the elbow tracking movement of subject B.

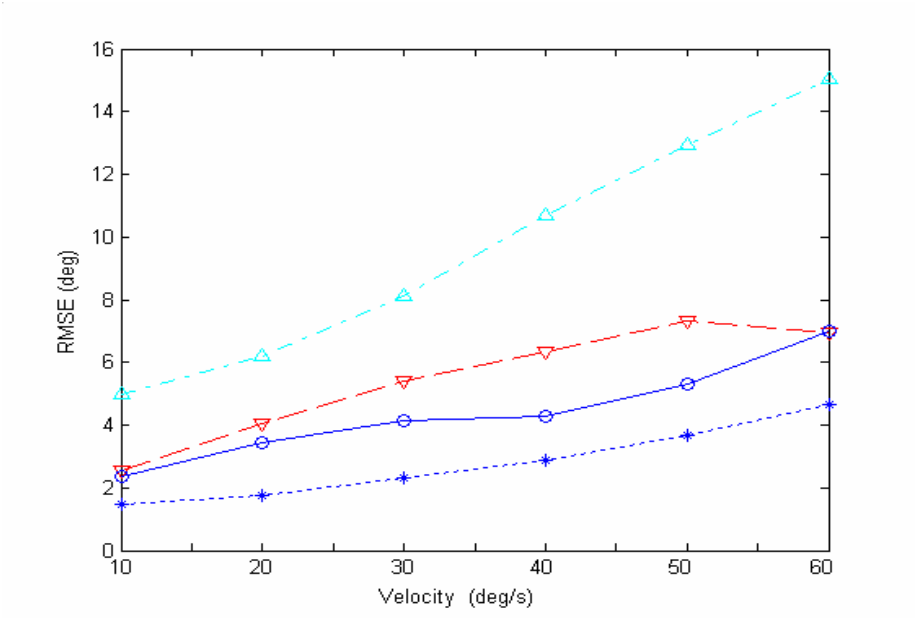

Fig. 3.37 Comparison between the RMSE of the unaffected arm (O) and the affected arm (Δ) before the four-week training, and the RMSE of the unaffected arm (*) and the affected arm (∇) after the four-week training at six velocities (10, 20, 30, 40, 50 and 60 deg/s) during the elbow tracking movement of subject C.

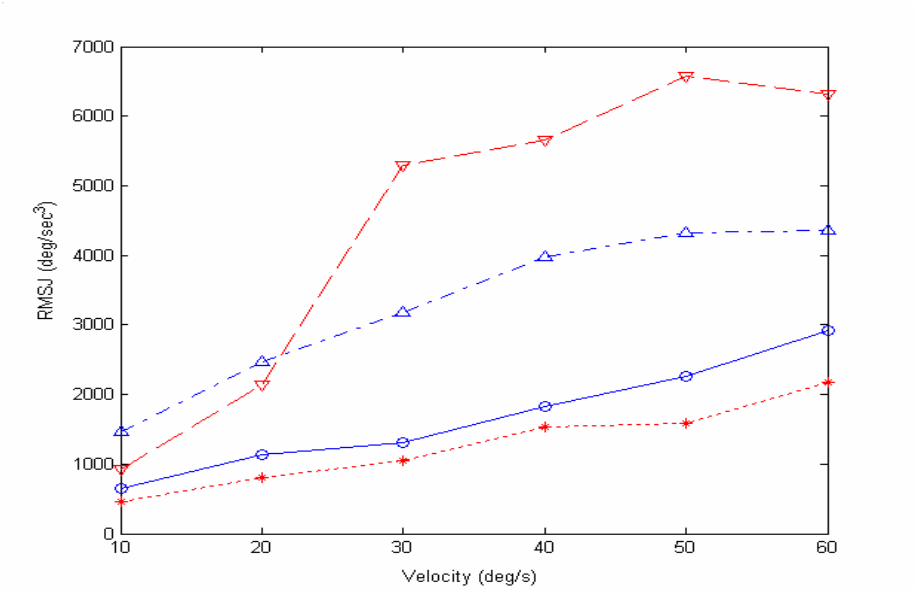

Fig. 3.38 Comparison between the RMSJ of the unaffected arm (O) and the affected arm (Δ) before the four-week training, and the RMSE of the unaffected arm (*) and the affected arm (∇) after the four-week training at six velocities (10, 20, 30, 40, 50 and 60 deg/s) during the elbow tracking movement of subject A.

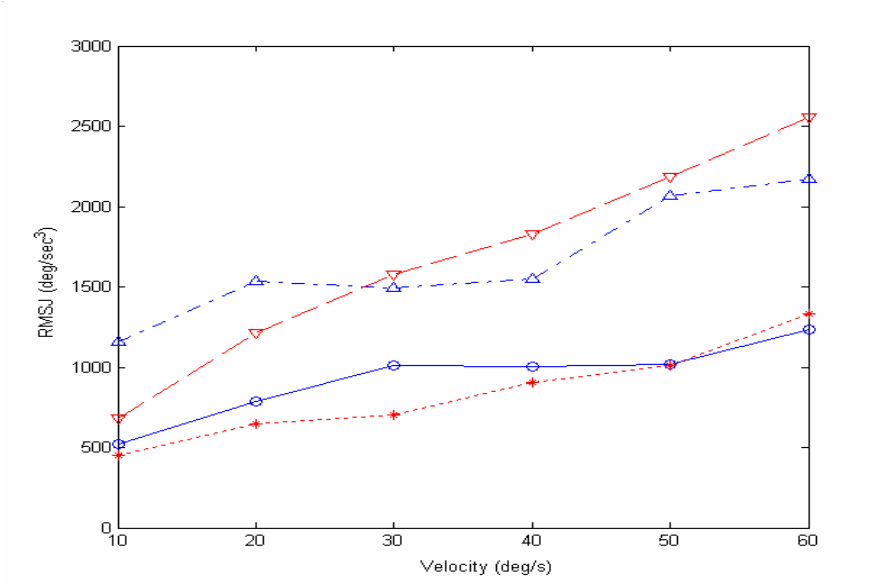

Fig. 3.39 Comparison between the RMSJ of the unaffected arm (O) and the affected arm (Δ) before the four-week training, and the RMSE of the unaffected arm (*) and the affected arm (∇) after the four-week training at six velocities (10, 20, 30, 40, 50 and 60 deg/s) during the elbow tracking movement of subject B.

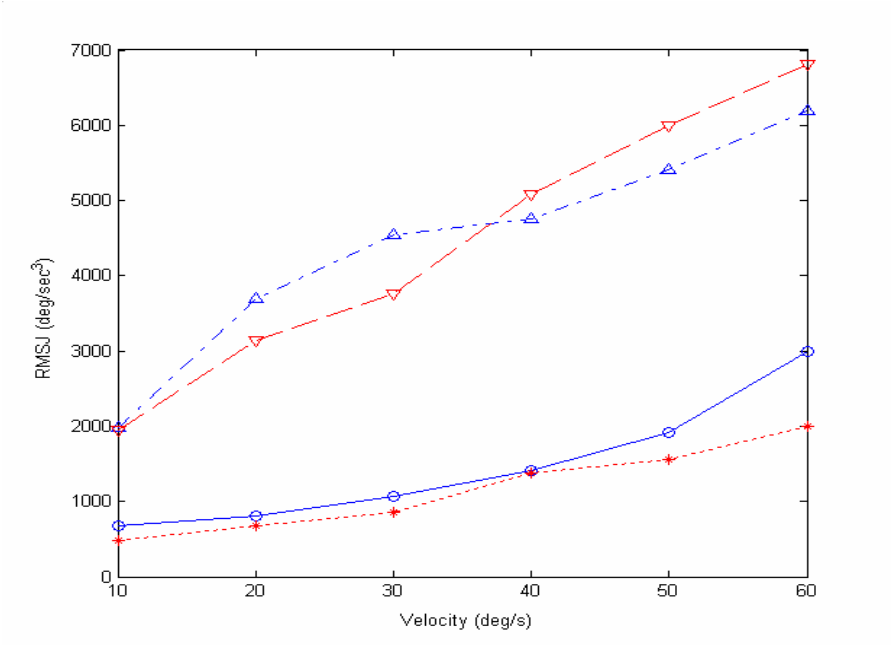

Fig. 3.40 Comparison between the RMSJ of the unaffected arm (O) and the affected arm (Δ) before the four-week training, and the RMSE of the unaffected arm (*) and the affected arm (∇) after the four-week training at six velocities (10, 20, 30, 40, 50 and 60 deg/s) during the elbow tracking movement of subject C.

Tables 3.9 and 3.10 showed the mean RD of the three trials for the affected and unaffected arm of each subject. Subjects A, B, and C showed a decrease in the RD at almost all the velocities after training both for the affected and unaffected arms. The results from subject A, B, and C also showed that the RD of the affected arm were larger than those of the unaffected arm at most of the situations both before and after the four-week training.

Velocity (deg/s)			10	20	30	40	50	60
Response Delay (ms)	Subject A	Pre-training	115	271	442	290	297	389
		Post-training	-27	124	175	132	240	282
	Subject B	Pre-training	289	378	288	374	235	286
		Post-training	-22	61	149	196	193	300
	Subject C	Pre-training	151	297	205	215	230	251
		Post-training	-2	62	51	128	168	171

Table 3.9 Response delay of the affected arm during the arm tracking experiment before and after the four-week rehabilitation training.

Velocity (deg/s)			10	20	30	40	50	60
Response Delay (ms)	Subject A	Pre-training	150	119	103	124	171	243
		Post-training	-34	38	44	87	116	138
	Subject B	Pre-training	141	148	298	281	253	290
		Post-training	52	81	124	153	276	268
	Subject C	Pre-training	57	64	38	83	79	121
		Post-training	-27	31	52	19	61	33

Table 3.10 Response delay of the unaffected arm during the arm tracking experiment before and after the four-week rehabilitation training.

3.4.5 Questionnaire

Table 3.11 showed the results from the subjective questionnaire on the four-week training with the myoelectrically controlled system (range 0-36) (Appendix II). Results showed that there was no adverse subjective opinion from the three subjects on the four-week rehabilitation training in terms of the nine questions.

Questions		Subject A	Subject B	Subject C	Mean
1	You are given a clear instruction before using the myoelectrically controlled system for training.	4	4	4	4
2	It is easy to put on the myoelectrically controlled system.	3	3	3	3
3	It is comfortable when you use the myoelectrically controlled system.	4	3	4	3.7
4	The appearance of the myoelectrically controlled robotic system looks acceptable.	3	3	4	3.3
5	The steps using the myoelectrically controlled system to carry out the training are simple to follow.	3	3	3	3
6	The range of motion of elbow is improved after using the myoelectrically controlled system.	4	3	3	3.3
7	The elbow becomes less stiff after using the myoelectrically controlled system.	3	3	3	3
8	The myoelectrically controlled system improves your ability to carry out activities of daily living.	3	3	3	3
9	Overall you are satisfied with the function of the myoelectrically controlled robotic system.	3	3	3	3
	Overall	30	28	30	
	Mean	3.3	3.1	3.3	

Table 3.11 Questionnaire on the effect of the robotic system in the four-week training. Subjective scoring system: 0 =strongly disagree; 1 =disagree; 2 = indifferent; 3 =agree; 4 =strongly agree.

CHAPTER 4 DISCUSSIONS

4.1 Recurrent neural network model

4.1.1 Recurrent neural network model for normal subjects

In order to find out how to control the robotic system with the electromyographic (EMG) signals of muscles at the elbow joint, a suitable control strategy should be proposed for the robotic system. The primary motivation to develop this recurrent neural network (RANN) model was to control the robotic system based on the EMG signals to assist subjects after stroke in daily activities or in rehabilitation training.

4.1.1.1 Structure of the RANN model

In this part, a recurrent artificial neural network together with an inverse dynamic model was constructed to predict the elbow torque during voluntary elbow movement in the horizontal plane. The voluntary movements with different loads and different speeds were analyzed based on the RANN model.

At the modeling stage, the neural network structure was a very important issue that affected the prediction accuracy and the model's robustness (Brown et al., 1994; Tong, 1997). The complexity of the neural network depended on the number of hidden nodes. The optimum number of hidden nodes not only depended on the structure of the neural network model but also on the inputs and outputs. The results shown in Fig. 2.11 were consistent with the argument that a sufficient number of hidden nodes achieved superior generalization when the network complexity was enough for the question (Tong, 1997; Hirose et al., 1991). If the model complexity was not enough for the problem, underfitting would occur (hidden nodes less than five in Fig. 2.11). Thus, increasing the hidden node could improve the performance of the model. If the model was too complex for the mapping, the training error still decreased but the test error increased. The network might fit together with noise. Larger test error would be generated in the test data because of overfitting. In order to make the network more generalized, it was very important to choose the suitable number of hidden nodes in the experiment in order to avoid underfitting and overfitting. At the same time, the number of iterations was another issue that should be considered in order to achieve the optimum results. The training process should be stopped, if the training error did

not have any significant improvement. The stop criterion was consistent with that found in the literatures (Au et al., 2000; Uchiyama et al., 1998).

4.1.1.2 Comparison with previous studies

There is a similarity between our results and those in Luh ’s study in which a three-layer fully connected feed-forward ANN model was built to predict the isokinetic elbow joint torques from EMG signals during the performance of single-joint movements (Luh et al., 1999). The mean root mean square error (RMSE) from all subjects was 1.67 Nm in learning and 8.27 Nm in tests. Luh et al. investigated EMG torque relationship at constant angular velocity. In their experimental setup, the subjects did not have fully voluntary control and needed external torque to keep the elbow moving at a constant velocity. Their model investigated only the biceps and the triceps, but the contribution of brachioradialis to the elbow torque was neglected, which could be one source of the errors. Au et al. (2000) used a time delayed artificial neural network to predict the shoulder and elbow kinematics among subject without impairment and subjects after spinal cord injury with EMG signals. The average relative error was 9.2% to 20.2% among normal subjects and was 10.7% to 23.4% among subjects after spinal cord injure. In our study, the average relative error for normal subjects were 2.84%±0.50% in the training data and 5.96%±1.54% in the test data if the joint angle and angular velocity of the elbow were added as inputs.

Under the voluntary dynamic movement, which consisted of the acceleration and the deceleration phases, the joint torque could not be directly measured by a torque sensor. Only under an isometric contraction or under a constant velocity, would the joint torque be directly measured by the torque sensor. Therefore the inverse dynamic model was applied to calculate the output torque in this study. In the inverse dynamic model, there were two parameters that would affect the output torque: (1) angular acceleration and (2) moment of inertia. The moment of inertia would be changed with different loads. In our study, trials with different loads and different frequencies were trained in one RANN model. Then the trained RANN model could be adapted to different loads. In the inputs of the RANN, this load information was not included; only EMG and kinematics were used. The results demonstrated the ability of RANN in responding to different loads and frequencies.

4.1.2 Model limitations for subjects after stroke

Although the RANN model seemed feasible with the data obtained from the subjects without impairment, the model did not have a similar performance when used with the data from subjects after stroke upon a review of the model's relative error and the cross correlation coefficient. Many factors could explain the results. First, the trajectory of a subject after stroke was less smooth than that of a normal subject, which increased the difficulty on the prediction ability with the RANN model. The increase in the root mean square jerk (RMSJ) could reflect the decrease of smoothness in the affected arm (Fig. 3.18). The increase in the RMSE also reflected the increase of abnormality in the trajectory. Many studies reported the abnormal EMG cocontraction (Chae et al., 2002a; McLellan et al., 1985) which might disturb the training and predicting. The RANN model was expected to predict the elbow torque during voluntary movement for subjects after stroke. However, the model suffered from over complex situation and was difficult to be applied as a robust control strategy at this stage. Therefore proportional control algorithm based on the EMG signal from the triceps was an alternative. It was a reliable control method which eliminated the effect of excessive muscle activation occurring in biceps of the affected arm (Canning et al., 2000). The EMG signal of the triceps was relatively clean during elbow extension, and the control based on the EMG signal could reflect the subject's intention.

4.2 Myoelectric control of the robotic system

4.2.1 Mechanisms that affected the movement of subjects after stroke

The interruption of the descending pathway and the immobilization after stroke would cause contracture which consisted of a shortening of muscle and loss of muscle compliance (O'Dwyer et al., 1996; Williams, 1988). This change in passive mechanical properties made patients after stroke exert additional effort to counteract the passive torque generated by the stiff and shortened muscle during the movement within the available range.

Apart from the changes in the biomechanical properties of the muscles, Koo et al. (2003) reported a position-dependent joint weakness of the elbow extensors which might be caused by the reduced activation of the agonists in an extended position.

Ada et al. (2000) found that the flexor strength of subjects after stroke was less affected by the joint angle whereas their extensor strength was more affected compared with the subjects without impairment. Ada et al. (2003) found that patients after stroke had selective muscle weakness at a shortened position. These facts imply that it is harder for subjects after stroke to extend their forearm at the extended positions across the range of motion of the elbow joint.

Muscle cocontraction was also found in subjects after stroke which reflected the impairment of the ability to selectively activate flexor and extensors (McLellan et al., 1985). This often occurred in biceps activation during elbow extension, while the triceps muscle was less affected. This was confirmed by the facts found in the sinusoidal arm tracking experiment (Fig. 4.1). Fig. 4.1 shows the EMG activation of the biceps and triceps from both the affected and the unaffected arms during sinusoidal arm tracking experiment. During the elbow flexion, there was less triceps activation both in the affected and the unaffected arms. However, during the elbow extension, there was excessive biceps activation in the affected arm but not in the unaffected arm. The biceps of the affected arm at this time generated involuntary torque which would interfere with the extension movement.

Some subjects after stroke could not extend their forearm to the fully extended position, and the movement was also disturbed by the involuntary torque generated by the biceps. The objective of designing the robotic system was to assist the subjects after stroke to perform elbow movement. In order to help them to perform elbow extension more easily, the current study used the static EMG from the triceps and the MIVE torque to construct the gain value and control the robotic system to provide an additional assistive torque in proportion to the amplitude of the triceps during the arm tracking movement. Additional external resistive loads which were based on the MIVE torque were also applied to the robotic system in order to investigate the movement performance under different loads and prepare the suitable parameter settings for the experiment at the next stage.

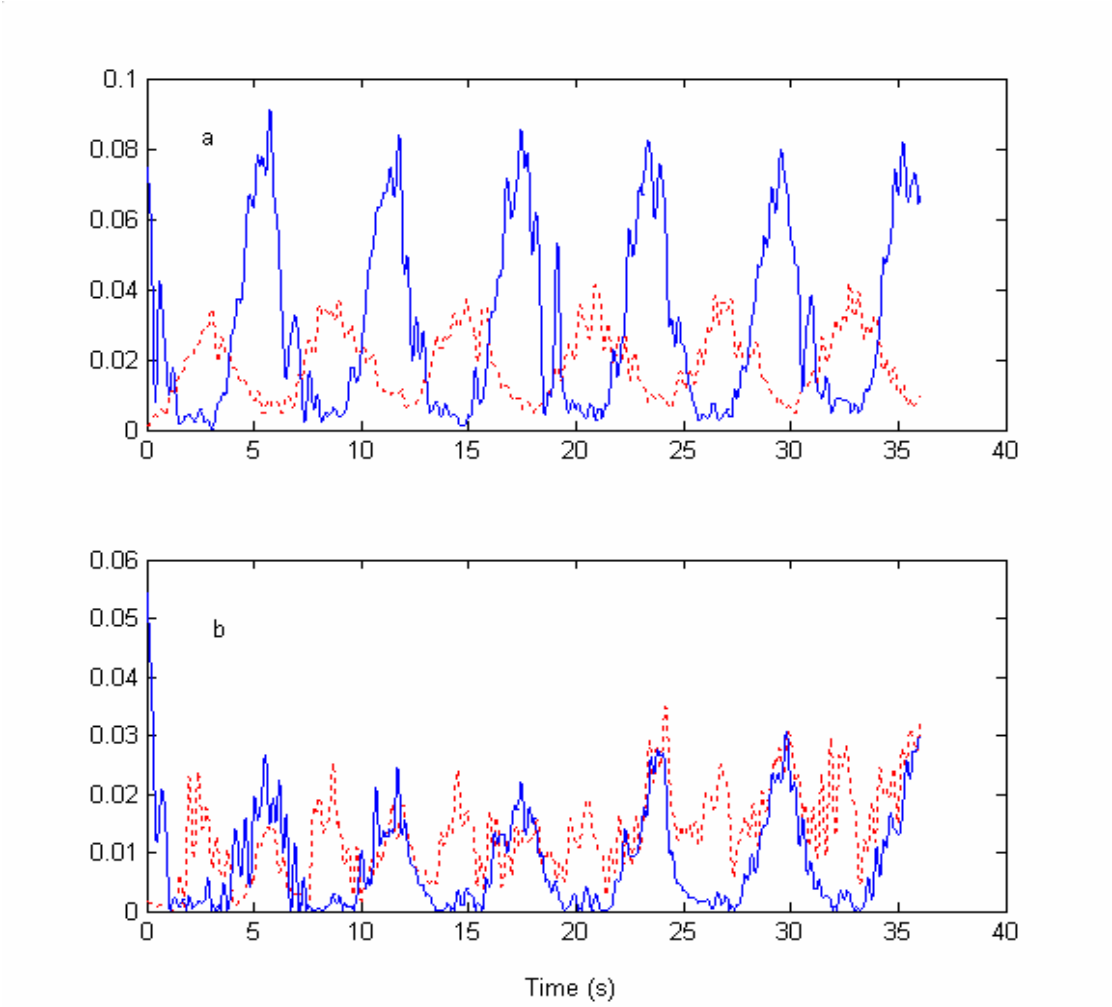

Fig. 4.1 The band-pass filtered (10-500 Hz), rectified and low-pass filtered (3 Hz) EMG signals of biceps (dotted line) and triceps (solid line) from the unaffected arm (a) and the affected arm (b) from a subject after stroke during the sinusoidal arm tracking experiment (the tracking velocity was at 20 deg/s).

4.2.2 Performance indices

The results of the tracking experiments revealed that with the increase in the gain, the NEMG of the triceps decreased. This meant that less effort was needed by subjects with the assistive torque from the robotic system. On the other aspect, the results showed that the ability of subjects after stroke to perform arm movement had been improved with the assistance of the robotic system. Subjects had more capacities to contradict the effect from stiff muscle and tissue, excessive muscle activation, and weak triceps during elbow extension. The increase in the extension range confirmed

the effect of the myoelectrically controlled system. The group mean RMSE even decreased with the assistance of the myoelectrically controlled robotic system in comparison with that without the assistance, while there was no significant difference in the most of the pairwise comparisons. There was a significant decrease in the RMSE at 100% of the gain as compared to that at 0 % of gain. The results showed that the assistance from the system did not bring the deterioration in the control of elbow. The experiment presented an increase in the RMSJ with the increase in the gain. The RMSJ reflected the smoothness of the trajectory and the results showed a deterioration in the smoothness when the gain increased. It was recommended that 100% and 50% assistive torques be used for the training, because the 150% assistive torque could not bring further improvement in the extension range and the RMSE. The system did not consider damping effect which might be a reason to cause an increase in jerk with the increase in the gain and the load. In our training protocol, the velocity was at a relatively low velocity. As subjects could easily control their affected forearm together with the manipulandum to follow the target at this velocity, the limitation could be relieved. For further investigation at a higher velocity or a more complex velocity profile, a damping component should be considered into the control strategy design in order to get a smoother trajectory.

4.2.3 Comparison of current system with other assistive devices

The exoskeleton system developed by Rosen's group (Rosen et al., 2001; Cavallaro et al., 2005) used EMG signals as the primary command signal to provide torque control in performing elbow movement with a scaled-down loading on the subject without impairment. A Hill-type muscle model was used to map between the EMG signals and the output torque and the system had not been applied among subjects after stroke. Cheng et al. (2003) also reported an EMG-controlled robot device to give assistive torque to subjects after stroke to perform elbow tracking and reaching in the vertical plane. Processed EMG signals from the biceps and triceps determined the amplitude of the torque which was applied by the motor through an adaptive filter. Both systems used EMG signals from the biceps and triceps to estimate a summed torque at the elbow joint. However, interference would occur due to the muscle co-contraction or spasticity if these systems were applied among subjects after stroke. Involuntary torque might originate from the excessive biceps activation. Cheng et al. (2003) used their system on subjects after stroke and reported that excessive co-contraction could

lead to instability of the robotic system. Their study merely investigated the performance within the range of 30 deg and did not provide any improvement in the extension range with the assistance of the robotic system. Moreover, there was a lack of long-term evaluation of the effect of their system on the upper limb functions.

In order to help subjects after stroke to perform elbow extension, some modifications were made to the two systems mentioned above. Only the EMG signal from the affected triceps was considered in this study, since the biceps was antagonist and did not have direct assistance to the movement. Moreover, our system did not want to amplify the involuntary effect on the biceps. The effectiveness of the system may be seen in the increase of the extension range for these subjects. Moreover, it took less effort for subjects after stroke to perform the same movement from 90 deg to 60 deg with a larger gain. Therefore, this design was also used in the next experiment which investigated the training effect of the myoelectrically controlled robotic system in a four-week rehabilitation training program for subjects after stroke.

4.3 Functional evaluation using the sinusoidal arm tracking system

4.3.1 Root mean square error

The damage in the motor cortex and immobilization after stroke would interfere with the sensorimotor control function of the upper limb, which might affect both the efferent and afferent motor control of the affected arm. The arm tracking experiments in this study used the RMSE as a performance indicator to reflect the elbow control function. The larger RMSE values from the affected arms when compared with the unaffected arms showed that it was more difficult for subjects to control their affected arms to follow the target. When the target velocity was increased, the difficulty of the task also increased, and a monotonic increase in RMSE also occurred in both the affected and the unaffected arms. The results showed that the RMSE was an effective parameter to be integrated with the arm tracking task in the functional evaluation of the elbow. A study done by Patten et al. (2003) also evaluated the perceptual motor control among hemiparetic adults with an upper limb trajectory tracking task. In their study, subjects performed an elbow flexion-extension task against a low-resistance isotonic load at three speeds: 25, 45 and 65 deg/s from 10 deg extension to 75 deg flexion. However, their results were contrary to what we found. In their experiment, the best performance occurred at the velocity of 45 deg/s for the affected arms, while

the RMSE in our experiment showed a monotonic increase with the increased tracking velocity. Several possible reasons might explain such difference. First, a one ft-lb additional torque in their experiment was applied to the elbow, which might have affected the tracking results. Second, it took time for subjects to adapt to the trajectory. Each of their subjects only performed two cycles of reciprocal extension and flexion which might have caused the large variation. In our results, the RMSE of the first few cycles was often larger than the succeeding cycles, which could be seen in Fig. 3.15. Furthermore, the different ranges of motion and starting points in these two experiments were also the factors that affected the results.

4.3.2 Root mean square jerk

From Flash and Hogan's minimum-jerk model (Flash et al., 1985; Wiegner et al., 1992), the natural voluntary movements are smooth, which can be reflected from minimized jerk cost. Therefore, the jerk cost could be used to evaluate the smoothness of the voluntary movements. In this study, the RMSJ of the affected arms exhibited a higher value at the elbow joint when compared to the unaffected arms, which was caused by the impaired control function after stroke. These results were consistent with Ju et al's work (Ju et al., 2002), who also found a significant increase in the integration of squared jerks (ISJ) for the affected arms of patients after stroke as compared with the unaffected arms during elbow tracking at 10 deg/s. The RMSJ could be used to describe the different smoothness between the affected and unaffected side in Fig. 3.16. Fig. 3.16 shows that there are more fluctuations in velocity, acceleration and jerk from the affected arm during the tracking test compared to those from the unaffected arm. The fluctuations could be explained by the changes in the mechanical properties of the elbow joint after stroke. The mechanical properties of the joint were time varying during cyclic voluntary movement (Bennet et al., 1992; Winter et al., 1988). In order to complete a task, the subjects rely on adjusting the mechanical properties of their arm, which reflects the combined influence of the muscle, the tendon and the proprioceptive feedback. The biceps and triceps would be expected to provide some damping effect to the elbow joint during the movement. For subjects after stroke, hypertonia often occurred in the affected muscles of the elbow, and the Ashworth scale was used to reflect the hypertonicity (Yeh et al., 2004). Significant correlations between the Ashworth scale and biomechanical model indices had been found during a constant velocity stretch

which suggested that the mechanical properties of affected muscles had changed on persons after stroke (McCrea et al., 2003; Pisano et al., 2000; Damiano et al., 2002). The higher RMSJ from the affected arms and the significant correlation between the RMSJ and the modified Ashworth scale in this study reflected that the change of the mechanical properties of the affected muscles interfered with the voluntary movement and resulted in a less smooth trajectory.

4.3.3 Response delay (RD)

The RD in this study showed the overall delay throughout the full cycle. The RD was significantly longer in the affected arms than in the unaffected arms and this could be related to lesions which caused specific impairments in the processing and efferent mechanisms of the central nervous system. The longer delay in initiation of the movement of the affected arm could be quantitatively reflected from the parameter. This finding was consistent with the report of other studies which concluded that there was a significantly longer initial and termination of the muscle force in the affected wrists than the unaffected wrists (Chae et al., 2002b). In our study, during the low velocity tracking (10 deg/s), a large deviation in the delay was found among subjects (Fig. 3.19); some had lags and some had advances between the target and the actual trajectory. When the velocity increased, it was harder for the subjects to follow the trajectory which resulted in an increase in the RD, thus the actual angle was mostly behind the target. The deficiency of the control ability on the affected arms resulted in a larger RD when the tracking velocity was from 20 deg/s to 60 deg/s.

The RMSE reflected the overall control ability. The RMSJ was related to the mechanical properties of the agonist and antagonist muscle pairs during a voluntary movement. The RD reflected the response action in the central nervous system to receive feedback signals and to control the movement. Although the three parameters reflected the motion quality from different aspects, they were inter-correlated; the longer RD and the larger RMSJ would also affect the RMSE value.

The voluntary elbow tracking task based on the system could be used to quantitatively evaluate the elbow motor control function of subjects after stroke. The results showed significant differences in the RMSE, RMSJ and RD when the affected and the unaffected arms were compared during the arm tracking experiment. The RMSE and

RMSJ increased with the increase in the tracking velocity for both the affected arms and the unaffected arms. These three parameters could be used as quantitative measurements during the rehabilitation training to evaluate the upper limb control function on persons after stroke in order to monitor the effect of different kinds of treatments and rehabilitation devices.

One factor which could interfere with the RMSE and RMSJ was the range of motion that subjects could perform. The subjects were instructed to follow the sinusoidal trajectory from 30 deg to 90 deg. They could finish this task better at lower velocities when using their affected arms. However, the subjects had difficulty in following the target at higher velocities which resulted in the decrease in the range of motion (Fig. 3.23). This phenomenon only occurred on the affected arm and the reasons might be as follows. Firstly, this phenomenon reflected the weakness of the affected muscle and its slowness to develop torque for subjects after stroke (Canning et al., 1999; Lum et al., 2004). Secondly, the cocontraction at the elbow joint could also affect the tracking performance (Chae et al, 2002a). Thirdly, a higher velocity might easily trigger the spasticity which could interfere with the subjects' tracking ability.

4.4 Effects of the training using the myoelectrically controlled robot

4.4.1 Possible mechanisms underlying this method

For subject after stroke, it was hard to move their affected arms. Therefore, they preferred to use their unaffected arms. This immobilization caused further deterioration of their upper limb function. The over-reliance on the unaffected arm also had an adverse effect on the function restoration of their affected arm. This was the theory of 'learned no use' that was applied in the constraint-induced movement therapy (CIMT) (Mark et al., 2004). The myoelectrically controlled robotic system was applied on the three subjects after stroke to investigate its long-term effect over a four-week period. The CIMT focused on the limitation of the unaffected arm in order to force the subjects to use their affected arm. In contrast, our design focused on amplifying the residual voluntary function of the affected arm in order to promote them to use their affected arm. This method was similar to Ward's hypothesis-driven approaches that rehabilitation could be promoted by the reduction of the somatosensory input from the intact hand and by the increase in somatosensory input from the paretic hand (Ward et al., 2004).

The myoelectrically controlled robotic system could assist subjects after stroke to extend their arm to a more extended position. In the first few sessions, the subjects might not be able to extend their arms to the fully extended position, but they could reach the extended position that they could not achieve in the horizontal plane through their own voluntary efforts (Fig. 3.29). Ada et al. (2003; 2000) suggested that the training at shortened muscle length was more effective in developing muscle strength at such muscle length. However, subjects after stroke often had difficulties in training the triceps at such position. It was hard or even impossible to reach such range due to contracture, muscle cocontraction or muscle weakness. The assistive function of the myoelectrically controlled robotic system could enable subjects after stroke to train at this range, which might have a potential beneficial effect. After several training sessions, the results showed that subjects could reach a more extended position even without the assistance from the robotic system. After the four-week training, two of the subjects could reach the fully extended position (0 deg) and the extension range of one subject also improved.

Different gains and loads were used in different sessions in order to familiarize the subjects with the different training environments and to help them adapt better. The gain could assist the subjects to move in a larger range, and the load could act as a resistive element to strengthen the muscle group during training. Virtual feedback on the elbow angle helped the subjects to correct the movement with their own intention through their own muscle under the assistance of the myoelectrically controlled robot system.

4.4.2 Functional improvement after the four-week rehabilitation training

The results showed that training using the myoelectrically controlled robotic system had positive effect to the subjects' affected arms. Quantitative measurements during each session with the robotic system could enable us to characterize their rates of improvement on a daily basis. The decrease of RMSE between the measured elbow angle and the target angle with the ongoing of the rehabilitation training reflected the continuous functional improvement during the training.

After the four-week training, there were increases of the muscle strength in the elbow flexors and elbow extensors of all the subjects after stroke, which seemed to be related

to the resistant loading during the training. This result was consistent with other studies on the effect of resistance strength training (Weiss et al., 2000; Ouellette et al., 2004). The evaluation based on the Fugl-Meyer scale and the modified Ashworth scale also showed the functional improvement in the affected arms.

The sinusoidal arm tracking experiment was also conducted to evaluate the upper limb function for subjects after stroke before and after the four-week training. In the test, six sinusoidal tracking velocities were investigated in order to reflect the functional improvement in different dynamic situations. After the four-week training, there were improvements in the RMSE and RD across all the velocities from the sinusoidal tracking test. The improvement in the RMSJ was also found at lower tracking velocities.

Subjective follow-up questionnaire among the subjects would be useful for future developments and adjustments on our robotic system and training protocol. All three subjects agreed that it was easy to manipulate the myoelectrically controlled robotic system. They also agreed that their elbow function together with their ability to carry out daily activities improved after training. Overall, they were satisfied with the rehabilitation training.

4.4.3 Other features of the robotic system

One advantage of this system was its multifunctionality. The system not only provided a training function but also provided an evaluation function. RMSE between the target trajectory and the elbow angle of each trial was displayed on the screen to provide visual feedback on the performed tracking. The RMSE value reflected the subject's tracking ability which could give useful guidance to these subjects. The angle, torque and EMG signals were captured during the training for off-line analysis. These data were useful to investigate the relationship among these variables during the training. The system gave us an open architectural platform on designing different control strategies for different applications through Labview programming for future developments.

4.4.4 Comparison of the system with other robotic devices for stroke rehabilitation

Passive movements have been showed to have beneficial effects on restoring the upper limb functions (Nelles et al., 2001). Cozens (1999) suggested that a robotic system should provide sufficient assistance to compensate for patients' impairments, but this should not transform the active exercise into a passive manipulation. It would be better if the subjects could perform motor relearning training voluntarily. The recent developments on rehabilitation robots also worked towards this interactive control, which allowed the robotic systems reacting to subjects efforts. MIT-MANUS was an interactive system, whose low inertia and adjustable guidance facilitate some patients with hemiplegia to move with their own effort. Admittance control in Colombo's robotic systems could also reduce the inertia and facilitate the subjects to use the system based on an interactive way. MIT-MANUS has been validated by large samples for its effectiveness including randomized controlled experiments (Krebs, et al., 1999; 2000 Volpe et al., 2000). Colombo's rehabilitation robotic systems were applied on 16 subjects in a three-week rehabilitation program. The MIME system and Bi-manu-tracking trainer could assist subjects to train their affected upper limb by following the trajectory from the unaffected limb. However, the control signal was not directly from the affected arm and it was indirectly controlled by the movement from the unaffected arm. Less compliant in the MIME system prevented weak subjects to move in a voluntary mode if the effort was from the affected arm. Although these current robotic devices have their advantages in the interactive control, none of them could provide voluntary support to the subjects who could not move the robotic system through their own effort using the affected arm. With the design in our system, the subject's effort could be detected from his/her EMG signal. The effort was directly linked to the assistance from the robotic system. Different loads and gains were added to enable the subject to train in different situations, and there was no assistant torque without the subject's effort. The system can be applied to subjects after stroke at different levels, especially for people who have problems in moving their arms, to perform an arm movement in a voluntary way if they have the residual voluntary triceps EMG signal on the affected arm. Rehabilitation training with cognitive investment for these subjects after stroke might promote motor relearning.

4.4.5 Comparison of the system with myoelectrically controlled functional electrical stimulation (FES) system

The sensorimotor integration theory suggests that the voluntary efferent output as well as the afferent input might assist in reorganizing the damaged brain area (Cauraugh et al., 2000). Therefore, it was better if the subject could keep efferent efforts to their affected arms rather than merely receiving afferent input in a simple passive training. In order to realize an active voluntary training, capturing the human's intention to build a man-machine interface and synchronizing the external stimulation with the human's intention were essential. The myoelectrically controlled FES system which was introduced in section 1.2.4 had realized this cognitive investment using the residual voluntary EMG signal of the affected muscle to control the FES system. However, the EMG-controlled FES system also had disadvantages which limited its application. It was known that the stimulation could cause secondary responses of the muscle which were added to the recorded EMG signals and caused instability (Fisher 1992). Robotic devices have demonstrated their advantages, and exoskeletons with EMG control strategy have also been reported to realize a natural control as assistive devices both for unimpaired subjects (Rosen et al, 2001) and for subjects after stroke (Cheng et al., 2003). Less effort is needed with the assistance of the devices than without the assistance. To apply such assistive robotic systems in the upper limb rehabilitation training for subjects after stroke was the main objective of this study. The surface EMG signals of the affected muscles would be captured as input signals to the robotic system, which could reflect the human's intention from the partial paralyzed muscle. The robotic system could provide the corresponding assistive and resistive torque during training. The cognitive investment and the performance improvement would encourage the subject to be actively and confidently involved into the voluntary rehabilitation training

4.4.6 Limitations of the current system

Since the myoelectrically controlled robotic system has one degree of freedom (DOF), only the affected elbow can be trained with this system. The myoelectrically controlled robotic system was developed and applied at a relatively low velocity (10 deg/s) in this study. For higher velocities or more complex velocity profiles, the control strategy needs further development in order to be easily controlled by the subjects. A damping component may be needed in order to get a smoother trajectory

in the future development for higher velocity application. The preliminary results of the four-week training showed that the system had the potential to restore the upper limb function for persons after stroke. Further studies should be undertaken to confirm its clinical efficacy with a large-scale randomized controlled experiment.

CHAPTER 5 CONCLUSIONS AND FUTURE STUDIES

5.1 Summary

The key objectives of this study were to develop a myoelectrically controlled robotic system, and to investigate its feasibility and effectiveness on assisting control of the elbow movement and on restoring upper limb function in the four-week training program for subjects after stroke.

The key contributions of this study were as follows. Firstly, a myoelectrically controlled robotic system with one degree of freedom (DOF) was developed. With the application of the proportional control, the system could provide assistive extension torque which was proportional to the subjects' processed and normalized triceps EMG signal during elbow extension. The system could also provide a resistive torque during elbow flexion and extension, the levels of which were based on the maximum isometric voluntary flexion (MIVF) torque and the maximum isometric voluntary extension (MIVE) torque, respectively.

Secondly, elbow movement with the assistance of the myoelectrically controlled robotic system was investigated on subjects after stroke. The effect of the different combinations of EMG-torque gain and resistive load to the performance of the elbow extension was evaluated on the affected arms of nine subjects after stroke. Results showed that the design could enable subjects with weak triceps to extend their affected elbows to a more extended position with the assistance of the current system and it took less effort for subjects after stroke to perform the same movement when the EMG-torque gain increased.

Thirdly, a four-week training using the myoelectrically controlled robotic system was conducted on three subjects after stroke. Results showed that there was a functional improvement in the affected arm of all three subjects after the four-week training. Outcome measurements on the muscle strength at the elbow joint showed that there were increases in the MIVE and MIVF torques for all the subjects after the four-week rehabilitation training. There was an increase in the extension range for the three subjects without the assistance of the robotic system after the four-week rehabilitation training. Moreover, the functional improvements in the affected arm could also be reflected from the changes in the modified Ashworth scale and the Fugl-Meyer score for the three subjects.

Finally, sinusoidal arm tracking experiments was designed in this study to quantitatively evaluate the elbow control function for subjects after stroke in dynamic situations. The experimental results showed that there were increases in the root mean square error (RMSE) and root mean square jerk (RMSJ) in both the affected and the unaffected arms with the increase in tracking velocity. The RMSE and RMSJ of unaffected arms were significantly lower than those of the affected arms at all the velocities. The response delay (RD) of the affected arms was larger than that of the unaffected arms at the velocities of 20, 30, 40 and 60 deg/s. There were significant correlations between the RMSJ and the modified Ashworth scale at the velocities of 10, 20, 30, 40 and 60 deg/s. The sinusoidal arm tracking experiment was also used as an evaluation tool in the four-week training program, and the functional improvement in the affected arms of the three subjects after stroke could be reflected from the deceases in the RMSE and RD after the four-week training.

5.2 Future studies

Based on the results in this study, further studies could be conducted in the following parts:

In this study, we investigated the long-term training effect of the myoelectrically controlled robotic system. Although positive effect had been found in all three subjects after the four-week training, the research suffered from limited number of subjects. In order to further confirm the efficacy of the myoelectrically controlled robotic system in the rehabilitation training, a large-scale randomized control experiment should be conducted and compared with conventional methods or other robotic devices.

The myoelectrically controlled robotic system could only be used to train the elbow at this time, it would be better if the rehabilitation training with the robotic system could be extended to more joints. Therefore, the system can be further developed for other joints such as wrist, shoulder and ankle. Moreover, a myoelectrically controlled robotic system with multiple degrees of freedom can be developed for more muscle groups, and the movements in the rehabilitation training can be related to activities of daily living.

I hope all the efforts in this study could benefit the persons after stroke in the rehabilitation and for the future development in the robot-aided rehabilitation.

REFERENCES

Ada L, Canning C, Dwyer T. Effect of muscle length on strength and dexterity after stroke. Clin Rehabil; 14(1):55-61 (2000).

Ada L, Canning CG, Low SL. Stroke patients have selective muscle weakness in shortened range. Brain; 126(Pt 3):724-31 (2003).

Aisen ML, Krebs HI, Hogan N, McDowell F, Volpe BT. The effect of robot-assisted therapy and rehabilitative training on motor recovery following stroke. Arch Neurol; 54(4):443-6 (1997).

An KN, Kwak BM, Chao EY, Morrey BF. Determination of muscle and joint forces: a new techniques to solve the indeterminate problem. Trans ASME J Biomech Engng; 106:364-367 (1984).

Angeleri F, Angeleri VA, Foschi N, Giaquinto S& Nolfe S The influence of depression, social activity, and family stress on functional outcome after stroke. Stroke; 24: 1478-1483 (1993).

Ashworth B. Preliminary trial of carisprodol in multiple sclerosis. Practition; 192:540-542 (1964).

Au ATC and Kirsch RF. EMG-Based Prediction of shoulder and elbow kinematics in able-bodied and spinal cord injured individuals. IEEE Trans on Rehab Eng; 8: 471-480 (2000).

Basmajian JV, Gowland C, Brandstater ME, Swanson L, Trotter J. EMG feedback treatment of upper limb in hemiplegic stroke patients: a pilot study. Arch Phys Med Rehabil; 63: 613-16 (1982).

Basmajian JV, Deluca CJ. Muscles Alive: Their Functions Revealed by Electromyography. Baltimore: Williams & Wilkins; 561 p (1985).

Bennett DJ, Hollerbach JM, Xu Y, Hunter IW. Time-varying stiffness of human elbow joint during cyclic voluntary movement. Exp Brain Res; 88: 433-442 (1992).

Bobath B. Adult hemiplegia: evaluation and treatment. London: William Heinemann, 1–29, 31–157 (1990).

Bode RK, Heinemann AW, Semik P, Mallinson T. Relative importance of rehabilitation therapy characteristics on functional outcomes for persons with stroke. Stroke; 35(11):2537-4, (2004).

Bohannon RW, Smith MB. Interrater Reliability of a Modified Ashworth Scale of Muscle Spasticity. Phys Ther; 67:206-207 (1986).

Bradley L, Hart BB, Mandana S, Flowers K, Riches M, Sanderson P. Electromyographic biofeedback for gait training after stroke Clin Rehab; 12: 11–22 (1998).

Brodal A. Self-observations and neuro-anatomical considerations after a stroke. Brain; 96:675-694 (1973).

Broeren J, Rydmark M, Sunnerhagen KS. Virtual reality and haptics as a training device for movement rehabilitation after stroke: a single-case study. Arch Phys Med Rehabil; 85(8): 1247-50 (2004).

Brown M, Harris C. Neurofuzzy adaptive modelling and control. Prentice hall; (1994).

Burgar CG, Lum PS, Shor PC, Machiel Van der Loos HF. Development of robots for rehabilitation therapy: The Palo Alto VA/Stanford experience. J Rehabil Res Dev; 37 (6): 663-673 (2000).

Canning CG, Ada L, O'Dwyer NJ. Slowness to develop force contributes to weakness after stroke. Arch Phys Med Rehabil; 80:66–70 (1999).

Canning CG, Ada L, O'Dwyer NJ. Abnormal muscle activation characteristics associated with loss of dexterity after stroke. J Neurol Sci; 176(1):45-56 (2000).

Carlo J. Luca D. The use of surface electromyography in biomechanics, Wartenweiler Memorial Lecture (the International Society for Biomechanics) 5, (1993).

Carr JH and Shepherd RB. A Motor Relearning Program for Stroke (2nd ed.) London: Heinemann Physiotherapy; (1987).

Cauraugh J, Light K, Kim S, Thigpen M, Behrman A. Chronic motor dysfunction after stroke: recovering wrist and finger extension by electromyography-triggered neuromuscular stimulation. Stroke;31(6):1360-1364 (2000).

Cavallaro E, Rosen J, Perry JC, Burns S, Hannaford B. Hill-type model as a myoprocessor for a neural controlled powered exoskeleton arm- parameters optimization. IEEE ICRA2005 4525-4530 (2005).

Chae J, Bethoux F, Bohine T, Dobos L, Davis T, Friedl A. Neuromuscular stimulation for upper extremity motor and functional recovery in acute hemiplegia. Stroke; 29: 975–9 (1998).

Chae J, Yang G, Park BK, and Labatia I. Muscle weakness and cocontraction in upper limb hemiparesis: relationship to motor impairment and physical disability. Neurorehabil Neural Repair; 16: 241–248 (2002a).

Chae J, Yang G, Park BK, Labatia I. Delay in initiation and termination of muscle contraction, motor impairment, and physical disability in upper limb hemiparesis. Muscle Nerve; 25(4): 568-75 (2002b).

Cheng HS, Ju MS, Lin CCK. Improving elbow torque output of Stroke patients with assistive torque controlled by EMG signals. J Biomech Eng; 125: 881-886 (2003).

Cheron G, Draye J P, Bourgeios M, Libert G. A dynamic neural network identification of electromyography and arm trajectory relationship during complex movements' IEEE Trans Biomed Eng; 43: 552-558 (1996).

Collen FM, Wade DT, Robb GF, Bradshaw CM. The Rivermead Mobility Index: a further development of the Rivermead Motor Assessment. International Disability Studies; 13: 50-54 (1991).

Colombo R, Pisano F, Micera S, Mazzone A,. Delconte C, Carrozza MC, Dario P, Minuco G. Robotic Techniques for Upper Limb Evaluation and Rehabilitation of Stroke Patients. IEEE Trans Neural Sys Rehab Eng; 13(3): 311- 324 (2005).

Cornu C, Goubel F, Fardeau M. Muscle and joint properties during elbow flexion in. Duchenne muscular dystrophy. Journal of Physiology; 533(2): 605-616 (2001).

Cozens JA. Robotic assistance of an active upper limb exercise in neurologically impaired patients. IEEE Trans. On Rehab Eng; 7:254-256 (1999).

Cram JR, Kasman GS, Holtz J. Introduction to Surface Electromyography. Gaithersburg: Aspen Publishers; (1998).

Damiano DL, Quinlivan JM, Owen BF, Payne P, Nelson KC, Abel MF. What does the Ashworth scale really measure and are instrumented measures more valid and precise? Dev Med Child Neurol; 44(2): 112-8 (2002).

Deutsch J, Merians A, Adamovich S, Poizner H, Burdea G. Development and application of virtual reality technology to improve hand use and gait of individuals post-stroke. Restor Neurol Neuros; 22(3-5):371-86 (2004).

Delp SL, Loan JP. A graphics-based software system to develop and analyze models of musculoskeletal structures. Comput Biol Med; 25:21-34 (1995).

Dewald JP, Pope PS, Given JD, Buchanan TS, Rymer WZ. Abnormal muscle coactivation patterns during isometric torque generation at the elbow and shoulder in hemiparetic subjects. Brain; 118 (2):495-510 (1995).

Dickstein R, Shefi S, Marcovitz E, Villa Y. Electromyographic activity of voluntarily activated trunk flexor and extensor muscles in post-stroke hemiparetic subjects. Clin Neurophysiol; 115(4):790-6 (2004).

Dipietro L, Sabatini AM, Dario P. Artificial neural network model of the mapping between electromyographic activation and trajectory patterns in free-arm movements. Med Biol Eng Comp; 41: 125-132 (2003).

Dobkin BH. Strategies for stroke rehabilitation. Lancet Neurol; 3: 528-536 (2004).

Fasoli SE, Krebs HI, Hogan N. Robotic technology and stroke rehabilitation: translating research into practice. Top Stroke Rehabil; 11(4):11-19 (2004).

Feng CJ, Mak AF. Three-dimensional motion analysis of the voluntary elbow movement in subjects with spasticity. IEEE Trans Rehabil Eng; 5(3):253-262 (1997).

Feng CJ, Mak AFT. Neuromuscular model for the stretch reflex in passive movement of spastic elbow joint. In: IEEE Biomedical Engineering Proceedings (1998).

Feng J, Mak AFT, Koo TKK. A surface EMG driven musculoskeletal model of the elbow flexion-extension movement in normal subjects and in subjects with spasticity. J Musculoskeletal Res; 3:109-123 (1999).

Ferraro M, Demaio JH, Krol J, Trudell C, Edelstein L, Christos P, England J, Fasoli S, Aisen ML, Krebs HI, Hogan N, Volpe BT. Assessing the motor status score: A scale for the evaluation of upper limb motor outcomes in patients after stroke. Neurorehabil Neural Repair;16: 283–289 (2002).

Fisher CM. Concerning the mechanism of recovery in stroke hemiplegia. Can J Neurol Sci; 19:57-63 (1992).

Fisher MA. AAEM minimonograph #13: H reflexes and F waves: Physiology and clinical indications. Muscle Nerve; 15:1223–1233 (1992).

Fitts PM. The information capacity of the human motor system in controlling the amplitude of movement. J Exp Psychol; 47(6): 381-391 (1954).

Flash T, Hogan N. The coordination of arm movements: An experimentally confirmed mathematical model. J Neurosci; 5: 1688-1703 (1985).

Fugl-Meyer AR, Jaasko I, Leyman I, Olssom S, Steglind S. The post-stroke hemiplegic patient. I. A method for evaluation of physical performance. Scand J Rehab Med; 7:13-31 (1975).

Gregson JM, Leathley MJ, Moore AP, Smith TL, Sharma AK, Watkins CL. Reliability of measurements of muscle tone and muscle power in stroke patients. Age Ageing; 29(3):223-8 (2000).

Given JD, Dewald JP, Rymer WZ. Joint dependent passive stiffness in paretic and contralateral limbs of spastic patients with hemiparetic stroke. J Neurol Neurosurg Psychiatry; 59(3):271-9 (1995).

Greshman GE, Alexander D, Bishop DS, Giuliani C, Goldberg G, Holland A, Kelly-Hayes M, Linn RT, Roth EJ, Stason WB, Trombly CA. Rehabilitation. Stroke; 28: 1522-1526 (1997).

Gonzalez EG, Myers SJ, Edelstein JE, Lieberman JS, Downey JA. Physiological Basis of Rehabilitation Medicine. 3rd Edition, Butterworth-Heinemann Publishers, Woburn MA, pp 890, (2001).

Graupe D. EMG pattern analysis for Patient-Responsive Control of FES in Paraplegics for Walker-Supported Walking, IEEE Trans Biomed Eng; 36(7): 711-719 (1989a).

Graupe D, Kohn KH, Basseas.SP. Control of electrically-stimulated walking of paraplegics via above and below-lesion EMG signature identification. IEEE Trans on Automatic Control; 34(2): 130-138 (1989b).

Gribble PL, Mullin LI, Cothros N, Mattar A. Role of cocontraction in arm movement accuracy. J Neurophysiol; 89(5): 2396-405 (2003).

Gregor RJ, Komi PV, Browning RC, Jarvinen M. A comparison of the triceps surae and residual muscle moments at the ankle during cycling. J Biomech; 24: 287-97 (1991).

Gurbuz H, Kivrak E, Soyupak S, Yerli SV. Predicting dominant phytoplankton quantities in a reservoir by using neural networks. Hydrobiologia; 504: 133-141 (2003).

Haaland KY, Harrington DL, Yeo R. The effects of task complexity on motor performance in left and right CVA patients. Neuropsychologia; 25(5):783-94 (1987).

Hallett M. Plasticity of the human motor cortex and recovery from stroke. Brain Res. Rev; 36: 169–174 (2001).

Hammond M. Fitts S, Kraft G, Nutter R. Trotter M, Robinson L. co-contraction in the hemiparetic forearm: quantitative EMG evaluation. Arch Phys Med Rehabil; 69: 348-351 (1988).

Hatano S. Experience from a multicentre stroke register: a preliminary report. Bulletin of the World Health Organisation; 54; 541-553 (1976).

He JP, Norling WR, Wang Y. A dynamic neuromuscular model for describing the pendulum test of spasticity. IEEE Trans Biomed Eng; 44:175-184 (1997).

Heine R, Manal K, Buchanan TS. Using Hill-type muscle models and EMG data in a forward dynamic analysis of joint moment: evaluation of critical parameters. J Mech Med Biol; 3(2): 169-186, (2003).

Hesse S, Schulte-Tigges G, Konrad M, Bardeleben A, Werner C. Robot-assisted arm trainer for the passive and active practice of bilateral forearm and wrist movements in hemiparetic subjects. Arch Phys Med Rehabil; 84:915–920 (2003).

Hill AV. The heat of shortening and the dynamic constants of muscle. Proc Roy Soc B; 126:136-195 (1938).

Hirose Y, Yamashita K, Hijiya S. Back-propagation algorithm which varies the number of hidden units. Neural Networks; 4: 61–66 (1991).

Hof AL, Van Den Berg J. EMG to force processing I: An electrical analogue of the Hill muscle model. J Biomech; 14:747-758 (1981a).

Hof AL, Van Den Berg J. EMG to force processing II: Estimation of parameters of the Hill muscle model for the human triceps surae by means of a calfergometer. J Biomech; 14:759-770 (1981b).

Hof AL, Van Den Berg J. EMG to force processing III: Estimation of model parameters for the human triceps surae msucle and assessment of the accuracy by means of a torque plate. J Biomech; 14:771-785 (1981c).

Hogan, N An organizing principle for a class of voluntary movements. J Neurosci; 4: 2745-2754 (1984).

Hogan N. Impedance control: An approach to manipulation, parts i, ii, iii. ASME J Dyn Syst Meas Contr; 107: 1-24 (1985).

Hogan, N, Krebs HI, Charnnarong J, Srikrishna P, Sharon A. MIT-MANUS: a workstation for manual therapy and training. I. Robot and Human Communication, 1992. Proceedings, IEEE International Workshop on, 1-3: 161 -165 (1992).

Homma K and Arai T. Design of an upper limb motion assist system with parallel mechanism. Proc of the IEEE International Conference on Robotics and Automation; 1302-1307 (1995).

Hong Kong Hospital Authority Statistical Report 1994-2002. http://www.ha.org.hk/hesd/nsapi/?MIval=ha_view_template&group=IFN&Area=PBL&Subj=STR (2004).

International Bobath Tutors Association. http://www.bobath.org.uk/BobathConceptToday.html (2000).

Inglis J, Donald MW, Monga TN, Sproule M, Young MJ. Electromyographic biofeedback and physicaltherapy of the hemiplegic upper limb. Arch PhysMed Rehabil; 65: 755-59 (1984).

Jack D, Boian R, Merians AS, Tremaine M, Burdea GC, Adamovich SV, Recce M, Poizner H. Virtual Reality-Enhanced Stroke Rehabilitation, IEEE Trans Neural Sys Rehab Eng; 9(3): 308-318, (2001).

Jonkman EJ, de Weerd AW, Vrijens NLH Quality of life after first ischemic stroke. Longterm developments and correlations with changes in neurological deficits, mood and cognitive impairment. Acta Neurol Scand; 98: 169-175 (1998).

Johnson GR, Carus DA, Parrini G, Scattareggia Marchese S, Valeggi R. The design of a five-degree-of-freedom powered orthosis for upper limb. Proc Instn Mech Engrs; 215: 275-284 (2001).

Johansson BB, Brain Plasticity and Stroke Rehabilitation. Stroke; 31 223-230 (2000).

Ju MS, Chen JJ, Lee HM, Lin TS, Lin CC, Huang YZ. Time-course analysis of stretch reflexes in hemiparetic subjects using an on-line spasticity measurement system. J Electromyogr Kinesiol; 10:1-14 (2000).

Ju MS, Lin CCK, Chen JR, Cheng HS, Lin CW. Performance of elbow tracking under constant torque disturbance in normotonic stroke patients and normal subjects. Clin Biomech; 17:640-649, (2002).

Ju MS, Lin CCK, Lin DH, Hwang IS, Chen SM. A rehabilitation robot with force-position hybrid fuzzy controller: hybrid fuzzy control of rehabilitation robot. IEEE Trans Neural Sys Rehab Eng; 13(3): 349- 358 (2005).

Kahn LE, Zygman ML, Rymer WZ, Reinkensmeyer DJ. Effect of robot-assisted and unassisted exercise on functional reaching in chronic hemiparesis. Engineering in Medicine and Biology Society, 2001. Proceedings of the 23rd Annual International Conference of the IEEE, 2: 25-28 (2001) P 1344 -1347 vol.2

Kamper DG, Rymer WZ. Impairment of voluntary control of finger motion following stroke: role of inappropriate muscle coactivation. Muscle Nerve; 24(5):673-81 (2001).

Karni A, Meyer G, Jezzard P, Adams MM, Turner R, Ungerleider LG. Functional MRI evidence for adult motor cortex plasticity during motor skill learning. Nature; 377:155-8, (1995).

Katz RT, Rymer WZ. Spastic hypertonia: Mechanisms and measurement. Arch Phys Med Rehabil; 70:144-155 (1989).

Keith RA, Granger CV, Hamilton BB, Sherwin FS. The functional independence measure: a new tool for rehabilitation. In: Eisenberg MG, Grzesiak RC (ed.). Advances in clinical rehabilitation volume 1. New York: Springer-Verlag; p. 6-18 (1987).

Koike Y, Kawato M. Estimation of dynamic joint torques and trajectory formation from surface electromyography signals using a neural network model' Biol Cybernet; 73: 291–300 (1995).

Koo TK, Mak AF, Hung LK, Dewald JP. Joint position dependence of weakness during maximum isometric voluntary contractions in subjects with hemiparesis. Arch Phys Med Rehabil; 84: 1380-1386 (2003).

Koo TKK, Mak AFT Feasibility of using EMG driven neuromusculoskeletal model for prediction of dynamic movement. J Electromyogr Kinesiol; 15:12-26 (2005).

Krebs HI, Hogan N, Aisen ML, Volpe BT. Robot-aided neurorehabilitation. IEEE Trans Rehabil Eng; 6(1): 75-87 (1998).

Krebs HI, Volpe BT, Aisen ML, Hogan N. Increasing productivity and quality of care: Robot-aided neuro-rehabilitation. J Rehabil Res Dev; 37 (6): 639-652 (2000).

Krebs HI, Hogan N, Volpe BT, Aisen ML, Edelstein L, Diels C. Overview of clinical trials with MIT-MANUS: a robot-aided neuro-rehabilitation facility. Technol Health Care; 7: 419-423 (1999).

Lafleur M, Jackson P, Malouin F, Richards C, Evans A, Doyon J. Motor learning produces parallel dynamic functional changes during the execution and imagination of sequential foot movements. NeuroImage; 16(1): 142-57 (2002).

Lai JC, Woo J, Hui E. Chan WM. Telerehabilitation - a new model for community-based stroke rehabilitation. Journal of Telemedicine & Telecare. 10(4):199-205, 2004.

Lance JW. Symposium Synopsis. In: Feldman RG, Young RR, Koella WP eds. Spasticity: Disordered Motor Control. Chicago: Year Book Publishers; p.485-494 (1980).

Langhammer B. Bobath or motor relearning programme? A. comparison of two different approaches of physiotherapy in. stroke rehabilitation: a randomized controlled study, Clin Rehabil; 14: 361–369 (2000).

Langhammer B, Stanghelle JK. Bobath or Motor Relearning Programme? A follow-up one and four years post stroke. Clin. Rehabil. 17(4): 731-734 (2003).

Lee S, Sankai Y. Power Assist Control for Leg with HAL-3 based on Virtual Torque and Impedance Adjustment, Proc. of IEEE SMC (2002).

Lennon SM, Johnson L. The modified Rivermead Mobility Index; validity and reliability. Disabil Rehabil; 22:833-839 (2000).

Levy CE, Nichols DS, Schmalbrock PM, Keller P,Chakeres DW. Functional MRI evidence of corticalreorganization in upper-limb stroke hemiplegia treated with constraint-induced movement therapy. Am J Phys Med Rehabil; 80:4–12 (2001).

Liepert J, Miltner WH, Bauder H, Sommer M, Dettmers C, Taub E, Weiller C. Motor cortex plasticity during constraint-induced movement therapy in stroke patients. Neurosci Lett; 250(1): 5-8 (1998).

Liepert J, Bauder H, Wolfgang HR, Miltner WH, Taub E, Weiller C. Treatment-induced cortical reorganization after stroke in humans. Stroke; 31: 1210–1216 (2000).

Lin CC, Ju MS, Lin CW. The pendulum test for evaluating spasticity of the elbow joint. Arch Phys Med Rehabil; 84(1): 69-74 (2003).

Lin DC, Rymer WZ. A quantitative analysis of pendular motion of the lower leg in spastic human subjects. IEEE Trans Biomed Eng; 38: 906-918 (1991).

Lincoln N, Leadbitter D. Assessment of motor function in stroke patients. Physiotherapy; 65: 48-51 (1979).

Liu MM, Herzog W, Savelberg HCM. Dynamic muscle force predictions from EMG: an artificial neural network approach. J Electromyogr Kinesiology; 9: 391–400 (1999).

Lloyd DG, and Besier TF. An EMG-driven musculoskeletal model to estimate muscle forces and knee joint moments in vivo. J Biomech; 36: 765-776 (2003).

Luh JJ, Chang GC, Cheng CK, Lai JS and Kuo ES. Isokinetic elbow joint torques estimation from surface EMG and joint kinematic data: using an artificial neural network model. J. Electromyogr. Kinesiology; 9: 173-183 (1999).

Luke C, Dodd KJ, Brock K. Outcomes of the Bobath concept on upper limb recovery following stroke. Clini Rehabil; 18(8): 888-98 (2004).

Lum PS, Burgar CG, Kenney DE, Van der Loos HF. Quantification of force abnormalities during passive and active-assisted upper-Limb reaching Movements in post-stroke hemiparesis. IEEE Trans Biomed Eng; 46(6): 652-62 (1999).

Lum PS, Burgar CG, Shor PC. Evidence for improved muscle activation patterns after retraining of reaching movements with the MIME robotic system in subjects with post-stroke hemiparesis. IEEE Trans Neural Syst Rehabil Eng; 12(2): 186-94 (2004).

Lum PS, Patten C, Kothari D, Yap R. Effects of velocity on maximal torque production in poststroke hemiparesis. Muscle Nerve. 30(6): 732-42 (2004).

Manal K, Gonzalez RV, Lloyd DG, Buchanan TS. A real-time EMG-driven virtual arm, Comput Biol Med; 32: 25-36 (2002).

Manal K, Buchanan TS. A one-parameter neural activation to muscle activation model: Estimating isometric joint moments from electromyograms. J Biomech; 36: 1197-1202 (2003).

Mark VW, Taub E. Constraint-induced movement therapy for chronic stroke hemiparesis and other disabilities. Restor. Neurol. Neurosci. 22: 317-36 (2004).

Martini FH. Fundamentals of Anatomy and Physiology. New Jersey: Prentice Hall (1995).

McCrea PH, Eng JJ, Hodgson AJ. Linear spring-damper model of the hypertonic elbow: reliability and validity. J Neurosci Methods; 128:121-128 (2003).

McCrea PH. Eng JJ. Consequences of increased neuromotor noise for reaching movements in persons with stroke. Exp Brain Res; 162(1):70-7 (2005).

McLellan DL, Hassan N, Hodgson JA. Tracking tasks in the assessment of spasticity. In: Delwaide PJ. Young RR, editors, Clinical neurophysiology in spasticity. Amsterdam: Elsevier; 131-9 (1985).

Mescheriakov S, Holzmuller G, Molokanova E, Berger M. A new method of fitting and analysis of simple uni-joint arm movements. Eur J Appl Physiol Occup Physiol; 74(5):484-486 (1996).

Mima T, Toma K, Koshy B, Hallett M. Coherence between cortical and muscular activities after subcortical stroke. Stroke; 32(11): 2597-2601 (2001).

Mirbagheri MM, Barbeau H, Kearney RE. Intrinsic and reflex contributions to human ankle stiffness: variation with activation level and position. Exp Brain Res; 135:423–436 (2000).

Mirbagheri MM, Barbeau H, Ladouceur M, Kearney RE. Intrinsic and reflex stiffness in normal and spastic, spinal cord injured subjects. Exp Brain Res. 141(4):446-59 (2001).

Misener DL,mMorin EL. An EMG to force model for the human elbow derived from surface EMG IEEE-EMBC and CMBEC; 1205-1206 (1995).

Morris SL, Dodd KJ, Morris ME. Outcomes of progressive resistance strength training following stroke: a systematic review. Clin Rehabil;18(1):27-39 (2004).

Murray WM, Delp SL, Buchanan TS. Variation of muscle moment arms with elbow and forearm position. J Biomech; 28(5):513-25 (1995).

Murray WM, Buchanan TS, and Delp SL Scaling of peak moment arms of elbow muscles with dimensions of the upper extremity. J Biomech; 35:19-26 (2002).

Nakano E, Imamizu H, Osu R, Uno Y, Gomi H, Yoshioka T, Kawato M. Quantitative examinations of internal representations for arm trajectory planning: minimum commanded torque change model. J Neurophysiol; 81(5): 2140-55 (1999).

Nef T, Riener R. ARMin-design of a novel arm rehabilitation robot. Proceedings of IEEE ICORR 57-60 2005.

Nelles G, Jentzen W, Jueptner M, Muller S, Diener HC. Arm training induced brain plasticity in stroke studied with serial positron emission tomography. Neuroimage; 13:1146-54 (2001).

National Institute of Neurology Disorder and Stroke, US, http://www.ninds.nih.gov/disorders/stroke/poststrokerehab.htm, (2005)

O'Dwyer NJ, Ada L, Neilson PD. Spasticity and muscle contracture following stroke. Brain; 119 (Pt 5):1737-49 (1996).

Ouellette MM， LeBrasseur NK， Bean JF， Phillips E， Stein J， Frontera WR， Fielding RA. High-intensity resistance training improves muscle strength, self-reported function, and disability in long-term stroke survivors. *Stroke*；35(6):1404-9, (2004).

Pandy, MG Computer modeling and simulation of human movement. Annu Rev Biomed Eng; 3: 245-73 (2001).

Pandyan AD, Johnson GR, Price CIM, Curless RH, Barnes MP, Rodgers H. A review of the properties and limitations of the Ashworth and modified Ashworth scales as a measure of spasticity. Clin Rehabil; 13: 373-83 (1999).

Pandyan AD, Cameron M, Powell J, Stott DJ, Granat MH. Contractures in the post-stroke wrist: a pilot study of its time course of development and its association with upper limb recovery. Clin Rehabil; 17(1):88-95 (2003).

Patten C, Kothari D, Whitney J, Lexell J, Lum PS. Reliability and responsiveness of elbow trajectory tracking in chronic poststroke hemiparesis. J Rehabil Res Dev; 40(6): 487–500 (2003).

Pigeon P, Yahia L, and Feldman AG. Moment arms and lengths of human upper limb muscles as functions of joint angles. J Biomech; 29: 1365–1370 (1996).

Pisano F, Miscio G, Del Conte C, Pianca D, Candeloro E, Colombo R. Quantitative measures of spasticity in post-stroke patients Clin Neurophysiol; 111: 1015-1022 (2000).

Pollack MR, Disler PB. 2: Rehabilitation of patients after stroke. Medical Journal of Australia; 177(8): 452-6 (2002).

Poole JL, Whitney SL. Motor assessment scale for stroke patients: concurrent validity and interrater reliability. Arch Phys Med Rehabil; 69:195-197 (1988).

Reinkensmeyer DJ, Hogan N, Krebs HI, Lehman SL and Lum PS. Rehabilitators, Robotics and Guides: New Tools for Neurological Rehabilitation 1992. Biomechanics and Neural Control of Posture and Movement; 38: 516-534 (2000).

Reinkensmeyer DJ, Dewald JPA, Rymer WZ. Guidance-Based Quantification of Arm Impairment Following Brain Injury: A Pilot Study. IEEE Trans Rehab Eng; 7(1): 1-11 (1999).

Reinkensmeyer DJ, Kahn LE, Averbuch M, McKenna-Cole AN, Schmit BD, Rymer WZ. Understanding and treating arm movement impairment after chronic brain injury: Progress with the ARM Guide. J Rehabil Res Dev; 37(6): 653-662 (2000).

Riener R, Nef T, Colombo G. Robot-aided neurorehabilitation for the upper extremities. Med Biol Eng Comp; (43): 2-10 (2005).

Riener R, Straube A. Inverse dynamics as a tool for motion analysis: arm tracking movements in cerebellar patients. J. Neurosci Methods; 72: 87-96 (1997).

Robertson IH, Murre JMJ. Rehabilitation of brain damage: Brain plasticity and Principles of guided recovery. Psycological Bulletin; 125: 544-575, (1999).

Rosen J, Brand M, Fuchs MB, Arcan M. A myosignal-based powered exoskeleton system. IEEE T Sys Man Cy B; 31(3): 210-222 (2001).

Rosen J, Fuchs MB, Arcan M. Performances of hill-type and neural network muscle models - towards a myosignal based exoskeleton. Comput Biomed Res; 32: 415-439 (1999).

Rushton DN. Functional Electrical Stimulation. Physiol. Meas; 18: 241-275 (1997).

Rymer WZ, Katz RT. Mechanisms of spastic hypertonia. Phys Med Rehab; 8: 442-453 (1994).

Sabari JS, Kane L, Flanagan SR, Steinberg A. Constraint-induced motor relearning after stroke: a naturalistic case report. Arch. Phys. Med. Rehabil; 82:524-527 (2001).

Schmit BD, Dhaher Y, Dewald JPA, Rymer WZ. Reflex torque response to movement of the spastic elbow: theoretical analyses and implications for quantification of spasticity. Ann Biomed Eng; 27: 815-829 (1999).

Sivenius J, Pyorala K, Heinonen OP, Salonen JT, Riekkinen P. The significance of intensity of rehabilitation of stroke-a controlled trial. Stroke; 16(6): 928-31 (1985).

Stein J. Motor recovery strategies after stroke. Top Stroke Rehabil; 11(2):12-22 (2004).

Takahashi CD, Reinkensmeyer DJ. Hemiparetic stroke impairs anticipatory control of arm movement. Exp Brain Res; 149(2): 131-40 (2003).

Teasell RW, Foley NC, Bhogal SK, Speechley MR. An evidence-based review of stroke rehabilitation. Top Stroke Rehabil; 10(1):29-58 (2003).

Trombly A, Radomski MV. Occupational therapy and physical dysfunction. Philadelphia, Lippincott Williams & Wilkins (2002).

Tong KY. Artificial neural network control of FES gait using virtual kinematic sensors. Ph.D thesis, University of Strathclyde (1997).

Tosiyasu L. Kunii: Creating and retargetting motion by the musculoskeletal human body model. The Visual Computer; 16(5): 254-270 (2000).

Uchiyama T, Bessho T, Akazawa K. Static torque-angle relation of human elbow joint estimated with artificial neural network technique. J Biomech; 31: 545-554 (1998).

Uno Y, Kawato M, Suzuki R. Formation and control of optimal trajectory in human multijoint arm movement—minimum torque-change model. Biol Cybern; 61: 89–101 (1989).

Van Bogart J, McGuire J, Harris GF. Upper extremity motion assessment in adult ischemic stroke patients: a 3-D kinematic model. Proceedings of the 23rd Annual EMBS international Conference, 1190-1192, (2001).

Van del Helm FCT. Large-Scale Musculoskeletal System: Sensorimotor Integration and Optimization 1994. Biomechanics and Neural Control of Posture and Movement; 32: 407-424 (2000).

van Vliet PM, Lincoln NB, Foxall A. Comparison of Bobath based and movement science based treatment for stroke: a randomised controlled trial. J Neurol Neurosurg Psychiatry; 76(4):465-6 (2005).

Vint PF, Mclean SP, Harron GM. Electromechanical delay in isometric actions initiated from nonresting levels. Med Sci Sports Exerc; 33 (6): 978-983 (2000).

Volpe BT, Krebs HI, Hogan N, Edelstein OTR L, Diels C, Aisen M. A novel approach to stroke rehabilitation: robot-aided sensorimotor stimulation. Neurology; 54(10): 1938-44 (2000).

Wade DT, Collin C. The Barthel ADL Index: a standard measure of physical disability? Int Disabil Stud; 10(2): 64-7 (1988).

Wang L, Buchanan TS. Prediction of joint moments using a neural network model of muscle activations from EMG signals. IEEE Trans Neur Sys Rehab Eng; 10: 30-37 (2002).

Ward NS, Cohen LG. Mechanisms Underlying Recovery of Motor Function After Stroke. Arch Neurol; 61(12): 1844-1848 (2004).

Weiss A, Suzuki T, Bean J, Fielding RA. High intensity strength training improves strength and functional performance after stroke. Am J Phys Med Rehabil; 79(4): 369-76 (2000).

Wiegner AW, Wierzbicka MM. Kinematic models and human elbow flexion movements: Quantitative analysis. Exp Brain Res; 88: 665-673 (1992).

Williams PE. Effect of intermittent stretch on immobilised muscle. Ann Rheum Dis; 47(12): 1014-6 (1988).

Winters JM, Stark L. Estimated mechanical properties of synergistic muscles involved in movements of a variety of human joints. J Biomech; 21:1027-1041 (1988).

Winters JM. Hill-type muscle models: A systems engineering perspective In Winters JM and Woo SLY. (Eds.) Multiple muscle systems: Biomechanics and movement organization. Spring-Verlag, Berlin; 69–93 (1990).

Wolf SL, Binder-Macleod SA. Electromyographic biofeedback applications to the hemiplegic patient. Changes in upper extremity neuromuscular and functional status. Phys Ther; 63:1393- 403 (1983).

Wyller TB, Holmen J, Laake P, Laake K. Correlates of subjective well-being in stroke patients. Stroke; 29: 363- 367 (1998).

Yang N, Zhang M, Huang C, Jin D. Motion quality evaluation of upper limb target-reaching movements. Med Eng Phys; 24(2): 115-20 (2002).

Yeh CY,Chen JJ,Tsai KH. Quantitative analysis of ankle hypertonia after prolonged stretch in subjectswith stroke. J Neurosci Methods; 137(2): 305-14 (2004).

Zajac FE. Muscles and tendon: Properties, models, scaling, and application to biomechanics and motor control. Crit Rev Biomed Eng; 17:359-411 (1989).

Zajac FE, Winter JM. Modeling musculo-skeletal movement system: joint and body segmental dynamics, musculo-skeletal actuation, and neuromuscular control In Winters JM, and Woo SLY. (Eds.) ‘Multiple muscle systems’, Spring-Verlag, Berlin; 121-148 (1990).

Zhang LQ, Rymer WZ. Simultaneous and nonlinear identification of mechanical and reflex properties of human elbow joint muscles. IEEE Trans Biomed Eng; 44:1192-1209 (1997).

Zhang YT, Herzog W, Liu MM. Adaptive demodulation of muscular force from myoelectric signals obtained during locomotion” IEEE-EMBC and CMBEC 1401-1402 (1997).

APPEDIX I: FUGL-MEYER SCORE

UPPER LIMB SUBSET

Shoulder/Elbow/Forearm				
Stage	Instruction	Response	Scoring Criteria	
I&II. reflex Activity	Tap the biceps and finger Flexor tendons Tap the triceps tendons	__ Stretch reflex at Elbow and or/fingers __ Stretch reflex	0= no reflex can be Elicited 2= reflex can be elicited	
III. Voluntary Movement within synergy	Flexor synergy "Turn your affected hand palm up and touch your ear" Extensor Synergy " Turn your hand palm down and reach to touch your unaffected"	Flexor Synergy __ Shoulder retraction __ Shoulder elevation __ Shoulder abduction to 90 deg __ Shoulder external rotation __ Elbow flexion __ Forearm Supination Extensor Synergy __ Shoulder Abduction & internal rotation __ Elbow extension __ Forearm pronation	(For each of 9 details) 0= can not perform 1= can perform partly 2= can perform faultlessly	
IV. Voluntary movement mixing flexor and extensor synergies	"Show me how you would put a belt around you [or tie an apron]" "Reach forward to take [object held in front of patient]"	__ Affected hand moves to lumbar spine area __ Reaches into 90 of shoulder flexion	0= can not perform 1= hand must actively pass anterior-superior iliac spine 2= faultless 0= elbow flexes or shoulder abducts immediately 1= if there occur later in motion 2= faultless	

	"Put your arm to your side & bend your elbow. Turn your palm up & down."	__ Pronates and supinates forearm with elbow at 90 deg and shoulder at 0 deg	0= if cannot position or can not pronate or supinate 1= Shoulder and elbow joints correctly positioned and beginning pronation & supination seen 2= faultless	
V. Voluntary movement out side of synergies	"Turns your palm down and reach over here to touch [object held out to side]"	__ Abducts shoulder to 90 deg with elbow extend to 0 & forearm pronated	0= initial elbow flexion or loss of pronation 1= partial motion or elbow flexes and forearm supinates later in motion 2= faultless	
	Reach as high as you can toward the ceiling	__ Flexes shoulder from 90 deg to 180 deg with elbow at 0 deg	0= elbow flexes or shoulder abducts immediately 1= if those occur later in motion 2= motion faultless	
	"Reach your arm Directly forward and turn your palm up & down"	__ Flexes shoulder to 30 deg -90 deg extends elbow to 0 and supinates and pronates	0=if can not position arm or cannot rotate 1= correct position and beginning rotation 2= faultless	
VI. Normal reflex activity (tested if patient scores 6 in stage V tests)	Tap on biceps, triceps and finger flexor tendons	__ Normal reflex response	0= >= 2 reflexes are markedly hyperactive 1= 1 reflex hyperactive or 2 reflexes lively 2= no more than 1 reflex lively and	

			none hyperactive	
Upper Arm Subtotal Score (36 points)				
Wrist				
Stage	Instruction	Response	Scoring Criteria	
Wrists stability with elbow flexed	Put the shoulder in 0 deg elbow in 90 deg flexion, and forearm pronated "life your wrist and hold it there."	__ Patient extends wrist to 15 deg. Therapist can hold upper arm in position	0= cannot extend 1= can extend, but not against resistance 2= can maintain against slight resistance	
Wrists stability with elbow extended	Put the elbow in 0 "lift your wrist and hold it there"	__ As above	As above	
Active Motion with elbow flexed and shoulder at 0	"Move your wrist up and down a few times"	__ Patient moves Smoothly from full Flexion to full extension. Therapist can hold upper arm.	0= no voluntary Movement 1= moves, but less than full range 2= faultless	
Active motion with elbow extended	"move your wrist up and down a few times"	__ As above	As above	
Circumduction	"Turn your wrist in a circle like this [demonstrate]."	__ Make a full circle-ombining flexion & extension with ulnar & radial deviation	0= cannot perform 1= jerky or incomplete motion 2= faultless	
Wrist Subtotal Score (10 points)____				
Hand				
Stage	Instruction	Response	Scoring Criteria	
I. Mass Flexion	"Make a fist"	__ Patient flexes fingers.	0= no flexion 1= less than full flexion as compared to other hand 2= full active flexion	
II. Hook Grasp	"Hold this hopping bag by the handles"	__ Grasp involves MCP extension and PIP& DIP flexion.	0= cannot perform 1= active grasp, no resistance 2= maintains grasp against great resistance	

III. Finger Extension	"Let go or me Shopping bag" "Open your Wide"	__ From full active or passive flexion, patient extends all fingers.	0= no extension 1= partial extension or able to release grasp 2= full range of motion as compared to other hand	
IV. Lateral Prehension	"Take hold of this sheet of paper [or playing card]."	__ Patient grasps between thumb & index finger.	0= cannot perform 1= can hold paper but not against tug 2= holds paper well against tug	
V. Palmar Prehension	" Take hold of this Pencil as if you Were going to write."	__ Therapist holds Pencil upright and patient grasps it.	Scoring as above	
VI. Cylindrical Grasp	"Take hold of this paper cup [or pill bottle]"	__ Therapist holds the object and patient grasps with 1st & 2th fingers together	Scoring as above	
VII. Spherical Grasp	"Take hold of this tennis ball [or apple]."	__ Patient grasps with fingers abducted.	Scoring above	
Hand subtotal Score (14 points) _____				
Coordination/Speed				
Stage	Instruction	Response	Scoring Criteria	
Normal movement	"Close your eyes. now, and touch your nose you're your fingertip. Do that as fast as you can 5 times."	Patients does Finger-to-nose test __ Tremor __ Dysmetria __ Speed (Compare to unaffected side)	Tremor: 0= marked 1=slight 2=none Dymetria: 0= pronounced or Unsystematic 1= slight and Systematic 2= none Speed: 0= > 6 sec lower	

			1= 2-5 sec lower 2= <2 sec lower	
Speed and Coordination Subtotal Score (6 points) _____				
TOTAL UPPER EXTRMITY SCORE (66 points) _____				
NT: not test, because recovery is sequential, more advanced movement are not tested if the patient fails movements in the earlier stage.				

(Trombly A, Radomski MV. Occupational therapy for physical dysfunction. Philadelphia, Lippincott Williams & Wilkins 2002)

Name 姓名: Sex 性別: Age 年齡: Contact Number 電話:

Hemiplegic Side 偏癱邊旁: Time since Stroke 發病時間: Time since using the myoelectrically controlled robotic system 使用肌電驅動電機時間:

	非常同意 Strongly Agree	同意 Agree	沒有分別 Indifferent	不同意 Disagree	非常不同意 Strongly Disagree
在使用肌電驅動電機前，你獲得足夠的指導 You were given a clear instruction before using the myoelectrically controlled robotic system for training					
容易操作肌電驅動電機 It is easy to put on the myoelectrically controlled robotic system					
操作肌電驅動電機時，感到舒適 It is comfortable when you use the myoelectrically controlled robotic system					
肌電驅動電機的外觀可接受 The appearance of the myoelectrically controlled robotic system looks acceptable					
操作肌電驅動電機的步驟簡單 The steps using the myoelectrically controlled robotic system to carry out the training is simple to follow					
手肘的移動幅度(範圍)有所改善 The range of motion of elbow is improved after using the myoelectrically controlled robotic system					
手肘的情況有所改善 The elbows become less spastistic after using the myoelectrically controlled robotic system					
使用肌電驅動電機能改善你進行日常活動的能力 The myoelectrically controlled robotic system improves your ability to carry out activities of daily living					
整體上你對肌電驅動電機感到滿意 Overall you are satisfied with the function of the myoelectrically controlled robotic system					

To improve the design of the myoelectrically controlled robotic system, any comment? 其他意見?

APPENDIX III: CONSENT FORM

I, _____ (name of subject), hereby consent to participate in, as a subject, “Rehabilitation Robot using Motor-relearning Exercises to Improve Upper Limb Impairment for Persons after Stroke”.

- I have understood the experimental procedures presented to me.
- I have given an opportunity to ask questions about the experiment, and these have been answered to my satisfaction.
- I realize I can discontinue the experiment with no reasons given and no penalty received during the experiment.
- I realize that the results of this experiment may be published, but that my own results will be kept confidential.
- I realize that the results of this experiment are the properties of The Hong Kong Polytechnic University.
- I agree that the PI and the project research members, who obtained the authorization from the PI, can use my experimental data for this project study.

Subject name: _____ Signature: _____

Witness: _____ Signature: _____

Date: _____

同意書

我，_____(受試者姓名), 在此同意作為受試者參加康复机器手中風康复測試研究。

- 我已明白到該測試的步驟。
- 我已給予機會詢問有關該測試的問題, 並已獲得滿意的回答。
- 我已知道我可以終止測試而無需給予任何理由, 或由此而受到任何懲罰。
- 我已知道這個測試的結果可被發表, 但有關我個人的結果將獲得保密。
- 我已知道這個測試的結果屬香港理工大 學 。
- 我同意本項目負責人及其受權的項目研究人員使用我的實驗記錄以作此項目的研究。

受試者姓名_____ 簽署_____

作證人姓名_____ 簽署_____

日期_____